Interactions of Nucleobase Appended Tri-Cationic Water-Soluble Porphyrins and Metalloporphyrins with DNA and Donor-Acceptor Systems Based on Axially Substituted Tin(IV) Porphyrins

A Thesis

Submitted for the Degree of

DOCTOR OF PHILOSOPHY

By

G. Premaladha

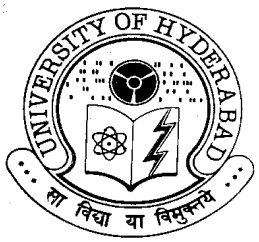

School of Chemistry
University of Hyderabad
Hyderabad - 500 046
INDIA

December 2005

School of Chemistry
University of Hyderabad
Central University P.O.
Hyderabad 500 046
India

Statement

I hereby declare that the matter embodied in this thesis is the result of investigations carried out by me in the School of Chemistry, University of Hyderabad, Hyderabad, India under the supervision of **Late Prof. Bhaskar G. Maiya**.

In keeping with the general practice of reporting scientific observations, due acknowledgements have been made wherever the work described is based on the findings of other investigators.

G. Premaladha

School of Chemistry
University of Hyderabad
Central University P.O.
Hyderabad 500 046
India

Certificate

Certified that the work contained in this thesis entitled **"Interactions of Nucleobase Appended Tri-Cationic Water-Soluble Porphyrins and Metalloporphyrins with DNA and Donor-Acceptor Systems Based on Axially Substituted Tin(IV) Porphyrins"** has been carried out by **G. Premaladha** under the supervision of **Late Prof. Bhaskar G. Maiya** and that the same has not been submitted elsewhere for a degree.

Dean
School of Chemistry

Prof. K. C. Kumara Swamy
Thesis Co-Supervisor

Acknowledgements

It gives me immense pleasure to express my deep sense of gratitude and profound respect to my supervisor **Late Prof. Bhaskar G. Maiya** for his constant guidance, encouragement and above all for the freedom he gave me in carrying out my research. His commitment to the work with a great sense of discipline and patience are highly admirable and truly inspiring. My association with him in this lab was a rewarding experience, which I never wish to forget.

I express my sincere thanks to Prof. K. C. Kumara Swamy, for his helpful discussions, suggestions and corrections of the papers as well as my thesis. His patience, co-operation and help towards the last stages of my work cannot be expressed in words.

I thank Prof. M. Periasamy, Dean, School of Chemistry, former Deans and all the faculty members of School of Chemistry especially Prof. Anunay Samanta, Prof. Samudranil Pal and Dr. Abani Kumar Bhuyan for their help on various occasions.

I thank my seniors Dr. L. Giribabu, Dr. C. V. Sastri, Dr. A. Ashok Kumar, Dr. D. Raghunath Reddy, Dr. P. Prashanth Kumar, Dr. M. Mariappan and my labmates Tamal Ghosh, A. Narahari and S. Prathap Chandran for the discussions and above all for creating a pleasant atmosphere in this laboratory.

Also, I would like to thank Prof. J. K. M. Sanders and Dr. N. Bampos, (University of Cambridge, Cambridge, U. K.); Prof. A. Osuka (Kyoto University, Kyoto, Japan) for their help in collecting mass (MALDI) data for some of the samples. Central Drug Research Institute, Lucknow is acknowledged for the FAB mass spectral data.

I would like to thank Mr. Satyanarayana, Mr. Bhaskar Rao, Mr. Raghavaiah and Mrs. Ayesa Parwez for their technical assistance. I also thank Mr.

Shetty and other non-teaching staff of the school of chemistry for their help. The assistance of Mr. Suresh for EPR and CD spectra is also gratefully appreciated.

Dr. T. Rajendiran and Prof. H. Surya Prakash Rao of Pondicherry University are remembered for their wonderful teaching, encouragement and affection.

Financial assistance from DST and CSIR is gratefully acknowledged.

I thank all my friends and well wishers for making my stay in the campus a memorable one.

Synopsis

This thesis entitled "**Interactions of Nucleobase Appended Tri-Cationic Water-Soluble Porphyrins and Metalloporphyrins with DNA and Donor-Acceptor Systems Based on Axially Substituted Tin(IV) Porphyrins**" deals with two aspects: (i) design, synthesis, spectroscopy of a new series of water-soluble tri-cationic porphyrins and metalloporphyrins and their interactions with DNA and (ii) design, synthesis, spectroscopy and photochemical properties of metalloid porphyrins that are substituted at the axial positions with aromatic donor subunits. Studies revealing the binding and cleaving ability of DNA have been carried out for the newly synthesized water-soluble porphyrins. Main observations of the research carried out with the donor-acceptor (D-A) systems include photoinduced electron transfer (PET) reactions.

Porphyrins and their metal/metalloid derivatives constitute a versatile class of compounds having applications in various research areas such as biomimetic photosynthesis, molecular electronics, molecular catalysis and photodynamic therapy. Water-soluble**,** cationic porphyrin systems are receiving attention because of their affinity for DNA and the potential they have for applications in photodynamic therapy. A variety of moieties have been connected to porphyrins to increase the binding affinity, to regulate the sequence specificity or to include chemical functionalities for inducing specific reactions. A great variety of D-A type porphyrin systems have been built those generally involve PET and EET as the key principles. While majority of D-A systems have been constructed by linking the donor/acceptor subunits at the porphyrin peripheral (i.e. β-pyrrole and meso) positions, relatively less number of such systems have been synthesized by utilizing the axial site/s on the central metal/metalloid ion of a porphyrin.

Chapter 3 of this thesis deals with a series of derivatives of 5,10,15,20-tetra-(N-methyl-4-pyridiniumyl)porphyrin (**H_2T4**) appended with nucleobase moieties (**AT4**, **TT4**, **GT4** and **CT4**). The metal insertion into the porphyrin chromophore leading to the possibility of change in the mode of binding has been utilized in the next chapter to synthesize Cu(II) and Zn(II) complexes of adenine appended tri-cationic porphyrins (**CuAT4** and **ZnAT4**) (chapter 4). Detailed studies on the binding with DNA using UV-visible, fluorescence, circular dichroism and thermal melting studies have been carried out. Photocleavage of DNA in the presence of light and the possible mechanism which is responsible for the cleavage also have been investigated. Chapter 5 deals with the interactions of nucleobase appended tri-cationic porphyrins and copper(II) metallated adenine appended tri-cationic porphyrin with DNA hairpins. In chapter 6 the synthesis, characterization and photochemical properties of 'axial-bonding' type compounds (**M3PY**, **M4PY**, **A3PY** and **A4PY**) based on the tin(IV) porphyrin scaffold are discussed. The ground state and excited state properties of dimers **A3PY** and **A4PY** are compared with that of their monomeric triads (**M3PY**, **M4PY)** and corresponding precursor compounds.

Overall, the work embodied in this thesis has been divided into seven chapters. A brief, chapter-wise account of the specific contents is presented below.

Chapter 1. Introduction

Recent literature on DNA interactions of cationic porphyrins, photodynamic therapy and donor-acceptor (D-A) systems based on axially substituted porphyrins, have been reviewed in this chapter.

Chapter 2. Materials and methods

This chapter presents a list of chemicals, a general description of the synthetic procedures, spectroscopic techniques, techniques used for monitoring DNA interactions, electrochemical and photophysical techniques employed during the research work.

Chapter 3. Nucleobase (A, T, G and C) appended tri-cationic water-soluble porphyrins: Synthesis, characterization, binding and photocleavage studies with DNA

It is interesting to investigate the DNA interactions of covalently linked cationic porphyrin chromophores (which exhibit versatile DNA binding ability) and nucleobase moieties, that are part of the building blocks of the DNA. In this regard, our efforts resulted in a series of nucleobase appended tri-cationic porphyrins (**AT4**, **TT4**, **GT4** and **CT4**) (Fig. 1).

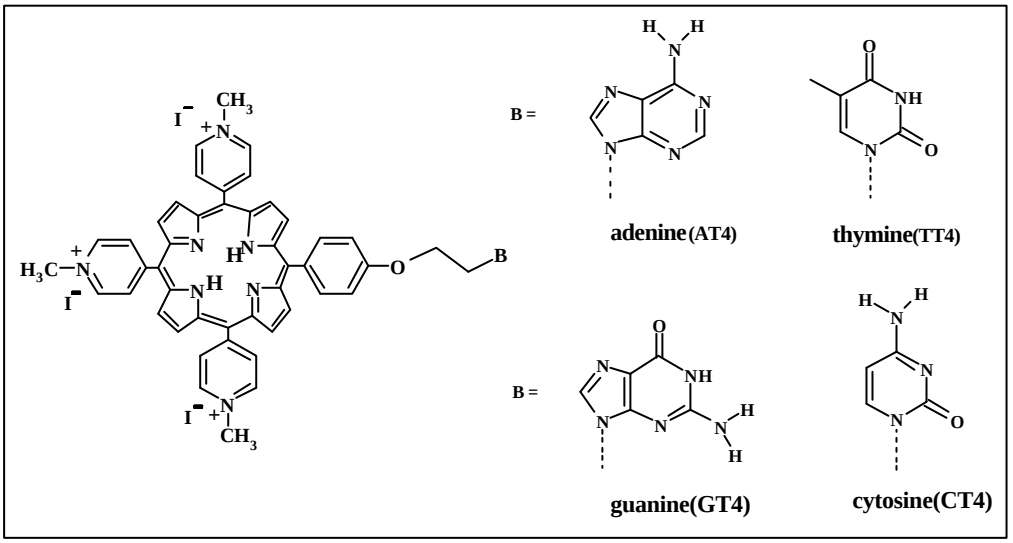

Fig. 1 Nucleobase appended tri-cationic water-soluble porphyrins synthesized in this study.

All these nucleobase appended tri-cationic porphyrins have been characterized by mass (FAB/MALDI), UV-visible and proton nuclear magnetic resonance (1D and ^{1}H-^{1}H COSY) spectroscopic techniques. The ground state spectroscopic data of these newly synthesized porphyrins as probed by the UV-visible and ^{1}H NMR spectroscopies collectively indicate that there exists minimum interaction between π-planes of the porphyrin chromophore and the nucleobase moiety. Fluorescence studies indicate that linking of nucleobase does not have any adverse effect on the singlet state properties of these nucleobase-linked porphyrins.

The binding interactions with CTDNA have been monitored using UV-visible, fluorescence, circular dichroism and thermal melting methods. The Soret band of the porphyrin tends to shift to a higher wavelength and decreases in the absorption intensity during addition of CTDNA. The shift in the wavelength maxima, percentage of hypochromism and the calculated binding constant values reveal that the behavior of these nucleobase porphyrins with CTDNA is similar to **H_2T4**. Analogous to **H_2T4**, increase in the emission intensity was observed for all these newly synthesized porphyrins with CTDNA and the results obtained are comparable to that of the absorption titrations. Circular dichroism spectra (350-500 nm) were run to analyze the possible mode of binding interaction of these porphyrins with CTDNA. The intercalating efficiency of the porphyrin present in nucleobase appended porphyrins follows the order **GT4** > **H_2T4** > **TT4** > **AT4** ~ **CT4**. These differences may be attributed due to the ability to form keto-enol tautomerism, propensity to form hydrogen bonding and extended conjugation. The conformational changes on DNA (CD spectra recorded at 220-300 nm) observed in the UV-visible region also support these conclusions. Thermal melting studies also suggest the same. Extent of cleavage (in the presence of light) of these porphyrins with pBR322 DNA was calculated through photocleavage experiments

and it was found that only **GT4** photocleaves more effectively than the other nucleobase appended porphyrins and **H_2T4** may be because stacked guanine moieties (arising due to the intercalation of guanine connected to porphyrin in between the base pairs) are more reducing than a single guanine residue. The singlet oxygen mechanism, which is responsible for the cleavage of DNA, is confirmed by conducting photocleavage inhibition experiments using various inhibitors.

Chapter 4. Adenine appended tri-cationic water-soluble metalloporphyrins: Synthesis, characterization, binding and photocleavage studies with DNA

Investigation of the interaction of adenine appended tri-cationic porphyrin (**AT4**) with CTDNA showed only very weak binding, particularly intercalation (chapter 3). Since metallation of porphyrins can vary the binding mode of porphyrin to nucleic acid duplexes, we have synthesized Cu(II) and Zn(II) complexes of adenine appended tri-cationic metalloporphyrins to investigate their binding interactions with DNA.

This chapter presents the details of the design, synthesis and characterization of the Cu(II) and Zn(II) complexes of adenine appended tri-cationic porphyrins (**CuAT4** and **ZnAT4**) (Fig. 2). Both the adenine appended tri-cationic metalloporphyrins synthesized have been characterized by mass (FAB/MALDI), UV-visible, proton nuclear magnetic resonance (1D and ^{1}H-^{1}H COSY) and electron spin resonance spectroscopic techniques.

Interactions of these metalloporphyrins with CTDNA have been investigated using UV-visible, fluorescence, circular dichroism and thermal melting experiments. The results are compared with those obtained for **AT4** and Cu(II) or Zn(II) complex of **H_2T4**.

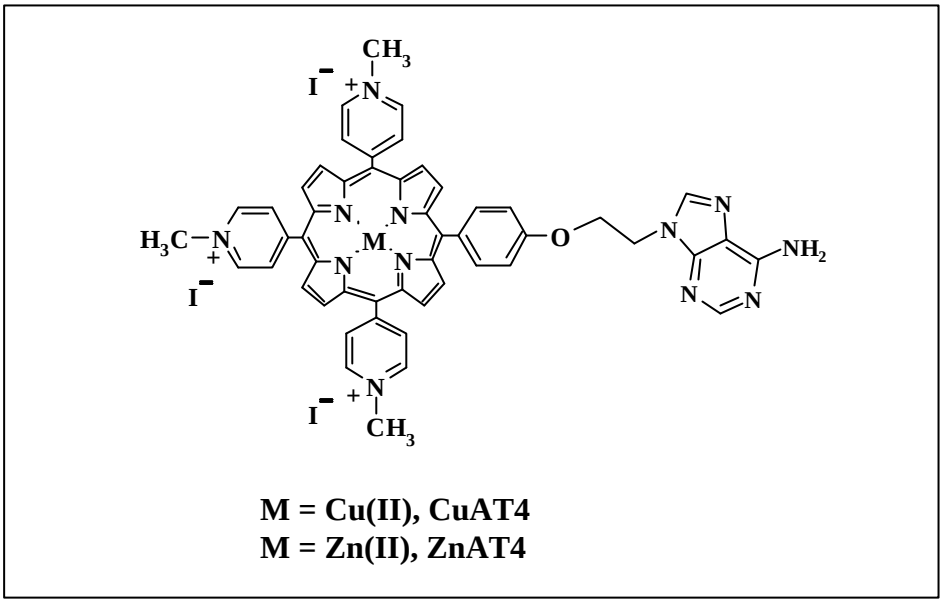

Fig. 2 Adenine appended tri-cationic water-soluble metalloporphyrins synthesized in this study

The ground state spectroscopic data of these newly synthesized metalloporphyrins as probed by the UV-visible, ^{1}H NMR and electron spin resonance spectroscopies collectively indicate that there exists minimum interaction between π-planes of the metalloporphyrin chromophore and the adenine moiety. Fluorescence studies indicate that metallation of porphyrin chromophore with Zn(II) does not have any adverse effect on the singlet state properties of **ZnAT4**.

The bathochromicity and hypochromism observed for **CuAT4** are higher than that for **ZnAT4**. The shift in the wavelength maxima, percentage of hypochromism and the calculated binding constant values reveal that the interactions of the **CuAT4** and **ZnAT4** with CTDNA are similar to that of **CuT4** and **ZnT4**, respectively. Circular dichroism spectra reveal that porphyrin in **CuAT4** intercalates more efficiently than **CuT4** in the duplex. The binding of the

adenine moiety may drive the copper metalated porphyrin to the proximity of the DNA, which results in strong intercalation of porphyrin in **CuAT4** than **CuT4**. In contrast to **ZnT4** (which binds externally), the porphyrin in **ZnAT4** interacts through external binding with self-stacking along the DNA helix. This may be due to two reasons: a) binding of adenine moiety with DNA may restrict the free disperse of porphyrin in **ZnAT4** and b) cluster formation of porphyrin molecules near one another at the early stages of DNA addition. Thermal melting studies performed also support these conclusions. The photocleaving efficiency of **ZnAT4** is slightly lesser than that of **ZnT4**. Similar to **CuT4**, **CuAT4** also did not show any photocleaving efficiency probably due to the paramagnetic nature of metal ion.

Chapter 5. Binding studies of nucleobase appended tri-cationic porphyrins and metalloporphyrin with DNA hairpins

It was of interest to utilize the DNA hairpins in order to study their interactions with our newly synthesized porphyrins. Analysis of the interactions of nucleobase appended tri-cationic porphyrins (**AT4**, **TT4**, **GT4** and **CT4**) and Cu(II) complex of adenine appended porphyrin (**CuAT4**) with DNA hairpins is done in this chapter. The results are compared with their references **H_2T4** and **CuT4**, respectively. The results with AT rich DNAs suggest that the nucleobase appended tri-cationic porphyrins bind only through external binding in a manner similar to **H_2T4** but to a lesser extent. The lesser external binding nature of these porphyrins may be due to the presence of only three positive charges that result in decrease in the affinity. Porphyrin in **GT4** shows slightly more external binding than the porphyrins connected to **AT4**, **TT4** and **CT4**. The presence of more acidic protons to exhibit keto-enol tautomerism, extended conjugation and ability to form more number of hydrogen bonds of the bound form of guanine in **GT4**

may drive the porphyrin moiety into the proximity of DNA and account for strong external interaction.

Parallel to the previous reports, DNA containing at least 50% G≡C base pairs (CG[T4] and CCGG[T4]) supports intercalative binding simply because a robust hydrogen bonding framework stabilizes the intercalated adduct and inhibits distortions that favor external binding. With CG[T4] DNA, the intercalating tendency of the nucleobase appended porphyrins and standard decreases in the order **H_2T4** > **GT4** > **TT4** > **CT4** ~ **AT4,** whereas with the 20 mer CCGG[T4], the order followed was **GT4** > **H_2T4** > **TT4** > **CT4** ~ **AT4**. Similar to the interactions with CTDNA, the changes observed here may be attributed due to the ability to form keto-enol tautomerism, propensity to form hydrogen bonding and extended conjugation. Interestingly, with the long stem DNA [CCGG[T4]], porphyrin in **GT4** shows more intercalation than **H_2T4**, whereas the situation was quite opposite with CG[T4] DNA. Both the co-operarive effect (which depends on the strength of the hydrogen bond of DNA hairpin) and the ability of guanine moiety bound to DNA to bring the porphyrin chromophore into the proximity of DNA may account for the efficient intercalation of porphyrin in **GT4** than **H_2T4** with CCGG[T4]. Experiments reveal that change in the loop sequence of the DNA also affects binding. The binding properties of **CuAT4** and **CuT4** as shown by absorption spectra and CD are similar to each other. Finally a stepwise energy analysis has been provided to illustrate the competing effects that influence the binding.

Chapter 6. Bis(aryloxo) derivatives of azo-benzene bridged tin(IV) porphyrins: Synthesis, spectroscopy and photochemistry

The 'axial-bonding' theme is utilized in this chapter to synthesize monomeric (**M3PY** and **M4PY**) and dimeric (**A3PY** and **A4PY**) scaffolds based

on tin(IV) porphyrins (Fig. 3). All these new compounds have been characterized by the mass (FAB/MALDI), UV-visible, proton nuclear magnetic resonance (1D and ^{1}H-^{1}H COSY) and also by the cyclic- and differential pulse voltammetric techniques.

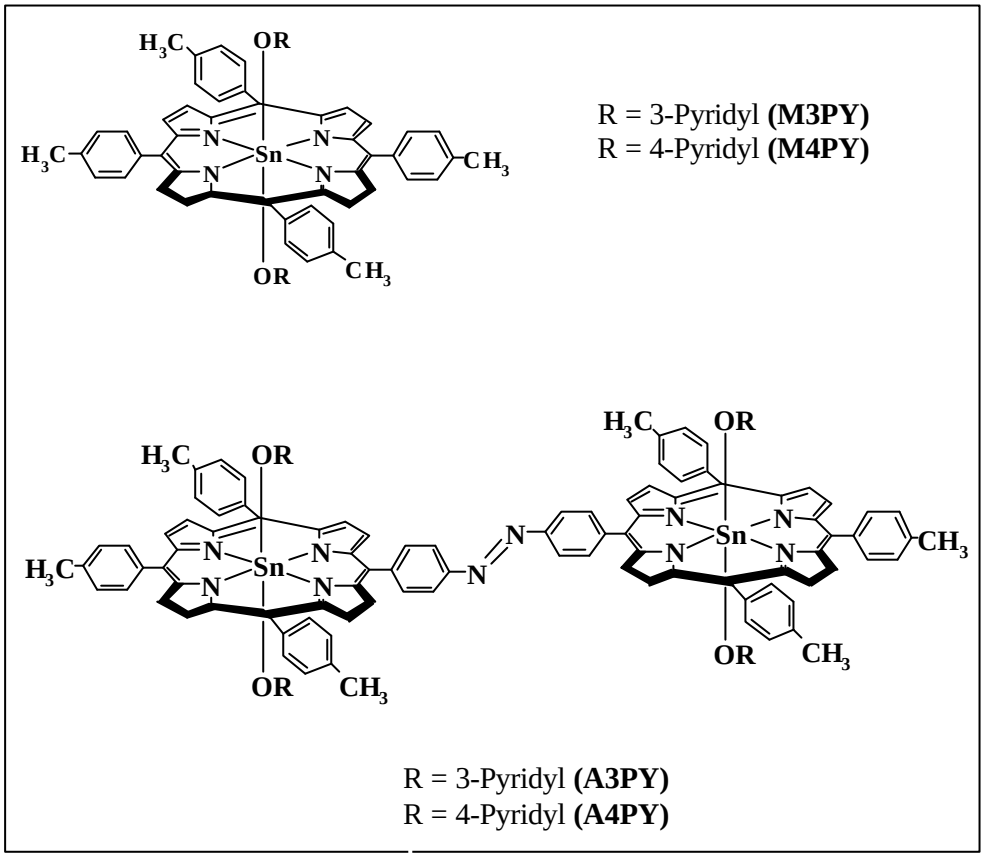

Fig. 3 Bis(aryloxo) derivatives of azo-benzene bridged tin(IV) porphyrins and their monomeric scaffolds synthesized in this study.

The Soret band of **$[L^{3}Sn(OH)_2]$** is broader when compared with the monomeric compound, **$[L^{1}Sn(OH)_2]$** indicating a ground state interaction of the azobenzene and porphyrin chromophore. The same trend is observed for **A3PY**

and **A4PY** with respective to their monomers **M3PY** and **M4PY**. Excitation of porphyrin at 600 nm results in quenching of fluorescence intensity. An intramolecular photoinduced electron transfer (PET) mechanism has been suggested to occur from axial ligand to porphyrin by the combined application of redox and emission data. Although we could not effect *cis-trans* isomerism of **A3PY** and **A4PY** triads under our experimental conditions, further investigations (perhaps under laser induced conditions) may provide fruitful results.

Chapter 7. Conclusions

This chapter presents general conclusions based on the investigations carried out in this work.

Contents

CHAPTER 1

Introduction

Current interest in the chemistry of porphyrins and related macrocyclic compounds is mostly due to the potential applications of these species in research areas such as biomimetic photosynthesis, molecular electronics, supramolecular catalysis, organic synthesis, magnetic resonance imaging (MRI) and photodynamic therapy (PDT).[1] A plethora of porphyrin systems have been built for use in many of these applications. Water-soluble, cationic porphyrin systems are receiving attention because of their affinity for DNA and the potential they have for applications in photodynamic therapy.[1] A variety of moieties have been connected to porphyrins to increase the binding affinity, to regulate the sequence specificity or to include chemical functionalities for inducing specific reactions.

This thesis deals with two aspects: (i) Design, synthesis, characterization and DNA interactions of nucleobase appended cationic porphyrins and (ii) Design, synthesis, characterization and photoinduced electron transfer (PET) reactions of donor-acceptor (D-A) systems in which the donor subunits are connected to the axial sites of metalloid porphyrin. While majority of the D-A systems have been constructed by linking the donor/acceptor subunits at the porphyrin peripheral (i.e. β-pyrrole and meso) positions, relatively less D-A systems have been synthesized by utilizing the axial site/s (central metal/nonmetal ion) of a porphyrin. This chapter provides a survey of the recent literature on DNA interactions of cationic porphyrins, photodynamic therapy and D-A systems based on axially substituted porphyrins, as relevant to the present study.

1.1 DNA Interactions of cationic porphyrins

Fiel and co-workers first showed that readily available tetracation **1** and its copper(II) derivative **2** (among the available tetracations **1**-**10**) are capable of intercalating into B-form DNA.[2,3] This was a remarkable observation because intramolecular steric forces prevent the pyridyl substituents from residing in the plane of the porphyrin. Three modes of interactions are possible for porphyrin to interact with DNA: (i) intercalation between the base pairs, (ii) external binding in the minor groove or with the phosphate backbone and (iii) through external stacking of porphyrins along the helix. In addition to the DNA binding studies of **1**, Fiel's group has also investigated the interaction of **11**, **12** and **13** with calf thymus DNA (CTDNA) and synthetic polynucleotides.[4,5] They found out that the location and orientation of the positively charged substituents alter the intercalation of a meso substituted porphyrin.

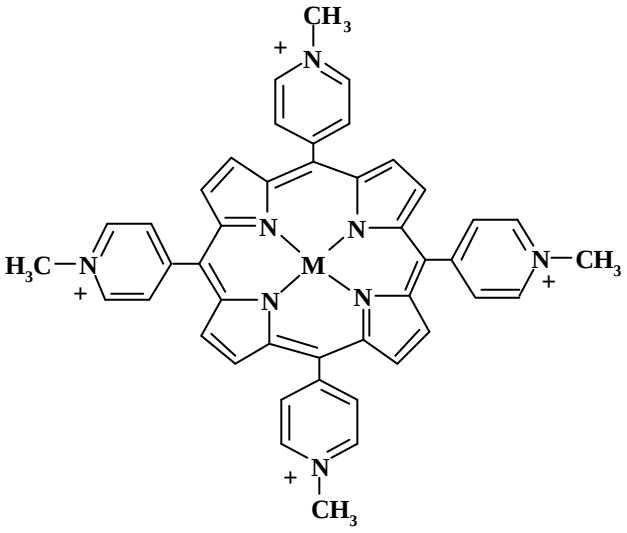

M = 2H (**1**), Cu(II) (**2**), Pd(II) (**3**), Pt(II) (**4**), Mn(III) (**5**), Fe(III) (**6**), Zn(II) (**7**), Co(II) (**8**), V(IV)=O (**9**), Ni(II) (**10**)

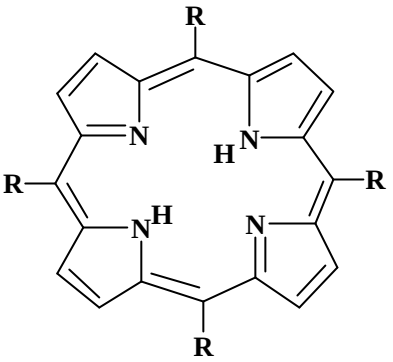

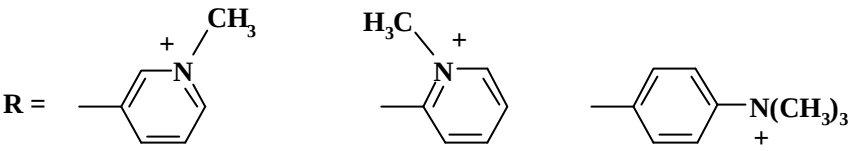

11 **12** **13**

Kelly and co-workers have reported a comparative study of the interaction of **1** and **7** with DNA using absorption, fluorescence spectroscopy and topoisomerisation.[6] Topoisomerisation of pBR 322 DNA shows that **1** unwinds DNA as efficiently as ethidium bromide confirming that it intercalates at many sites whereas **7** may cause only limited winding. The fluorescence intensity of either **1** or **7** is enhanced in the presence of poly (A-T), whereas in the presence of poly(G-C) the fluorescence intensity of **7** is unaffected and that of **1** is markedly reduced. Waring and co-workers found out the preference of both AT and GC protected sites by porphyrins **1** and **10** during their footprinting experiments.[7] Footprinting analysis also has been carried out by Dabrowiak co-workers to delineate the DNA binding specificity of transition metal complexes of **1**.[8] Analysis revealed that complexes **5**, **6**, **7** and **8** which are 5- or 6- coordinate were found to bind in the AT regions; by contrast, the 4-coordinate complexes **2** and **10** bind both in the AT and GC regions of the fragment.

Interactions of cationic porphyrins with several native and synthetic DNAs were studied using NMR (^{31}P and ^{1}H) spectroscopy and viscosity mesurements.[9-12] Increase in viscosity of linear DNA was observed with **1** and **10** whereas slight decrease in viscosity was observed with porphyrin **7**. A characteristic ^{31}P NMR signal at ~ -0.9 ppm relative to trimethyl phosphate and pronounced upfield shifts of some of the imino ^{1}H signals were observed due to intercalation. Detailed analysis of NMR spectra confirms the selective intercalation at 5′-CG-3′. Pasternack and co-workers have utilized stopped-flow and temperature-jump techniques to investigate the interactions of nucleic acids with porphyrins and metalloporphyrins. Results reveal that the reaction of both axially and nonaxially liganded porphyrins at AT sites is too rapid to be measured by these kinetic methods, whereas at GC sites the interaction of the nonaxially liganded porphyrins is in the millisecond time range. Both CTDNA and synthetic homopolymers [poly(dG-dC) and poly(dA-dT)] have been employed for these studies.[13]

The interactions of **1** and its transition metal complexes with the hexadeoxyribonucleotides have been reported using resonance Raman and/or UV-visible spectroscopy by Nakamoto and co-workers.[14] The results indicate that the hexamers containing the 5′CG3′ as well as the 5′GC3′ site and also the mismatched hexamer d(TGTGCA)$_2$ are capable of intercalating the **1**, **2** and **10** porphyrins. ^{1}H NMR spectra of d(CGTACG)$_2$ mixed with **2** have provided further evidence for the intercalation and for the other hexamers outside binding by localized electrostatic interaction is suggested. Possible reasons for different binding properties of long and short helices are also discussed by them.

Mode of binding of porphyrins is influenced by coulombic, hydrophobic and steric constraints, which can be varied by modifying the structure of the porphyrin as well as the composition of DNA. The mode of binding also depends

on the [porphyrin]/[DNA] ratio. At low [porphyrin]/[DNA] ratios, the groove binding mode[3,15-20] and intercalation[11,21-23] have been suggested for **1** complexed with AT and GC site of DNA, respectively. In the groove binding mode, whether the crescent-shaped side of **1** fits into the minor groove or it binds near the minor groove is still unclear, while porphyrin intercalates between the base pairs in the 5′CG3′ site.[24-27] As the ratio increases, the outside binding mode, represented by a bisignate excitonic circular dichroism (CD) in the Soret region, dominates for both AT-rich and GC-rich DNAs.[4,24-27]

Interaction of the metalloporphyrins with nucleic acid duplexes also has been extensively studied since the binding mode of porphyrin to nucleic acid duplexes, i.e., intercalative or outside binding mode can be easily tuned by varying the metal center.[28-31] For example, the thin square planar porphyrins **2**, **3** and **4** are capable of intercalating into the pocket between two adjacent base pairs of B-DNA, since these metalloporphyrins are not ligated at their vacant axial site by aquo ligands. On the other hand, **5**, **6**, **7** and **8** can bind only to the outside of the DNA duplex due to one or two axial aquo ligands.[32,33] The DNA binding studies of **9** clearly show the inability for intercalation since there is increase in DNA viscosity and an AT preference similar to **7**.[34] Insertion of various metal ions in the porphyrin ring makes it suitable for specific interactions. Shreiner and co-workers have observed that **3** binds edge-on in the major groove at an ApT step.[35]

Crystallographic analysis of metalloporphyrin **2**-oligonucleotide complexes has shown that intercalation or groove binding of cationic porphyrin causes a distortion of B-DNA significantly.[29,30] Williams *et al*. have reported the X-ray structure of a complex in which **2** flips a base out of hexamer DNA helical ($[d(CGATCG)]_2$) stack. The porphyrin binds by normal intercalation between the C and G of 5′TCG3′ and by extruding the C of 5′CGA3′. Two pyridyl rings are

located in each groove of the DNA and the complex appears to be extensively stabilized by electrostatic interactions between positively charged nitrogen atoms of the pyridyl rings and negatively charged phosphate oxygen atoms of the DNA. The extrusion of a base appears to be facilitated by pyridyl-DNA steric clashes.

Uno *et al*. have studied the binding properties of **1** and **2** with RNA and DNA·RNA hybrid duplexes.[36] The porphyrin **1** was found to bind in a single step to poly(rI)·poly(rC), poly(rG)·poly(rC) and poly(rG)·poly(dC) and in a multistep manner to poly(rA)·poly(rU), poly(rA)·poly(dT) and poly(rI)·poly(dC). The induced CD spectra suggested that the porphyrin preferred to bind to the RNA duplexes with self-stacking along the polymer surface and to the hybrids with intercalation at higher duplex load. This observation implied a distinct conformational difference between the RNA duplexes and DNA·RNA hybrids, and a porphyrin molecule is able to recognize the difference. Relative to the free-base **1**, its copper (II) complex **2** binds to poly(rA)·poly(dT) and poly(rA)·poly(rU) with a greatly increased binding constant.[37] The external self-stacking of the porphyrin **2** on the surface of the polymers was evident from the strong conservative type induced CD signals. Thus, the bound porphyrin may impose an ordered architecture on the polymer surface, the stacking being facilitated by the more planar nature of the **2** than the nonmetal counterpart. Kim and co-workers have studied the interaction of **1** with triplex DNA.[38] Since the third strand in the triplex inhibits the formation of **1** assembly, stacking occurs in the major groove of both the $d(A)_{12}·d(T)_{12}$ and the $d(G)_{12}·d(C)_{12}$ duplexes.

The interaction of **1** with DNA has been investigated at ionic strength (IS) values of 0.01 and 0.20 M (pH 6.8) using the flash-photolysis technique along with optical absorption and fluorescence data. At low IS the quenching constant of the porphyrin triplet states by molecular oxygen (k_q) value for **1** externally bound to the GC sites is five times lower than that for the free porphyrin and

twice as high as that for the intercalated one. At high IS the binding of **1** reduces the k_q three-fold for the AT sites in the minor groove and 16-fold in the major groove compared to the free one.[39]

Hurley and co-workers have extensively investigated the interaction of cationic porphyrins with G-tetrad (**14**) that stabilizes the quadruplex DNA. The results reveal that **1** binds to the intramolecular quadruplex DNA by stacking externally to the guanine tetrad at the GT step, while **12** binds predominantly via external binding to the TTA loop.[40-42]

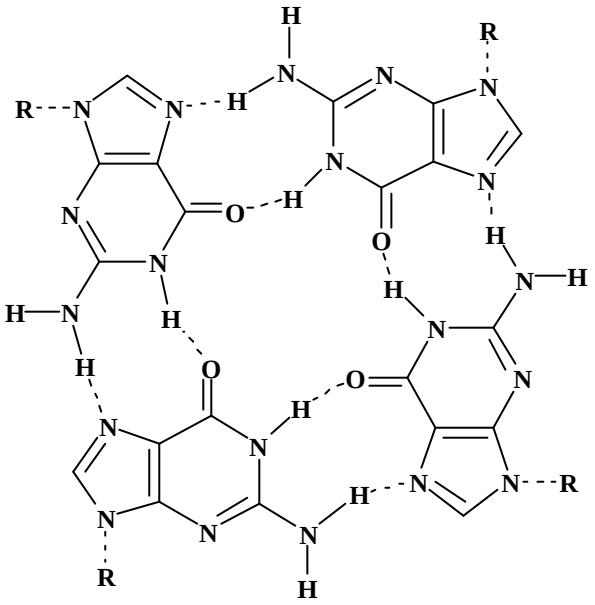

G-tetrad structure **(14)**

Further work on structure activity relationship reported by Hurley *et al*. led to the following conclusions: (i) stacking interactions are critical for telomerase inhibition, (ii) positively charged substituents are important but may be interchanged and combined with hydrogen-bonding groups and (iii)

substitution is tolerated only on the meso positions of the porphyrin ring and the bulk of the substituents should be matched to the width of the grooves in which they putatively lie.[43] Sheardy and co-workers have shown that the affinity for **1** with simple G4T4 quadruplex is twice as that with duplex DNA (CGCGATAT).[44] Meunier and co-workers have investigated the oxidative damage of the quadruplex with **5**. They found out that the high-valent porphyrin $Mn^{(V)}$=O species obtained by the activation of **5** by $KHSO_5$ could mediate efficient oxidative cleavage of the quadruplex. The location of damage showed that the metalloporphyrin bind to the last G-tetrad of the quadruplex structure via an external interaction. They also conclude that the oxo-metalloporphyrin is very reactive that could mediate both electron-abstraction or H-abstraction on G or T residues, respectively within the DNA quadruplex target.[45] The same group also has synthesized a series of aminoquinoline derivatives of tri-cationic metalloporphyrins and the degradation of quadruplex DNA has been assayed *in vitro* with the manganese derivatives.[46] They have concluded that these complexes were capable of inhibiting the telomerase enzyme with IC_{50} values in the micromolar range through telomeric repeat amplification protocol (TRAP) assay experiments.

Recently a series of cationic metalloporphyrin derivatives have been prepared by making variations on the porphyrin skeleton of **1**.[47] The DNA binding properties of nickel(II) and manganese(III) porphyrins were studied by surface plasmon resonance and the capacity of the nickel porphyrins to inhibit telomerase was tested by TRAP assay. The nature of the metal influences the kinetics (the process is faster for Ni than for Mn) and the mode of interaction (stacking or external binding). The chemical alterations did not lead to increased telomerase inhibition. The best selectivity for G-quadruplex DNA was observed for **5**, which exhibits a tenfold preference for quadruplex over duplex. Szalai and co-workers

have studied the interactions of **2** with parallel standard quadruplexes.[48] They found a 2:1 binding stoichiometry for G-quadruplex of d($T_4G_4T_4$) and a 3:1 binding stoichiometry for G-quadruplex of d($T_4G_8T_4$) with **2**, respectively using the method of continuous variation analysis. Induced emission spectra of **2** with any of this G-quadruplex indicate a mode of binding in which the ligand is protected from the solvent. Electron paramagnetic resonance spectra of **2** with added oligonucleotide show an increase in the Cu-N superhyperfine coupling constant as the length of the oligonucleotide increases. On the basis of these data, it has been proposed that with both quadruplexes, metalloporphyrin **2** externally stack at each end of the run of guanines, similar to other planar G-quadruplex ligands. Data obtained are consistent with intercalation of a **2** molecule into the G-quadruplex of d($T_4G_8T_4$).

Recently Ishikawa *et al*. have reported that an antiparallel quadruplex structure was found to be stabilized greatly by the meta-isomers than by the para-isomers and the well-studied **1**, as revealed by the increase in melting temperature of the quadruplex.[49] One mole equivalent of these isomers was sufficient to stabilize the quadruplex. From the experiments carried out, the unique site for the porphyrin binding is suggested to be the external guanine tetrad or groove of the quadruplex. Jenkins and co-workers have examined the porphyrin binding to intermolecular and intramolecular quadruplex DNA from Oxytricha and human telomers and a thrombin-binding aptamer.[50] The results indicate binding by threading intercalation at each closely similar GpG site, possibly without invoking neighbor exclusion for adjacent sites, rather than through either external electrostatic processes or end-pasted stacking modes. Von Hoff and co-workers have identified a series of porphyrins (freebase and metal complexes of **1** and tetraquinoline porphyrin) as G-quadruplex interacting agents that stabilize the telomeric G-quadruplex DNA and thereby inhibit human telomerase.[51] The results

suggest that relevant biological effects of porphyrins can be achieved at concentrations that do not have general cytotoxic effects on cells. Moreover, the data support the concept that a rational, structure-based approach is possible to design novel telomere-interactive agents with application to a selective and specific anticancer therapy.

Balton and co-workers have found that porphyrins are highly fluorescent in the presence of quadruplex but not with duplex DNA, which offer a route to the specific detection of the former DNA under biologically important conditions. [52] They have even revealed that there is selectivity between the quadruplex types for porphyrins.

The complexation of **1** with free and encapsidated DNA of T7 bacteriophage was investigated by Csik and co-workers.[53] The studies reveal two main binding types of **1**, e.g., external binding and intercalation both in free and in encapsidated DNA. Increase in the strand separation temperature of both free and native phage DNA and also the unchange of phase transition temperature of phage capsid proteins with **1** led to the conclusion that binding of the porphyrin does not influence the protein structure and/or the protein-DNA interaction.

The interaction of **1** with the oligonucleotide DNA duplex $[d(GCACGTGC)]_2$ has been studied by Leontis *et al*.[23] The binding of **1** to $[d(GCACGTGC)]_2$ produced a single set of mostly upfield-shifted DNA resonances in slow exchange with the resonances of the free DNA. The observed intra- and intermolecular NOEs (Nuclear Overhauser Effect) in this complex showed that the porphyrin intercalates at the central 5′CG3′ step of the DNA duplex without disrupting the flanking base pairs.

Molecular dynamics calculations by Ford and co-workers indicated that contacts in the major groove involving thymine methyl groups of DNA and pyridinium groups of **1** could inhibit full intercalation of the porphyrin into a

5′TpA3′ step.[7] But the uridine replacement studies carried out by McMillin group confirm that the steric bulk of the thymine methyl group does not prevent **1** from intercalating in A=T-rich regions of DNA.[54] The latter group has also reported the interactions of **1** and **2** with hairpin-forming oligonucleotides to label the binding motifs and the sequence specificity. The results suggest that the robust hydrogen bonding within the B-form duplex promotes the intercalative binding of **1** and **2** since it stabilizes the intercalated adduct and inhibits distortions that favor external binding. Intercalation occurs if the composition of the DNA has atleast 50% G≡C even in the absence of G≡C step whereas interaction with a run of four A=T results in groove-binding.[54,55] Inosine-for-guanine replacement in DNA hairpin hosts reveals that the intercalative binding of **2** depends upon strong hydrogen bonding within the stem.[56,57] Luminescence properties of the intercalation of **2** into DNA also have been investigated by McMillin group.[58] The results indicate that the distribution of porphyrin between the two types of sites (AT site and GC site) depends on the nucleotide-to-copper ratio and intercalation is favored at moderate ratios. Novel emission with a lifetime of about 20 ns is observed from the tripdoublet and tripquartet excited states of intercalated **2**. This emission is normally quenched by a mechanism, which involves coordination of the solvent at an axial position of the copper center. Solvent-induced quenching occurs when the complex is externally bound but not when the complex is intercalated because the axial coordination sites are blocked.

Turpin and co-workers have studied the dynamics and mechanism of the photoinduced reversible process of formation and decay of an exciplex species formed between **2** and poly(dA-dT).[59] They have found that the binding of one of the CO-groups of T or U to **2** in its lowest excited triplet state results in a shortening of the triplet-state lifetime. In addition, a population of an excited $^2[d_{z^2},d_{x^2-y^2}]$ state, i.e., the most low-lying and long-lived excited state for the five-

coordinated state of **2** (exciplex state), occurs in the process of excitation relaxation. The studies also reveal the promotion of one of the copper d electrons into the half-filled $d_{x^2-y^2}$ orbital and the expansion of the porphyrin core to accommodate the occupation of this d orbital. The exciplex deactivation process is accompanied by the CO-group detachment with a disruption of the exciplex into initial components.

The same group also has investigated the dynamics and mechanisms of photoexcitation relaxation of **10** bound to DNA polynucleotides using time-resolved picosecond transient absorption (TA) and nanosecond resonance Raman (RR) spectroscopies.[60] A long-lived transient species has been assigned to the excited intramolecular metal-centered (d,d) state $^3B_{1g}$ of the 4-coordinate Ni porphyrin intercalated between G-C base pairs. Studies also support the existence of atleast two types of interaction of **10** with poly(dA-dT)$_2$, each having its own kinetics of TA decay and transient RR spectra. The data show that a major part of Ni porphyrin molecules yields a photophysical behavior typical for a 4-coordinate species (the excited (d,d) state $^3B_{1g}$ playing the key role in relaxation processes), while a minor part of **10** also participates in axial ligand binding/release photoprocesses. Since the comparative studies show that no 6-coordinate $^3B_{1g}$(L)2 transient species is photogenerated in the complex with poly(dA-dT)$_2$, the axial coordination of only one extra-ligand molecule (most probably from the surrounding water solution) to the porphyrin central Ni ion is proposed. Turpin *et al*. have also confirmed the exciplex formation that results from the photoinduced interaction of **2** with calf-thymus DNA using resonance Raman (RR) spectroscopy by both ~10 ns and ~50 ps laser pulses.[61]

The exciplex formation of **2** with various DNAs (double stranded, single stranded and calf thymus DNA) have been analysed using picosecond time-resolved resonance Raman (ps-TR3) technique.[62] It is shown that reversible

exciplex is formed between photoexcited **2** and C=O groups of thymine residues in all thymine-containing sequences of nucleic acids. It has been reported that although the binding mode of the porphyrin actually depends on the base sequence, there is no preferential binding of **2** to the various sites of DNA and there is no photoinduced ultrafast porphyrin translocation from GC to AT sites of DNA also. In addition, it is shown that the two exciplex species formed (with the surrounding water molecules and with thymine residues) can be distinguished from each other by their relaxation kinetics: the lifetime of the exciplex formed with water lies in the 3-12 ps range, while that of the exciplex formed with nucleic acids lies in the nanosecond time domain (1-3 ns).

Highly efficient exciplex formation has also been found between **2** with adenine-containing poly-(dA) and cytosine-containing oligo$(dC)_9$.[63] Since adenine has no exocyclic C=O group, one of its basic endocyclic nitrogens (N1, N3 or N7) is proposed to interact as an axial ligand with electronically excited **2** to form **2***N exciplexes. The importance of an adequate geometry for fixation of **2** to the polynucleotide for exciplex formation is also confirmed, since the exciplex is barely observed with poly(rA) and poly(rC) and even less in guanine-containing poly(dG) and poly(rG) despite of the presence of C6=O, N3 and N7 potential ligands.

The binding interactions of **1** with a self-complementary duplex DNA, $d(GCTTAAGC)_2$ reveal that the porphyrin binds to the major groove of the TTAA region.[64] Binding properties of the tri-cationic porphyrin monomer with a phenolic substituent at the periphery and the porphyrin dimer conjugated with hydrophilic triethylene glycol were investigated by Kim and co-workers.[65] The spectral properties of the polynucleotides and porphyrin monomer were the same as **1**, indicating that the substitution at one peripheral pyridiniumyl ring did not affect the binding mode. Interaction of porphyrin dimer with poly$(dG\text{-}dC)_2$

indicates that one of the porphyrin moiety of the dimer intercalate initially and than the other one also intercalate consecutively within a few hours, on the other hand with poly $(dA\text{-}dT)_2$ the porphyrins are stacked along the polynucleotide stem even at a very low [porphyrin]/[DNA base] ratio. All these results collectively suggest that porphyrin moiety tilts strongly relative to the polynucleotide helical axis.

Verchere-Beaur *et al*. have investigated binding of tri-cationic amino acid derivatized porphyrins (**15**) to a variety of natural and synthetic DNAs.[66] The studies indicate that the intercalating efficiency of amino acid porphyrin derivatives are less than that of **1** perhaps due to the presence of only three positive charges on the porphyrin ion and/or an increased specificity toward specific DNA sequences arising from amino acid linkage. The same group has also reported the synthesis of copper pyridinium group (which can hydrolyse phosphodiester bonds) appended metalloporphyrins (**16** and **17**) and their interactions with DNA.[67] They showed that these porphyrins interact with DNA via external association and intercalation.

Meunier and co-workers have shown that **5** exerts good affinity for nucleic acids and is capable of oxidizing the sugar C-H bonds of the deoxyribose units, resulting in efficient DNA cleavage.[68] The same group also has synthesized a variety of porphyrins and investigated their binding and/or cleaving abilities of DNA.[69-75] For example, oligonucleotides conjugated to a tri-cationic manganese(III) porphyrin complex have been synthesized and their DNA cleaving ability relative to **5** is analysed. The studies indicate that the oligonucleotide conjugated porphyrin is a highly efficient artificial endonuclease which is able to hydroxylate C-H bonds of DNA sugars at nanomolar concentrations.[76]

Meunier and co-workers have also synthesized a conjugate molecule by associating a tri-cationic metalloporphyrin motif to Hoechst 33258 (H 33258) (**18** and **19**), a DNA minor groove binding dye known for its selective affinity for AT tracts.[77,78] The Gel-electrophoresis cleavage experiments support strong and selective interaction of the metalloporphyrin-dye hybrid with DNA and allow an estimate of 10 basepairs (bp) as an average size for the affinity site of an isolated

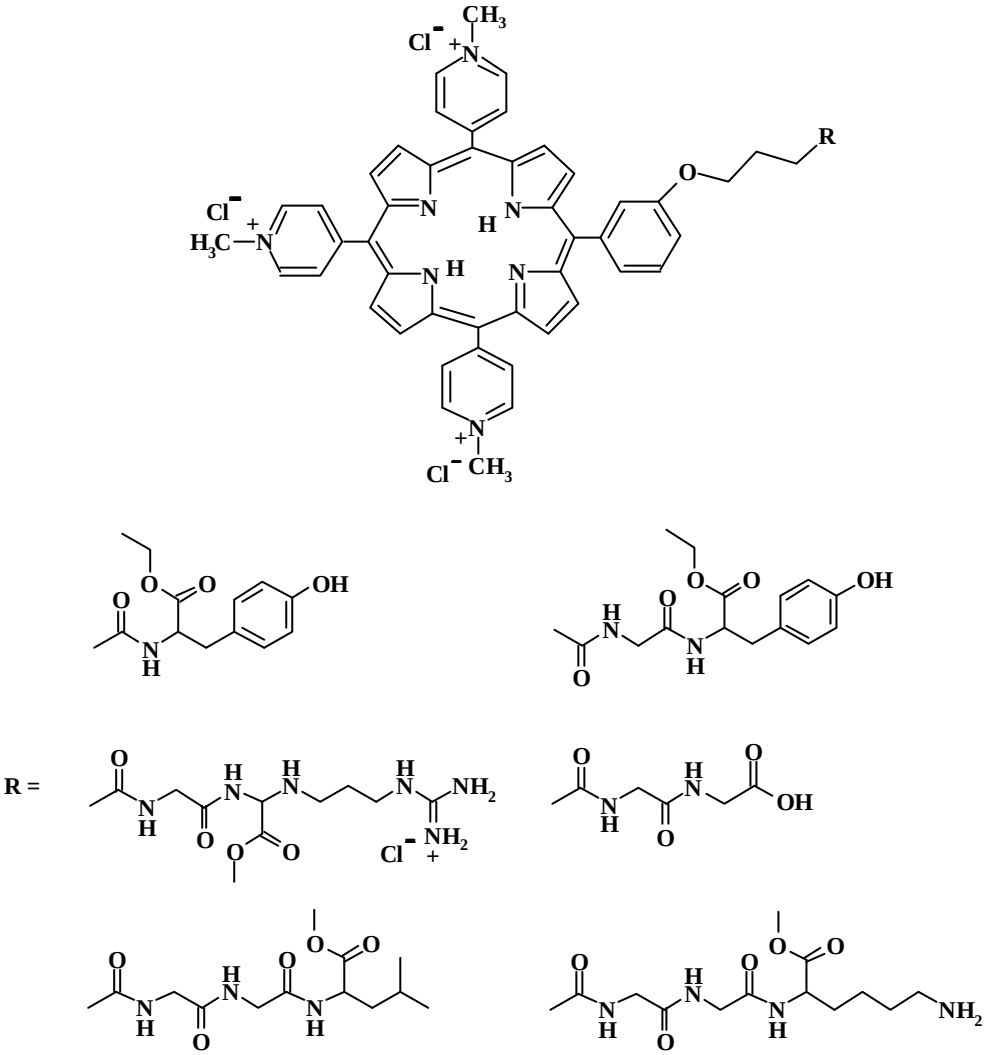

15

conjugate molecule. Binding studies indicated a preferential interaction of only the H33258 moiety with DNA (with the porphyrin entity pushed out of the groove) for higher concentrations of H33258 conjugate and self-aggregation of the H33258 conjugate all along the DNA strand in a nonselective mode for the highest concentrations.

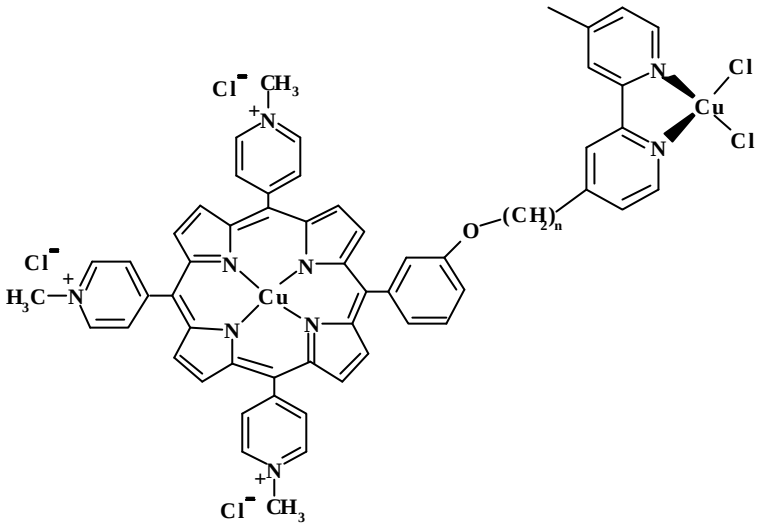

n = 5 (**16**), 9 (**17**)

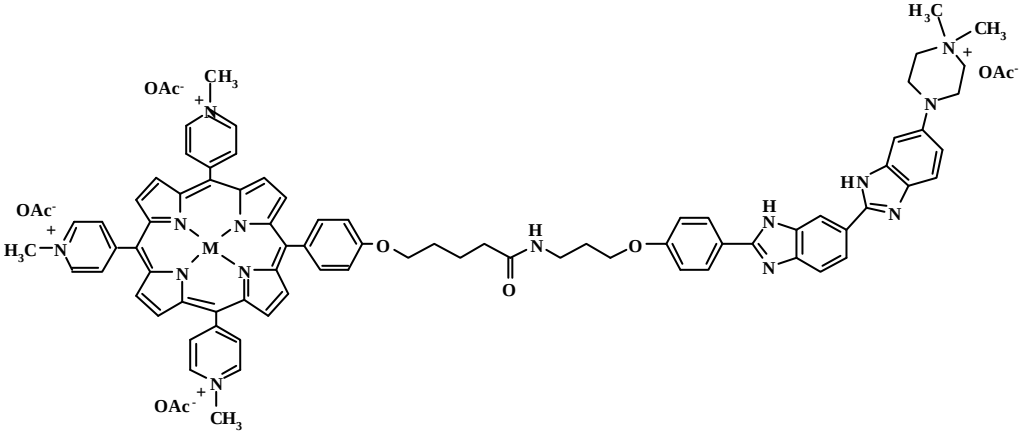

M = Mn (III) (**18**), Ni (II) (**19**)

A cationic manganese(III) porphyrin-peptide nucleic acid (PNA) (**20**) conjugate has been prepared to cleave a double-stranded DNA target.[79] Cleavage experiments were performed with a 247-base pair restriction DNA fragment containing a 10-base pair homopurine binding target for the PNA. Oxidative activation by **20** leads to sequence specific, 3′-staggered cleavage of both DNA strands near the strand displacement junction. Further the porphyrin **20** binds over 100-fold better to double-stranded DNA compared to the native PNA.

Several structurally modified metalloporphyrin-oligonucleotide conjugates have been synthesized in order to find out the most efficient compound for *in vitro* DNA cleavage.[80] The nature and the length of the tether were modulated, the

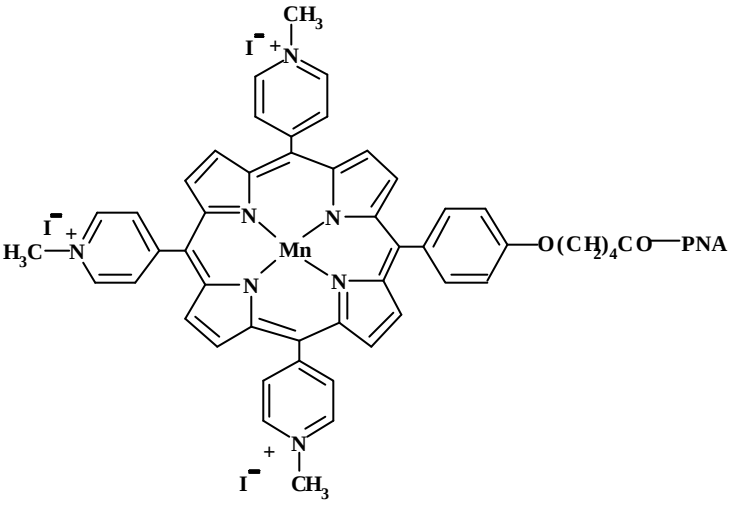

PNA = TTJTTJTTTT-(ado)$_n$-TTTTCTTCTT-NH_2

J = pseudo isocytosine

Ado = 8-amino-3,6-dioxaoctanoyl[-$NH(CH_2CH_2O)_2CH_2CO$-]

20

metalloporphyrin entity was modified (metal and ligand) and different ways of activation of the metalloporphyrin were assayed. It has been noticed that the location of the peptidic bond within the linker could greatly affect the cleavage

efficiency of the different conjugates. The most efficient conjugate for oxidative DNA cleavage was a manganese(III) tetracationic porphyrin-oligonucleotide.[81]

Czuchajowski and co-workers have synthesized H-phosphonate derivative of tri-cationic porphyrin (**21**) and the conjugates were photoactivated in the presence of the target 22-mer and 16-mer oligonucleotides. Photoactivation of porphyrin-oligonucleotide conjugates resulted in site-specific DNA modification characterized by a main reaction site size of ~5 bases.[82]

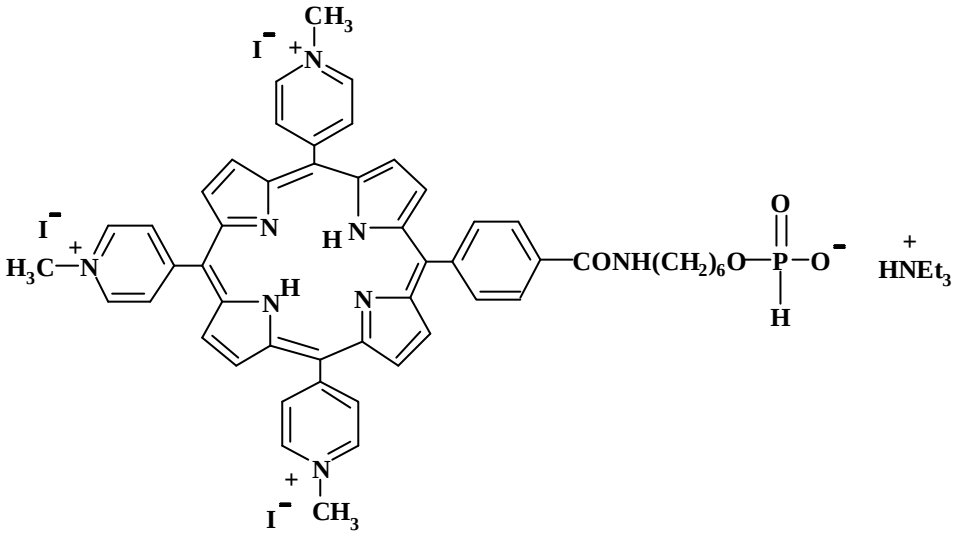

21

A series of porphyrins with mono- and disubstituted cationic substituents introduced at various peripheral positions (**22**-**29**) are synthesized and investigated by Pandey and co-workers for their ability to bind and cleave DNA in the presence of light.[83] The metalloporphyrins **26** and **29** bind to DNA via intercalation, which is in contrast to the previously reported outside-binding mode for **7**. Except the monocationic porphyrin **22** and Ni(II) dicationic porphyrin **27**, all the other porphyrins were efficient photocleavers of DNA. The DNA

photocleavage characteristics of this series of cationic porphyrins were found to depend on the structural characteristics of the porphyrins such as (a) length of the side chain of the cationic substituents (**23** *vs* **25**), (b) the position of the side chain on the porphyrin ring (**25** *vs* **28**) and (c) the presence of the chelating metal in **24**, **26** and **29** as compared to the nonmetallo porphyrins **23**, **25** and **28**, respectively.

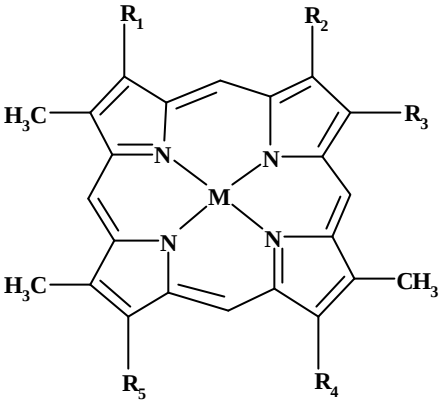

R_1= H, R_2 = CH_3, R_3 = –CH=CH-CH_2-$N^+(CH_3)_3I^-$, R_4 = R_5 = $(CH_2)_2CO_2CH_3$, M = 2H **(22);** R_1 = R_3 = –CH_2-$N^+(CH_3)_3I^-$, R_2 = CH_3, R_4 = R_5 = $(CH_2)_2CO_2CH_3$, M = 2H **(23);** R_1 = R_3 = –CH_2-$N^+(CH_3)_3I^-$, R_2 = CH_3, R_4 = R_5 = $(CH_2)_2CO_2CH_3$, M = Zn(II) **(24);** R_1 = R_3 = –CH=CH-CH_2-$N^+(CH_3)_3I^-$, R_2 = CH_3, R_4 = R_5 = $(CH_2)_2CO_2CH_3$, M = 2H **(25);** R_1 = R_3 = –CH=CH-CH_2-$N^+(CH_3)_3I^-$, R_2 = CH_3, R_4 = R_5 = $(CH_2)_2CO_2CH_3$, M = Zn(II) **(26);** R_1 = R_3 = –CH=CH-CH_2-$N^+(CH_3)_3I^-$, R_2 = CH_3, R_4 = R_5 = $(CH_2)_2CO_2CH_3$, M = Ni(II) **(27);** R_1 = R_4 = –CH=CH-CH_2-$N^+(CH_3)_3I^-$, R_3 = CH_3, R_2 = R_5 = $(CH_2)_2CO_2CH_3$, M = 2H **(28);** R_1 = R_4 = –CH=CH-CH_2-$N^+(CH_3)_3I^-$, R_3 = CH_3, R_2 = R_5 = $(CH_2)_2CO_2CH_3$, M = Zn(II) **(29)**

The interactions of DNA with **30** and **31** have been examined and compared with their corresponding porphyrins (**8** and **32)** by Dabrowiak *et al.*[17] The results show that the metalloporphyrins are not intercalated whereas non-

metalloporphyrins having four freely rotating meso-aryl groups intercalate between the base pairs of DNA. In the presence of $KHSO_5$, the cobalt(III) porphyrins cleave closed circular PM2 DNA in a single strand manner. A kinetic analysis of the cleavage data revealed that cleavage rates are in the order of **8** > **30** > **31** with the difference being due to different DNA affinities rather than differences in cleavage rate-constants.

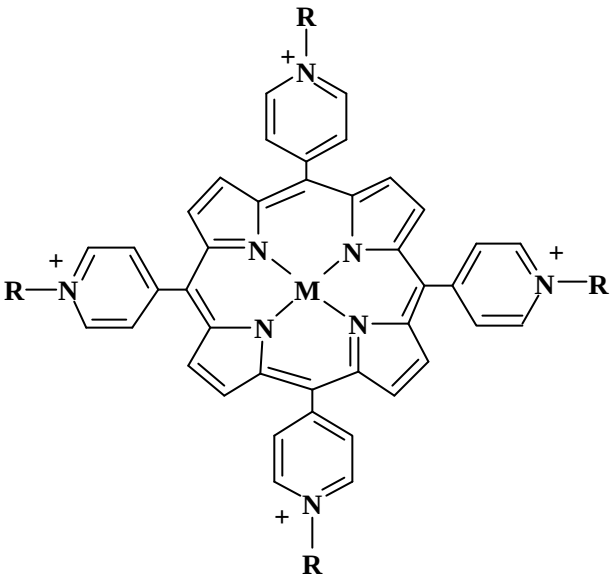

M	R	counterion
Co(III)	$-(CH_2)_3-CH_3$ (**30**)	$4BF_4^-$
Co(III)	$-(CH_2)_7-CH_3$ (**31**)	$4Cl^-$
2H	$-(CH_2)_3-CH_3$ (**32**)	$4BF_4^-$

Thirty-three free-base/metallo porphyrins corresponding to the general formula *[meso-(N*-methyl-4(or 3 or 2)-pyridiniumyl)$_n$(aryl)$_{4-n}$]porphyrinato(M), (M = 2H**,** Cu(II) or Fe(III)Cl) (**33**) with n = 2-4, have been synthesized and characterized by Mansuy and co-workers.[84] Studies of porphyrin-DNA

interactions showed that not only the tetracationic, but also the corresponding tri- and dicationic porphyrins were able to intercalate into CTDNA. The cis dicationic meso-bis(N-methyl-2-pyridiniumyl)diphenylporphyrin, which involved only two freely rotating meso-aryl groups in a cis position, was also able to intercalate. The other porphyrins, which involved either zero, one or two trans freely rotating meso-aryl groups, could not intercalate into DNA. These results show that only half of the porphyrin ring is necessary for intercalation to occur.

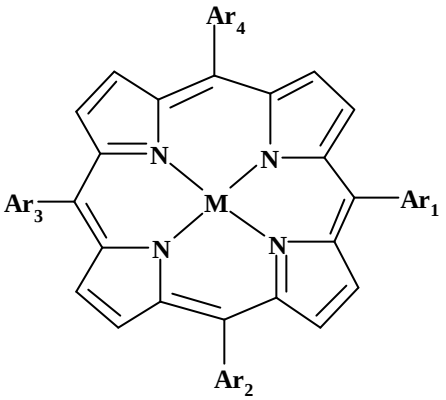

33

To target selectively the major groove of double-stranded B-DNA, Perree-Fauvet and co-workers have designed and synthesized a bis(arginyl) conjugate of a tri-cationic porphyrin (**34**).[85-87] The theoretical results indicate preferential binding to a sequence encompassing the palindrome GGCGCC encountered in the primary binding site of the HIV-1 retrovirus. Spectroscopic studies carried out on the complexes with poly(dG-dC) and poly(dA-dT) and a series of oligonucleotide duplexes having either a GGCGCC, CCCGGG or TACGTA sequence indicate intercalation of the porphyrin in poly(dG-dC) and all the oligonucleotides. The melting temperature of the oligonucleotides having the GGCGCC sequence was increased whereas the melting temperature of sequences having CCCGGG or

TACGTA in place of GGCGCC was unaltered. This indicates a preferential binding of BAP to GGCGCC, consistent with the theoretical predictions. IR spectroscopy on d(GGCGCC)$_2$ indicated that the guanine absorption bands were shifted by the binding of BAP, indicative of the interactions of the arginine arms in the major groove.

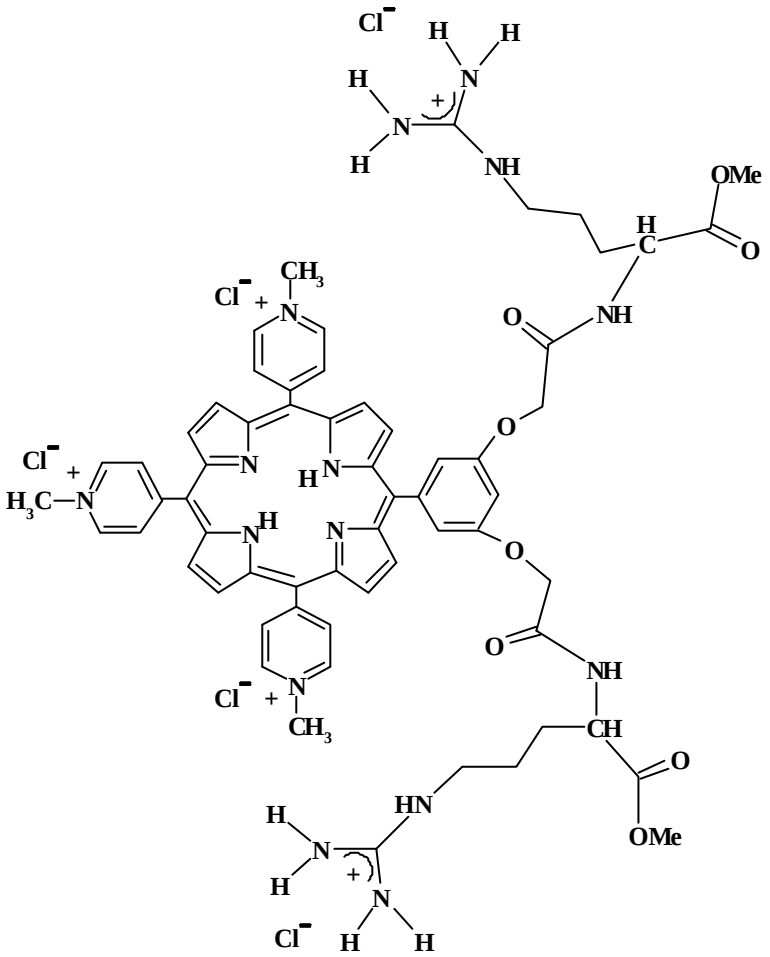

34

Organocobalt derivatives of tetracationic water-soluble porphyrins have been synthesized and their binding to CTDNA and to the synthetic DNA polymers, [poly(dA-dT)]$_2$ and [poly(dG-dC)]$_2$ was studied by Marzilli *et al.*[88]

The studies showed that the porphyrin are outside binders. Binding to all the DNA polymers, the Soret bands exhibit blue shifts suggesting that the $[CH_3Co(por)]^{4+}$ cations, particularly $[CH_3CoTMAP]^{4+}$, become five coordinate on DNA binding which was a first good evidence for the presence at equilibrium of five-coordinate $CH_3Co(III)(N4)$ forms in water.

Pasternack and co-workers have reported the extended, organized assemblies of trans-bis(N-methylpyridinium-4-yl)diphenylporphine and its copper(II) derivative (**35** and **36)** on DNA.[26,89-94] Experiments reveal extended porphyrin aggregates form remains dispersed on the DNA.

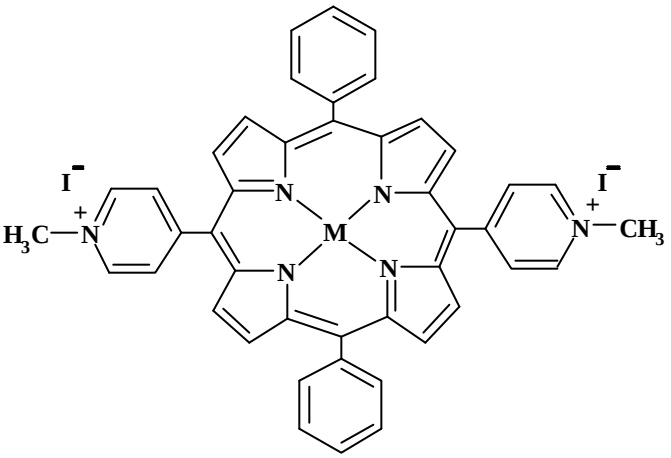

M = 2H (**35**), Cu(II) (**36**)

McMillin and co-workers have reported a surprising result that dicationic porphyrins (**37-40**), which are sterically less demanding, bind with DNA only through intercalation irrespective of the base pairs.[95,96] However, for **38** and **40** the binding constants are smaller because uptake requires the loss of an axial ligand.[96] Sequences that contain mainly adenine-thymine base pairs easily depart from the canonical B-form DNA structure and generally accommodate bulky porphyrins in external binding sites. But intercalation becomes the preferred mode

of binding even in [poly(dA-dT)]$_2$, since the steric requirements are so minimal with **37** and **39**. The intercalated form of the **41** is less stable, probably because of frontal strain associated with the (*N*-methyl)pyridinium-2-yl groups. Further the studies carried out by McMillin group with **38** reveal that the adduct formation depends even on the loop sequence present in the hairpin substrates.[97]

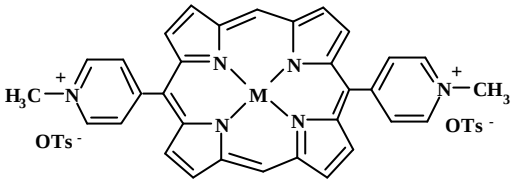

M = 2H (**37**), Zn(II) (**38**)

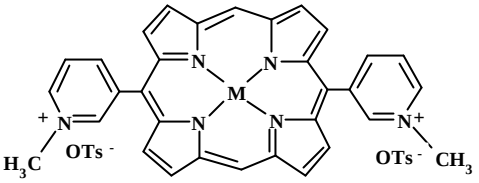

M = 2H (**39**), Zn(II) (**40**)

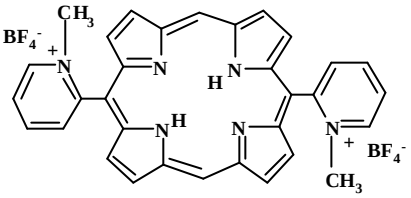

M = 2H (**41**)

Uno and co-workers have synthesized a series of cationic bis-porphyrins with various lengths of diamino alkyl linkage and analysed their photo-induced DNA cleaving ability.[98] The cationic bis-porphyrins were found to self-aggregate by the formation of an intermolecular dimer. Outside self-stacking on the DNA surface has been assigned as mode of binding since conservative-type CD spectra of the bis-porphyrins were induced in the Soret region on binding to calf thymus DNA. Their photonuclease activity using plasmid DNA decreased as the number of hydrocarbons increased which could be correlated with their tendency for dimerization. The same group also has prepared Zinc(II) complexes of cationic bis-porphyrins to improve the less DNA photocleavage activities of the metal-free

bis-porphyrins linked with a series of aliphatic diamines.[99] The zinc(II) insertion into the metal-free cationic bis-porphyrins completely removed their self-aggregation properties, most probably due to steric hindrance between axial ligands of zinc(II) chromophores of the cationic bis-porphyrins. The DNA photocleavage activities of the zinc(II) complexes were fully enhanced, which were three times larger than that of **1**. Genady *et. al*. have synthesized cationic porphyrin dimers (liked via alkylation of the nitrogen atoms of 4,4′-bipyridine and 1,2-di-(4-pyridyl)ethane) and proved that they can interact and cleave the DNA.[100]

Tjahjono and co-workers have synthesized cationic porphyrins bearing five-membered rings at the meso-positions (**42** and **43**) and studied their interaction with CTDNA.[101] The spectroscopic results revealed that **42** binds outside to the minor groove of CTDNA while **43** intercalates into CTDNA. The same group has also studied the interaction of transition metal complexes (**44**-**47**) with CTDNA. Metalloporphyrins **45** and **46** intercalate into the 5'GC3' step of CTDNA whereas **44** is bound edge-on at the 5'TA3' step of the minor groove of CTDNA.[102] The zinc(II) complex (**47**) is bound face-on at the 5'TA3' step of the major groove of CTDNA. These results have revealed that the kind of central metal ions of metalloporphyrins influences the binding characteristics of the porphyrin to DNA.

A series of DNA binding tri-cationic platinum(II) conjugates (**48**-**51**) have been synthesized with different spacer ligands and used for appropriate coordination to platinum(II) complexes.[103] Compound **50** exhibited *in vivo* antitumor activity superior to *cis*-platin against the leukemia L1210 cell line.

Marzilli co-workers have observed extensive self-stacking along the DNA surface during the interactions between the water-soluble tentacle porphyrin **52** and DNA (CTDNA, poly $(dA\text{-}dT)_2$ and poly $(dC\text{-}dG)_2$).[104-107]

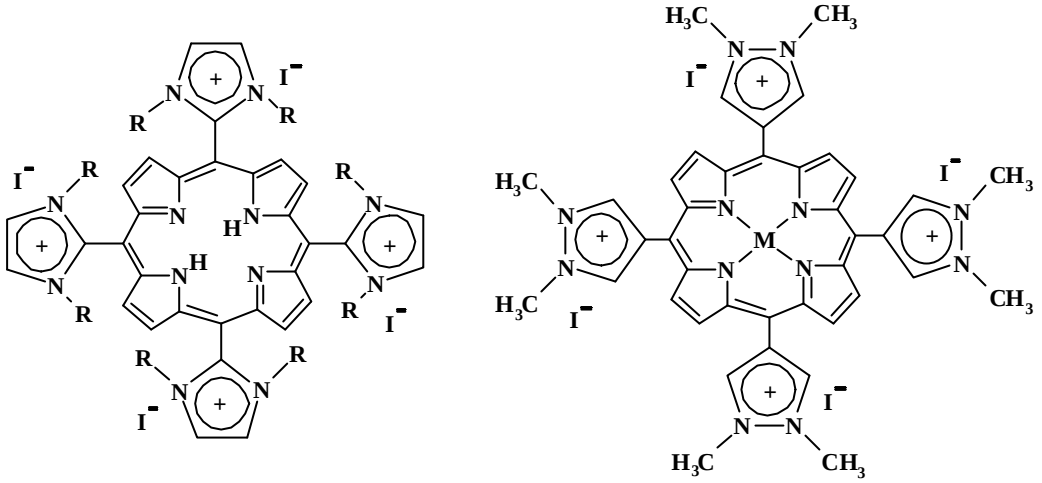

R = -CH_3 (**42**) M = 2H (**43**), Mn (III) (**44**), Ni(II) (**45**), Cu(II) (**46**), Zn(II) (**47**)

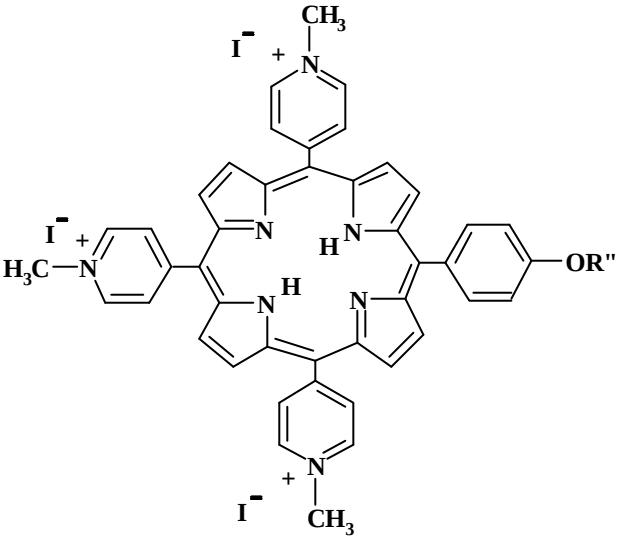

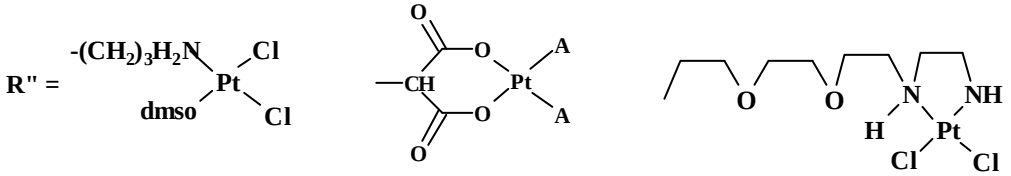

48 A = dmpda (**49**), dach (**50**) **51**

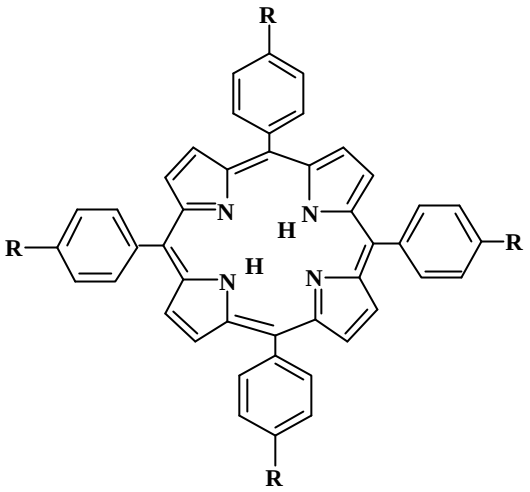

R = -$OCH_2CH_2CH_2N^+(Me)_3$ Cl^- (**52**)

Meunier co-workers have synthesized the ellipticene appended cationic porphyrins and investigated the interaction with DNA as well as the cytotoxicity of leukemia cell.[108] The studies reveal that these molecules show high affinity constant for double stranded DNA. A few other cationic porphyrin interactions with DNA also have been investigated using Raman spectroscopy.[109,110] A series of alkylamido and acrylamido derivatives of porphyrins have been synthesized and their interaction with DNA and antibacterial activity has been reported by Czuchajowski.[111,112] EPR technique has been employed by few groups to investigate the interactions of cationic porphyrins with DNA.[113-115] Binding and photo physical properties of **1** and **7** bound to DNA also have been studied.[116-119] Energy and electron-transfer processes involving palladium porphyrins bound to DNA has been reported by Harriman group.[120]

1.2 Photodynamic therapy

Photodynamic therapy (PDT) is a newly introduced modality for treating cancer in which a photosensitizing agent acts against malignant tumor under the

influence of light.[121,122] PDT have been used to treat cancers of the lung,[123] gastrointestinal tract,[124,125] the head and neck region,[126-128] bladder,[129] prostate,[130] and nonmelanoma skin cancers and actinic keratosis.[131] PDT were employed in cancerous treatments such as psoriasis[132,133] and age-related macular degeneration (ARMD).[134-136] Ex *vivo* procedures have also been examined for treating leukemia patients bone marrow and hematopoietic stem cell grafts.[137] Successful treatment of atherosclerosis or arterial plaque with PDT has been reported.[138]

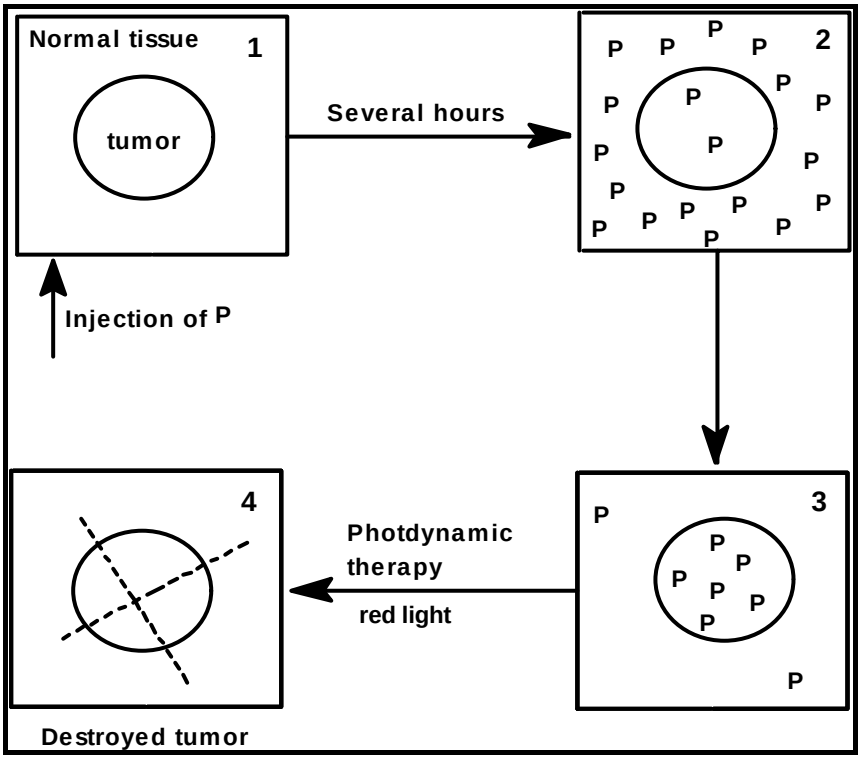

Fig. 1.2.1 Schematic representation of the action of PDT in cancer therapy

The technique of PDT in cancer therapy involves the intravenous injection of a photosensitizer (P), which over a period of time, is selectively retained by the neoplastic tissue. Subsequent irradiation with visible light using a laser generates

singlet oxygen (or other cytotoxic species) within the tumour, ultimately leading to cell necrosis and tumor regression.[139] A diagrammatic representation of the action of PDT in cancer therapy is shown in Fig. 1.2.1.

Two different kinds of mechanisms, Type I and Type II, have been proposed for the PDT action and in both the mechanisms involve the formation of excited triplet sensitizer (^3S), where S is the sensitizer.

$$S \xrightarrow{hn} {}^1S \qquad (1.2.1)$$

$$^1S \xrightarrow{ISC} {}^3S \qquad (1.2.2)$$

Type I

$$^3S + R \longrightarrow S^+ + R^- \qquad (1.2.3)$$

$$^3S + R \longrightarrow S^- + R^+ \qquad (1.2.4)$$

Type II

$$^3S + {}^3O_2 \longrightarrow S + {}^1O_2 \qquad (1.2.5)$$

$$^1O_2 + \text{biomolecules} \longrightarrow \text{Products} \qquad (1.2.6)$$

In the Type I mechanism, ^3S interacts directly with the substrate molecule (R), either by hydrogen atom abstraction or by electron transfer to produce the reactive radical species. These radicals may interact with oxygen to produce cytotoxic products such as $O_2^{\bullet-}$, $OH^{\bullet}$, H_2O_2 etc. In the Type II mechanism, ^3S reacts with the ground state triplet oxygen producing singlet oxygen, which is a highly reactive species that selectively attacks electron rich substrates to give peroxides or other oxidized species. Recent *in vitro* and *in vivo* studies indicate

that generation of singlet oxygen is a crucial step in the PDT cytotoxicity.[139] Fig 1.2.2, a modified Joblanski diagram for a typical photosentizer, outlines the principal photophysical processes of interest. The importance with regard to PDT is that the excited photosensitizer can undergo the nonradiative process of inter-system crossing (ISC, route 4, Fig 1.2.2). This is a spin-forbidden process, as it requires spin inversion, thereby converting the photosensitizer to a triplet state (T_1). Any 'forbidden pathway' is the less likely than an allowed process, but a good photosensitizer undergoes the 'forbidden' ISC pathway with very high efficiency. The molecule can relax from the triplet state via at least two pathways: radiatively by phosphorescence and non-radiatively by spin exchange with another triplet state molecule.

Phosphorescence involves a spin inversion and thus is also spin-forbidden, imposing a relatively long lifetime on the triplet state. This allows interaction of the excited photosensitizer with molecules in the vicinity of the sensitizer. One such interaction is spin exchange (also corresponding to energy transfer) with triplet oxygen, which generates the highly reactive singlet oxygen species. (route 6, Fig. 1.2.2). Singlet oxygen is a very reactive species with a lifetime in water of roughly four microseconds. It undergoes several reactions with biological substrates such as oxidation and cycloaddition, all of which are quite disruptive to biological processes. As a result, the efficiency of transferring the energy of the absorbed light from the triplet state of the photosensitizer to triplet oxygen and thereby generating singlet oxygen, defined as the singlet oxygen quantum yield.

The ideal photosensitizer should meet the following requirements: It should be chemically pure and of known composition, have minimal dark toxicity and only be cytotoxic in the presence of light, be preferentially retained by the target tissue, be rapidly excreted from the body to provide low systemic toxicity, have a high quantum yield for the photochemical event (which is often the

generation of singlet oxygen ($^1O_2$) or superoxide (O_2^-)) and have strong absorbance with a high extinction coefficient in the 600-800 nm range where tissue penetration of light is at a maximum and where the wavelengths of light are still energetic enough to produce singlet oxygen.[140]

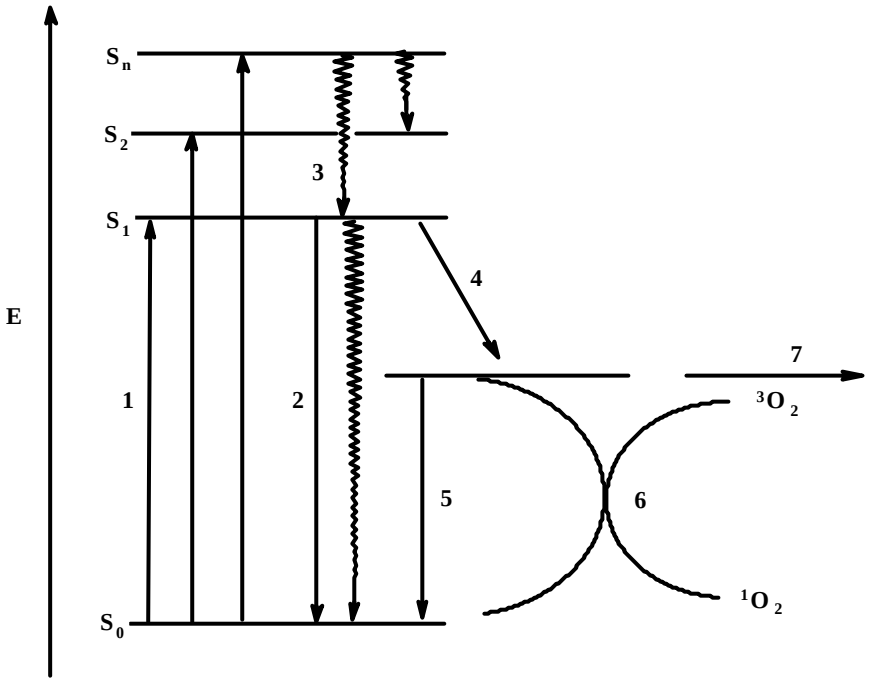

1. Absorption of light, 2. Fluorescence, 3. Internal conversion, 4. Inter-system crossing. 5. Phosphorescence, 6. Singlet oxygen photoprocess (Type II photo process), 7. Hydrogen or electron transfer (Type II photo process-photobleaching)

Fig. 1.2.2 Modified Joblanski diagram for a typical photosensitizer

Porphyrins and related compounds are the best-known PDT photosensitizers since they possess most qualities that are expected for an ideal PDT photosensitizer.[140] Among the first generation photosensitizers,

hematoporphyrin derivative (HpD) (**53**) and its commercial variant, photofrin II® have been used for clinical testing.[139,141] HpD is a complex mixture of hematoporphyrin, (Hp), hydroxyethylvinyldeuteroporphyrin (Hvd) and protoporphyrin together with dimers and higher oligomers of these porphyrins joined with ether or ester linkages. photofrin II® is a purified preparation of the active fraction of HpD. Despite of the utility of photofrin II important disadvantages are: (i) it is a complex and variable mixture of porphyrin oligomers linked with ether, ester or carbon-carbon linkages, which are not stable either during storage or after administration, (ii) it has only one weak absorption peak in the relevant part of the spectrum at about 630 nm, but absorbs much more strongly at shorter wavelengths in the visible and near UV regions and (iii) it is not very selective and causes skin photosensitivity.

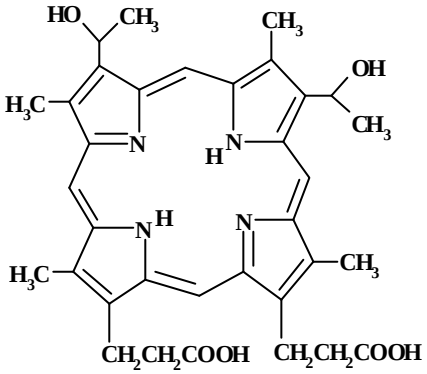

53

The tetra(p-sulfonatophenyl)porphyrin ($TPPS_4$), an excellent producer of $^1O_2$ has very good water solubility. $TPPS_4$ is membrane permeable, displays lysosomal accumulation in cells, accumulates in tumors, and is effective both *in vitro* and *in vivo*, but its clinical ambitions ended after reported neurotoxicity in mice exposed to high doses of $TPPS_4$.[142,143]

Recent work with porphyrin derivatives suggests some novel approaches to porphyrin delivery. Dendrimeric porphyrin derivatives with a porphyrin ring as the dendrimer core have been prepared[144] and touted as effective photosensitizers *in vitro*.[145] Tetraphenylporphyrin derivatives bearing amino acids, peptides or diamines have demonstrated excellent surface recognition for potassium channels.[146] These two different classes of porphyrin molecules suggest different ways of targeting porphyrin-based photosensitizers, which may be developed in the future.

Substituent changes in the meso positions of the porphyrins have little impact on the wavelengths of absorption of the porphyrin chromophore. Longer-wavelength-absorbing porphyrins (band I absorption maxima of ~665 nm) have been prepared by substituting a chalcogen atom (S or Se) for an NH at the 21-position of the porphyrin ring.[147,148] Such molecules are called core-modified porphyrins, and sulfonated analogues of the 21-thia- and 21-selenaporphyrins have been evaluated as photosensitizers for PDT.[149-151] Replacing a second core hetero atom with S or Se gives 21, 23-core-modified porphyrins with even longer wavelength band I absorption maxima, 695-700 nm.[152,153]

5-Aminolevulinic acid (**54**, ALA) is a naturally occurring amino acid that is a precursor to protoporphyrin IX (**55**, PpIX).[154-156] PpIX is actively under investigation as a photosensitizer for PDT. PpIX is converted into heme through the action of the enzyme ferrochelatase. Skin photosensitization with PpIX is limited to 1-2 days, which offers a distinct advantage relative to PDT with photofrin II. The topical administration of **55** and its derivatives has also been found to be effective at producing PpIX on various surface lesions.

Phthalocyanines absorb very strongly in the red region of the spectrum with absorption maxima 670-780 nm and greater ε values. The zinc, aluminum and silicon phthalocyanines are efficient

generators of singlet oxygen with long-lived triplet states and have been found to be useful photosensitizers for PDT.[157-161]

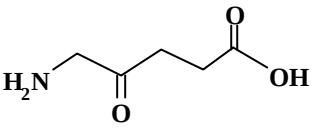

ALA (**54**)

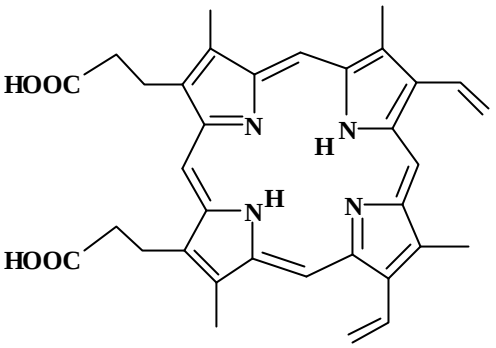

Protoporphyrin IX (**55**)

Reduction of a pyrrole double bond on the porphyrin periphery gives the chlorin core, and further reduction of a second pyrrole double bond on the chlorin periphery gives the bacteriochlorins. Both of these classes of molecules have band I absorption maxima at longer wavelengths (λ_{max} = 650-670 nm for chlorins and λ_{max} = 730-800 nm for bacteriochlorins) than the porphyrins and yet still remain efficient generators of $^1O_2$.[162]

The naturally occurring chlorin e_6 was the first evaluated chlorin which has a band I absorption maximum of 654 nm with a value of ε near 40,000 $M^{-1}cm^{-1}$. Unfortunately, chlorin e_6 showed long-term skin photosensitization[140] and requires high doses to be effective. In contrast alkyl esters of chlorin e_6 and its derivatives such as mono-L-aspartyl chlorin e_6 have been found to be more bioavailable and more effective at lower doses. Benzobacteriochlorin derivatives and their metal derivatives show limited skin photosensitization.[140,163]

Another class of synthetic porphyrin-related molecules is the core-expanded porphyrins or texaphyrins.[164] These molecules have five N atoms in the expanded core, which can accommodate metals with larger ionic radii such as

lutetium and gadolinium. The metalated texaphyrins have unusual biological properties, which make them of interest for PDT and radiation therapy.[165] Lutetium texaphyrin has a long wavelength absorption maximum of 732 nm with ε of 42,000 $M^{-1}cm^{-1}$ and is an efficient generator of $^1O_2$.[140]

1.3 Donor-Acceptor (D-A) systems based on axially substituted porphyrins

Donor/acceptor subunits can be connected at the axial sites of a metallo/metalloid (M) porphyrin *via* M–N, M–O etc. bonds characterized by either coordinative or covalent interactions.

1.3.1 Basic theory of PET and EET reactions

Molecules, upon photoexcitation become powerful donors or acceptors and hence can be involved in electron and/or energy transfer reactions. Photoinduced electron transfer reaction has attracted the interest of chemists in many respects that include synthesis of organic molecules, development of solar energy storage/conversion systems and understanding of natural/artificial photosynthetic systems.[166-169] Similarly, excitation energy transfer reactions are also important from the point of view of photosynthetic antenna function,[170] polymer photophysics,[171] molecular electronic devices etc.[172,173] Equally significant is the theoretical understanding of the electron and energy transfer reactions and, this has added further impetus to the study of these important processes.[174-179] Fig. 1.3.1 depicts pathways through which electron and energy transfer processes can occur. In electron transfer, the excited state (*) can act either as a donor (D) or as an acceptor (A) whereas in energy transfer, the excited state will always be a donor.

Marcus theory of electron transfer process provides a convenient way of discussing certain key aspects involved in the PET reactions.[174-177] According to

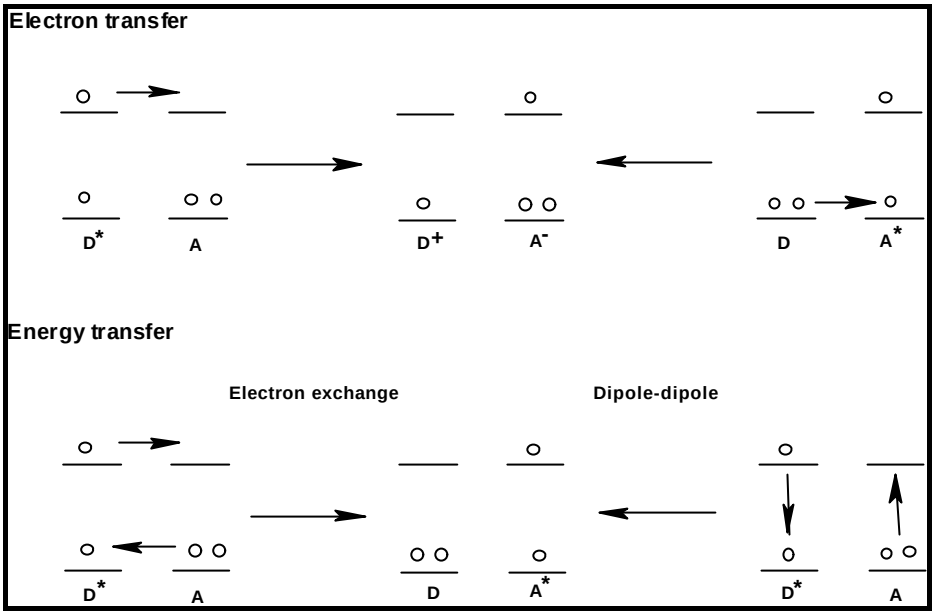

Fig. 1.3.1 Electron and energy transfer involving excited donor (D*) and acceptor (A*) systems.

this theory, the rate constant for electron transfer (k_{ET}) is given by the expression

$$k_{ET} = \frac{k_{el}\, \nu_n \exp(-\Delta G^0 + \lambda)}{4\, k_B\, T} \qquad (1.3.1).$$

Here, k_{el} is the electronic transmission coefficient, ν_n is the frequency of nuclear motion through the transition state, ΔG^0 is the standard Gibb's free energy change for the overall ET reaction, λ is the reorganization energy needed to orient the initial complex to have a suitable configuration for electron transfer, k_B is the Boltzman's constant and T, the absolute temperature. $\Delta G^{\#}$ is the free energy of activation, and it is related to ΔG^0 and λ, the reorganization energy, by the expression

$$\Delta G^{\#} = \frac{(\lambda + \Delta G^{0})^2}{4\lambda} \qquad (1.3.2).$$

For exoergic reactions, when $-\Delta G^0 < 0$, k_{ET} increases with increasing exoergicity. It reaches a maximum at $-\Delta G^0 = \lambda$ and decreases again when $-\Delta G^0 > \lambda$. This region of decrease of k_{ET} with respect to increasing exoergicity is termed as the "Marcus inverted region".

Electronic energy transfer reactions can, in principle, operate by two mechanisms:

(i) Dipole-dipole mechanism which involves mutual Columbic interaction of electrons (Forster's theory) [178]

(ii) Exchange mechanism which involves mutual exchange of electrons (Dexter's theory) [179]

Forster has developed an expression for the rate of electronic energy transfer due to dipole-dipole interaction in terms of the experimentally obtainable parameters. According to this theory, the rate constant for energy transfer, $k_{EnT,}$ is given by eqn. 1.3.3.

$$k_{EnT} = \frac{8.8x10^{-25}\kappa^2 \phi_D}{n^4 \tau_D R^6} \int F_D(\bar{\nu}) \varepsilon_A(\bar{\nu}) \bar{\nu}^{-4} d\bar{\nu} \qquad (1.3.3)$$

In the above equation, $\bar{\nu}$ is the wave number, $F_D(\bar{\nu})$ is the spectral distribution of the donor emission in quanta normalized to unity, $\varepsilon_A(\bar{\nu})$ is the molar extinction coefficient for the acceptor absorption and n is the refractive index of the solvent. κ^2 is a function of relative orientation of transition dipole moments of the donor and the acceptor. ϕ_D is the quantum yield of donor emission, τ_D is the donor emission lifetime (in seconds) and R is the distance between the donor and acceptor molecules (in centimeters).

From the photophysical point of view, the fundamental processes that originate from the singlet state are depicted in Fig. 1.3.2.

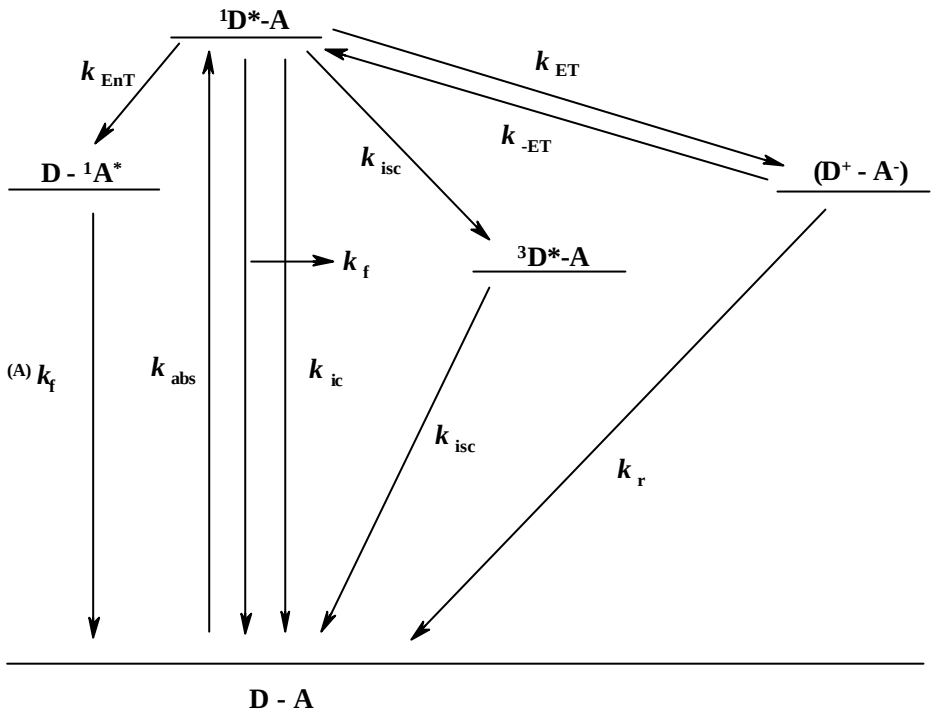

Fig. 1.3.2 Fundamental processes originating from the singlet excited state.

Here, superscripts 1 and 3 refer to the singlet and the triplet states, respectively. k_f ($^{(A)}k_f$), k_{ic}, k_{isc}, k_{ET}, k_{-ET}, k_r and k_{EnT} are the rate constants for fluorescence, internal conversion, intersystem crossing, forward electron transfer, reverse electron transfer, charge recombination and energy transfer reactions, respectively. For an efficient electron/energy transfer to occur, k_{ET} and k_{EnT} have to compete with other processes *viz*. fluorescence, internal conversion, intersystem crossing etc.

Table 1.3.1 summarizes determinants of EET and PET reactions derived from the theories of electron and energy transfer reactions as well as the processes competing with these reactions discussed above.

Table 1.3.1

Determinants of electron and energy transfer	
Electron transfer	Distance and orientation (electronic coupling, orbital overlap); Free energy change (driving force); Reorganization in D and A; Orientation polarization of medium
Excitation energy transfer	Distance and orientation (coupling of excited states); Spectral overlap of emission and absorption of D and A; refractive index of the medium.
Processes competing with electron and energy transfer	
Electron transfer	(i) Nonradiative relaxation of D* by photoisomerization and other conformational changes; Excited state proton transfer; Intersystem crossing; Chemical reactions.
	(ii) Back reaction to the ground state D-A
Excitation energy transfer	Same as (i)

1.3.2 M - O bonded D-A systems

Shimidzu and co-workers have reported a series of "wheel-and-axle" type phosphorus(V) porphyrin arrays in which porphyrin units are linked to each other *via* the central phosphorus(V) ions.[180-184] The excited state properties of a few compounds in this series of oligomers have been investigated. Singlet lifetimes of these 'wheel-and-axle' type dimers have been reported to decrease with increasing solvent polarity. The decrease in lifetime suggested the enhancement of non-radiative decay through the charge transfer (CT) state. In addition, the trimers showed strong fluorescence quenching than that of the corresponding dimers. Electrochemically synthesized D-A polymers, which contain axial oligothiophene (electron donor) and basal phosphorus(V) porphyrin (electron acceptor) subunits have also been reported.[185]

Segawa and co-workers have reported a series of center-to-edge type phosphorus porphyrin arrays in which porphyrin units are linked axially to each other *via* the central phosphorus(V) ions.[186] In these systems, the excited state charge transfer was considered to be responsible for the quenching of fluorescence. The same group has reported axially substituted dialkoxo phosphorus(V) porphyrin derivatives.[187] Photochemistry of these systems has not been investigated.

Rao and Maiya have reported aryloxo derivatives of phosphorus(V) porphyrin-based trimers and D-A systems.[188,189] While steady state fluorescence data of the former systems have been analyzed in terms of energy transfer from the phosphorus(V) porphyrin to the axial porphyrin subunits and a PET in the reverse direction, those of the latter systems has been interpreted in terms of a PET reaction from the axial aryloxo 'donor' ligands to the singlet phosphorus(V) porphyrin.

Hirakawa and Segawa have reported phosphorus(V) porphyrin-pyrene triads in which two pyrene subunits are connected to a central phosphorus(V) ion through various bridges.[190] These triads are characterized by π - π interaction between the pyrene and porphyrin moieties. As a result, emission from the photoexcited states of both the pyrene and the porphyrin subunits were quenched through energy and/or electron transfer process.

Goh and Czuchajowski have reported synthesis of novel axial dinucleoside bearing phosphorus(V) porphyrins.[191] In these complexes, phosphorus(V) porphyrin units are axially connected through the 5′-O-thymidine-3′-O bridges.

The scope of carboxylate binding by tin(IV) porphyrins and the solution geometries of the resulting complexes **(56)** have been explored using NMR spectroscopy by Hawley *et al.*[192] Sanders and co-workers have suggested the use

of ‘axial-bonding’ type tin(IV) porphyrins as NMR shift reagents and as supramolecular protecting groups.[193]

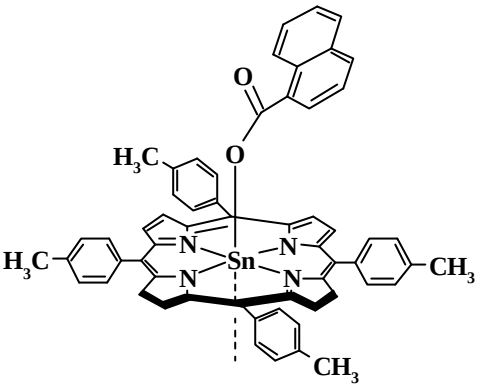

56a

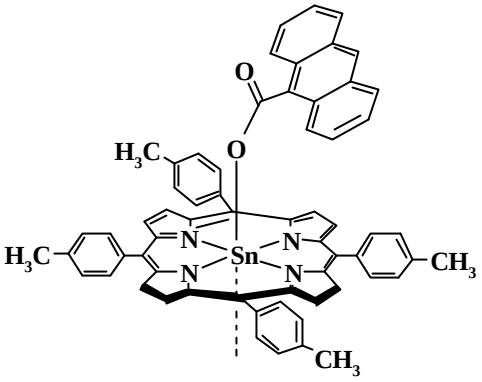

56b

In an interesting study, Webb and Sanders have reported a series of cyclic, mixed-metalloporphyrin trimers (**57**) having cavities lined with different carboxylate groups.[194] The influence of these carboxylate-lined cavities on the binding of pyridyl ligands to the ruthenium(II) centers of these hosts was investigated. The rich hydrogen-bonding environment provided by a D-quinate-lined cavity **57e** was found to enhance the binding of 4-methanolpyridine to the ruthenium(II) center.

Aluminium(III) porphyrin based ‘axial-bonding’ type dimers and trimers have been reported recently.[195] Fluorescence quantum yields and singlet state lifetimes were found to be lowered for these complexes in comparison with those of the monomeric chromophores. EET from the aluminum(III) porphyrin to the free base subunit and a PET in the reverse direction has been invoked to explain the observed fluorescence quenching.

Shiragami *et al*. reported antimony(V) porphyrin systems bearing axial aryl groups. Fluorescence spectra of (2-naphthoxy)polyoxalkoxyantimony(V) tetraphenylporphyrin complex were analyzed under the excitation of naphthoxy

and porphyrin chromophores.[196,197] The excitation energy of naphthoxy chromophore was observed to be transferred to the porphyrin moiety with nearly equal rates irrespective of methylene bridge length. The emission of porphyrin chromophore was quenched by naphthoxy chromophore with rate constants of 10^7 – 10^{10} s^{-1} depending on both the solvent used and the length of the methylene bridge. Under excitation of the naphthoxy chromophore of the triad system involving porphyrin, 2-naphthoxy and 4-methoxyphenoxy chromophores, the excited singlet state of the porphyrin chromophore generated by the energy transfer from the naphthoxy chromophore was quenched by the naphthoxy and the methoxyphenoxy chromophores *via* non-radiative processes involving electron transfer.

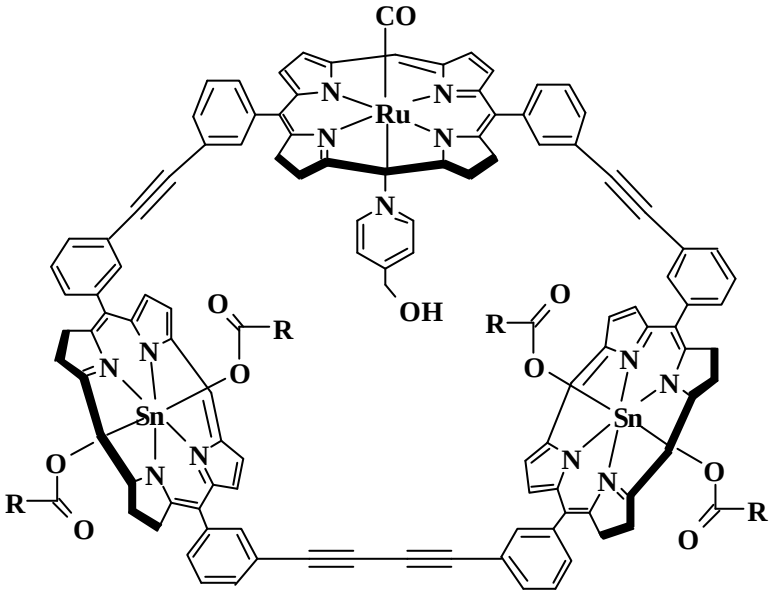

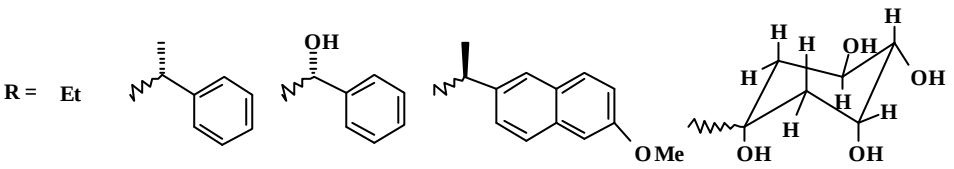

57a **57b** **57c** **57d** **57e**

1.3.3 Both M – N and M – O bond containing D-A Systems

Sanders and co-workers have reported heterometallic oligoporphyrins, **58** and **59**, using cooperative Ru – N/Zn – N and Sn – O coordination.[198-200] These oligomers were designed to exploit the complementary geometries and cooperative binding properties of tailor-made metalloporphyrin building blocks.

Recently, a photochemically-functional, axial-bonding type hybrid porphyrin trimer, **60**, has been self-assembled by an advantageous utilization of the well-known hard and soft acid-base (HSAB) principle and metal ion recognition by a ditopic ligand.[201] Steady state emission results have been interpreted in terms of a PET from the axial ruthenium(II) porphyrin to the excited state of the basal tin(IV) porphyrin.

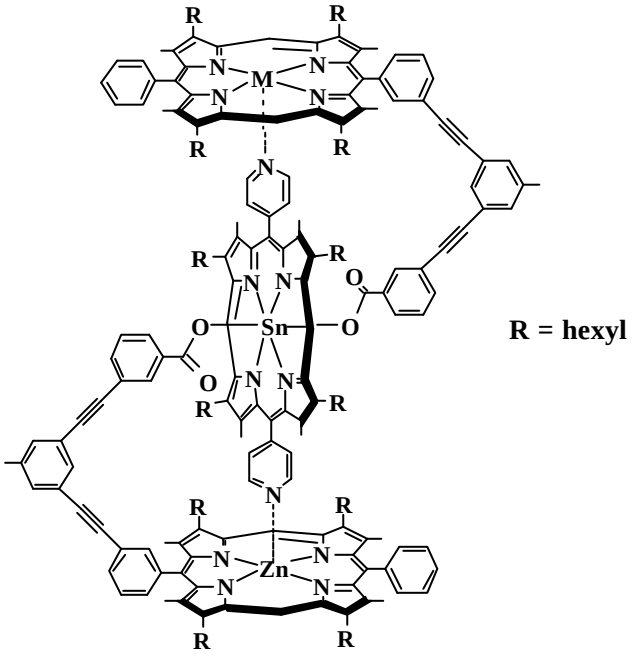

M = Zn(II) (**58a**), M = Ru(II) (**58b**)

R = hexyl

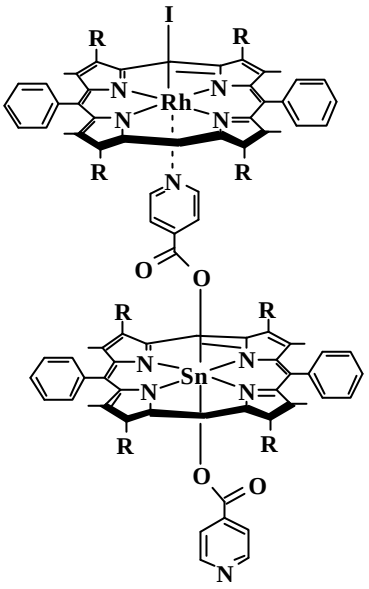

59a

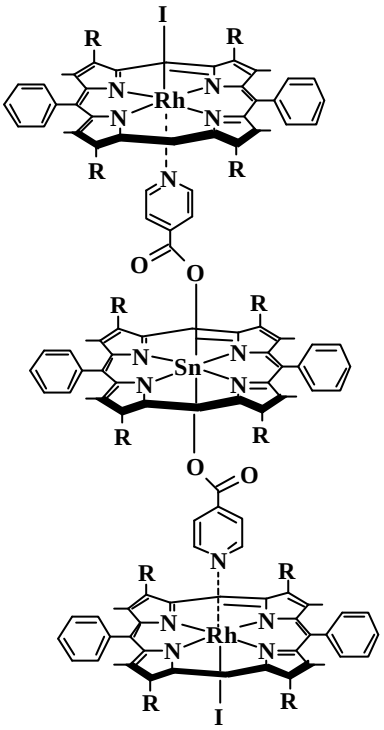

R = hexyl

59b

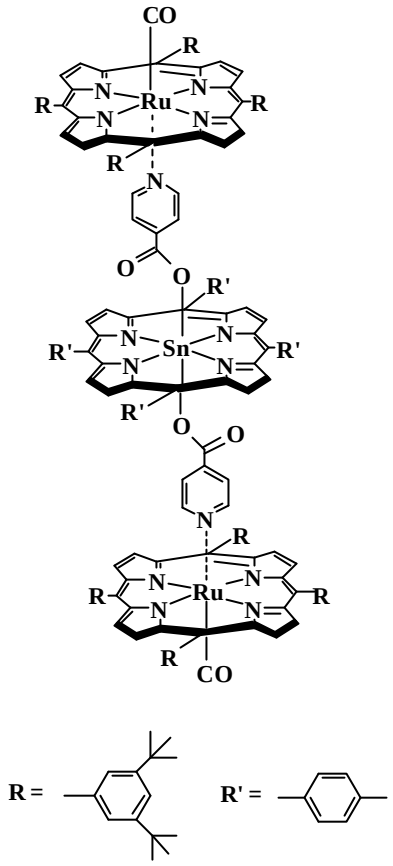

R =

R' =

60

1.4 Summary

In this chapter, recent developments in cationic porphyrins and their DNA interactions, basic principles of PDT agents and also porphyrin based D-A systems highlighting their PET and EET reactions as applicable to the subject matter of the present thesis have been reviewed.

1.5 Objectives of the present work

The primary objectives of the present work are (i) to develop a new series of tri-cationic water-soluble porphyrins and metalloporphyrins and investigate

their DNA interacting ability and (ii) to develop a series of donor acceptor (D-A) systems and address their photoinduced electron transfer (PET) and excitation energy transfer (EET) reactions. Specifically, the following systems have been explored:

i. Synthesis of nucleobase appended tri-cationic porphyrins to address their interactions with calf thymus DNA (CTDNA),

ii. Insertion of metal ion into tri-cationic porphyrins linked with adenine to monitor their binding and cleaving ability with CTDNA,

iii. Analysis of the interactions of nucleobase appended tri-cationic porphyrins and adenine appended tri-cationic Cu(II) metallated porphyrin with DNA hairpins and

iv. Synthesis of axially linked bis(aryloxo) derivatives of azo-benzene bridged tin(IV) porphyrin dimers and evaluation of their PET and EET properties.

1.6 References

1. Henderson, B. W.; Dougherty, T. J. *Photochem. Photobiol.* **1992**, *55*, 145.
2. Fiel, R. J.; Howard, J. C.; Mark, E. H.; Datta Gupta, N. *Nucleic Acids Res.* **1979**, *6*, 3093.
3. Fiel, R. J.; Munson, B. R. *Nucleic Acids Res.* **1980**, *8*, 2835.
4. Carvlin, M. J.; Fiel, R. J. *Nucleic Acids Res.* **1983**, *11*, 6121.
5. Carvlin, M. J.; Mark, E.; Fiel, R. J.; Howard, J. C. *Nucleic Acids Res.* **1983**, *11*, 6141.
6. Kelly, J. M.; Murphy, M.; McConnell, D. J.; OhUigin, C. *Nucleic Acids Res.* **1985**, *13*, 167.
7. Ford, K.; Fox, K. R.; Neidle, S.; Waring, M. J. *Nucleic Acids Res.* **1987**, *15*, 2221.

8. Ward, B.; Skorobogaty, A.; Dabrowiak, J. C. *Biochemistry* **1986**, *25*, 7827.
9. Banville, D. L.; Marzilli, L. G.; Strickland, J. A. *Biopolymers* **1986**, *25*, 1837.
10. Strickland, J. A.; Marzilli, L. G.; Wilson, W. D.; Zon, G. *Inorg. Chem.* **1989**, *28*, 4191.
11. Marzilli, L. G.; Banville, D. L.; Zon, G.; Wilson, W. D. *J. Am. Chem. Soc.* **1986**, *108*, 4188.
12. Banville, D. L.; Marzilli, L. G.; Wilson, W. D. *Biochem. Biophys. Res. Commun*. **1983**, *113*, 148.
13. Pasternack, R. F.; Gibbs, E. J.; Villafranca, J. J. *Biochemistry* **1983**, *22*, 5409.
14. Biitje, K.; Schneider, J. H.; Kim, J. P.; Wang, Y.; Ikuta, S.; Nakamoto, K. *J. lnorg. Biochem.* **1989**, *37*,119.
15. Kuroda, R.; Tanaka, H. *J. Chem. Soc., Chem. Commun*. **1994**, 1575.
16. Schneidr, H.-J.; Wang, M. *J. Org. Chem*. **1994**, *59*, 7473.
17. Sehlstedt, U.; Kim, S. K.; Carter, P.; Goodisman, J.; Vollano, J. F.; Norden, B.; Dabrowiak, J. C. *Biochemistry* **1994**, *33*, 417.
18. Yun, B. H.; Jeon, S. H.; Cho, T.-S.; Yi, S. Y.; Sehlstedt, U.; Kim, S. K. *Biophys. Chem.* **1998**, *70*, 1.
19. Lee, Y.-A.; Lee, S.; Cho, T.-S.; Kim, C.; Han, S. W.; Kim, S. K. *J. Phys. Chem. B* **2002**, *106*, 11351.
20. Lee, S.; Jeon, S. H.; Kim, B.-J.; Han, S. W.; Jang, H. G.; Kim, S. K. *Biophys. Chem*. **2001**, *92*, 35.
21. Hui, X. W.; Gresh, N.; Pullman, B. *Nucleic Acids Res*. **1990**, *18*, 1109.
22. Ford, K. G.; Neidle, S. *Bioorg. Med. Chem*. **1995**, *6*, 671.
23. Guliaev, A. B.; Leontis, N. B. *Biochemistry* **1999**, *38*, 15425.

24. Carvlin, M. J.; Datta-Gupta, N.; Fiel, R. J. *Biochem. Biophys. Res. Commun.* **1982**, *108*, 66.

25. Pasternack, R. F.; Brigandi, R. A.; Abrams, M. J.; Willams, A. P.; Gibbs, E. *J. Inorg. Chem*. **1990**, *29*, 4483.

26. Pasternack, R. F.; Gibbs, E. J.; Collings, P. J.; DePaula, J. C.; Turzo, L. C.; Terracina, A. *J. Am. Chem. Soc*. **1998**, *120*, 5873.

27. Strickland, J. A.; Marzilli, L. G.; Gay, K. M.; Wilson, W. D. *Biochemistry* **1988**, *27*, 8870.

28. Pasternack, R. F.; Gibbs, E. J. *Met. Ions Biol. Syst.* **1996**, *33*, 367.

29. Lipscomb, L. A.; Zhou, F. X.; Presnell, S. R.; Woo, R. J.; Peek, M. E.; Plaskon, R.R.; Williams, L.D. *Biochemistry* **1996**, *35*, 2818.

30. Bennett, M.; Krah, A.; Wien, F.; Garman, E.; Mckenna, R.; Sanderson, M.; Niedle, S. *Proc. Natl. Acad. Sci. U.S.A.* **2000**, *97*, 9476.

31. Barnes, N. R.; Schreiner, A. F.; Finnegan, M. G.; Johnson, M. K.; *Biospectroscopy* **1998**, *4*, 341.

32. Chirvony, V. S. *J. Porphyrins Phthalocyanines* **2003**, *7*, 766.

33. Pasternack, R. F.; Gibbs, E. J.; Villafranca, J. J. *Biochemistry* **1983**, *22*, 2406.

34. Lin, M.; Lee, M.; Yue, K. T.; Marzilli, L. G. *Inorg. Chem.* **1993**, *32*, 3217.

35. Barnes, N. R.; Stroud, P. D.; Robinson, K. E.; Horton, C. Schreiner, A. F.; *Biospectroscopy* **1999**, *5*, 179.

36. Uno, T.; Hamasaki, K.; Tanigawa, M.; Shimabayashi, S. *Inorg. Chem.* **1997**, *36*, 1676.

37. Uno, T.; Aoki, K.; Shikimi, T.; Hiranuma, Y.; Tomisugi, Y.; Ishikawa, Y. *Biochemistry* **2002,** *41*, 13059.

38. Lee, Y-A.; Kim, J.-O.; Cho, T.-S.; Song, R.; Kim, K. S. *J. Am. Chem. Soc*. **2003**, *125*, 8106.

39. Borissevitch, I. E.; Gandini, S. C. M. *J. Photochem. Photobiol. B.* **1998**, *43*, 112.
40. Han, F. X.; Wheelhouse, R. T.; Hurley, L. H. *J. Am. Chem. Soc.* **1999**, *121*, 3561.
41. Wheelhouse, R. T.; Sun, D.; Han, H.; Han, F. X.; Hurley, L. H. *J. Am. Chem. Soc.* **1998**, *120*, 3261.
42. Han, H.; Langley, D. R.; Rangan, A.; Hurley, L. H. *J. Am. Chem. Soc.* **2001**, *123*, 8902.
43. Shi, D. F.; Wheelhouse, R. T.; Sun, D. Y.; Hurley, L. H. *J. Med. Chem.* **2001**, *44*, 4509.
44. Anantha, N. V.; Azam, M.; Sheardy, R. D. *Biochemistry* **1998**, *37*, 2709.
45. Vialas, C.; Pratviel, G.; Meunier, B. *Biochemistry* **2000**, *39*, 9514.
46. Maraval, A.; Franco, S.; Vialas, C.; Pratviel, G.; Blasco, M. A.; Meunier, B. *Org. Biomol. Chem*. **2003**, *1*, 921.
47. Dixon, I. M.; Lopez, F.; Esteve, J-P.; Tejera, A. M.; Blasco, M, A.; Pratviel, G.; Meunier, B. *Chem. Bio. Chem* **2005**, *6*, 123.
48. Keating, L. R.; Szalai, V. A. *Biochemistry* **2004,** *43*, 15891.
49. Yamashita, T.; Uno, T.; Ishikawa, Y. *Bioorg. Med. Chem.* **2005**, *xxx* xxx.
50. Haq, I.; Trent, J. O.; Chowdhry, B. Z.; Jenkins, T. C. *J. Am. Chem. Soc.* **1999,** *121*, 1768.
51. Izbicka, E.; Wheelhouse, R. T.; Raymond, E.; Davidson, K. K.; Lawrence, R. A.; Sun, D.; Windle, B. E.; Hurley, L. H.; Von Hoff, D.D. *Cancer Res.* 1999, *59*, 639.
52. Arthanari, H.; Basu, S.; Kawano, T. L.; Bolton, P. H. *Nucleic Acids Res.* **1998**, *26*, 3724.
53. Zupan, K.; Herenyi, L.; Toth, K.; Majer, Z.; Csik, G. *Biochemistry* **2004,** *43*, 9151.

54. Thomas, K. E.; McMillin, D. R. *J. Phys. Chem. B*, **2001**, *105*, 12628.

55. Eggleston, M. K.; Crites, D. K.; McMillin, D. R. *J. Phys. Chem. A* **1998**, *102*, 5506.

56. Tears, D. K. C.; McMillin, D. R. *Chem. Commun.* **1998**, 2517.

57. Lugo-Ponce, P.; McMillin, D. R. *Coord. Chem. Rev.* **2000**, *208*, 169.

58. Hudson, B. P.; Sou, J.; Berger, D. J.; McMillin, D. R. *J. Am. Chem. Soc.* **1992**, *114*, 8997.

59. Kruglik, S. G.; Galievsky, V. A.; Chirvony, V. S.; Apanasevich, P. A.; Ermolenkov, V. V.; Orlovich, V. A.; Chinsky, L.; Turpin, P.-Y. *J. Phys. Chem.* **1995**, *99*, 5732.

60. Galievsky, V. A.; Chirvony, V. S.; Kruglik, S. G.; Ermolenkov, V. V.; Orlovich, V. A.; Otto, C.; Mojzes, P.; Turpin, P.-Y. *J. Phys. Chem.* **1996**, *100*, 12649.

61. Shvedko, A. G.; Kruglik, S. G.; Ermolenkov, V. V.; Orlovich, V. A.; Turpin, P.-Y.; Greve, J.; Otto, C. *J. Raman Spectrosc.* **1999**, *30*, 677.

62. Kruglik, S. G.; Mojzes, P.; Mizutani, Y.; Kitagawa, T.; Turpin, P.-Y. *J. Phys. Chem. B* **2001**, *105*, 5018.

63. Mojzes, P.; Kruglik, S. G.; Baumruk, V.; Turpin, P.-Y. *J. Phys. Chem. B* **2003**, *107*, 7532.

64. Takako, O.; Hajime, M.; Yasuhiko, Y. *Biophys. Chem*. **2005**, *113*, 53.

65. Kim, J.-O.; Lee, Y.-A.; Jin, B.; Park, T.; Song, R, Kim, S. K. *Biophys. Chem*. **2004**, *111*, 63.

66. Catherine, V.-B.; Martine, P.-F.; Eric, T.; Gilles, A.-H.; Nathalie, B.; Alain, G. *Tetrahedron* **1996**, *52*, 13589.

67. Laine, M.; Richard, F.; Tarnaud, T.; Bied-Charreton, C.; Verchere-Beaur, C. *J. Biol. Inorg. Chem.* **2004**, *9*, 550.

68. Pitie, M.; Pratviel, G.; Bernadou, J.; Meunier, B.; *Proc. Natl. Acad. Sci. U.S.A.* **1992**, *89*, 3967.
69. Dubey, I.; Pratviel, G.; Meunier, B. *Perkin 1* **2000**, *18*, 3088.
70. Chaloin, L.; Bigey, P.; Loup, C.; Marin, M.; Galeotti, N.; Piechaczyk, M.; Heitz, F.; Meunier, B. *Bioconjugate. Chem*. **2001**, 12, 691.
71. Lapi, A.; Pratviel, G.; Meunier, B. *Metal-Based Drugs* **2001**, 8, 47.
72. Wietzerbin, K.; Muller, J. G.; Jameton, R. A.; Pratviel, G.; Bernadou, J.; Meunier, B.; Burrows, C. J. *Inorg. Chem* **1999**, *38*, 4123.
73. Drexler, C.; Hosseini, M. W.; Pratviel, G.; Meunier, B. *Chem. Commun.* **1998**, *13*, 1343.
74. Jakobs, A, J.; Bernadou, J. B.; Meunier, B. *J. Org. Chem.* **1997**, *62*, 3505.
75. Marguerite, P.; Meunier, B. *J. Biol. Inorg. Chem.*, **1996**, *1*, 239.
76. Casas, C.; Lacey, J.; Meunier, B. *Bioconjugate Chem.* **1993**, *4*, 366.
77. Frau, S.; Bernadou, J.; Meunier, B. *Bioconjugate Chem.* **1997**, 8, 222.
78. Silvana, F.; Jeanoseph, B.; Meunier, B.; Jean-Claude, D.; Joseph, V. *New. J. Chem.* **1995**, 19, 873.
79. Bigey, P.; Sonnichsen, S. H.; Meunier, B.; Nielsen, P. E. *Bioconjugate Chem*. **1997**, 8, 267.
80. Mestre, B.; Pitie, M.; Loup, C.; Claparols, C.; Pratviel, G.; Meunier, B. *Nucleic Acids Res.* **1997**, *25*, 1022.
81. Mestre, B.; Jakobs, A.; Pratviel, G.; Meunier, B. *Biochemistry* **1996**, *35*, 9140.
82. Li, H.; Fedorova, O. S.; Trumble, W. R.; Fletcher, T. R.; Czuchajowski, L.; *Bioconjugate Chem.* **1997**, *8*, 49.
83. Mettath, S.; Munson, B. R.; Pandey, R. K.; *Bioconjugate Chem.* **1999,** *10*, 94.

84. Sari, M. A.; Battioni, J. P.; Dupri, D.; Mansuy, D.; Le Pecqa, J. B. *Biochemistry* **1990,** ***29,*** 4205.

85. Mohammadi, S.; Perree-Fauvet, M.; Gresh, N.; Hillairet, K.; Taillandier, E.; *Biochemistry* **1998,** *37,* 6165.

86. Steenkeste, K.; Enescu, M.; Tfibel, F.; Perree-Fauvet, M.; Fontaine-Aupart, M.-P.; *J. Phys. Chem. B* **2004**, *108,* 12215.

87. Perree-Fauvet, M.; Gresh, N. *Tetrahedron Lett.* **1995**, *36,* 4227.

88. Trommel, J. S.; Marzilli, L. G. *Inorg. Chem.* **2001,** *40,* 4374.

89. Pasternack, R. F.; Gibbs, E. J.; Bruzewicz, D.; Stewart, D.; Shannon, K.; Engstrom. *J. Am. Chem. Soc.* 2002, 124, 3533.

90. Scolaro, L. M.; Romeo, A.; Pasternack. R. F. *J. Am. Chem. Soc.* **2004**, 126, 7178.

91. Pasternack, R. F.; Bustamante, C.; Collings, P. J.; Giannetto, A.; Gibbs, E. J. *J. Am. Chem. Soc.* **1993**, *115,* 5393.

92. Pasternack, R. F.; Collings, P. J. *Science* **1995**, *269,* 935.

93. Pasternack, R. F.; Goldsmith, J. I.; Szep, S.; Gibbs, E. J.; *Biophys. Chem.* **1998**, *75,* 1024.

94. Pasternack, R. F.; Ewen, S.; Rao, A.; Meyer, A. S.; Freedman, M. A. *Inorg. Chim. Acta* **2001**, *317,* 59.

95. Wall, R. K.; Shelton, A. H.; Bonaccorsi, L. C.; Bejune, S. A.; Dube, D.; McMillin, D. R. *J. Am. Chem. Soc.* **2001**, *123,* 11480.

96. Bejune, S. A.; Shelton, A. H.; McMillin, D. R. *Inorg. Chem*. **2003**, *42,* 8465.

97. Bejune, S. A.; McMillin, D. R. *Chem. Commun.* **2004**, 1320.

98. Yamakawa, N.; Ishikawa, Y.; Uno, T. *Chem. Pharm. Bull.* **2001**, *49,* 1531.

99. Ishikawa, Y.; Yamakawa, N.; Uno, T. *Bioorg. Med. Chem.* **2002**, *10*, 1953.

100. Genady, A. R.; Gabel, D. *Tetrahedron Lett.* **2003**, *44*, 2915.

101. Tjahjono, D. H.; Akutsu, T.; Yoshioka, N.; Inoue, H. *Biochim. Biophys. Acta* **1999**, *1472*, 333.

102. Tjahjono, D. H.; Mima, S.; Akutsu, T.; Yoshioka, N.; Inoue, H. *J Inorg. Chem.* **2001**, *85*, 219.

103. Song, R.; Kim, Y.-S.; Lee, C. O.; Soo. Y. S.; *Tetrahedron Lett*. **2003**, *44*, 1537.

104. Marzilli, L. G.; Petho, G.; Lin. M.; Kim, M. S.; Dixon. D. W. *J. Am. Chem. Soc*. **1992**, *114*, 7575.

105. Mukundan, N. E.; Petho, G.; Dixon, D. W.; Marzilli. L. G. *J Inorg. Chem.* **1995**, *34*, 3677.

106. Mukundan, N. E.; Petho, G.; Dixon, D. W.; Kim, M. S.; Marzilli, L. G. *Inorg. Chem.* **1994**, *33*, 4676.

107. Petho, G.; Nancy, B. E.; Kim, M. S.; Lin, M.; Dixon, D. W.; Marzilli, L. G. *Chem. Commun.* **1993**, 1547.

108. Ding, L.; Etemad-Moghadam, G.; Cros, S.; Auclair, C.; Meunier, B. *J. Med. Chem.* **1991**, *34*, 900.

109. Gray, T. A.; Yue, K. T.; Marzilli, L. G. *J. lnorg. Biochem.* **1991**, *41*, 205.

110. Wheeler, G. V.; Chinsky, L.; Miskovsky, P.; Turpin, P.-Y. *J. Biomol. Struct. Dyn.* **1995**, *13*, 399.

111. Li, H.; Fedorova, O. S.; Grachev, A. N.; Trumble, W. R.; Bohach, G. A.; Czuchajowski, L. *Biochim. Biophys. Acta* **1997**, *1354*, 252.

112. Li, H.; Czuchajowski, L.; Trumble, W. R. *J. Heterocyclic Chem.* **1997**, *34*, 999.

113. Dougherty, G. *J. Inorg. Biochem.* **1988**, *34*, 95.

114. Chikira, M.; Suda, S.; Nakabayashi, T.; Fujiwara, Y.; Ejiri, T.; Yoshikawa, M.; Kobayashi, N.; Shindo, H. *J. Chem. Soc., Dalton Trans.* **1995**, *8*, 1325.

115. Dougherty, G.; Pastemack, R. F. *Biophys. Chem.* **1992**, *44*, 11.

116. Chirvony, V. S.; Victor, G. A.; Sergei, T. N.; Boris, D. M.; Vladimir, E. V.; Turpin, P.-Y. *Biospectroscopy* **1999**, *5*, 302.
117. Kruk, N. N.; Shishporenok, S. I.; Korotky, A. A.; Galievsky, V. A.; Chirvony, V. S.; Turpin, P. -Y. *J. Photochem. Photobiol B.* **1998**, *45*, 67.
118. Kruk, N. N.; Dzhagarov, B. M.; Galievsky, V. A.; Chirvony, V. S.; Turpin. P. -Y. *J. Photochem. Photobiol. B.* **1998**, *42*, 181.
119. Chirvony, V. S.; Galievsky, V. A.; Kruk, N. N.; Dzhagarov, B. M.; Turpin, P. -Y. *J. Photochem. Photobiol B.* **1997**, *40*, 154.
120. Anne, B. M.; Harriman, A. *J. Am. Chem. Soc.* **1994**, *116*, 10383.
121. Jesionek, A.; von Tappeiner, H. *Arch. Klin. Med.* **1905**, *82*, 223.
122. Detty, M. R.; Gibson, S. L.; Wagner, S. J. *J. Med. Chem.* **2004**, *47*, 1.
123. Kato, H. *J. Photochem. Photobiol. B.* **1998**, *42*, 96.
124. Puolakkainen, P.; Schroder, T. *Dig. Dis.* **1992**, *10*, 53.
125. Moesta, K. T.; Schlag, P.; Douglas, H. O. Jr.; Mang, T. S. *Lasers Surg. Med.* **1995**, *16*, 84.
126. Bellnier, D. A.; Greco, W. R.; Loewen, G. M.; Nava, H.; Oseroff, A. R.; Pandey, R. K.; Tsuchida, T.; Dougherty, T. J. *Cancer Res.* **2003**, *63*, 1806.
127. Prosst, R. L.; Wolfsen, H. C.; Gahlen, J. *Endoscopy* **2003**, *35*, 1059.
128. Dilkes, M. G.; Benjamin, E.; Ovaisi, S.; Banerjee, A. S. *J. Laryngol. Otol.* **2003**, *117*, 713.
129. Jichlinski, P.; Leisinger, H.-J. *Urol. Res.* **2001**, *29*, 396.
130. Nathan, T. R.; Whitelaw, D. E.; Chang, S. C.; Lees, W. R.; Ripley, P. M.; Payne, H.; Jones, L.; Parkinson, M. C.; Emberton, M.; Gilliam, A. R.; Mundy, A. R.; Bown, S. G. *J. Urol.* **2002**, *168*, 1427.
131. Pariser, D. M.; Lowe, N. J.; Stewart, D. M.; Jarratt, M. T.; Luck, A. W.; Pariser, R. J.; Yamauchi, P. S. *J. Am. Acad. Dermatol.* **2003**, *48*, 227.

132. Szoimies, R. M.; Landthalor, M.; Karror, S. *J. Dermatol. Treat.* **2002**, *13*, S13.
133. Loman, J. A.; Morton, C. A. *Expert Opin. Biol. Ther.* **2002**, *2*, 45.
134. Rechtman, E.; Ciulla, T. A.; Criswell, M. H.; Pollack, A.; Harris, A. *Expert Opin. Pharmacother.* **2002**, *3*, 931.
135. Keam, S. J.; Scott, L. J.; Curran, M. P. *Drugs* **2003**, *63*, 2521.
136. Mueller, V. A.; Ruokonen, P.; Schellenbeck, M.; Hartmann, C.; Tetz, M. *Ophthalmic. Res.* **2003**, *35*, 60.
137. Miyagi, K.; Sampson, R. W.; Sieber-Blum, M.; Sieber, F. *J. Photochem. Photobiol. B* **2003**, *70*, 133.
138. Hayase, M.; Woodbaum, K. W.; Perlroth, J.; Miller, R. A.; Baumgardner, W.; Yock, P. G.; Yeung, A. *Cardiovasc. Res.* **2001**, *49*, 449.
139. Henderson, B. W.; Dourgherty, T. J.; Eds.; Marcel Dekker: New York, **1992**.
140. Sharman, W. M.; Allen, C. M.; van Lier, J. E. *Drug Discovery Today* **1999**, *4*, 507.
141. Kessel, D.; Woodburn, K. *Int. J. Biochem.* **1993**, *25*, 1377.
142. Sema, A. A. F.; Kennedy, J. C.; Blakeslee, D.; Robertson, D. M. Can. *J. Neurol. Sci.* **1981**, *8*, 105.
143. Winkelman, J. W.; Collins, G. H. *Photochem. Photobiol.* **1987**, *46*, 801.
144. Harth, E. M.; Hecht, S.; Helms, B.; Malmstrom, E. E.; Frechet, J. M. J.; Hawker, C. J. *J. Am. Chem. Soc.* **2002**, *124*, 3926.
145. Nishiyama, N.; Stapert, H. R.; Zhang, G.-D.; Takasu, D.; Jiang, D.-L.; Nagano, T.; Aida, T.; Kataoka, K. *Bioconjugate Chem.* **2003**, *14*, 58.
146. Gradl, S. N.; Felix, J. P.; Isacoff, E. Y.; Garcia, M. L.; Trauner, D. *J. Am. Chem. Soc.* **2003**, *125*, 12668.

147. Latos-Grazynski, L.; Lisowski, J.; Olmstead, M. M.; Balch, A. L. *Inorg. Chem.* **1989**, *28*, 1183.

148. Latos-Grazynski, L.; Pacholska, E.; Chmielewski, P. J.; Olmstead, M. M.; Balch, A. L. *Inorg. Chem.* **1996**, *35*, 566.

149. Ziolkowski, P.; Milach, J.; Symonowicz, K.; Chmielewski, P.; Latos-Grazynski, L.; Marcinkowska, E. *Tumori* **1995**, *81*, 364.

150. Marcinkowska, E.; Ziolkowski, P.; Pacholska, E.; Latos-Grazynski, L.; Chmielewski, P.; Radzikowski, C. Z. *Anticancer Res.* **1997**, *17*, 3313.

151. Hilmey, D. G.; Abe, M.; Nelen, M. I.; Stilts, C. E.; Baker, G. A.; Baker, S. N.; Bright, F. V.; Davies, S. R.; Gollnick, S. O.; Oseroff, A. R.; Gibson, S. L.; Hilf, R.; Detty, M. R. *J. Med. Chem.* **2002**, *45*, 449.

152. Ulman, A.; Manassen, J. *J. Chem. Soc., Perkin Trans. 1* **1979**, *4*, 1066.

153. Ulman, A.; Manassen, J.; Frolow, F.; Rabinovich, D. *Tetrahedron Lett.* **1978**, 167.

154. Gaullier, J. M.; Berg, K.; Peng, Q.; Anholt, H.; Selbo, P. K.; Ma, L. W.; Moan, J. *Cancer Res.* **1997**, *57*, 1481.

155. Kennedy, J. C.; Pottier, R. H.; Pross, D. C. *J. Photochem. Photobiol. B* **1990**, *6*, 143.

156. Kennedy, J. C.; Marcus, S. L.; Pottier, R. H. *J. Clin. Laser Mod. Surg.* **1996**, *14*, 289.

157. Paquette, B.; Boyle, R. W.; Ali, H.; MacLennan, A. H.; Truscott, T. G.; van Lier, J. E. *Photochem. Photobiol.* **1991**, *53*, 323.

158. Margarone, P.; Gregoire, M.-J.; Scasnart, V.; Ali, H.; van Lier, J. E. *Photochem. Photobiol.* **1996**, *63*, 217.

159. Berg, K.; Bommer, J. C.; Moan, J. *Photochem. Photobiol.* **1989**, *49*, 587.

160. Colussi, V. C.; Feyes, D. K.; Mulvihill, J. W.; Li, Y.-S.; Kenney, M. E.; Elmets, C. A.; Oleinick, N. L.; Mukhtar, H. *Photochem. Photobiol.* **1999**, *69*, 236.
161. Boyle, R. W.; Paquette, B.; van Lier, J. E. Biological activities of phthalocyanines XIV. *Br. J. Cancer* **1992**, *65*, 813.
162. Kostenich, G. A.; Zhuravkin, I. N.; Zhavrid, E. A. *J. Photochem. Photobiol. B* **1994**, *22*, 211.
163. Li, G.; Graham, A.; Chen, Y.; Dobhal, M. P.; Morgan, J.; Zheng, G.; Kozyrev, A.; Oseroff, A.; Dougherty, T. J.; Pandey, R. K. *J. Med. Chem.* **2003**, *46*, 5349.
164. Sessler, J. L.; Hemmi, G.; Mody, T. D.; Murai, T.; Burrell, A.; *Acc. Chem. Res.* **1994**, *27*, 43.
165. Sessler, J. L.; Miller, R. A.; *Biochem. Pharmacol.* **2000**, *59*, 733.
166. *Photoinduced Electron Transfer*, Parts A-D; Fox, M. A., Chanon, M., Eds.; Elsevier: Amsterdam, **1988**.
167. *Photoinduced Electron Transfer* A series in *Topics in Current Chemistry* Mattay, J.; Ed.; Springer-verlag: New York, **1991**.
168. Marcus, R. A.; Sutin, N. *Biochim. Biophys. Acta* **1985**, *811*, 262.
169. *Photosynthesis;* Amesz, J.; Ed.; Elsevier: Amsterdam, **1987**.
170. Gust, D.; Moore, T. A.; Moore, A. L. *Acc. Chem. Res*. **1993**, *26*, 198.
171. Guillet, J. E. in *Polymer Photophysics and Photochemistry*; Cambridge University Press: Cambridge, **1985**.
172. Bloor, D. *Physica Scripta.* **1991**, *39*, 380.
173. Pope, M. *Mol. Cryst. Liq. Cryst.* **1993**, *228*, 1.
174. Marcus, R. A. *J. Chem. Phys*. **1956**, *24*, 966.
175. Marcus, R. A. *J. Chem. Phys*. **1965**, *43*, 679.

176. Marcus, R. A. *in Light Induced Charge Separation in Biology and Chemistry*; Gerischer, H.; Katz, J. J., Eds.; Verlag Chemie: Berlin, **1979**, p. 15.
177. Marcus, R. A. *Angew. Chem., Int. Ed. Engl*. **1993**, *32*, 1111.
178. Forster, Th. *Discuss. Faraday Soc*. **1959**, *27*, 7.
179. Dexter, D. L. *J. Chem. Phys*. **1953**, *21*, 836.
180. Shimadzu, T.; Segawa, H. *Thin Solid Films* **1996**, *273*, 14.
181. Susumu, K.; Kunimoto, K.; Segawa, H.; Shimidzu. *J. Phys. Chem.* **1995**, *99*, 29.
182. Segawa, H.; Kunimoto, K.; Susumu, K.; Taniguchi, M.; Shimidzu, T. *J. Am. Chem. Soc*. **1994**, *116*, 11193.
183. Susumu, K.; Segawa, H.; Shimidzu, T. *Chem. Lett*. **1995**, 929.
184. Susumu, K.; Kunimoto, K.; Segawa, H.; Shimidzu, T. *J. Photochem. Photobiol. A: Chem*. **1995**, *92*, 39.
185. Segawa, H.; Nakayama, N.; Shimidzu, T. *Chem. Commun*. **1992**, 784.
186. Susumu, K.; Tanaka, K.; Shimidzu, T.; Takeuchi, Y.; Segawa, H. *J. Chem. Soc., Perkin Trans. 2* **1999**, 1521.
187. Segawa, H.; Kunimoto, K.; Nakamoto, A.; Shimidzu, T. *J. Chem. Soc., Perkin Trans. 1* **1982**, 939.
188. Rao, T. A.; Maiya, B. G. *Chem. Commun*. **1995**, 939.
189. Rao, T. A.; Maiya, B. G. *Inorg. Chem*. **1996**, *35*, 4829.
190. Hirakawa, K.; Segawa, H. *J. Photochem. Photobiol. A: Chem*. **1999**, *123*, 67.
191. Goh, G, K.-M.; Czuchajowski, L. *J. Porphyrins Phthalocyanines* **1997**, *1*, 281.
192. Hawley, J. C.; Bampos, N.; Abraham, R. J.; Sanders, J. K. M. *Chem. Commun*. **1998**, 661.

193. Tong, Y.; Hamilton, D. G.; Meillon. J.-C.; Sanders, J. K. M. *Org. Lett.* **1999**, *1*, 1343.

194. Webb, S. J.; Sanders, J. K. M. *Inorg. Chem*. **2000**, *39*, 5920.

195. Prashanth K, P.; Maiya, B. G. *New J. Chem*. **2003**, *27*, 619.

196. Andou, Y.; Shiragami, T.; Shima, K.; Yasuda, M. *J. Photochem. Photobiol. A: Chem*. **2002**, *147*, 191.

197. Shiragami, T.; Andou, Y.; Hamasuna, Y.; Yamaguchi, F.; Shima, K.; Yasuda, M. *Bull. Chem. Soc. Jpn.* **2002**, *75*, 1577.

198. Redman, J. E.; Feeder, N.; Teat, S. J.; Sanders, J. K. M. *Inorg. Chem*. **2001**, *40*, 2486.

199. Kim, H.-J.; Bampos, N.; Sanders, J. K. M. *J. Am. Chem. Soc*. **1999**, *121*, 8120.

200. Stulz, E.; Mak, C. C.; Sanders, J. K. M. *J. Chem. Soc., Dalton Trans*. **2001**, 604.

201. Maiya, B. G.; Bampos, N.; Kumar, A. A.; Feeder, N.; Sanders, J. K. M. *New J. Chem*. **2001**, *25*, 797.

CHAPTER 2

Materials and Methods

2.1 Introduction

This chapter presents a listing of all the chemicals and other materials employed at various stages of the research work. Procedures followed for the purification of solvents and chemicals are also given here. Further, a brief discussion of the physicochemical techniques as well as biochemical techniques employed during the course of the investigation is presented.

2.2 Materials

Chemicals required for the present study were procured from Aldrich or from local manufacturers (i.e., SISCO, E-Merck, BDH). They were purified when required by standard procedures.[1,2]

Supercoiled DNA pBR 322 (cesium chloride purified) was obtained from Bangalore Genei (India). Agarose (low melt, 65 ^{o}C, Molecular Biology grade for DNA gels) was purchased from Bio-Rad Laboratories Inc. (U.S.A). Highly polymerized calf thymus DNA (CTDNA), ethidium bromide and bromophenol blue were procured from Sigma (U.S.A). These biochemicals were used as received. Tris(hydroxylmethyl) aminomethane (Tris), sucrose, sodium chloride, ethylenediaminetetraacetic acid disodium salt (EDTA-Na_2), disodium hydrogen phosphate (Na_2HPO_4) and sodium dihydrogen phosphate (NaH_2PO_4) were of Molecular Biology grade, obtained from Sisco Research Laboratories (India).

Integrated DNA Technologies supplied the hairpin forming oligonucleotides 5′-GATTACTTTTGTAATC-3′ (TT[T4]), 5′- GATAACTTTTGTTATC-3′ (TA[T4]), 5′-GACGACTTTTGTCGTC-3′ (CG[T4]), 5′-GATTACGGGAGTAATC-3′ (TT[GA3]) as well as the 20-mer variant 5′-GACCGGACTTTTGTCCGGTC- 3′ (CCGG[T4]). The commercial supplier provided the extinction coefficients, ε_{260} = 153 700 M^{-1} cm^{-1} for TT[T4] and TA[T4], ε_{260} = 146 100 M^{-1} cm^{-1} for CG[T4], ε_{260} = 168 000 M^{-1} cm^{-1} for TT[GA3] and ε_{260} = 180 700 M^{-1} cm^{-1} for CCGG[T4].

Nitrogen gas was obtained from Indian Oxygen Limited (India). It was further purified and dried by passing it through alkaline pyrogallol solution, sulfuric acid, and potassium hydroxide pellets.

2.3 Solvents

The common solvents employed during the research work were purified according to the standard procedures.[1,2] Chloroform, methylenechloride and methanol were extensively purified as described below, for spectroscopic purposes.

The LR grade methylene chloride was washed twice with sulfuric acid and then with water. This was washed twice with sodium bicarbonate solution and then with water. The solvent was dried over calcium chloride and distilled over phosphorus pentoxide. It was stored over basic alumina until use. Chloroform (LR) was washed 3 - 4 times with water, stored over calcium chloride overnight and distilled over phosphorus pentoxide. It was stored in the dark over basic alumina. Methanol (LR) was initially purified by distillation through an efficient fractionating column then warmed with magnesium turnings and iodine until the color of iodine has disappeared and all the magnesium was converted to magnesium methoxide. Finally it was distilled off and stored over Linde type 4Å molecular sieves until use.

2.4 Physical methods

The FAB mass spectra were recorded on a JEOL SX 102/DA-6000 mass spectrometer/data system using xenon (6 kV, 10 mA) as the FAB gas. The accelerating voltage was 10 kV and the spectra were recorded at room temperature with m-Nitrobenzyl alcohol (NBA) was used as the matrix. MALDI-TOF spectra were recorded on a Kompact MALDI 4 mass spectrometer (Kratos Analytical Ltd). The instrument was operated in reflection time of flight mode with an accelerating potential of 20 KV and in the negative ion recording mode. LC MS spectra were recorded on a LCMS-2010A Shimadzu mass spectrometer.

The UV-visible spectra were recorded with either a Shimadzu model 160A or a Shimadzu model UV-3101PC UV-vis spectrophotometer. A matched pair of quartz cuvettes were employed (path length = 1 cm each). Concentrations of the various investigated compounds employed for this purpose ranged from ca. 2×10^{-6} (porphyrin Soret band) to 5×10^{-5} M (porphyrin Q- and other bands/bands due to other compounds).

Steady state fluorescence spectra were recorded either on a Spex Model Fluoromax-3 or a Jasco Model FP 777 spectrofluorometer using a 1 cm quartz cell. Right angle detection technique was employed for these measurements. The excitation and emission slit widths employed were 3 nm. Concentration of the samples was adjusted such that the optical densities at the excitation wavelengths were less than ca. 0.2 for emission spectra and ~ 1×10^{-7} M (or the optical density at the emission wavelength, $\lambda_{em} < 0.2$) for excitation spectra. A Rhodamine 6G quantum counter was employed for spectral corrections at wavelengths < 600 nm. Fluorescence quantum

yields (ϕ) were estimated by integrating the areas under the fluorescence curves using the expression of Austin and Gouterman (eqn. 2.1).[3]

$$\mathbf{f}_{\mathbf{sample}} = \frac{\mathbf{O.D}_{\mathbf{standard}} \mathbf{x}\, \mathbf{A}_{\mathbf{sample}}}{\mathbf{O.D}_{\mathbf{sample}} \mathbf{x}\, \mathbf{A}_{\mathbf{standard}}} \mathbf{x}\ \mathbf{f}_{\mathbf{standard}} \qquad (2.1)$$

Here, A is area under the emission spectral curve and O.D. is optical density of the compound at the wavelength of exciting light. ϕ_{sample} and $\phi_{standard}$ are the fluorescence quantum yields of the sample under investigation and the standard used, respectively. The fluorescence standards employed were 5,10,15,20-tetraphenylporphyrin (**H_2TPP**) (ϕ_f = 0.13 in CH_2Cl_2),[4] 5,10,15,20-tetraphenylporphyrinatozinc(II) (**ZnTPP**) (ϕ_f = 0.036 in CH_2Cl_2),[4,5] 5,10,15,20-tetra(*N*-methylpyridinium-4-yl)porphyrin (**H_2T4**) (ϕ_f = 0.047 in H_2O)[6] and 5,10,15,20-tetra(*N*-methylpyridinium-4-yl)porphyrinatozinc(II) (**ZnT4**)[6] (ϕ_f = 0.025 in H_2O). Refractive index corrections have been employed while estimating the ϕ values in various solvents.[7]

^{1}H NMR spectra were recorded with either a Bruker NR-200 AF-FT or a Bruker DRX-400 spectrometer using $CDCl_3$ or CD_3OD or DMSO-d_6 as the solvent. Tetramethylsilane (TMS) was the internal standard employed while recording these samples. The sample concentration was typically ~ 1 - 3 x 10^{-3} M.

ESR spectra were run on a JEOL JES-FA200 X-band ESR spectrometer for the copper(II) systems at 100 ± 3 K. Diphenylpicrylhydrazide (DPPH) was used as the g-marker.

Cyclic- and differential pulse voltammetric experiments were performed on a CH Instruments model CHI 620A electrochemical analyzer. Tetrabutylammonium perchlorate (TBAP) was used as the supporting electrolyte in all the cases. The working and the auxillary (counter) electrodes employed were always platinum and the reference electrode chosen was a saturated calomel electrode (SCE). A salt bridge containing the same concentration of base electrolyte as that of the bulk solution was positioned between the nitrogen-purged bulk-test-solution and the reference electrode to reduce the effect due to liquid junction potentials. Fc^+/Fc (Fc = ferrocene) couple was used to calibrate the redox potential values and it could be reversibly oxidized under these experimental conditions.

2.5 DNA binding experiments with CTDNA

The stock solution of CTDNA was made by dissolving in appropriate buffers and kept overnight at 4 ^oC for complete dissolution. The concentration of CTDNA was measured by using its known extinction coefficient at 260 nm (6600 $M^{-1}cm^{-1}$).[8]

2.5.1 Absorption titrations

Absorption titration experiments with CTDNA were carried out in a phosphate buffer containing 0.006 M Na_2HPO_4, 0.02 M NaH_2PO_4, 0.001 M ethylenediaminetetraacetic acid (EDTA) (pH = 6.8) and sufficient NaCl to give a final ionic strength of μ = 0.5 M, by varying r_0, $0.5 \leq r_0 \leq 135$ (r_0 is defined as the ratio of the total concentration of nucleic acids (in base pairs) to that of porphyrin) and maintaining the porphyrin concentration constant (3.2 μM). Absorbance values were recorded after each successive addition of DNA solution and equilibration (ca. 5 min.). The apparent binding constant, K_{app}, was determined from the plot of $(\varepsilon_p-\varepsilon_{app})$ *vs.* (ε

$_{app}$-ε_p)/[DNA]$_{total}$, where [DNA] is the concentration of DNA in base pairs, ε_{app} is the apparent extinction coefficient (obtained by calculating A_{obsd}/[complex]) and ε_p refers to the extinction coefficient of the free porphyrin. The data were fitted to eqn. 2.2.[9-11]

$$(e_p - e_{app}) = \{(e_{app} - e_p)/[DNA]_{total}\}\{1/K_{app}\} + De \qquad (2.2)$$

where ε_p is the molar absorptivity of the free porphyrin, ε_{app} is the absorbance of a given solution divided by the total porphyrin concentration, and $\Delta\varepsilon$ is ε_p - ε_b. Thus, a plot of ε_p-ε_{app} vs. (ε_{app} - ε_p)/[DNA]$_{total}$ should yield a straight line of slope l/K_{app} and an intercept of $\Delta\varepsilon$ where $\Delta\varepsilon$ is ε_p- ε_b in which ε_b refers to extinction coefficient of bound porphyrin.

2.5.2 Fluorescence titrations

A procedure analogous to that used for the absorbance titration experiments was used for fluorescence titration experiments. Fluorescence titrations were also performed in the same buffer, in which absorption titrations have been carried out. The concentration of porphyrin employed was between 10^{-6} and 10^{-5} M and that of DNA varied between 10^{-6} and 10^{-3} M (base pairs). The data obtained were analyzed using eqn. 2.3.

$$C_F = C_T[(I / I_0) - P] / [1 - P] \qquad (2.3)$$

Here C_T is concentration of the porphyrin added, C_F is concentration of the free porphyrin, and I_0 and I are the fluorescence intensities in the absence and in the

presence of DNA, respectively. P is the ratio of the observed fluorescence quantum yield of the bound probe to the free porphyrin. The value of P was obtained from a plot of I/I_0 vs 1/[DNA] such that the limiting fluorescence quantum yields is given by the y-intercept. The amount of bound porphyrin (C_B) at any concentration was equal to $C_T - C_F$. A plot of r/C_F vs r, where r is equal to C_B/[DNA], was constructed according to the modified Scatchard equation, eqn. 2.4,

$$\mathbf{r/C_F = K_b(1\text{-}nr)[(1\text{-}nr)/[1\text{-}(n\text{-}1)\,r]]^{n-1}} \qquad (2.4)$$

given by McGhee and Von Hippel, where K_b is the intrinsic binding constant and n is the binding site size in base pairs.[12-14]

2.5.3 Circular dichroism

Circular dichroism spectra were recorded on JASCO, J810 spectropolarimeter using phosphate buffer containing 0.006 M Na_2HPO_4, 0.02 M NaH_2PO_4, 0.001 M EDTA, pH = 6.8. The same general procedure as for the UV-vis and fluorescence titrations was used to analyse the mixtures with different r_0 values ($3 \leq r_0 \leq 32$) by maintaining the concentration of the porphyrin constant (4.6 μM). All the spectra were recorded with steps of 0.5 nm and a response time of 4 s.[9,11,15,16]

2.5.4 Thermal denaturation

DNA melting experiments were carried out in 1.5 mM Na_2HPO_4, 0.5 mM NaH_2PO_4, 0.25 mM Na_2EDTA, pH 7.0 by monitoring the absorption (260 nm) of CTDNA (150 μM, nucleotide pairs, NP), using a Shimadzu model UV-160A spectrophotometer coupled with a temperature controller model Julabo-F12, at various

temperatures in the absence and in the presence of the porphyrin. The melting temperature (T_m) and the curve width σ_T (temperature range where 10%-90% of the absorption increase occurred) were calculated as previously described.[17,18]

2.6 DNA photocleavage and agarose gel electrophoresis

Electrophoresis through agarose is the standard method used to separate, identify or purify DNA fragments.[19-22] Using this technique, bands containing as little as 1-10 ng of DNA can be detected by direct examination of the agarose gel (stained with EtBr) in the UV light.[22] When an electric field is applied across the gel, DNA, which is negatively charged at neutral pH, migrate towards the anode. The intact supercoiled (Form I) DNA migrates faster than the single nicked (Form II) in the gel. This technique has been employed to identify the product/s of the DNA photocleavage, which was carried out in this work.

2.6.1 Buffers/Reagents

2.6.1.1 Tris-acetate ethylenediaminetetraacetate (TAE) electrolyte buffer (50 X stock)

Tris base (48.40 g) was dissolved in water (100 mL). EDTA disodium salt (7.44 g) was dissolved in water (50 mL) and the pH was adjusted to 8.0 using NaOH. This pH-adjusted EDTA solution was added to the tris solution followed by the addition of glacial acetic acid (11.42 mL). The volume was made up to 200 mL with H_2O and the resulting buffer was stored at 4 ^oC.

2.6.1.2 Sample buffer (6X)

A 0.25% bromophenol blue in 40% sucrose-H_2O was used as the sample buffer. This buffer was prepared by first dissolving sucrose (2.00 g) in water (3 mL) and then adding bromophenol blue (12.50 g) to this solution. The volume was made up to 5 mL. The resulting buffer was stored at 4 ^oC.

2.6.1.3 Ethidium bromide stock solution (10 mg/mL)

A 0.10 g of EtBr was dissolved in water (10 mL) by stirring in dark for several hours. The resulting solution was stored in a brown bottle at the ambient temperature. Working concentration of 0.5 µg/mL was used for staining the gels after electrophoresis.

2.6.2 Gel configuration and gel casting

A horizontal slab gel electrophoresis chamber (3.5 x 7.5 inches or 6.0 x 7.5 inches) made of polystyrene snaplock box obtained from Broviga Inc. (India) was used to carry out the agarose gel electrophoresis. Platinum wire was used as each of the two electrodes. A platform composed of four lantern slides glued together in a stack is cemented in the center of the box. A gel plate of 7.0 cm x 10.0 cm in size rests on this platform so that the gel is submerged just beneath the surface of the electrophoresis buffer. The details of gel casting are given below.

A 0.40 g of low melt agarose (Molecular Biology grade) was added to TAE buffer (50 mL). The slurry was then heated on a boiling water bath until the agarose dissolved completely. The solution was cooled to 50 ^oC. Both ends of the gel mold were closed with a clean autoclaved tape and a small quantity of agarose solution was applied with a pipette along the edges of the gel mold so as to seal it completely. Remaining warm agarose solution was poured onto the gel mold and immediately the comb was clamped into position near one end of the gel. The teeth of the comb formed

the sample wells. Care was taken to see that at least 0.5 - 1.0 mm of agarose was left between the bottom of the teeth and the base of the gel, so that the sample wells are completely sealed. After 35 - 40 min. (by which
time the gel was completely set), the comb and the autoclaved tape were removed carefully and the gel was mounted in the electrophoresis tank. Working buffer (200 mL, TAE) was poured into the gel until the gel was covered to a depth of about 1 mm.

2.6.3 Photolysis of pBR 322 DNA and separation of the products

Photolysis experiments were carried out for pre-incubated (1 h) samples of pBR 322 DNA (100 μM nucleotide phosphate, 4 μL) and the appropriate concentration of the porphyrin (~2.5 μM) placed in a quartz tube of 3 mm internal diameter. Tris-HCl buffer (pH 8.0) was used as the medium. Irradiation of the samples was done using a Xe arc lamp (150 W, Photon Technology International). The required wavelength for the irradiation was isolated from the source using a PTI Model S/N 1366 (10 nm band pass) monochromator. At times, photolysis was also carried out inside the sample chamber of a Jasco Model FP-777 spectrofluorometer with the slit width 5 nm. The temperature was maintained at 20 ^{o}C throughout irradiation.

After irradiation, 2 μL of sample buffer was added to the quartz tube containing the irradiated sample and the contents were directly loaded onto a 0.8% (w/v) agarose gel. The gel was run with standard TAE buffer pH 8.0 at 40 V for 4 h after which it was stained with 0.5 μg/mL solution of EtBr for 30 min. The data were documented using a UVITEC Gel Documentation center. The percentage of cleavage (C) was calculated using the expression[23]

$$C = \frac{[\text{Form II}] + 2[\text{Form III}]}{[\text{Form I}] + [\text{Form II}] + 2[\text{Form III}]} \quad (2.5)$$

In order to identify the actual reactive oxygen species responsible for DNA damage, a number of control experiments were carried out using various types of quenchers ('inhibitor studies').[24] Nitrogen gas was used to flush dioxygen, sodium azide (1 mM) was used as a $^1O_2$ quencher. DMSO (200 mM) and mannitol (100 mM) were used as $OH^{\bullet}$ scavengers. 4,5-dihydroxy-1,3-benzenedisulfonic acid disodium salt (Tiron, 10 mM) was used as a superoxide anion radical quencher. D_2O was used to increase the lifetime of singlet oxygen.

2.7 Binding experiments with hairpin DNA

Binding interactions of tri-cationic porphyrins with DNA Hairpins were also have been investigated during this work. The stock solution was made by dissolving each haipin DNA in appropriate buffer and kept overnight at 4 ^oC for complete dissolution. The concentration was measured by using its known extinction coefficient provided by the supplier at 260 nm.[25,26]

2.7.1 Absorption titration

Absorption titration experiments with hairpin DNA were carried out in a μ = 0.1, pH 6.8 phosphate buffer that included 0.05 M NaCl by varying r_0, $0.25 \leq r_0 \leq 15$ and maintaining the porphyrin concentration constant (1.7 μM). Absorbance values were recorded after each successive addition of DNA solution and equilibration (ca. 5 min.).[25-27]

2.7.2 Circular dichroism

Circular dichroism experiments were also performed with the DNA hairpins in the same buffer, in which absorption titrations have been carried out. To compensate for any offset, the baseline adjustment is such that each CD spectrum goes through zero at 480 nm. The spectra were recorded for $r_0 \sim 5$ maintaining the porphyrin concentration constant (1.7 μM).[25-27]

2.8 General considerations

Error estimation of the data, reconstruction of various spectra, calculations of rate constants, various regression analysis etc., that appear throughout this dissertation, have been carried out on an IBM compatible PC Pentium IV computer using the available in-house software/Origin 6.0 software package.

At all times, care was taken to avoid the entry of direct, ambient light into the samples in the spectroscopic and electrochemical experiments. Unless otherwise specified, all experiments were carried out at an ambient temperature (ca. 293 ± 3 K).

All hazardous chemicals were handled with appropriate precaution. Protective gloves, goggles, and safety mask were employed to minimize exposure to obnoxious chemicals, ultraviolet light etc.

The following are the standard error limits involved in various measurements (unless otherwise stated):

λ_{max} ± 1 nm; ε ± 10%; λ_{exc} ± 1 nm; λ_{em} ± 2 nm; ϕ ± 10%; $E_{1/2}$ ± 0.1 V; δ ± 0.01 ppm; J ± 1 Hz; K_{app} ± 10%; K_b ± 10%; T_m ± 1 ^oC; % DNA cleavage (C) ± 8%

2.9 References

1. *Vogel's Text Book of Practical Organic Chemistry* (Revised by Furniss, B. S.; Hannaford, A. J.; Smith, P. W. G.; Tatchell, A. R.), 5th ed.; Longmann (ELBS): Essex (U.K.), **1991**.
2. Perrin, D. D.; Armarego, W. L. F.; Perrin, D. R. *Purification of Laboratory Chemicals*, Pergamon: Oxford, **1980**.
3. Austin, E.; Gouterman, M. *Bioinorg. Chem*. **1978**, *9*, 281.
4. Quimby, D. J.; Longo, F. R. *J. Am. Chem. Soc*. **1975**, *97*, 5111.
5. Harriman, A.; Davila, J. *Tetrahedron* **1989**, *45*, 4737.
6. Kalyanasundaram. K. *Inorg. Chem*. **1984**, *23*, 2453.
7. Lackowicz, J. R. *Principles of Fluorescence Spectroscopy*; Plenum press: New York, **1983**.
8. Reichmann, M.E.; Rice, S. A.; Thomas, C. A.; Doty, P. *J. Am. Chem. Soc.* **1954,** *76*, 3047.
9. Fiel, R. J.; Howard, J. C.; Mark, E. H.; Dattagupta, N. *Nucleic Acids Res.* **1979**, *6*, 3093.
10. Pasternack, R. F.; Gibbs, E. J.; and Villafranca, J. J. *Biochemistry*, **1983**, *22*, 2406.
11. Carvlin, J. M.; Fiel, R. J. *Nucleic Acids Res.*1**983**, *11*, 6121.
12. McGhee, J. D.; von Hippel, P. H. *J. Mol. Biol*. **1974**, *86*, 469.
13. Kelly, J. M.; Murphy, J. M. *Nucleic Acids Res.*1**985**, *13*, 167.
14. Sari, M. A.; Battioni, J. P.; Mansuy, D.; Lepecq, J. B. *Biochem. Biophys. Res. Commun*. **1986**, *141*, 643.
15. Pasternack, R. F. *Chirality* **2003**, 15, 329.
16. Carvlin. M. J.; Mark, E.; Fiel. R. J.; Howard, J. C. *Nucleic Acids Res.* 1983, *11*, 6141.

17. Kelly, J. M.; Tossi, A. B.; McConnell, D. J.; OhUigin, C. *Nucleic Acids Res.*1**985**, *13*, 6017.
18. Marmur, J.; Doty, P. *J. Mol. Biol*. **1962**, *5*, 109.
19. Sambrook, J.; Russell, D. W. *Molecular Cloning A Laboratory Manual*; 3rd ed. Cold Spring Harbor Laboratory Press: New York, 2001.
20. Fisher, M. P.; Dingman, C. W. *Biochemistry* **1971,** *10*, 895.
21. Ajay, C.; Borst, P. *Biochim. Biophys. Acta* **1972,** *269*, 192.
22. Sugden, P. A. B.; Sambrook, J. *Biochemistry* **1973,** *12*, 3055.
23. Praseuth, D.; Gaudemer, A.; Verlhac, J-B.; Kraljic, I.; Sissoeff, I.; Guille, E. *Photochem. Photobiol*. **1986**, 44, 717.
24. Chatterjee. S. R.; Srivastava. T. S.; Kamat. J. P.; Devasagayam. T. P. A. *J. Porphyrins and Phthalocyanines* **1998**, *2*, 337.
25. Thomas, K. E.; McMillin, D. R. *J. Phys. Chem. B* **2001**, *105*, 12628.
26. Lugo-Ponce, P.; McMillin, D. R. *Coord. Chem. Rev*. **2000**, *208*, 169.
27. Eggleston, M. K.; Crites, D. K.; McMillin, D. R. *J. Phys. Chem. A* **1998**, *102*, 5506.

CHAPTER 3

Nucleobase (A, T, G and C) appended tri-cationic water-soluble porphyrins: Synthesis, characterization, binding and photocleavage studies with DNA

3.1 Introduction

Interest in cationic water-soluble porphyrins, particularly derivatives of N-methylpyridinium-4-yl porphyrins, is due to their versatile DNA binding ability that finds application in PDT,[1-4] or as antiviral agents.[5,6] Since cationic porphyrins bind with telomeric DNA, they also act as inhibitors of telomerase, an enzyme that has a significant role in extending the life time of tumor cells.[7-13] Interactions of tetra-cationic free-base porphyrins and metalloporphyrins with DNA have been extensively reported in the literature.[14-24] Dicationic porphyrins, which are sterically less demanding, bind with DNA only through intercalation irrespective of the base pairs.[25-27]

Recently, versatile binding nature of these porphyrins with DNA has been used to bring other moieties in the proximity of DNA. A variety of moieties have been connected to porphyrins to increase the binding affinity, to regulate the sequence specificity or to include chemical functionalities for inducing specific reactions.[28-37] Two novel cationic porphyrins bearing five-membered rings at the meso-positions, meso-tetrakis(1,3-dimethylimidazolium-2-yl)porphyrin and meso-tetrakis(1,2-dimethylpyrazolium-4-yl)porphyrin have been synthesized and their interactions with CTDNA were compared with that of 5,10,15,20-tetra-(N-methyl-4-pyridiniumyl)porphyrin (**H_2T4**).[38,39]

During the course of study with water-soluble porphyrins, it was found interesting to design nucleobase bearing cationic porphyrin analogous and to study the interactions of these with DNA. Nucleobase appended cationic

porphyrins have the potential to bind the duplex through multifunctional modes, i.e. *via* N-methylpyridinium group and the nucleobase subunit. We have synthesized nucleobase [A (adenine), T (Thymine), G (guanine) and C (cytosine)] appended tri-cationic porphyrins, **AT4**, **TT4**, **GT4** and **CT4**. The purine (A and G) and pyrimidine bases (C and T) were connected through N-9 and N-1 nitrogen atoms to the porphyrin, respectively by -O(CH_2)$_2$- spacer.[40] Here we discuss the synthesis and spectral characterization of all the four newly synthesized porphyrins (Scheme 3.1). Results of the experiments carried out to probe the DNA binding and photo cleavage proclivities are also analysed in this chapter.

3.2 Experimental section

Tosylate salt of **H_2T4** was obtained from Aldrich (U.S.A) and used as such. 5,10,15,20-Tetraphenylporphyrin (**H_2TPP**),[41] the reference compound employed during this investigation, was synthesized according to the reported procedure.

3.2.1 Synthesis of 5-(4-hydroxyphenyl)-10,15,20-tripyridyl porphyrin (1)

This compound was prepared by a modification of the reported procedure.[42] A solution of 4-pyridinecarboxaldehyde (8.0 g, 74 mmol) in 200 mL of propanoic acid was warmed to 120 °C with vigorous stirring for 30 min. 4-Hydroxybenzaldehyde (3.0 g, 24 mmol) and pyrrole (5.0 g, 75 mmol) were added and the resulting mixture was refluxed for 1 h. The solution was cooled to room temperature and the precipitate was filtered off, washed with methanol and dried. The solid was dissolved in $CHCl_3$ containing a few drops of methanol and was subjected to column chromatography (basic alumina) eluting with $CHCl_3$:CH_3OH (97:3, V/V). The first, fast moving fraction was identified as 5,10,15,20-tetra(4-pyridyl)porphyrin. The desired compound was eluted out when the eluent was

changed to $CHCl_3$:CH_3OH (93:7, V/V). The collections were evaporated to get **1**. Yield = 0.15 g (8%).

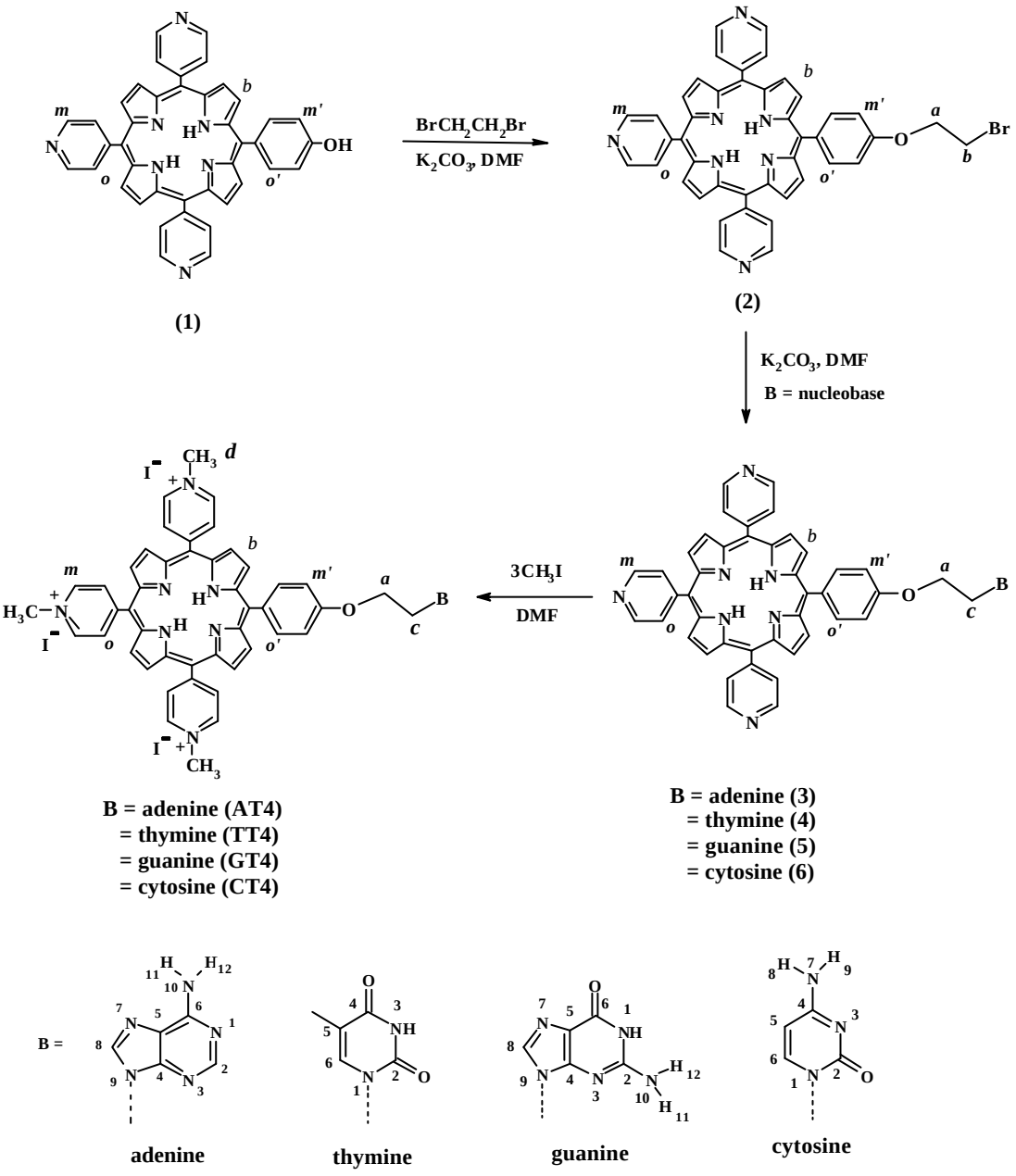

Scheme 3.1 Synthesis of nucleobase appended tri-cationic porphyrins

3.2.2 Synthesis of 5-(4-(2-bromoethoxy)phenyl)-10,15,20-tripyridyl porphyrin (2)

A mixture of **1** (0.2 g, 0.32 mmol), anhydrous K_2CO_3 (0.5 g, 3.62 mmol) and 1,2-dibromoethane (0.08 g 0.42 mmol) in dry dimethylformamide (30 mL) was stirred under nitrogen for 24 h. After the solvent was removed under vacuum, the remaining residue was dissolved in $CHCl_3$ and loaded on a silica gel column. Using $CHCl_3$:CH_3OH (97:3, V/V) as the eluent, the desired product **2** was eluted out. Yield = 0.14 g (60%).

3.2.3 Synthesis of 5-(4-(9-(2-oxyethyl)adenine)phenyl)-10,15,20-tripyridyl porphyrin (3)

A mixture of **2** (0.074 g, 0.1 mmol), anhydrous K_2CO_3 (1.7 g, 1.1 mmol) and adenine (0.015 g, 0.11 mmol) in dry dimethylformamide (15 mL) was stirred under nitrogen for 24 h. The solvent was removed under vacuum, the residue was dissolved in $CHCl_3$ containing a few drops of CH_3OH and loaded on a silica gel column. Using $CHCl_3$:CH_3OH (97:3, V/V) as the eluent, the first collected fraction was identified to be unreacted **2**. The desired product **3** was eluted out as the second band when the solvent was changed to $CHCl_3$:CH_3OH (95:5, V/V). Yield = 0.05 g (62%). MALDI MS: $[M]^+ = 794$, $[M–(C_7H_8N_5)]^+ = 632$.

3.2.4 Synthesis of 5-(4-(1-(2-oxyethyl)thymine)phenyl)-10, 15, 20-tripyridyl porphyrin (4)

A mixture of **2** (0.074 g, 0.10 mmol), anhydrous K_2CO_3 (1.7 g, 1.10 mmol) and thymine (0.014 g, 0.11 mmol) in dry dimethylformamide (30 mL) was stirred under nitrogen for 24 h. The solvent was removed under vacuum, the residue was dissolved in $CHCl_3$ containing a few drops of CH_3OH and loaded on a silica gel column. Using $CHCl_3$:CH_3OH (97:3, V/V) as the eluent, the first

fraction collected was identified to be unreacted **2**. The desired product **4** was eluted out as the second band when the solvent was changed to $CHCl_3$:CH_3OH (95:5, V/V). Yield = 0.04 g (53%). FAB MS: $[M+H]^+$ = 786, $[M–(C_7H_9N_2O_2)]^+$ = 633.

3.2.5 Synthesis of 5-(4-(9-(2-oxyethyl)guanine)phenyl)-10,15,20-tripyridyl porphyrin (5)

A mixture of **2** (0.074 g, 0.10 mmol), anhydrous K_2CO_3 (1.7 g, 1.10 mmol) and guanine (0.017 g, 0.11 mmol) in dry dimethylformamide (30 mL) was stirred under nitrogen for 24 h. The solvent was removed under vacuum, the residue was dissolved in $CHCl_3$ containing a few drops of CH_3OH and loaded on a silica gel column. Using $CHCl_3$:CH_3OH (97:3, V/V) as the eluent, the first fraction collected was identified to be unreacted **2**. The desired product **5** was eluted out as the second band when the solvent was changed to $CHCl_3$:CH_3OH (95:5, V/V). Yield = 0.03 g (40%). FAB MS: $[M+H]^+$ = 811, $[M–(C_7H_8N_5O)]^+$ = 633.

3.2.6 Synthesis of 5-(4-(1-(2-oxyethyl)cytosine)phenyl)-10,15,20-tripyridyl porphyrin (6)

A mixture of **2** (0.074 g, 0.10 mmol), anhydrous K_2CO_3 (1.7 g, 1.10 mmol) and cytosine (0.012 g 0.11 mmol) in dry dimethylformamide (30 mL) was stirred under nitrogen for 24 h. The solvent was removed under vacuum, the residue was dissolved in $CHCl_3$ containing a few drops of CH_3OH and loaded on a silica gel column. Using $CHCl_3$:CH_3OH (97:3, V/V) as the eluent, the first fraction collected was identified to be unreacted **2**. The desired product **6** was eluted out as the second band when the solvent was changed to $CHCl_3$:CH_3OH

(92:8, V/V). Yield = 0.04 g (45%). FAB MS: $[M+H]^+$ = 771, $[M-(C_6H_8N_3O)+3H]^+$ = 635.

3.2.7 Methylation of 3, 4, 5 and 6

All the nucleobase-appended porphyrins were methylated by stirring each of them with a large excess of methyl iodide (~90 equiv.) in dry dimethylformamide for 15 min at room temp. The reaction was monitored by TLC (silica gel) CH_2Cl_2:CH_3OH, (95:5, V/V) (Note: the product does not migrate on the TLC plate). The solvent and the excess methyl iodide were removed under vacuum. The residue was taken up in CH_3OH and precipitated with diethyl ether. All the tri-cationic nucleobase linked porphyrins **AT4**, **TT4**, **GT4** and **CT4** of **3**, **4**, **5** and **6**, respectively were obtained in nearly quantitative yields.

3.3 Results and discussion

Synthesis of all the four new compounds (**3-6**) has been accomplished in moderate yields, by a simple condensation between the ethylbromo porphyrin derivative and nucleobase. Reaction of excess ethylbromo porphyrin with nucleobase in presence of K_2CO_3 and DMF gives the corresponding nucleobase appended pyridyl porphyrins. Tri-cationic porphyrins (**AT4**, **TT4**, **GT4** and **CT4**) were obtained by methylating pyridyl porphyrins in the presence of DMF and methyl iodide. The pyridyl, methylated and their precursor porphyrins synthesized in this study were characterized by FAB/MALDI MS, NMR (^1H and ^1H-^1H COSY) and UV-visible spectroscopic methods.

3.3.1 Ground state properties

The MALDI MS spectrum of **3** is illustrated in Fig. 3.1. MALDI MS spectrum of **3** and FAB mass spectral data of **4-6** (see section 3.2) show the parent

ion peak, as expected. The MALDI MS spectral data of all the four methylated nucleobase bearing compounds show less intense peak (without the three counter ions) and intense peaks due to the fragments: MALDI MS **AT4**: $[M–3I]^+$ = 839, $[M–(CH_3I_3)]^+$ = 824, $[M–(C_9H_{15}N_5I_3)]^+$ = 647; **TT4**: $[M–3I]^+$ = 830, $[M–(C_9H_{16}N_2O_2I_3)]^+$ = 646; **GT4**: $[M–C_3H_9I_3]^+$ = 810, $[M–(C_9H_{15}N_5OI_3)]^+$ = 646; **CT4**: $[M–3I]^+$ = 815, $[M–(C_8H_{15}N_3OI_3)]^+$ = 646.

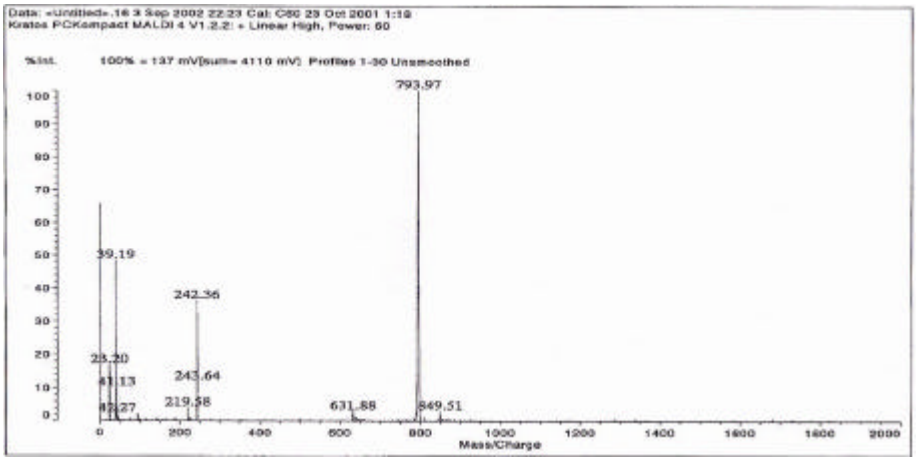

Fig. 3.1 MALDI MS spectrum of **3**

Fig. 3.2 illustrates the ^{1}H NMR spectrum recorded for **CT4** porphyrin in DMSO-d_6. ^{1}H NMR spectral data of all the new compounds along with their individual constituents are summarized in Table 3.1. Spectra were analyzed based on the resonance position and integrated intensity data. ^{1}H NMR data of the nucleobase tri-cationic porphyrins show peaks due to nucleobase moiety and confirm the presence of nucleobase in **3**-**6** as well as the methylated compounds (**AT4**, **TT4**, **GT4** and **CT4**). The -C*H* protons of purine porphyrins, **AT4** (2- and 8- position) and **GT4** (8-position) appear at 8-9 ppm. Among the pyrimidine

porphyrins, **CT4** clearly shows peaks corresponding to two -C*H* protons of cytosine, which resonate as doublets at 8.01 and 6.19 ppm.

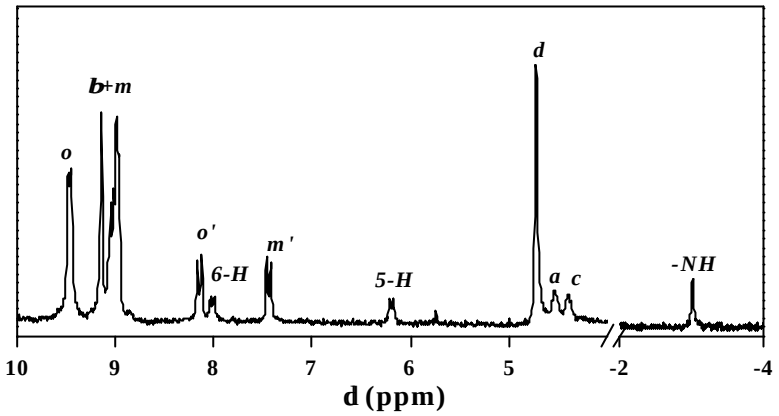

Fig. 3.2 ^{1}H NMR spectrum of **CT4** (200 MHz, 300 K) in DMSO-d_6, TMS. (for peak assignments please see Scheme 3.1)

Table 3.1 ^{1}H NMR data for **1**-**6**, **AT4**, **TT4**, **GT4** and **CT4** [a]

Compd.	d, ppm				
	Porphyrin	**Nucleobase**	**OCH_2**	**NCH_2**	**CH_2Br**
1 [b]	8.82 (8H, ***b***, bs), 8.93 (6H, *o*, d, J = 5.0 Hz), 8.20 (6H, *m*, d, J = 5.0 Hz), 7.93 (2H, *o¢*, d, J = 6.3 Hz), 7.15 (2H, *m¢*, d, J = 6.3 Hz)	-	-	-	-
2 [c]	9.00-8.75 (8H, ***b***, m), 9.06 (6H, *o*, d, J = 5.8 Hz), 8.35 (8H, *m+o¢*, m), 7.33 (2H, *m¢*, m), –2.87 (2H, *NH*, bs)	-	3.87 (2H, *a*, t)	-	4.58 (2H, *b*, t)
3 [b]	8.80 (8H, ***b***, bs), 8.96 (6H, *o*, d, J = 5.5 Hz), 8.14 (6H, *m*, d, J = 5.5 Hz), 8.04 (2H, *o¢*, d, J = 8.4 Hz), 7.22 (2H, *m¢*, m), –2.98 (2H, *NH*, bs)	8.32 (2H, *2-H+8-H*, s)	4.76 (2H, *a*, t)	4.57 (2H, *c*, t)	-
4 [c]	9.05-8.88 (8H, ***b***, m), 9.10 (6H, *o*, d, J = 5.7 Hz), 8.16 (8H, *m+o¢*, m), 7.28 (2H, *m¢*, m), –2.79 (2H, *NH*, bs)	8.25 (1H, *3-H*, s), 7.39 (1H, *6-H*, s), 2.05 (3H, *5-methyl*, s)	4.55 (2H, *a*, t)	4.35 (2H, *c*, t)	-

……continued

…..Table 3.1

5 [c]	9.00-8.78 (8H, ***b***, m), 9.06 (6H, *o*, d, J = 5.6 Hz), 8.25-8.08 (8H, *m*+*o*¢, m), 7.37 (2H, *m*¢, d, J = 5.0 Hz), –2.86 (2H, *NH*, bs)	7.31 (1H, *8-H*, s)	4.65 (2H, *a*, t)	4.49 (2H, *c*, t)	-
6 [b]	9.10-8.60 (14H, ***b*** +*o*, m), 8.13 (6H, *m*, d, J = 5.3 Hz), 8.08 (2H, *o*¢, d, J = 9.0 Hz), 7.24 (2H, *m*¢, m), –2.90 (2H, *NH*, bs)	7.55 (1H, *6-H*, d, J = 7.4 Hz), 5.70 (1H, *5-H*, d, J = 7.4 Hz)	4.45 (2H, *a*, bt)	4.25 (2H, *c*, bt)	-
AT4 [d]	9.30-8.85 (14H, ***b***+*m*, m), 9.46 (6H, *o*, d, J = 6.6 Hz), 8.12 (2H, *o*¢, d, J = 8.7 Hz), 7.41 (2H, *m*¢, d, J = 8.7 Hz), 4.80-4.60 (9H, *d*, bs), –3.02 (2H, *NH*, bs)	8.80 (1H, *2-H*, s), 8.78 (1H, *8-H*, s)	4.85 (2H, *a*, bt)	4.80-4.60 (2H, *c*, bs)	-
TT4 [d]	9.26-8.93 (14H, ***b***+*m*, m), 9.46 (6H, *o*, d, J = 6.4 Hz), 8.12 (2H, *o*¢, d, J = 8.3 Hz), 7.43 (2H, *m*¢, d, J = 8.3 Hz), 4.71 (9H, *d*, s), –3.00 (2H, *NH*, bs)	7.75 (1H, *6-H*, s), 1.86 (3H, *5-methyl*, s)	4.52 (2H, *a*, bt)	4.24 (2H, *c*, bt)	-
GT4 [d]	9.20-8.84 (14H, ***b***+*m*, m), 9.46 (6H, *o*, d, J = 7.0 Hz), 8.14 (2H, *o*¢, d, J = 8.3 Hz), 7.46 (2H, *m*¢, d, J = 8.3 Hz), 4.80-4.60 (9H, *d*, bs) –2.95 (2H, *NH*, bs)	9.93 (1H, *1-H*, s), 8.30 (1H, *8-H*, s)	4.80-4.60 (2H, *a*, bs)	4.54 (2H, *c*, bt)	-
CT4 [d]	9.30-8.80 (14H, ***b***+*m*, m), 9.46 (6H, *o*, d, J = 5.3 Hz), 8.14 (2H, *o*¢, d, J = 9.0 Hz), 7.44 (2H, *m*¢, d, J = 9.0 Hz), 4.72 (9H, *d*, s), –3.01 (2H, *NH*, bs)	8.01 (1H, *6-H*, d, J = 7.4 Hz), 6.19 (1H, *5-H*, d, J = 7.4 Hz)	4.53 (2H, *a*, bt)	4.34 (2H, *c*, bt)	-

[a] Error limits: δ, 0.01 ppm, J, ±1 Hz. [b] Spectra were recorded in $CDCl_3$ + CD_3OD. [c] Spectra were recorded in $CDCl_3$. [d] Spectra were recorded in DMSO-d_6.

Fig. 3.3 illustrates the ^1H-^1H COSY spectrum of **6**. The two cytosine protons of **6** appear as doublets at 7.67 ppm and 5.85 ppm and show proton-proton connectivity. The compound **TT4** shows two singlets at 1.86 and 7.75 ppm due to the -CH_3 and -C*H* protons, respectively. The resonance positions of the protons on porphyrin components (protons ***b***, *o*, *m*, *o*¢, *m*¢ and *d*; see Scheme 3.1 for proton assignments) of **3**, **4**, **5** and **6** are more or less similar to those of **1** and **2**. On the other hand, the resonance positions and the splitting patterns of the

protons on their tri-cationic porphyrins are quite different from those of **1** and **2**. The ortho protons of the methylated porphyrins are deshielded and resonate at around 9.45 ppm, which were resonating at around 9.00 ppm for the nucleobase appended pyridyl porphyrins. The methylated compounds **AT4**, **TT4**, **GT4** and **CT4** show a sharp singlet (9H) between 4.71-4.72 ppm (cf. δ(C*H*$_3$I): 2.18), which corresponds to the resonance of N-methyl protons. A comparison of these spectra with those of the precursor compounds reveal that the resonance positions of the various protons present either on the porphyrin macrocycle or the nucleobase moiety are not shifted considerably upon linking the two moieties *via* the -OCH_2CH_2- spacer.

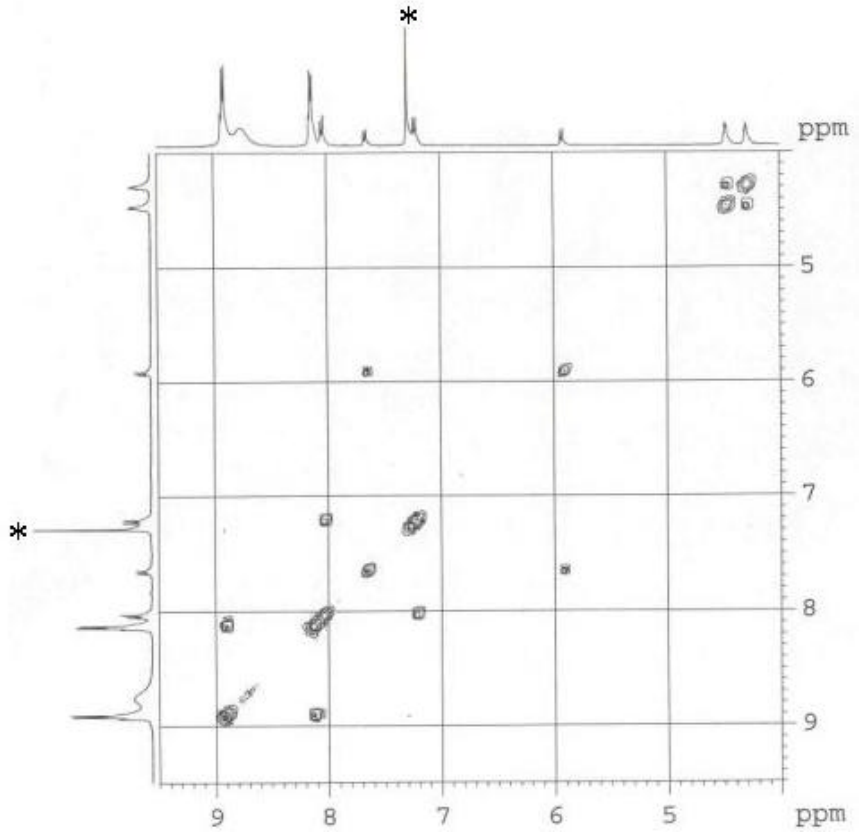

Fig. 3.3 ^{1}H-^{1}H COSY spectrum of **6** recorded in $CDCl_3$ + CD_3OD (* peak is due to solvent, 400 MHz, 300K).

The UV-visible spectra of **AT4**, **TT4**, **GT4** and **CT4** are shown in Fig. 3.4. The wavelengths of maximum absorbance (λ_{max}) and molar extinction coefficient (ε) values of the newly synthesized compounds and those of their constituent individual components, as obtained from the UV-visible studies, are summarized in Table 3.2. The UV-visible spectra of **3**, **4**, **5** and **6** show that the λ_{max} values lie in the same range as **1** and **2** and the corresponding nucleobase. The porphyrin Soret and Q-bands of **AT4**, **TT4**, **GT4** and **CT4** are close to the corresponding bands of $\mathbf{H_2T4}$.[43] Similarly the band, which is present in the UV region in these cationic porphyrins due to the absorption of the nucleobase moiety connected to porphyrin in each case, is close to the absorption of corresponding free nucleobase. The UV-visible spectra of these cationic systems reported here are quite similar to those of the monomers forming them. Thus, UV-visible data reveals that there is no π-π interaction between the porphyrin chromophore and the nucleobase moiety in solution.

Table 3.2 UV-visible data of pyridyl, tri-cationic nucleobase appended porphyrins and their precursors.[a]

Compd.	λ_{max}, nm (log e)		
	Soret band	**Q-band**	**Nucleobase**
1 [b]	419 (5.06)	647 (3.09), 590 (3.25), 550 (3.38), 515 (3.76)	-
2 [b]	418 (5.49)	645 (3.42), 590 (3.66), 548 (3.76), 514 (4.18)	-
3 [b]	418 (5.50)	645 (3.41), 590 (3.65), 548 (3.75), 514 (4.17)	270 (4.31)
4 [b]	418 (5.41)	645 (3.40), 590 (3.55), 548 (3.55), 514 (4.07)	265 (4.21)
5 [b]	418 (5.37)	645 (3.30), 589 (3.53), 548 (3.63), 514 (4.04)	270 (3.98)

….continued

…….Table 3.2

6 [b]	418 (5.37)	645 (3.29), 589 (3.53), 548 (3.63), 514 (4.04)	270 (4.11)
AT4 [c]	425 (5.20)	646 (3.20), 585 (3.62), 561 (3.66), 521 (3.96)	260 (4.41)
TT4 [c]	425 (5.26)	643 (3.31), 584 (3.76), 561 (3.78), 521 (4.06)	263 (4.44)
GT4 [c]	425 (5.20)	643 (3.25), 584 (3.71), 561 (3.72), 521 (3.99)	259 (3.94)
CT4 [c]	425 (5.15)	643 (3.28), 584 (3.71), 561 (3.73), 521 (3.94)	265 (4.27)
Adenine [b]	-	-	275 (3.56)
Thymine [b]	-	-	274 (3.67)
Guanine [d]	-	-	248 (4.04), 275 (3.87)
Cytosine [b]	-	-	275 (3.58)

[a] Error limits: λ_{max}, ± 1 nm, log ε, ± 10%. [b] Spectra were measured in DMF. [c] Spectra were measured in H_2O. [d] Spectrum was measured in 10 mL H_2O containing 2 drops of conc. HCl.

3.3.2 Excited state properties

Table 3.3 summarizes the fluorescence quantum yield (ϕ) values of the pyridyl and cationic porphyrins. The emission spectra of nucleobase tri-cationic appended porphyrins and their reference compound **H_2T4** in H_2O are shown in Fig. 3.5. Inspection of the data given in the Table reveals that the quantum yield and the emission peak maximum of nucleobase-linked pyridyl porphyrins **1-6** are close to those of their standard **H_2TPP**.[44] Similarly, the results obtained for tri-cationic nucleobase-linked porphyrins are close to those of their standard **H_2T4**.[43] Thus, linking of nucleobase does not have any adverse effect on the singlet state properties of these nucleobase-linked porphyrins.

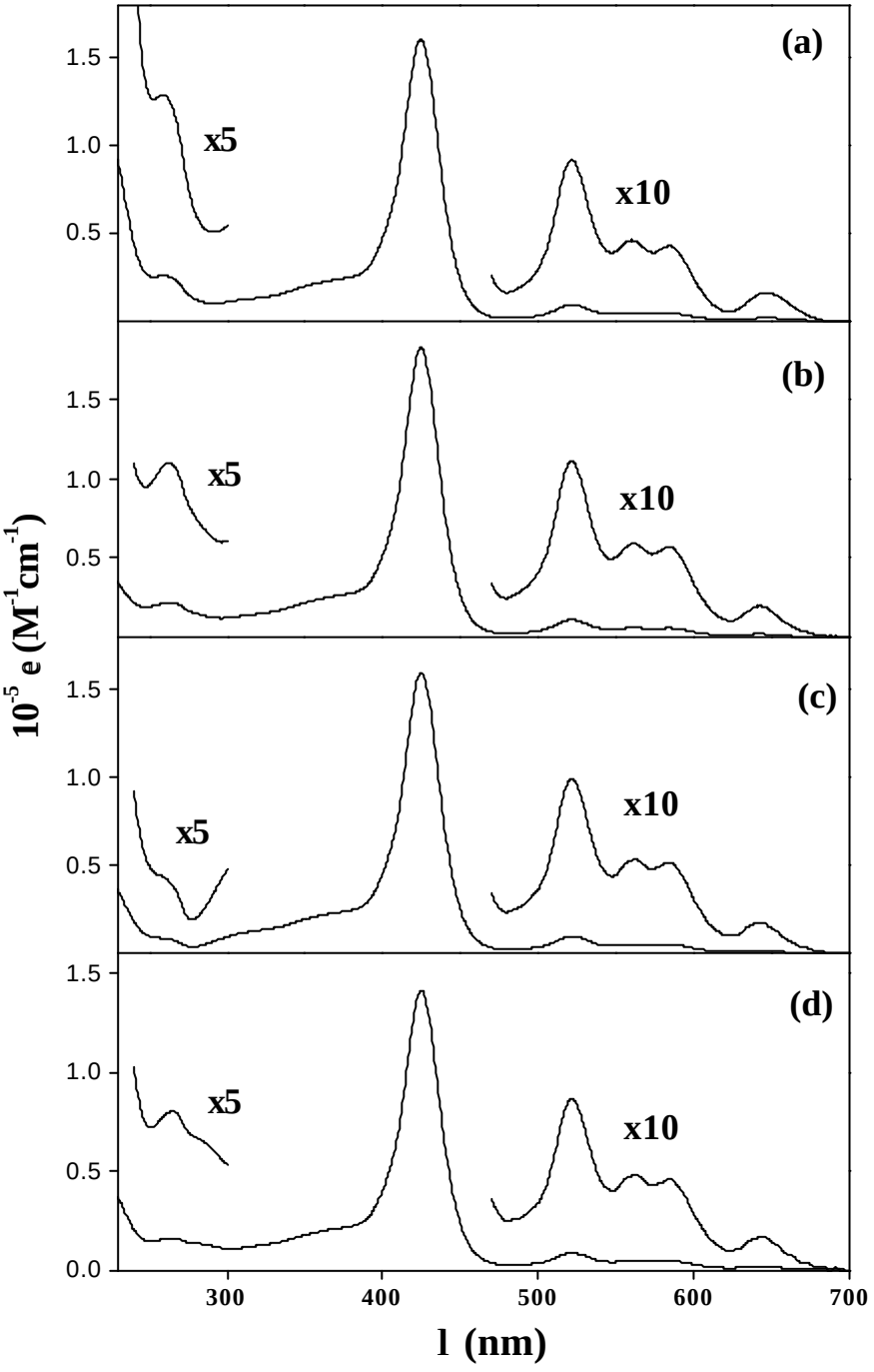

Fig. 3.4 UV-visible spectra of (a) **AT4** (b) **TT4** (c) **GT4** and (d) **CT4** in H_2O.

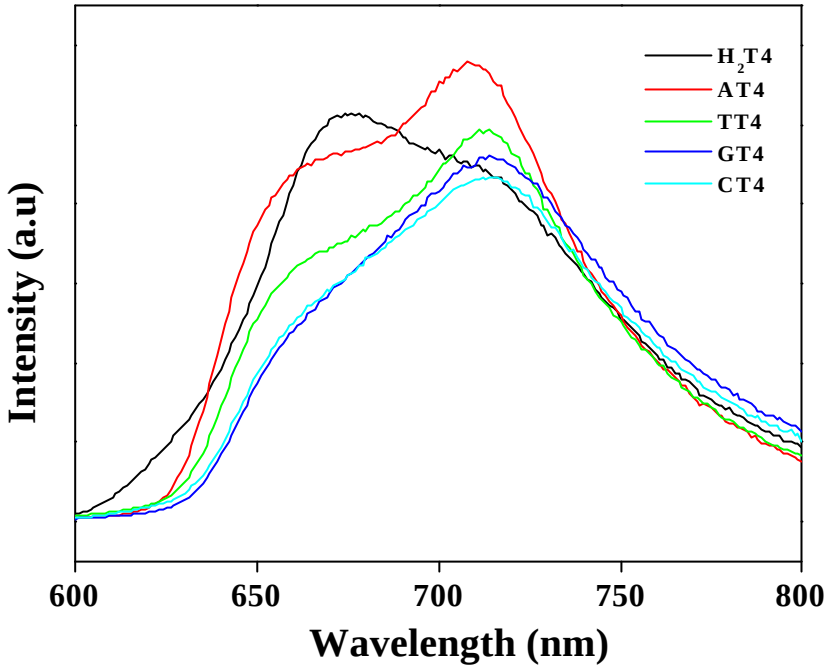

Fig. 3.5 Fluorescence spectra of **H_2T4** and nucleobase appended tri-cationic porphyrins in H_2O: λ_{ex} = 425 nm.

3.4 DNA binding

DNA binding by the newly synthesized tri-cationic porphyrins with CTDNA during this study has been monitored by absorption, luminescence, circular dichroism (CD) and thermal melting methods. All these porphyrins were present as monomers under the set of titration conditions.

Fig. 3.6 illustrates the absorption titration performed with the guanine-linked porphyrin (**GT4**) in the presence of CTDNA. Similar titrations were carried out for **AT4**, **CT4** and **TT4** cationic porphyrins. Absence of an isosbestic point observed is suggestive of two or more binding modes.[36] Table 3.4 summarizes change in the absorbance maxima and percentage of hypocromism

Table 3.3 Fluorescence data for pyridyl and tri-cationic nucleobase appended porphyrins and their precursors [a]

Compd.	λ_{em}, nm (f)
in DMF, λ_{ex} = 420 nm	
1	652, 716 (0.14)
2	649, 715 (0.13)
3	649, 715 (0.13)
4	649, 715 (0.12)
5	649, 715 (0.13)
6	652, 716 (0.14)
in H_2O, λ_{ex} = 425 nm	
AT4	713 (0.046)
TT4	714 (0.043)
GT4	714 (0.042)
CT4	716 (0.044)

[a] Error limits: λ_{em}, ± 1 nm; ϕ, ± 10 %

values for the porphyrins investigated during this study obtained from absorption titration experiments. The apparent DNA binding constants (K_{app}) obtained from the absorption titrations using eqn. 2.2 are also listed in Table 3.4. Due to the structural similarity of the purine bases (A and G) the spectral changes in **AT4** and **GT4** porphyrins can be compared with each other as well the pyrimidine bases (C and T) linked porphyrins **TT4** and **CT4**. Spectral changes observed for these porphyrins are then compared with those observed for **H_2T4** under the same conditions.[18,45,46] The Soret band of the **AT4**, **TT4** and **GT4** porphyrins show a

slightly higher bathochromic shift (9-10 nm) and lesser % hypochromicity (7-13 %) than the standard **H_2T4** porphyrin, which exhibits 7 nm bathochromic shift and 38 % hypochromicity at $r_0 \sim 40$.

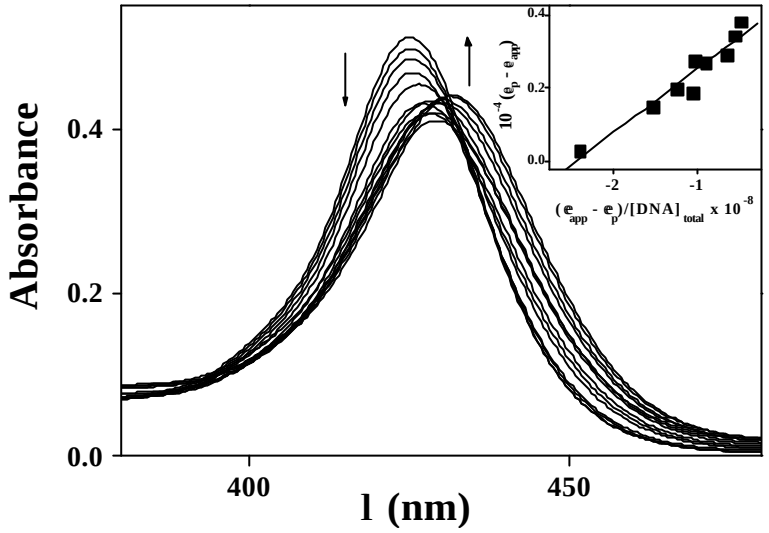

Fig. 3.6 Absorption titration of **GT4** performed with CTDNA in pH 6.8 phosphate buffer, μ = 0.5 M. The inset shows the binding isotherm for apparent binding constant (K_{app}) calculation.

CT4 porphyrin also shows a bathochromic shift of 9 nm but it exhibits hyperchromicity with same r_0 (r_0 = [DNA]/[porphyrin]) value. With smaller r_0 values decrease in the absorption intensity as well as bathochromic shift were observed but with higher r_0 values the absorbance intensity starts enhancing without change in the absorption maxima. In contrast, with **H_2T4** only decrease in the absorption intensity was observed even with higher r_0 values. The binding constant values are similar to that of the **H_2T4** porphyrin or slightly more. All these results reveal that the behavior of the newly synthesized nucleobase tri-cationic porphyrins is more or less similar to that of **H_2T4**, which interacts with the CTDNA through both by intercalation and external binding.

The fluorescence spectra of all the nucleobase tri-cationic porphyrins were recorded by exciting at λ_{ex} = 425 nm in the presence of large excess of CTDNA. Fig. 3.7 illustrates the fluorescence titration performed for **GT4** with CTDNA. Table 3.4 summarizes the λ_{max} values of the emission peaks and the calculated intrinsic binding constant (K_b) values using eqn. 2.4.[47] For these porphyrins, the interactions with CTDNA cause splitting of the broad fluorescence band into two distinct bands. In the case of **H_2T4**, the broad band splits into two distinct bands with maxima at 654 and 714 nm[48,49] whereas in the nucleobase linked porphyrins it splits into bands at 661 and 721 nm (centered at about 675 nm in the absence of CTDNA). Enhancement in intensity was observed with CTDNA for all the four compounds similar to that for **H_2T4**. Fluorescence titration experiments followed by binding constant calculations provided the K_b values (see Table 3.4) that were comparable to those obtained in the UV-visible experiments.

The porphyrins do not display circular dichroism in the absence of DNA, whereas spectra are induced in the Soret region when they are bound to natural or artificial DNA. The induced CD spectra for **H_2T4** and the newly synthesized nucleobase tri-cationic porphyrins were recorded in the presence of CTDNA with different r_0 ($3 \leq r_0 \leq 32$) values. The CD experiments were performed starting from r_0 ~3 to assure the formation of 1:1 adduct. Similar to **H_2T4**, all the porphyrins feature a positive and negative signal, reflecting the coexistence of the two modes of interaction i. e., intercalation and external interaction in the groove.[18,46,50,51]

Fig. 3.8 depicts the CD spectra of **GT4** porphyrin recorded in the presence of CTDNA with various r_0 values. Fig. 3.9 illustrates the spectra recorded between 350-500 nm for various nucleobase tri-cationic porphyrins and **H_2T4** at

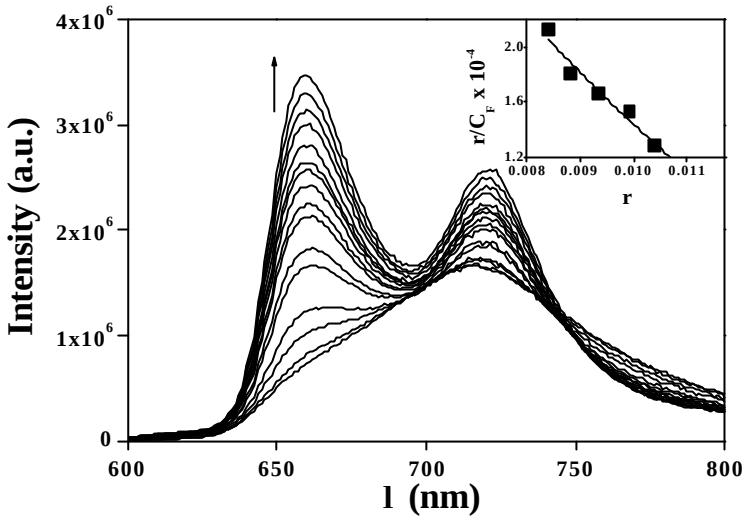

Fig. 3.7 Fluorescence titration of **GT4** with CTDNA in pH 6.8 phosphate buffer, μ = 0.5 M. The inset shows the binding isotherm for binding constant (K_b) calculation.

r_0 ~ 3.2. The data obtained from CD experiments are also summarized in Table 3.4. In the case of **GT4**, the intensity of the negative band decreases with increase in r_0, which means that the intercalation is favoured at low r_0 values whereas the other porphyrins do not show much change in intensities with increase in the r_0 values.[37] Analysis of CD spectra recorded at constant r_0 ratio reveals that the mode of interaction differs with different nucleobase tri-cationic porphyrins. At lower ratio r_0 ~ 3.2, only porphyrin connected to **GT4** and **H_2T4** porphyrin show positive peak due to external binding. From the earlier reported works with cationic porphyrins, a positive and a negative induced CD signals have been recognized as due to interaction of external binding and intercalation, respectively.[17]

Among the purine base containing porphyrins **AT4** and **GT4**, the former shows only a weak negative induced CD signal while the latter shows an intense

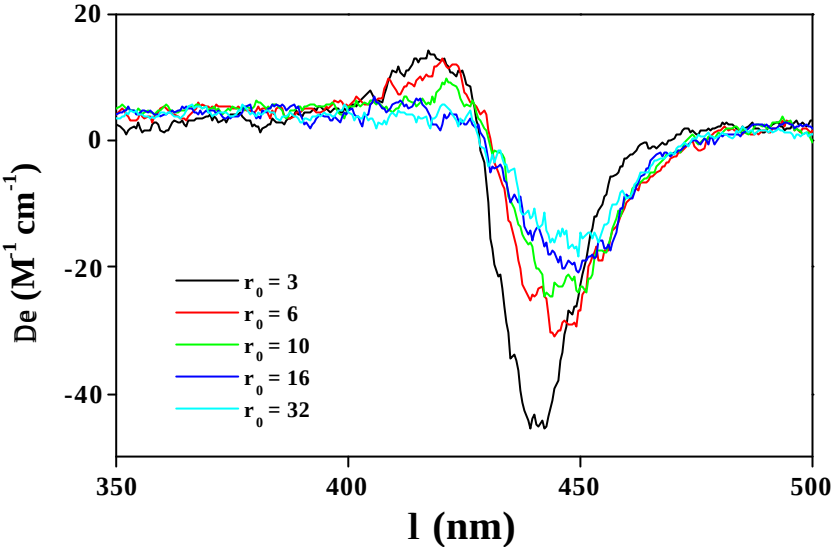

Fig. 3.8 CD spectra of **GT4** with CTDNA (350-500 nm) recorded in 0.017 M, pH 6.8 phosphate buffer at various r_0 values.

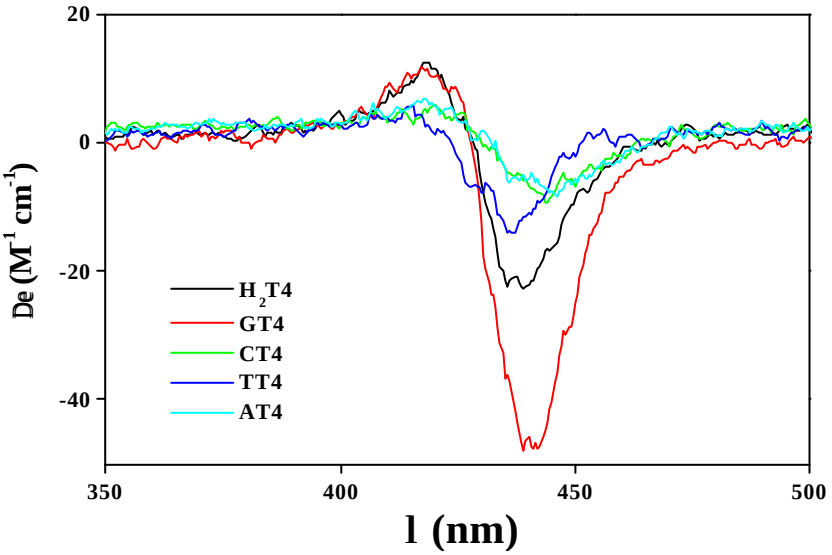

Fig. 3.9 CD spectra of nucleobase tri-cationic porphyrins and **H_2T4** with CTDNA (350-500 nm) recorded in 0.017 M, pH 6.8 phosphate buffer at r_0 ~ 3.2:1.

Table 3.4 Spectral data and binding constants for nucleobase appended tri-cationic porphyrins and **H_2T4** with CTDNA

Compound	Soret absorbance [a]		CD [d]	Emission [e]	
	D l, nm [b] (%H) [c]	K_{app} M^{-1} x 10^4	l, nm (De, $M^{-1}cm^{-1}$)	l, nm [f]	K_b M^{-1} x 10^4
AT4	9 (13)	2.40	417 (+7) 446 (-8)	662, 721	2.87
TT4	10 (7)	4.90	416 (+6) 437 (-14)	661, 720	4.44
GT4	9 (10)	5.62	417(+12) 439 (-48)	659, 721	6.36
CT4	9 (-3)	1.09	420 (+6) 444 (-9)	660, 721	3.24
H_2T4	7 (38)	2.29	418(+13) 439 (-23)	655, 716	3.45

[a] Spectra were recorded in μ = 0.5 M, phosphate buffer pH 6.8 at DNA base:porphyrin ratio 40:1. [b] Shift induced in Soret maximum. [c] Percent drop in absorbance intensity. [d] Spectra were recorded in μ = 0.017 M, phosphate buffer pH 6.8 at DNA base:porphyrin ratio 3.2:1 [e] Spectra were recorded in μ = 0.5 M, phosphate buffer, pH 6.8. [f] Maxima in the emission spectrum.

peak (than **H_2T4**). **CT4** and **TT4** also show difference in their mode of interaction with **H_2T4** porphyrin:**TT4** exhibits a peak more intense than **CT4**, but less intense than **H_2T4**. Intense negative CD peaks confirm that porphyrin in **GT4** and **TT4** intercalate readily whereas only less efficiency was observed for intercalation with the porphyrins in **AT4** and **CT4**.

The acidity of the NH sites in nucleobase follows the order: guanine (N10H11 and N1H) > thymine (N3H) > cytosine (N7H8) > adenine (N10H11).

The acidic protons present in the N1 and N3 of guanine and thymine favour keto-enol tautomerism in these nucleobases.[52] If only the porphyrin moiety intercalates and nucleobase is present in the unbound form, the efficiency of intercalation is expected to be more or less similar for these nucleobase appended porphyrins since the difference in the tautomerism is not going to affect the ability of the porphyrin interaction much, as the porphyrin and nucleobase moiety are connected through the alkyl chain.

The next case is that of the nucleobase in the bound form. The stability arising due to the keto-enol tautomerism of the bound nucleobase may increase the intercalation of porphyrin in the duplex. The weaker intercalating efficiency of porphyrins appended in **AT4** and **CT4** compared to **H_2T4** is possibly due to the presence of only three positive charges in **AT4** and **CT4**.[37] The CD spectra of adenine and cytosine porphyrins show a longer wavelength shift of 7 nm and 5 nm respectively in the negative region; this may be due to binding in a different mode compared to guanine and thymine porphyrins. Extended conjugation and ability to form three hydrogen bonds in guanine moiety may drive the porphyrin in **GT4** to intercalate better relative to porphyrin in **TT4**, which can form only two hydrogen bonds and less conjugation with only six membered ring.

Fig. 3.10 illustrates the CD spectra recorded for various nucleobase tri-cationic porphyrins and **H_2T4** at $r_0 \sim 3.2$ in the UV region between 220 and 300 nm. The CD spectrum of CTDNA recorded in the absence of porphyrins consists of a positive band at 284 nm (UV: λ_{max} 259 nm) due to base stacking and a negative band at 246 nm due to helicity and is characteristic of DNA in the right-handed B-form.[53] The spectral changes observed in the UV-region is due to the change in the conformation of the DNA. This conformational change could be due to the effect of porphyrin chromophore (since porphyrin also has little absorption in the same region) or due to the nucleobase moiety or even

combination of both. The transition in the conformation resulted by **TT4** is almost similar to that of **H_2T4**. Both the porphyrins do not show much change in the negative peak except that the positive peak disappears and a new negative peak arises at the same wavelength.

Upon addition of **AT4** and **CT4** porphyrins, the positive band of both becomes bisignate and the negative band appears the same with slightly lesser magnitude. Surprisingly with **GT4** both the positive and negative bands disappear and a new negative band emerges ~270 nm. All these data together reveal that the interaction of **AT4** and **CT4** with CTDNA are similar but differ from the other porphyrin (**GT4** and **TT4**) interactions. Thus the intercalating efficiency of the porphyrin present in nucleobase tri-cationic porphyrins and standard follows the order **GT4** > **H_2T4** > **TT4** > **AT4** ~ **CT4**.

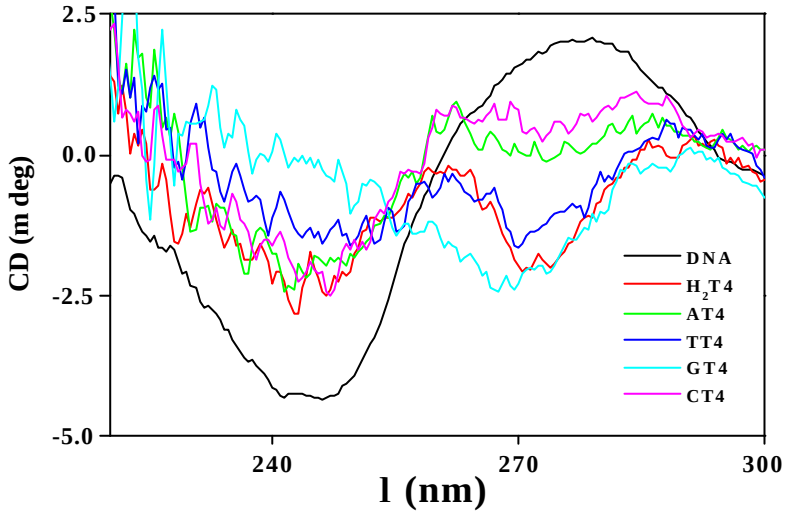

Fig. 3.10 CD spectra of nucleobase tri-cationic porphyrins and **H_2T4** with CTDNA (220-300 nm) recorded in 0.017 M, pH 6.8 phosphate buffer at r_0 ~ 3.2:1.

Fig. 3.11 illustrates the thermal melting curve for CTDNA obtained in the presence and absence of **GT4**. The thermal melting data are summarized in Table 3.5. The melting temperature (T_m) of DNA is sensitive to its double helix

stability. Binding of a porphyrin to DNA alters the T_m depending on the strength of its interaction. Hence, the tendency of the porphyrins binding to DNA and also their strength of binding could be ascertained. The change in melting temperature ΔT_m, is nothing but the difference between the thermal melting temperature of the CTDNA in the presence and absence of the porphyrin.

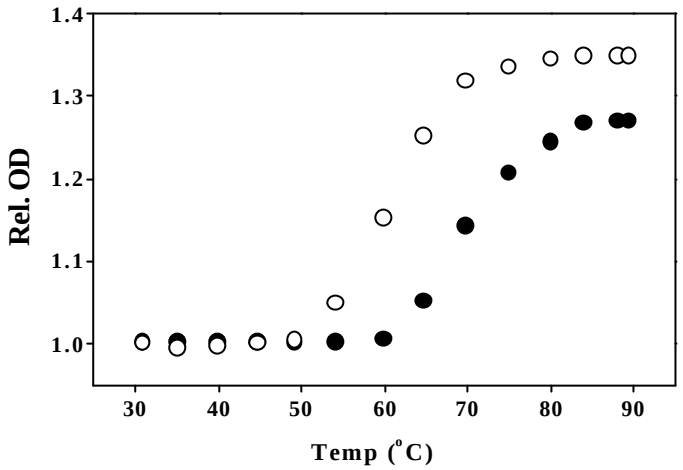

Fig. 3.11 Thermal melting curves for CTDNA in the absence (○) and in the presence (●) of **GT4** in 0.006 M, pH 7.0 phosphate buffer at r_0 ~ 40:1.

The difference between the change in thermal melting temperature of nucleobase-linked porphyrins and **H_2T4** ranges from 2.0 to 4.2 °C and **GT4** shows the maximum when compared to the other nucleobase-linked porphyrins.[18,54,55] This gives an additional support to conclude that **GT4** intercalates more when compared to the standard **H_2T4**.

3.5 Photocleavage studies

DNA photocleavage experiments have been carried out with the nucleobase appended tri-cationic porphyrins and the results are compared with cleavage obtained for **H_2T4**.[56,57] Fig. 3.12 summarizes the photocleavage

experiment carried out for nucleobase tri-cationic porphyrins. Control experiments have suggested that untreated pBR 322 DNA does not show any cleavage in the dark and even upon irradiation by a 425±5 nm light (compare Lanes 1 and 2 in Fig. 3.12).

Table 3.5 Thermal melting data for the Nucleobase linked porphyrins and **H_2T4** [a]

Compound	T_m °C
DNA	60.8
H_2T4	65.5
AT4	67.5
TT4	68.7
GT4	69.7
CT4	68.0

[a] Error limits: T_m, ±1 °C

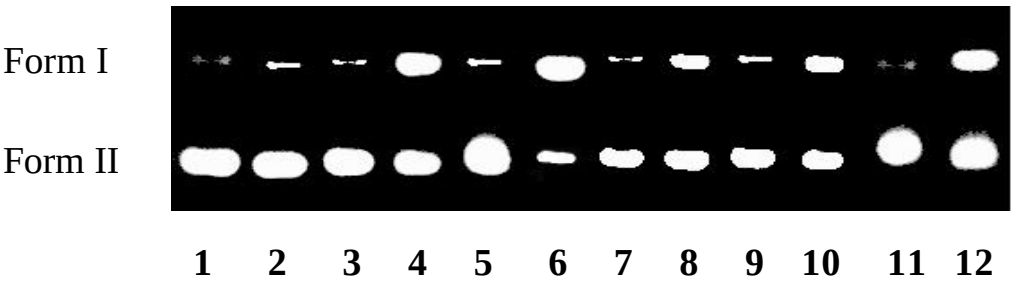

Fig. 3.12 Photocleavage experiments of nucleobase appended tri-cationic porphyrins and **H_2T4**. Dark and Light Experiments: Lanes 1 and 2: Untreated pBR 322 (100 μM) in the dark and upon irradiation. Lanes 3, 5, 7, 9 and 11: pBR 322 + **AT4**, pBR 322 + **GT4**, pBR 322 + **CT4**, pBR 322 + **TT4** and pBR 322 + **H_2T4**, respectively (2.5 μM) in dark. Lanes 4, 6, 8, 10 and 12: pBR 322 + **AT4**, pBR 322 + **GT4**, pBR 322 + **CT4**, pBR 322 + **TT4** and pBR 322 + **H_2T4**, respectively (2.5 μM) upon irradiation. λ_{irra} = 425±5 nm (60 min) in each case.

DNA nicking was observed for the newly synthesized porphyrins as well as the standard (**H_2T4**). Irradiation of DNA in the presence of **GT4** was seen to 20% more effectively photocleave when compared to **H_2T4**. This may be because stacked guanines moieties (arises due to the intercalation of guanine connected to porphyrin in between the base pairs) is more reducing than a single guanine residue.[58] All the other free-base porphyrins (**AT4**, **CT4** and **TT4**) show comparable photocleaving efficiency when compared to **H_2T4**.

Fig. 3.13 shows the bar diagram representation of photocleavege experiment conducted for **GT4** in the presence of various inhibitors. The singlet

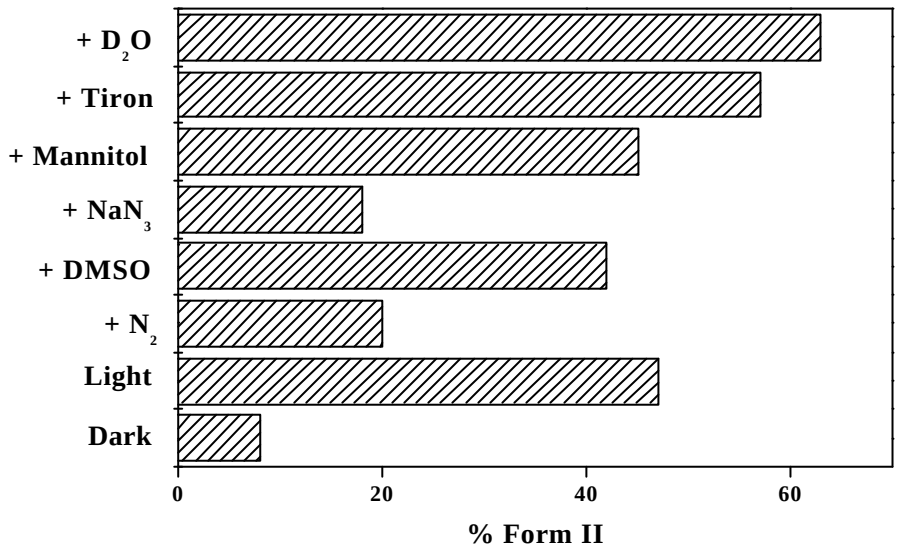

Fig. 3.13 Bar graph presentation of effects of 'inhibitors' on the light-induced nuclease activity of **GT4**. Irradiation time is 60 min in each case and λ_{irra} = 425 ± 5 nm. Lanes 1 and 2: Dark and Light experiments: pBR 322 and **GT4**. Lanes 3-7: Light experiments: pBR 322 + **GT4** in the presence of N_2, DMSO (200 mmol), NaN_3 (1 mM), mannitol (100 mmol), tiron (10mM) and D_2O, respectively, upon irradiation for 60 min at 425±5 nm in each case.

oxygen mechanism is confirmed by performing a representative run with **GT4** in the presence of various 'inhibitors'. NaN_3 - $^1O_2$ 'quencher', shows 60% inhibition of the photocleavage by **GT4** at 1 mM concentration.

Purging the reaction mixture with N_2 (15 min., to remove O_2) also shows inhibition of photocleavage. The amount of photocleavage was increased by addition of D_2O, which increases the lifetime of $^1O_2$. Addition of DMSO or mannitol ($^{\bullet}OH$ radical scavengers) did not show any inhibition from the cleavage of the porphyrin. These results suggest that, among the reactive oxygen species, only $^1O_2$ plays a major role in the DNA photocleavage mechanism of **GT4**. Interestingly, with Tiron (disodium salt of 4,5-dihydroxy-1,3-benzenedisulfonic acid,) a superoxide inhibitor, there is a 10% increase in conversion of Form I to Form II, probably due to the inhibition of the superoxide formation which in turn increases the formation of singlet oxygen resulting in more DNA cleavage.

3.6 Summary

In summary, four nucleobase (A, T, G and C) appended tri-cationic water-soluble porphyrins have been synthesized and well characterized by mass (FAB and MALDI MS), UV-visible and ^1H NMR (^1H and ^1H-^1H COSY) spectroscopic techniques. UV-visible and fluorescence titrations have been carried out to estimate the binding with CTDNA. The shift in the wavelength maxima, percentage of hypochromicity and the calculated binding constant values reveal that the behavior of these nucleobase tri-cationic porphyrins with CTDNA is similar to **H_2T4**. Circular dichroism spectra were run to analyze the possible mode of binding interaction of these porphyrins with DNA. At low r_0 values porphyrin in **GT4** intercalates more readily than the other nucleobase containing porphyrins. Porphyrin in **TT4** also intercalates with efficiency greater than porphyrins in **AT4** and **CT4**, but with lesser efficiency than **GT4** and **H_2T4**

porphyrins, at same r_0 value. These changes may be attributed due to the ability to form keto-enol tautomerism, propensity to form hydrogen bonding and extended conjugation. Thermal melting studies were performed to support these investigations. Amount of cleavage in DNA (in the presence of light) of these porphyrins with pBR 322 DNA was calculated through photocleavage experiments and it was found that **GT4** photocleaves more effectively than the other nucleobase appended porphyrins and **H_2T4**. The singlet oxygen mechanism, which is responsible for the cleavage of DNA, is confirmed by conducting photocleavage inhibition experiments using various inhibitors.

3.7 References

1. Henderson, B. W.; Dougherty, T. J. *Photochem. Photobiol.* **1992**, *55*, 145.
2. Ali, H.; van Lier, J. E. *Chem. Rev*. **1999**, *99*, 2379.
3. Ackroyd, R.; Kelty, C.; Brown, N.; Reed, M. *Photochem. Photobiol.* **2001**, *74*, 656.
4. Lane, N. *Sci. Am.* **2003**, *288*, 38.
5. Dixon, D. W.; Schinazi, R.; Marzilli, L. G. *Ann. N. Y. Acad. Sci.* **1990**, *616*, 511.
6. Kasturi, C.; Platz, M. S. *Photochem. Photobiol.* **1992**, *56*, 427.
7. Maraval, A.; Franco, S.; Vialas, V.; Patviel, G.; Blasco, M. A.; Meunier, B. *Org. Biomol. Chem.* **2003**, *1*, 921.
8. Han, F. X. G.; Wheelhouse, R. T.; Hurley, L. H. *J. Am. Chem. Soc.* **1999**, *121*, 3561.
9. Cech, T. R. *Angew. Chem., Int. Ed.* **2000**, *39*, 35.
10. Han, H.; Langley, D. R.; Rangan, A.; Hurley L. H. *J. Am. Chem. Soc.* **2001,** *123*, 8902.

11. Izbicka, E.; Wheelhouse, R. T.; Raymond, E.; Davidson, K. K.; Lawrence, R. A.; Sun, D.; Windle, E. B.; Hurley, L. H.; Von Hoff, D. D. *CANCER RESEARCH.* **1999**, *59*, 639.
12. Shi, D-F.; Wheelhouse, R. T.; Sun, D.; Hurley, L. H. *J. Med. Chem*. **2001**, *44*, 4509.
13. Haq, I.; Trent, J. O.; Chowdhary, B. Z.; Jenkins. T. C. *J. Am. Chem. Soc.* **1999**, *121*, 1768.
14. Pasternack, R. F.; Gibbs, E. J. In *Porphyrin and metalloporphyrin interactions with nucleic acids*; Elsevier: Amsterdam, The Netherlands, **1996**; Vol. 33, p. 367.
15. Marzilli, L. G. *New J. Chem.* **1990**, *14*, 409.
16. McMillin, D. R.; McNett, K. M. *Chem. Rev.* **1998**, *98*, 1201.
17. Fiel, R. J.; Munson, B. R. *Nucleic Acids Res.* **1980**, *8*, 2835.
18. Fiel, R. J.; Howard, J. C.; Mark, E. H.; Dattagupta, N. *Nucleic Acids Res.* **1979**, *6*, 3093.
19. Leontis, N. B. *Biochemistry,* **1999**, *38*, 15425.
20. Pasternack, R. F.; Gibbs, E. J.; Villafranca, J. J. *Biochemistry* **1983**, *22*, 2406.
21. Lipscomb, L. A.; Zhou, F. X.; Presnell, S. R.; Woo, R. J.; Peek, M. E.; Plaskon, R. R.; Williams, L. D. *Biochemistry* **1996**, *35*, 2818.
22. Bennett, M.; Krah, A.; Wien, F.; Garman, E.; McKenna, R.; Sanderson, M.; Neidle, S. *Proc. Natl. Acad. Sci. U.S.A.* **2000**, *97*, 9476.
23. Barnes, N. R.; Schreiner, A. F.; Finnegan, M. G.; Johnson. M. K. *Biospectroscopy* **1998**, *4*, 341.
24. Chirvony. V. S. *J. Porphyrins Phthalocyanines* **2003**, *7*, 766.
25. Bejune, S. A.; Shelton, A. H.; McMillin, D. R. *Inorg. Chem.* **2003**, *42*, 8465.

26. Wall, R. K.; Shelton, A. H.; Bonaccorsi, L. C.; Bejune, S. A.; Dube, D.; McMillin D. R. *J. Am. Chem. Soc.* **2001**, *123*, 11480.
27. Bejune, S. A.; McMillin, D. R. *Chem. Commun.* **2004**, 1320.
28. Dubey, I.; Pratviel, G.; Meunier, B. *Perkin 1* **2000**, *18*, 3088.
29. Chaloin, L.; Bigey, P.; Loup, C.; Marin, M.; Galeotti, N.; Piechaczyk, M.; Heitz, F.; Meunier, B. *Bioconjugate. Chem*. **2001**, *12*, 691.
30. Lapi, A.; Pratviel, G.; Meunier, B. *Metal-Based Drugs* **2001**, *8*, 47.
31. Wietzerbin, K.; Muller, J. G.; Jameton, R. A.; Pratviel, G.; Bernadou, J.; Meunier, B.; Burrows, C. J. *Inorg. Chem* **1999**, *38*, 4123.
32. Drexler, C.; Hosseini, M. W.; Pratviel, G.; Meunier, B. *Chem. Commun.* **1998**, *13*, 1343.
33. Jakobs, A, J.; Bernadou, J. B.; Meunier, B. *J. Org. Chem.* **1997**, *62*, 3505.
34. Bigey, P.; Soennichsen, S. H.; Meunier, B.; Nielsen, P. E. *Bioconjugate Chem.* **1997**, *8*, 267.
35. Pitie, M.; Meunier, B. *J Biol. Inorg. Chem.* **1996**, *1*, 239.
36. Laine, M.; Richard, F.; Tarnaud, E.; Bied-Charreton, C.; Verchere-Beaur, C. *J. Biol. Inorg. Chem.* **2004**, *9*, 550.
37. Verchere-Beaur, C.; Perr-Fauvet, M.; Catherine, V-B.; Martine, P-F.; Tarnaud, E.; Anneheim-Herbelin, G.; Bone, N.; Gaudemer, A. *Tetrahedron* **1996**, *52*, 13589.
38. Tjahjono, D. H.; Akutsu, T.; Yoshioka, T.; Inoue, H. *Biochim. Biophys. Acta*, **1999**, *85*, 333.
39. Tjahjono, D. H.; Mima, S.; Akutsu, T.; Yoshioka, N.; Inoue, H. *J. Inorg. Biochemistry* **2001**, 85, 219.
40. Sirish, M.; Maiya, B. G. *J. Porphyrins Phthalocyanines* **1998**, *2*, 1.
41. Fuhrhop, J.-H.; Smith, K. M.; In *Porphyrins and Metalloporphyrins*; Smith, K. M., Ed.; Elsevier: Amsterdam, **1975**; p. 769.

42. Casas, C.; Bernadette, S.J.; Loup, C.; Lacey, J.; Meunier, B. *J. Org. Chem.* **1993**, *58*, 2913.
43. Kalyanasundaram. K. *Inorg. Chem*. **1984**, *23*, 2453.
44. Quimby, D. J.; Longo. F. R., *J. Am. Chem*. *Soc*. **1975**, *97*, 5111.
45. Pasternack, R. F.; Gibbs, E. J.; and Villafranca, J. J. *Biochemistry* **1983**, *22*, 2406.
46. Carvlin, J. M.; Fiel, R. J. *Nucleic Acids Res.*1**983**, *11*, 6121.
47. McGhee, J. D.; von Hippel, P. H. *J. Mol. Biol*. **1974**, *86*, 469.
48. Kelly, J. M.; Murphy, J. M. *Nucleic Acids Res.*1**985**, *13*, 167.
49. Sari, M. A.; Battioni, J. P.; Mansuy, D.; Lepecq, J. B. *Biochem. Biophys. Res. Commun.* **1986**, *141*, 643.
50. Pasternack, R. F. *Chirality* **2003**, *15*, 329.
51. Carvlin. M. J.; Mark, E.; Fiel. R. J.; Howard, J. C. *Nucleic Acids Res.* **1983**, *11*, 6141.
52. Baker. E. S.; Gidden. J.; Ferzoco. A.; Bowers. M. T. *Phys. Chem. Chem. Phys*. **2004**, *6*, 2786.
53. Ivanov, V. I.; Minchenkova, L. E.; Schyolkina, A. K.; Poletayev, A.I. *Biopolymers* **1973**, *12*, 89.
54. Kelly, J. M.; Tossi, A. B.; McConnell, D. J.; OhUigin, C. *Nucleic Acids Res.* 1**985**, *13*, 6017.
55. Marmur, J.; Doty, P. *J. Mol. Biol*. **1962**, *5*, 109.
56. Fiel, R. J.; Beerman, T. A.; Mark, E. S.; Gupta, N. D. *Biochem. Biophys. Res. Commun.* **1982**, *107*, 1067.
57. Praseuth, D.; Gaudemer, A.; Verlhac, J-B.; Kraljic, I.; Sissoeff, I.; Guille, E. *Photochem. Photobiol.* **1986**, *44*, 717.
58. Prat, F.; Houk, K. N.; Foote, C. S. *J. Am. Chem. Soc*. **1998**, *120*, 845.

CHAPTER 4

Adenine appended tri-cationic water-soluble metalloporphyrins: Synthesis, characterization, binding and photocleavage studies with DNA

4.1 Introduction

A number of intensive studies on interactions of free-base and metalloporphyrin with DNA have been reported in the literature.[1-19] It has been shown that the binding mode of porphyrin to nucleic acid duplexes, e.g. intercalative or outside binding mode can be easily tuned by varying the metal center.[20-25] Crystallographic analysis of metalloporphyrin-oligonucleotide complexes has shown that intercalation or groove binding of cationic porphyrin causes a distortion of B-DNA significantly.[20,21]

Meunier co-workers have extensively investigated the interactions of cationic porphyrins and metalloporphyrins with DNA.[26-42] Water-soluble, cationic metalloporphyrins bearing various functional groups on the *meso* position of the macrocycle exhibit varying cytotoxicity toward cancer cells in vitro, depending on the nature of the central atom (Mn(III), Fe(II), Zn(II) and Ni(II)) and on the number of pyridinium groups.[43] Derivatives based on the tris-(methylpyridinium)porphyrin motif were the most active, with the Mn(III) complex exhibiting higher toxicity than the Fe(II) analogue while the Zn(II) and Ni(II) complexes were inactive. Hybrid molecules consisting of both metalloporphyrin and ellipticene moieties were synthesized in order to capitalize on the biological activities of both entities.[44] Relative to the metal-free H_2T4, CuT4 binds to poly(rA)·poly(dT) and poly(rA)·poly(rU) with a greatly increased binding constant and the bound metalloporphyrin may impose an ordered architecture on the polymer surface, the stacking being facilitated by the more

planar nature of the CuT4 than the nonmetal counterpart.[45,46] The copper-bipyridinium (which hydrolyzes phosphodiester bonds) appended copper metallated porphyrins have been synthesized and their oxidative and hydrolytic reactivity towards supercoiled plasmid DNA has been studied in vitro.[47,48] The metal complexes of *meso*-tetrakis(1,2-di-methylpyrazolium-4-yl)porphyrin has been studied and it was shown that the Ni(II) derivative and Cu(II) derivative are intercalated into the 5′GC3′ step of CTDNA whereas Mn(III) and Zn(II) derivatives are bound edge-on at the 5′TA3′ step of the minor groove and major groove of CTDNA, respectively.[49] Recently, striking evidence has been provided to show that the porphyrin chromophore in ZnD3 and ZnD4 loses its axial ligand and binds as an intercalator due to its reduced steric demands; in contrast, the bulkiness of the ZnT4 system regulates it to external binding.[50-53]

In this chapter, we describe the synthesis and spectral characterization of the newly synthesized adenine appended metalloporphyrins, Scheme 4.1. Interactions of Cu(II) and Zn(II) metal complexes of adenine appended tri-cationic water-soluble porphyrins with CTDNA (**ZnAT4** and **CuAT4**) were studied on the basis of changes in the Soret band, induced circular dichroism and thermal melting experiments. Results from the experiments carried out to probe the DNA photocleavage proclivities are also reported in this chapter.

4.2 Experimental section

4.2.1 Synthesis

The precursor **AtriPyP** [meso-5-(4-(9-(2-oxyethyl)adenine)phenyl)-10,15,20-tripyridylporphyrin] was synthesized as described in Chapter 3, section 3.2.3. The H_2T4 porphyrin was obtained commercially and converted to its zinc and copper complexes, **ZnT4** and **CuT4** [(5,10,15,20-tetra(*N*- methylpyridinium-4-yl)porphyrinato zinc(II) (tosylate salt)) and (5,10,15,20-tetra(*N*- methylpyridini-

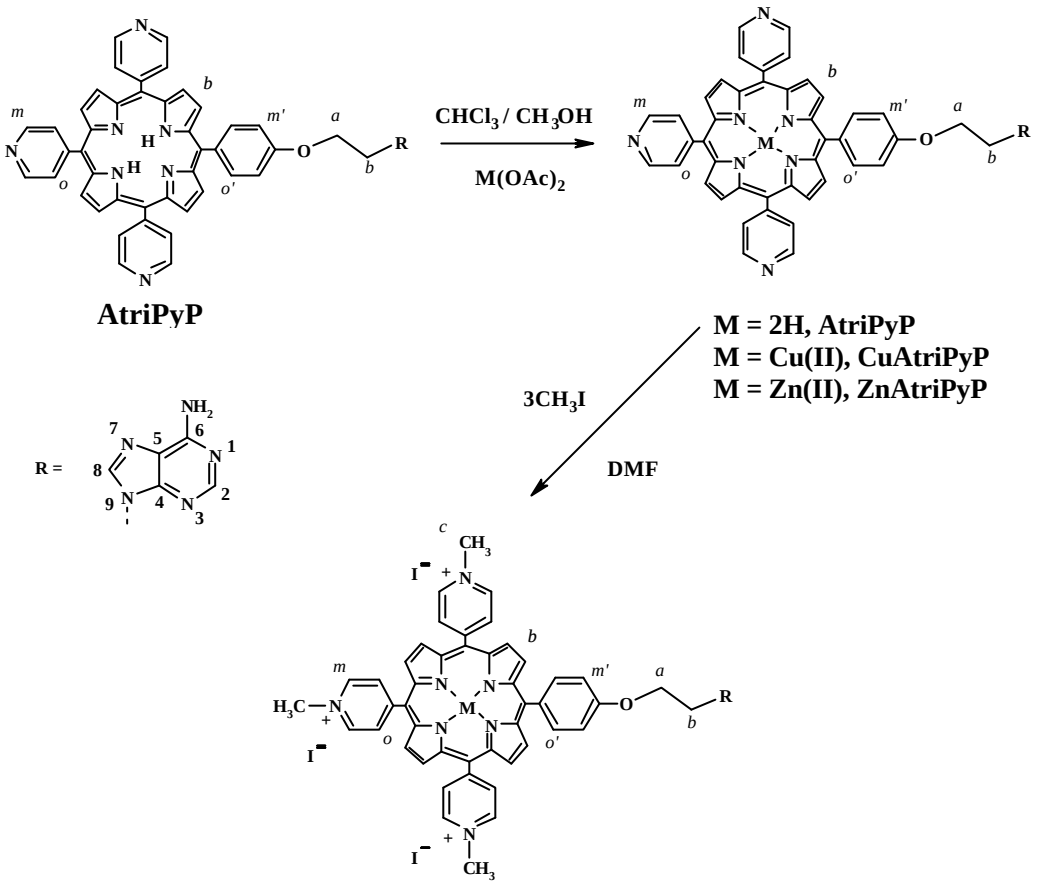

M = 2H**, AT4;** Cu(II)**, CuAT4;** Zn(II)**, ZnAT4**

Scheme 4.1 Synthesis of transition metal complexes of adenine appended tri-cationic porphyrins.

um-4-yl)porphyrinatocopper (II) (iodide salt))] respectively, by modified reported procedures.[54] **CuTPP** [5,10,15,20-tetraphenylporphyrinatocopper(II)] and **ZnTPP** [5,10,15,20-tetraphenylporphyrinatozinc(II)] were synthesized according to a reported procedure and used as standards for the ESR and fluorescence studies, respectively.[55,56] The DNA binding results obtained for **AT4** [meso-5-(4-(9-(2-oxyethyl)adenine)phenyl)-10,15,20-tri(*N*-methylpyridinium-4-yl)porphyrin]

with CTDNA (section 3.4) were also used as a reference for further DNA binding studies.

4.2.2 Synthesis of Cu(II)/Zn(II) complexes of AtriPyP (CuAtriPyP/ ZnAtriPyP)

Zn(II) or Cu(II) complexes were prepared by metallating the free-base **AtriPyP** with the corresponding metal acetates by standard methods.[56] Typically, 100 mg of **AtriPyP** (0.125 mmol) and ~100 mg of either $Cu(OAc)_2.H_2O$ or $Zn(OAc)_2.2H_2O$ were stirred in $CHCl_3/CH_3OH$ for 0.5 h at room temperature. The solvents were evaporated and the residue was purified by column chromatography using $CHCl_3$:CH_3OH (98:2, V/V) furnishing the pure product in each case. Yields ranged from 65 to 75%.

4.2.3 Synthesis of CuAT4 and ZnAT4 (Methylation of CuAtriPyP and ZnAtriPyP)

CuAtriPyP and **ZnAtriPyP** were methylated by stirring each of them with large excess of methyl iodide (~ 90 equiv.) in dry dimethylformamide for 15 min at room temperature. The reaction was monitored by TLC (silica gel) using CH_2Cl_2:CH_3OH (95:5, V/V; the product does not move on the TLC plate). The solvent and the excess methyl iodide were removed under vacuum. The residue was taken up in CH_3OH and precipitated with distilled acetone. Both the metallated tri-cationic nucleobase linked porphyrins, **CuAT4** and **ZnAT4** were obtained in nearly quantitative yields. MALDI MS, **CuAT4**: $[M\text{-}3I]^+$, 899; $[M\text{-}C_8H_{13}N_5\ I_3]^+$, 720; **ZnAT4**: $[M\text{-}3I]^+$, 901; $[M\text{-}C_8H_{13}N_5I_3]^+$, 723.

4.3 Results and discussion

The scheme for the synthesis of transition metal complexes of adenine appended tri-cationic porphyrins is given in Scheme 4.1. The copper and zinc complexes of adenine linked pyridyl complexes were obtained (~ 70 % yield) by metallation with corresponding metal acetates. The metallated pyridyl complexes were methylated with methyl iodide and obtained quantitatively. The tri-cationic metalloporphyrins and their precursors, synthesized in this study were characterized by MALDI MS, ^{1}H NMR, ESR and UV-visible spectroscopic methods.

4.3.1 Ground state properties

Fig 4.1 (a and b) illustrates the MALDI MS spectra recorded for **CuAT4** and **ZnAT4**, respectively. The MALDI MS spectral data shows less intense peak without the three counter ions at 899 and 901 for **CuAT4** and **ZnAT4**, respectively and intense peaks due to fragments. Fig 4.2 and Fig 4.3 exhibit the ^{1}H NMR spectra recorded for **ZnATriPyP** and **ZnAT4**, respectively and the data are summarized in Table 4.1. The spectra were analyzed on the basis of resonance positions and integrated intensity data. Both the complexes show peaks due to adenine (2-*H* and 8-*H*) between 7.80-8.50 ppm. The ortho protons which resonate at 8.82-8.50 ppm as multiplet in **ZnAtriPyP**, shifts to downfield at 9.46 ppm as a doublet in **ZnAT4**. The *b*-pyrrolic, *m* and *o′* protons of **ZnAtriPyP** appear as mutiplets at 8.37-7.80 ppm. In the case of **ZnT4** the *b*-pyrrolic and the meta protons are observed as mutiplets at 9.05-8.75 ppm but the *o′* protons appear as a doublet at 8.02 ppm. The *m′* protons resonate at 7.11 and 7.29 ppm for **ZnAtriPyP** and **ZnT4**, respectively as doublet. The resonance positions of the spacer protons *a* and *b* are seen to be unaltered in both the **ZnAtriPyP** and **ZnAT4** porphyrins. The sharp singlet at 4.50-4.90 ppm (cf. δ(C*H*$_3$I): 2.18) confirmed the N-methylation in **ZnAT4**.

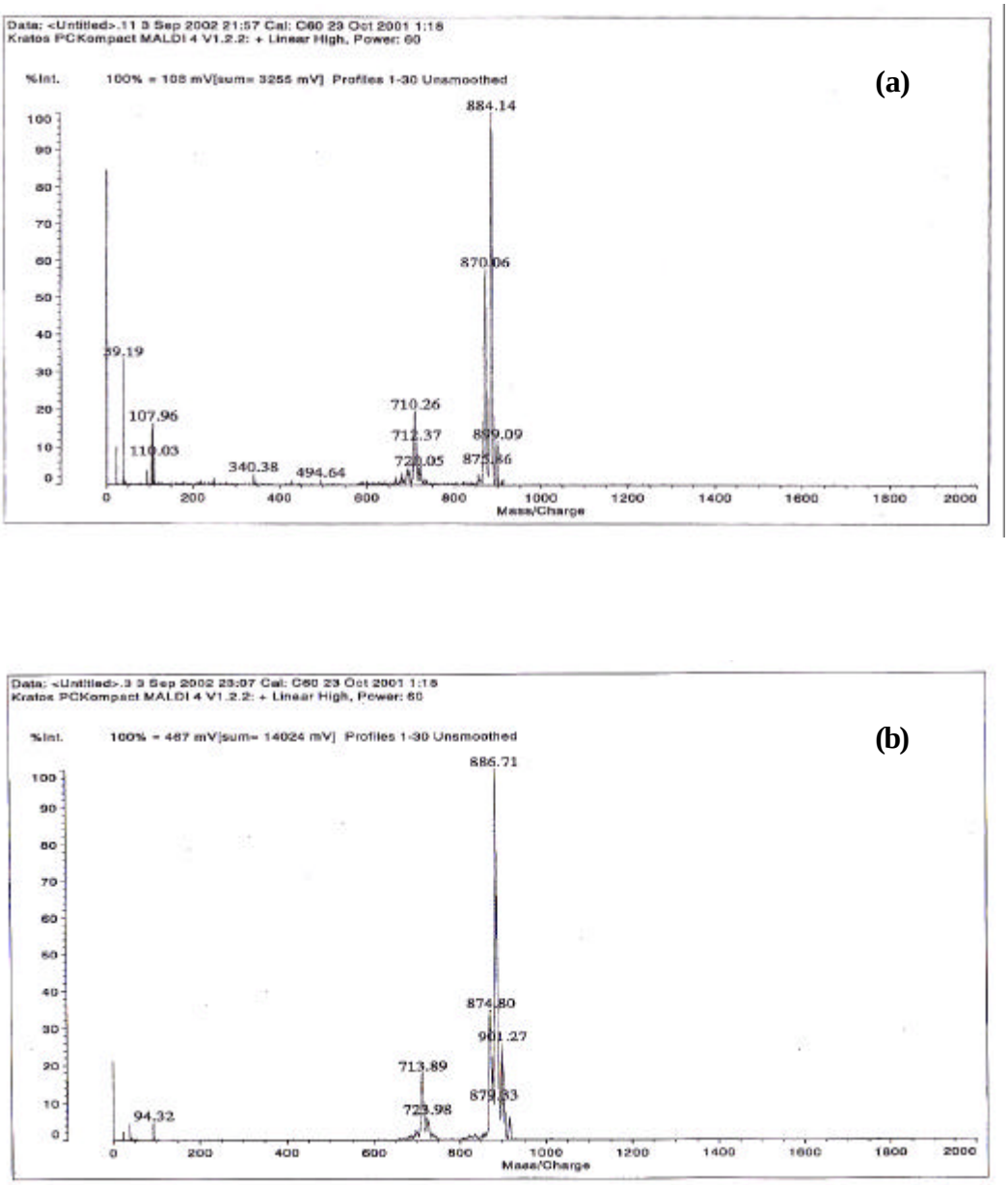

Fig 4.1 MALDI MS spectra of (a) **CuAT4** and (b) **ZnAT4**.

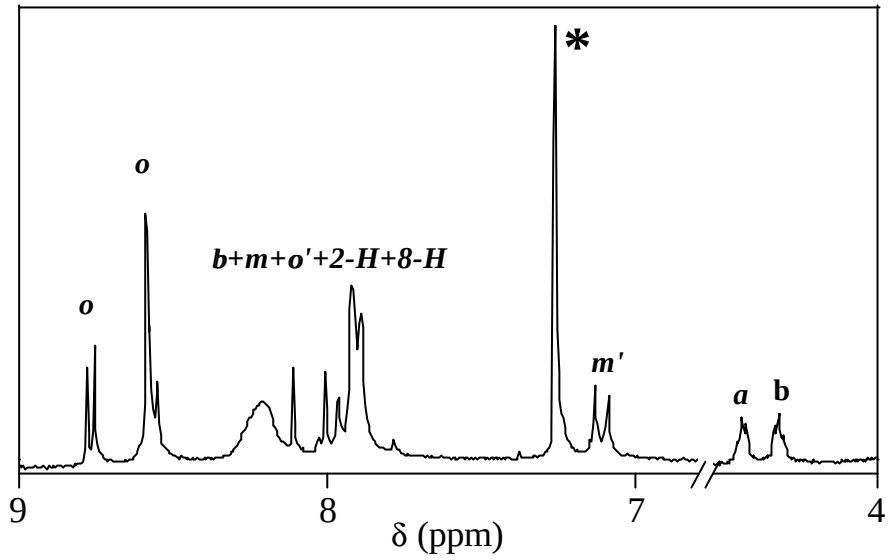

Fig. 4.2 ^{1}H NMR spectrum of **ZnAtriPyP** (200 MHz, 300 K) in $CDCl_3$+CD_3OD, TMS. (* peak is due to solvent).

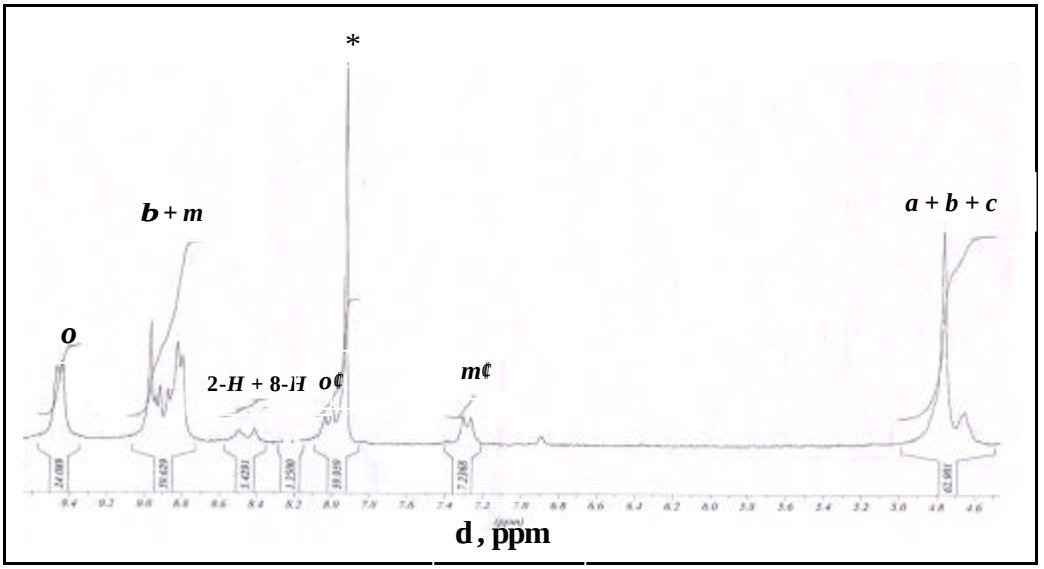

Fig. 4.3 ^{1}H NMR spectrum of **ZnAT4** (200 MHz, 300 K) in $CDCl_3$+DMSO-d_6, TMS. (* peak is due to solvent. See Scheme 4.1 for proton assignments and Table 4.1).

Table 4.1 ^{1}H NMR data of Zn(II) complexes of adenine linked pyridyl and tri-cationic porphyrins (see Scheme 4.1 for proton assignments).[a]

Compd.	d, ppm			
	Porphyrin	**Nucleobase**	**-OCH_2**	**-NCH_2**
ZnAtriPyP [b]	8.82-8.50 (6H, *o*, m), 8.37-7.80 (18H, ***b***+*m*+*o′*+2-$H_{adenine}$+8-$H_{adenine}$, m), 7.11 (2H, *m′*, d, J = 8.8 Hz).	8.37-7.80 (2H, 2-$H_{adenine}$+8-$H_{adenine}$, m)	4.76 (2H, *a*, t)	4.66 (2H, *b*, t)
ZnAT4 [c]	9.46 (6H, *o*, d, J = 5.3 Hz), 9.05-8.75 (14H, ***b***+*m*, m), 8.02 (2H, *o′*, d, J = 7.8 Hz), 7.29 (2H, *m′*, d, J = 7.8 Hz), 4.90-4.50 (9H, *c*, bs)	8.49 (1H, 2-$H_{adenine}$, s), 8.41 (1H, 8-$H_{adenine}$, s)	4.90-4.50 (2H, *a*, bs),	4.65 (2H, *b*, bs)

[a] Error limits: δ, 0.01 ppm, J, ±1 Hz.

[b] Spectrum was recorded in $CDCl_3$+CD_3OD.

[c] Spectrum was recorded in $CDCl_3$+DMSO-d_6.

The UV-visible spectra of **CuAT4**, **ZnAT4** and **AT4** are illustrated in Fig. 4.4. The data obtained from the UV-visible spectra are summarized in Table 4.2. An absorption in the UV-region similar to **AtriPyP** and **AT4** porphyrins was observed in all the porphyrins due to the presence of the adenine moiety. Similarly, the band which is present in the UV region in these metallo pyridyl and cationic porphyrins due to the absorption of the adenine moiety in each case, is close to the absorption of free adenine.[57] The Soret band and two Q-bands accompanied by a shoulder due to the absorption of the porphyrin chromophore appear at 426 nm and 465-640 nm, respectively for **ZnAtriPyP** porphyrin. Similarly for **ZnAT4**, the Soret band and Q-bands were observed at 435 nm and 500-670 nm, respectively.

For both the **CuAtriPyP** and **CuAT4** porphyrins the Soret-band absorbs at 416 nm and Q-band absorbs at 540 and 548 nm, respectively with a shoulder at 580-590 nm. The wavelength of maximum absorption (λ_{max}) values and the molar extinction coefficient values (ε) obtained from the UV-visible spectra of the transition metal complexes of adenine linked pyridyl and tri-cationic porphyrins are comparable to that of the free-base **AtriPyP** and **AT4** porphyrins (chapter 3 and Table 3.2), respectively. Thus, the UV-visible data reveal that there is no π-π interaction between the metalloporphyrin chromophore and the adenine moiety.

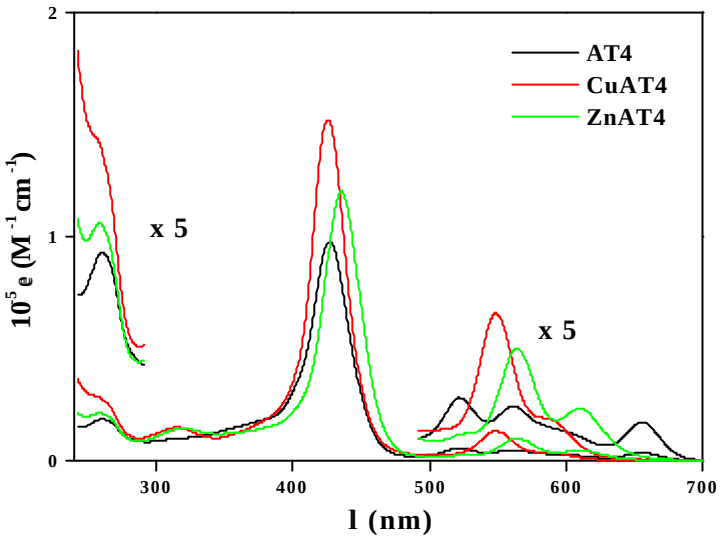

Fig. 4.4 UV-visible spectra of **AT4**, **CuAT4** and **ZnAT4** in H_2O.

ESR spectra of **CuAtriPyP** (in chloroform+methanol+toluene), **CuAT4** (ethanol) and the reference compound **CuTPP** (in toluene) (100 ± 3 K) have been recorded. Fig. 4.5 depicts the ESR spectra for **CuAtriPyP** and **CuAT4**; the data are summarized in Table 4.3.

Table 4.2 UV-visible data of adenine linked pyridyl, tri-cationic metalloporphyrins and their precursor [a]

Compound	λ_{max}, nm (log e)		
	Soret band	**Q-bands**	**Nucleobase**
CuAtriPyP [b]	416 (5.44)	540 (4.06)	268 (4.21)
ZnAtriPyP [b]	426 (5.52)	599 (3.65), 559 (4.12), 521 (3.33)	268 (4.26)
CuAT4 [c]	416 (5.18)	589 (3.59), 549 (4.13)	258 (4.47)
ZnAT4 [c]	435 (5.08)	610 (3.66), 564 (3.99)	259 (4.31)
Adenine [b]	-	-	275 (3.56)

[a] Error limits: λ_{max}, ± 1 nm, log ε, ± 10%. [b] Spectra were recorded in DMF. [c] Spectra were recorded in H_2O.

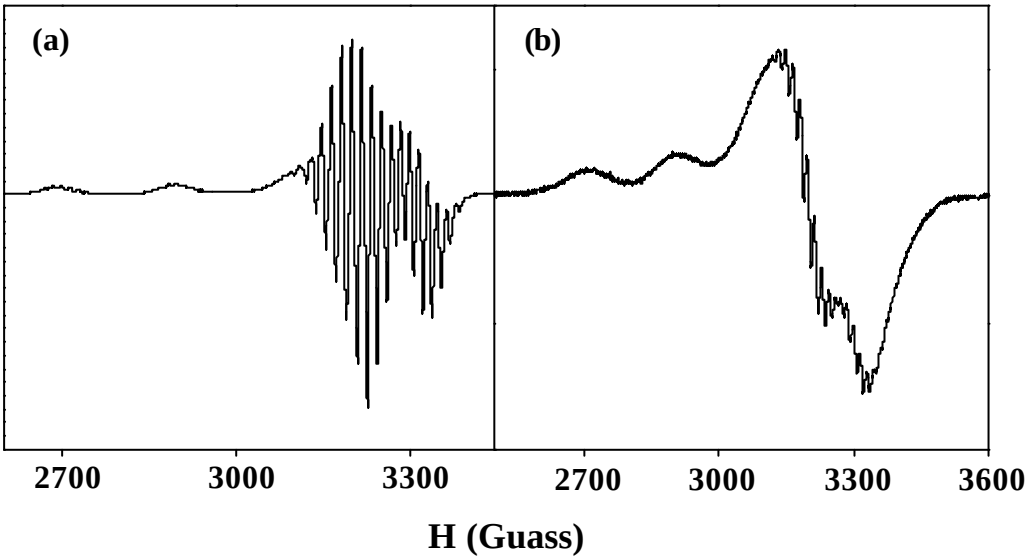

Fig. 4.5 ESR spectra of (a) **CuAtriPyP** (chloroform+methanol+toluene) and (b) **CuAT4** (ethanol), 100 ± 3K.

The spectra were analyzed using the spin-hamiltonians reported for the **CuTPP**.[58,59] The data given in Table 4.3 suggest that the spectral parameters ($g_{\hat{O}}$, $g_{\perp}$ and $A_{\hat{O}}^{Cu}$, $A_{\perp}^{Cu}$, $A_{\hat{O}}^{N}$ and $A_{\perp}^{N}$ (x 10^4 cm^{-1}) of **CuAtriPyP** and **CuAT4** are indistinguishable from those of **CuTPP** and **CuT4** values, respectively.[60] Invariance of g and A values in comparison with those of **CuTPP** or **CuT4** show that the supramolecular perturbation has no significant influence on the ESR parameters. Thus, both the ESR and UV-visible data indicate that there is no significant interaction between the metalloporphyrin and the adenine moiety in solution.

Table 4.3 ESR Spectral Data (100±3K) [a]

Compound	g	$g_{\wedge}$	x 10^{-4} cm^{-1}			
			A^{Cu}	$A_{\wedge}^{Cu}$	A^{N}	$A_{\wedge}^{N}$
CuTPP [b]	2.1454	2.0290	207	32.8	13.9	16.4
CuAtriPyP [c]	2.1792	2.0438	202	32.4	14.2	16.2
CuAT4 [d]	2.1562	2.0473	192	30.8	-	15.4

[a] Error limits: g = ± 0.005; A = ± 10%. [b] measured in toluene. [c] measured in chloroform+methanol+toluene. [d] measured in ethanol.

4.3.2 Excited state properties

Fig. 4.6 illustrates the steady state fluorescence spectra of **ZnAtriPyP** (DMF) and **ZnAT4** (H_2O) with their corresponding standards **ZnTPP** and **ZnT4**, respectively. The steady state fluorescence studies of **CuAtriPyP** and **CuAT4**

were found to be totally non-emissive probably due to the formation of a five-coordinate complex with solvent. The tripdoublet and tripquartet states of the five-coordinate complex are thought to decay via a short-lived d-d excited state.[17,60-65]

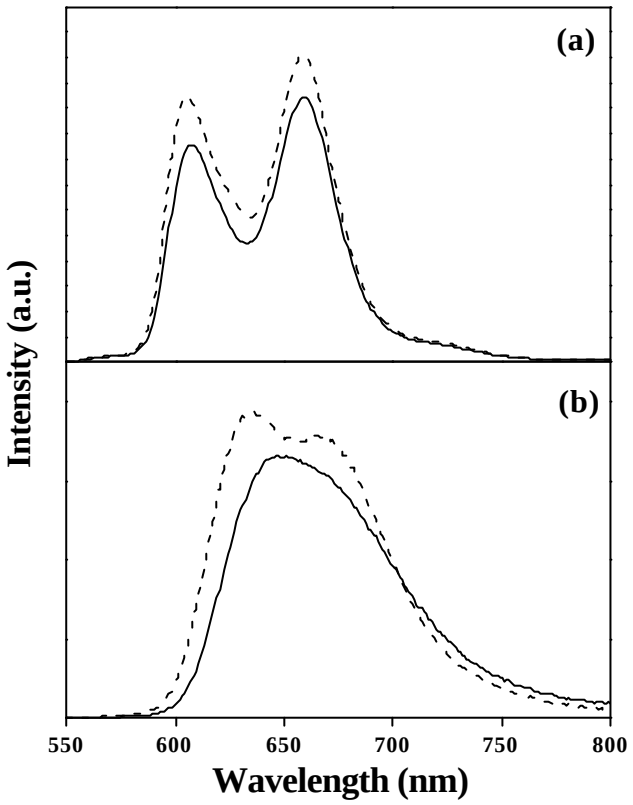

Fig. 4.6 Fluorescence spectra (equimolar solutions, ~0.2 OD) of (a) λ_{ex} = 425 nm: **ZnAtriPyP (————)** and **ZnTPP** (--------) in DMF (b) λ_{ex} = 435 nm: **ZnAT4** (————) and **ZnT4** (--------) in H_2O.

The fluorescence quantum yield values of the **ZnAtriPyP** and **ZnAT4** have been calculated by exciting at 425 and 435 nm, respectively. The excitation of the porphyrin core of **ZnAtriPyP** (DMF) leads to two emission peaks at 608 and 659 nm, whereas excitation of the porphyrin of **ZnAT4** (H_2O) leads to only

one emission peak at 649 nm. The calculated quantum yield values are 0.055 and 0.022, respectively for **ZnAtriPyP** and **ZnAT4**. The quantum yields and the emission peak maxima (Fig. 4.6a) of **ZnAtriPyP** and **ZnTPP** reveal that the emission properties are close to each other.[66] Similarly, the emission properties of **ZnAT4** are close to that for **ZnT4**.[67] Thus, metallation with Zn does not have any adverse effect on the singlet state properties of the adenine-linked metalloporphyrins.

4.4 DNA binding

DNA binding by the newly synthesized metalloporphyrins with CTDNA has been monitored by absorption, luminescence, circular dichroism and thermal melting methods. All these porphyrins were present as monomers under the set of titration conditions.

Table 4.4 summarizes the spectral data obtained for the interactions of adenine appended tri-cationic metalloporphyrins and their references with CTDNA. Fig. 4.7 shows the UV-visible titration performed for **CuAT4** with CTDNA. A similar titration has been performed for **ZnAT4** also. Absence of an isosbestic point observed is suggestive of two or more binding modes.[47] The UV-visible spectra recorded for **CuAT4** with CTDNA show 5 nm bathochromic shift in the Soret region and 20% hypochromicity, similar to **CuT4** at $r_0 \sim 40$ (r_0 = [DNA]/[porphyrin]). The bathochromicity obtained for both **ZnAT4** and **ZnT4** are comparable (2 nm) but the former shows hyperchromicity whereas the latter shows hypochromicity. These results reveal that the **CuAT4** intercalates in the DNA duplex in contrast the **ZnAT4** binds in the groove. For both the complexes, with smaller r_0 values decrease in the absorption intensity as well as bathochromic shift was observed but with higher r_0 values the absorbance intensity starts enhancing without change in the absorption maxima.

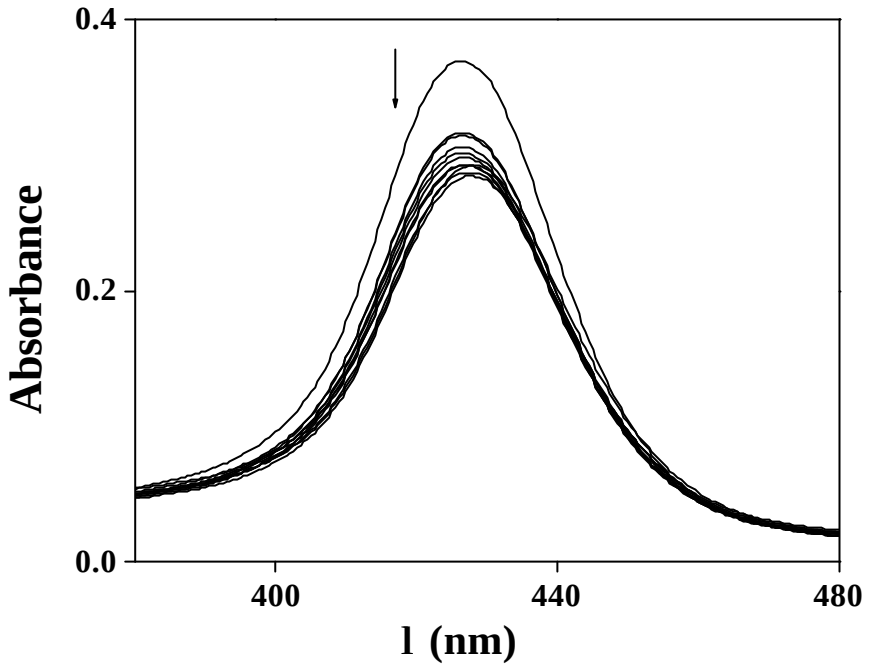

Fig. 4.7 Absorption titration of **CuAT4** performed with CTDNA in pH 6.8 phosphate buffer, μ = 0.5 M.

The apparent binding constants (K_{app}) calculated for **CuAT4** and **ZnAT4** with CTDNA from the UV-visible titrations are 3.60 x 10^5 M^{-1} and 1.09 x 10^4 M^{-1}, respectively. All these results reveal that the behavior of the **CuAT4** and **ZnAT4** are more or less similar to that of **CuT4** (interacts both by intercalation and external binding) and **ZnT4** (interacts only by external binding), respectively.[24,68]

The fluorescence titration has been performed for **ZnAT4** by exciting at λ_{ex} = 435 nm in the presence of large excess of CTDNA. Fig. 4.8 illustrates the fluorescence titration performed for **ZnAT4** with CTDNA. Similar to **ZnT4**, the interactions of **ZnAT4** with CTDNA cause splitting of the broad fluorescence

band into two distinct bands with peaks at 621 and 721 nm, which appeared as a single band with peak at 647 nm in the absence of DNA.[69] Enhancement in intensity was observed with addition of CTDNA. The intrinsic binding constant (K_b) calculated with CTDNA from fluorescence titration is 2.54 x 10^4 M^{-1}.

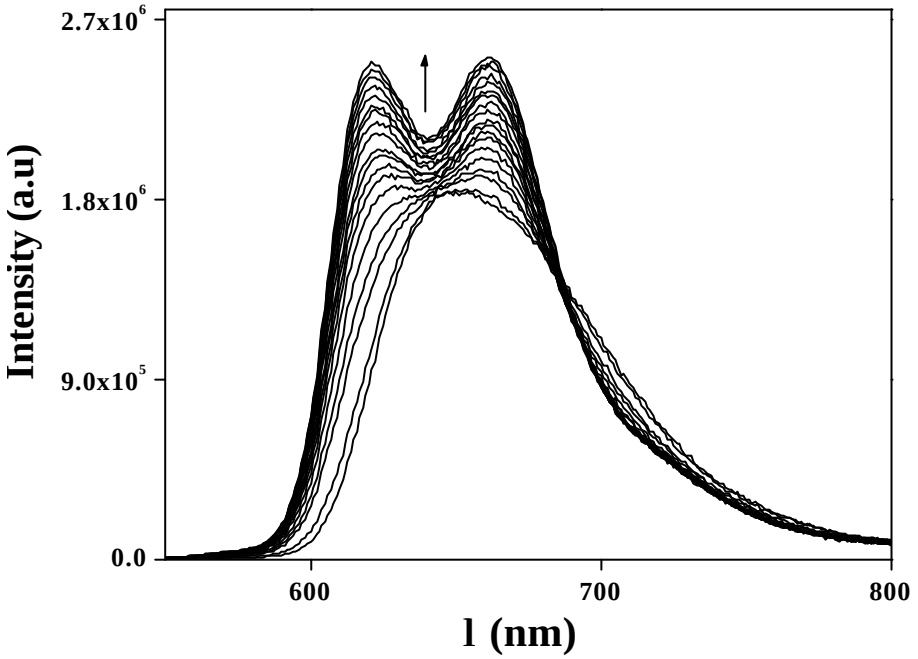

Fig. 4.8 Fluorescence titration of **ZnAT4** with CTDNA in pH 6.8 phosphate buffer, μ = 0.5 M. (λ_{ex} = 435 nm).

The porphyrins do not display circular dichroism in the absence of DNA, whereas spectra are induced in the Soret region, when they are bound to natural or artificial DNA. The induced CD spectra for **CuAT4** and **ZnAT4** were recorded in the presence of CTDNA with different r_0 ($3 \leq r_0 \leq 32$) values. The CD experiments were performed starting from r_0 ~3 to assure the formation of 1:1

adduct and ended up with r_0 ~32, where adduct formation becomes maximum. Fig. 4.9 and Fig. 4.10 show the CD spectra of **CuAT4** and **ZnAT4**, respectively recorded in the presence of CTDNA with various r_0 values. Fig. 4.11 and Fig. 4.12 illustrates the spectra recorded for **CuAT4** and **ZnAT4** with their standards, **AT4** and **CuT4** or **ZnT4** at r_0 ~ 3.2, respectively.

Fig. 4.9 reveals that similar to **H_2T4** and **CuT4**, the **CuAT4** also features a positive and negative signal, reflecting the coexistence of the two modes of interaction i. e., intercalation and external interaction in the groove.[24,47,70] At lower r_0 values a sharp negative peak at 439 nm and a positive peak at 416 nm with lesser intensity was observed. With increase in r_0 value decrease in both the positive and negative intensity were observed, means that the intercalation is favored at low r_0 values. From the earlier reported works with cationic porphyrins, a positive and a negative induced CD signals have been recognized as due to interaction of external binding and intercalation, respectively.[17,41]

Comparison of the CD spectra of **AT4**, **CuAT4** and **CuT4** given in Fig. 4.11 at constant lower r_0 value show difference in their interacting behaviour towards DNA. From Fig. 3.9 and section 3.4, it was suggested earlier that the intercalating efficiency of porphyrin connected to the adenine moiety was weak due to (i) the less acidic protons [to exhibit amino-imino tautomerism; acidity of the NH sites in nucleobase follows the order: guanine (N10H11 and N1H) > thymine (N3H) > cytosine (N7H8) > adenine (N10H11)], and (ii) the presence of only three positive charges.[71] But the metallation of the porphyrin core with Cu(II) ions promotes the intercalating efficiency of porphyrin in **CuAT4** than **AT4** may be due to the axial coordination of Cu(II) metal centers with the DNA nucleobase. The binding of the adenine moiety may drive the copper metalated porphyrin to the proximity of the DNA, which results in strong intercalation of porphyrin in **CuAT4** than **CuT4**.

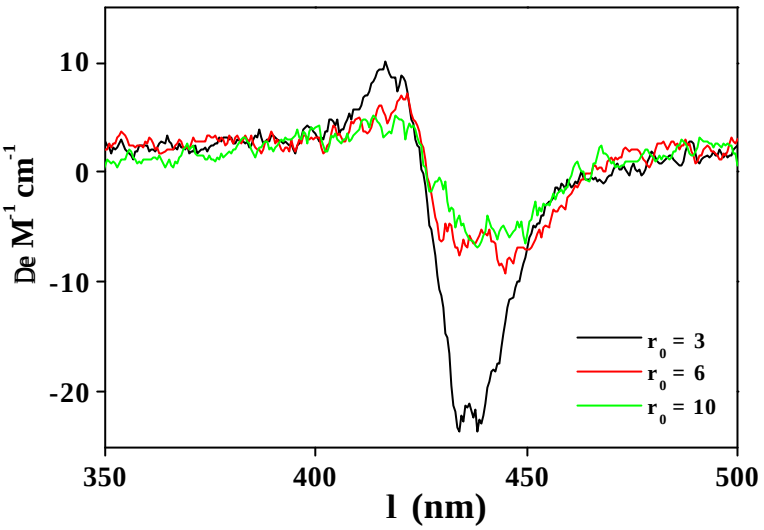

Fig. 4.9 CD spectra of **CuAT4** recorded with CTDNA in pH 6.8 phosphate buffer, μ = 0.017 M.

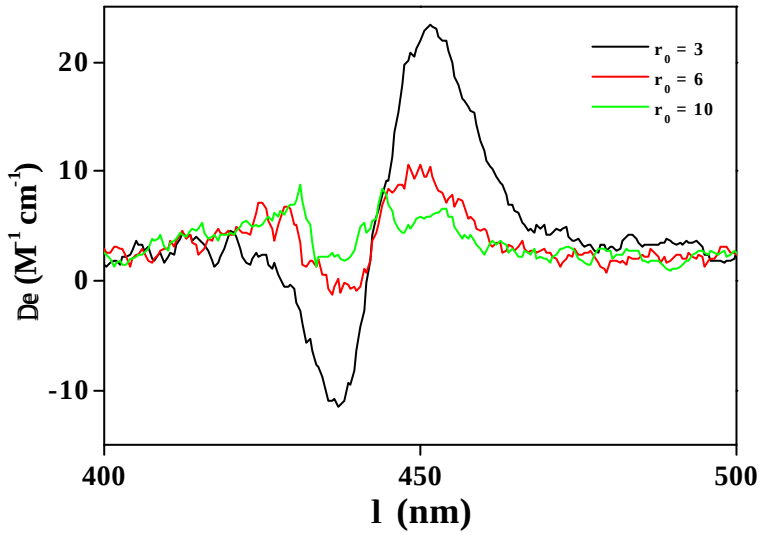

Fig. 4.10 CD spectra of **ZnAT4** recorded with CTDNA in pH 6.8 phosphate buffer, μ = 0.017 M.

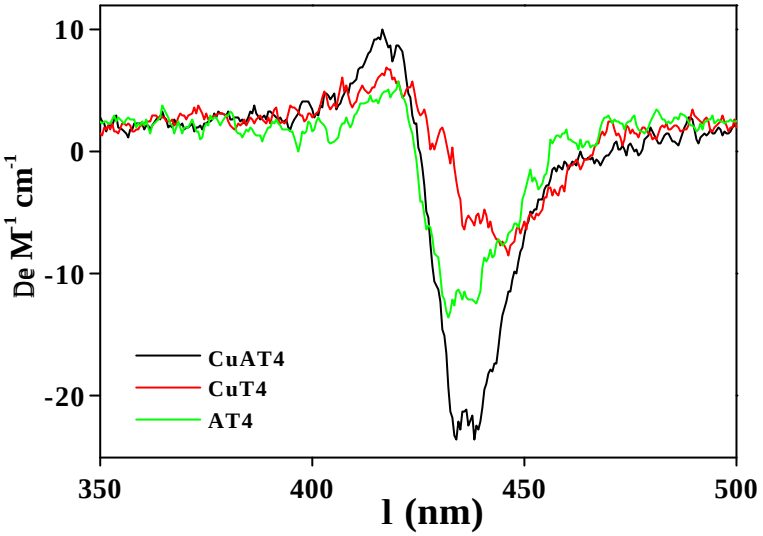

Fig. 4.11 CD spectra of **AT4**, **CuAT4** and **CuT4** porphyrins with CTDNA (350-500 nm) recorded in pH 6.8 phosphate buffer, μ = 0.017 M at r_0 = 3.2:1.

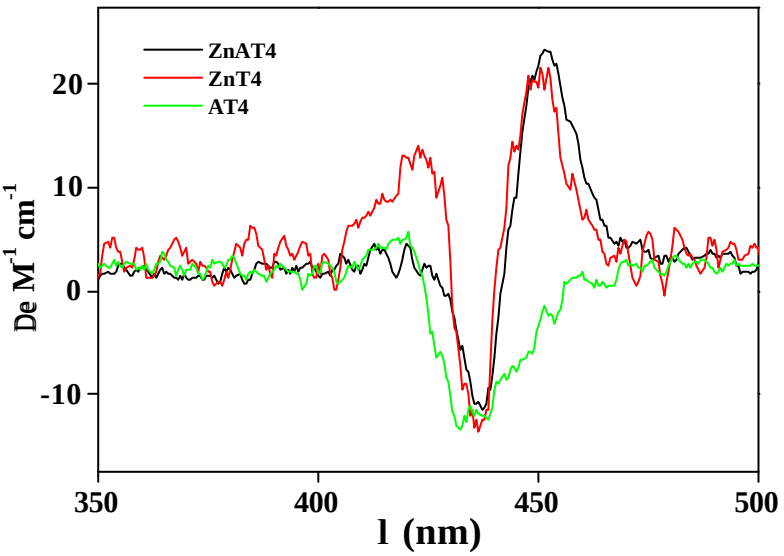

Fig. 4.12 CD spectra of **AT4**, **ZnAT4** and **ZnT4** porphyrins with CTDNA (350-500 nm) recorded in pH 6.8 phosphate buffer, μ = 0.017 M at r_0 = 3.2:1.

Table 4.4 Spectral data for adenine appended tri-cationic metalloporphyrins and their standards with CTDNA

Compd	Soret absorbance [a]		CD [d]	Emission [e]	
	Dl, nm [b] (%H) [c]	K_{app} M^{-1}	l, nm (De, $M^{-1}cm^{-1}$)	l, nm [f]	K_b M^{-1}
CuAT4	5 (20)	3.60×10^5	416 (+9) 436 (-22)	-	-
CuT4	6 (18)	5.40×10^4	418 (+5) 433 (-12)	-	-
ZnAT4	2 (-6)	0.80×10^4	417 (+3) 437 (-11) 451 (+23)	621, 661	2.54×10^4
ZnT4	2 (3)	1.09×10^4	423 (+13) 419(+13) 451 (+22)	618, 657	1.80×10^4

[a] Spectra were recorded in μ = 0.5 M, phosphate buffer pH 6.8 at DNA base:porphyrin ratio 40:1. [b] Shift induced in Soret maximum. [c] Percent drop in absorbance intensity. [d] Spectra were recorded in μ = 0.017 M, phosphate buffer pH 6.8 at DNA base:porphyrin ratio 3.2:1 [e] Spectra were recorded in μ = 0.5 M, phosphate buffer pH 6.8. [f] Maxima in the emission spectra

The porphyrin in **ZnAT4** shows a conservative spectrum, which is different from that of the **ZnT4** porphyrin (Fig 4.12). At lower r_0 ratio the CD spectrum of **ZnT4** shows two peaks in the positive region, which is characteristic of minor groove binding. In contrast, the porphyrin in **ZnAT4** shows a conservative CD spectrum, which is similar to the CD spectrum observed for the interactions of tetracationic tentacle porphyrins, [meso-tetrakis[4-[(3-(trimethylammonio)propyl)-oxy]phenyl]porphyrin] with DNA.[72-76] A positive band at 451 nm and a negative band at 437 nm accompanied by a small positive shoulder at 425 nm observed in **ZnAT4** similar to tentacle porphyrin have been attributed due to highly organized outside self stacking of porphyrin

chromophores in the DNA duplex. This may be explained due to two reasons (a) binding of adenine moiety with DNA may restrict the free disperse of porphyrin in **ZnAT4** and (b) cluster formation of porphyrin molecules near one another at the early stages of DNA addition. When the DNA is in large excess, the porphyrins are free to disperse to essentially independent binding sites. With increase in the r_0 value negative peak of **ZnAT4** disappears and two new peaks appear in the positive region at 449 nm and 430 nm, similar to **ZnT4** since minor groove binding becomes the preferential mode of binding. Similar to **ZnT4**, the porphyrin in **ZnAT4** also interacts externally with the DNA due to its ability to form fifth coordination.[5,6,24,69]

Fig 4.13 illustrates the thermal melting curve for CTDNA obtained in the presence and absence of **CuAT4**. The melting temperature (T_m) of DNA is sensitive to its double helix stability and the binding of compounds to DNA alters the T_m depending on the strength of interactions. Therefore, it can be used as an indicator of binding properties of porphyrins to DNA and their binding strength.

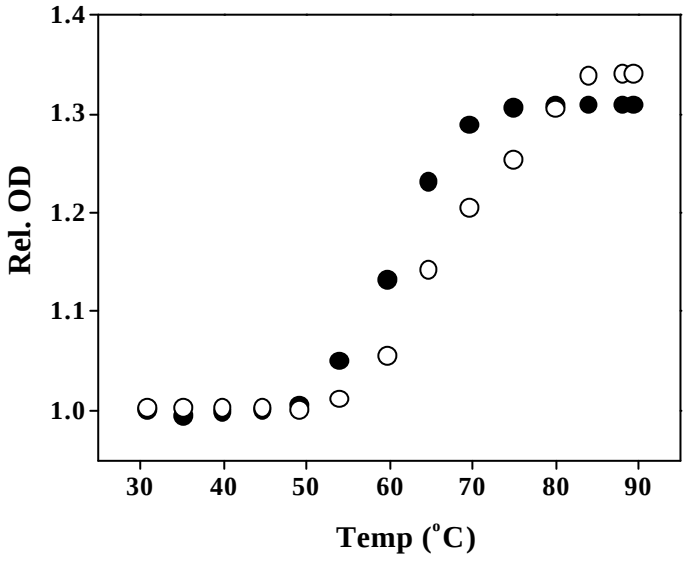

Fig. 4.13 Thermal melting curves for CTDNA in the absence (●) and in the presence (○) of **GT4** in 0.006 M, pH 7.0 phosphate buffer at r_0 = 40:1.

The change in melting temperature $\Delta T_{m,}$ is nothing but the difference between the thermal melting temperature of the CTDNA in the presence and absence of the porphyrin. The change in thermal melting temperature of **CuAT4** is 3.0 °C more than that of **CuT4** whereas it is slightly more for **ZnAT4** or unaltered compared to **ZnT4**. This gives an additional support to conclude that **CuAT4** intercalates and **ZnAT4** binds externally.

4.5 Photocleavage studies

DNA photo cleavage experiments have been carried out with the **ZnAT4** and **CuAT4** metalloporphyrins and the results are compared with photocleavage obtained for **ZnT4** and **CuT4**, respectively. Fig. 4.14 depicts the results of the photocleavage experiment carried out for **ZnAT4** and **ZnT4** porphyrins. Control experiments have suggested that untreated pBR 322 DNA does not show any cleavage in the dark and even upon irradiation by a 435±5 nm light for zinc com-

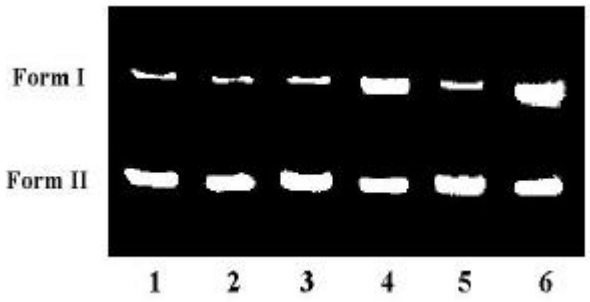

Fig. 4.14 Photocleavage experiments of **ZnAT4** and **ZnT4** porphyrins. Dark and Light Experiments: Lanes 1 and 2: Untreated pBR 322 (100 μM) in the dark and upon irradiation. Lanes 3 and 5: pBR 322 + **ZnAT4** and pBR 322 + **ZnT4**, respectively (2.5 μM) in dark. Lanes 4 and 6: pBR 322 + **ZnAT4** and pBR 322 + **ZnT4**, respectively (2.5 μM) upon irradiation. λ_{irra} = 435±5 nm (60 min) in each case.

plexes (compare Lanes 1 and 2 in Fig. 4.14). DNA nicking was observed for the zinc complexes upon irradiation of DNA in the presence of **ZnAT4** but shows slightly lesser cleaving efficiency than **ZnT4**. Copper complexes don't show nicking probably due to their paramagnetic behaviour.[77,78]

4.6 Summary

In summary, two transition metal complexes of adenine appended tri-cationic porphyrins have been synthesized and characterized by MALDI MS, UV-visible, ^{1}H NMR and ESR spectroscopic techniques. UV-visible and fluorescence titrations have been carried out to estimate the binding with CTDNA. The shift in the wavelength maxima, percentage of hypochromicity and the calculated binding constant values reveal that the behaviour of the **CuAT4** and **ZnAT4** with CTDNA are similar to **CuT4** and **ZnT4**, respectively. Circular dichroism spectra were run to analyze the possible mode of binding interaction of these porphyrins with CTDNA. Porphyrin in **CuAT4** intercalates more efficiently than **CuT4** in the duplex. In contrast to **ZnT4** (which binds externally), the porphyrin in **ZnAT4** interacts through external binding with self-stacking along the DNA helix. Thermal melting studies were performed to support these investigations. Extent of cleavage in DNA (in the presence of light) of these porphyrins with pBR 322 DNA was calculated through photocleavage experiments and it was found that **ZnAT4** photocleaves with slightly lesser efficiency than the standard **ZnT4**. Similar to **CuT4, CuAT4** also did not show any photocleaving efficiency probably due to the paramagnetic nature of metal ion.

4.7 References

1. Pasternack, R. F.; Garrity, P.; Ehrlich, B.; Davis, C. B.; Gibbs, E. J.; Orloff, G.; Giartosio, A.; Turano, C. *Nucleic Acids Res*. **1986**, *14*, 5919.

2. Carvlin, M. J.; Datta-Gupta, N.; Fiel, R. J. *Biochem. Biophys. Res. Commun*. **1982**, *108*, 66.
3. Banville, D. L.; Marzilli, L. G.; Strickland, J. A. *Biopolymers* **1986**, *25*, 1837.
4. Marzilli, L. G.; Banville, D. L.; Zon, G.; Wilson, W. D. *J. Am. Chem. Soc*. **1986**, *108*, 4188.
5. Banville, D. L.; Marzilli, L. G.; Wilson, W. D. *Biochem. Biophys. Res. Commun*. **1983**, *113*, 148.
6. Pasternack, R. F.; Gibbs, E. J.; Villafranca, J. J. *Biochemistry* **1983**, *22*, 5409.
7. Guliaev, A. B.; Leontis, N. B. *Biochemistry* **1999**, *38*, 15425.
8. Strickland, J. A.; Marzilli, L. G.; Gay, K. M.; Wilson, W. D. *Biochemistry* **1988**, *27*, 8870.
9. Sehlstedt, U.; Kim, S. K.; Carter, P.; Goodisman, J.; Vollano, J. F.; Norden, B.; Dabrowiak, J. C. *Biochemistry* **1994**, *33*, 417.
10. Fiel, R. J.; Munson, B. R. *Nucleic Acids Res.* **1980**, *8*, 2835.
11. Ward, B.; Skorobogaty, A.; Dabrowiak, J. C. *Biochemistry* **1986**, *25*, 7827.
12. Kuroda, R.; Tanaka, H. *J. Chem. Soc., Chem. Commun*. **1994**, 1575.
13. Carvlin, M. J.; Fiel, R. J. *Nucleic Acids Res.* **1983**, *11*, 6121.
14. Carvlin, M. J.; Mark, E.; Fiel, R. J.; Howard, J. C. *Nucleic Acids Res.* **1983**, *11*, 6141.
15. Fiel, R. J.; Howard, J. C.; Mark, E. H.; Datta Gupta, N. *Nucleic Acids Res.* **1979**, *6*, 3093.
16. Ford, K.; Fox, K. R.; Neidle, S.; Waring, M. J. *Nucleic Acids Res.* **1987**, *15*, 2221.
17. McMillin. D. R.; McNett. K. M. *Chem. Rev*. **1998**, *98*, 1201.
18. Kasturi. C.; Platz. M. *Photochem. Photobiol.* **1992**, *56*, 427.

19. Barnes, N. R.; Stroud, P. D.; Robinson, K. E.; Horton, C. Schreiner, A. F.; *Biospectroscopy* **1999**, *5*, 179.
20. Pasternack, R. F.; Gibbs, E. J. *Met. Ions Biol. Syst.* **1996**, *33*, 367.
21. Lipscomb, L. A.; Zhou, F. X.; Presnell, S. R.; Woo, R. J.; Peek, M. E. Plaskon, R. R.; Williams, L. D. *Biochemistry* **1996**, *35*, 2818.
22. Bennett, M.; Krah, A.; Wien, F.; Garman, E.; Mckenna, R.; Sanderson, M.; Niedle, S. *Proc. Natl. Acad. Sci. U.S.A.* **2000**, *97*, 9476.
23. Barnes, N. R.; Schreiner, A. F.; Finnegan, M. G.; Johnson, M. K. *Biospectroscopy* **1998**, *4*, 341.
24. Chirvony, V. S. *J. Porphyrins Phthalocyanines* **2003**, *7*, 766.
25. Pasternack, R. F.; Gibbs, E. J.; Villafranca, J. J. *Biochemistry* **1983**, *22*, 2406.
26. Pitie, M.; Pratviel, G.; Bernadou, J.; Meunier, B.; *Proc. Natl. Acad. Sci. U.S.A.* **1992**, *89*, 3967.
27. Maraval, A.; Franco, S.; Vialas, C.; Pratviel, G.; Blasco, M. A.; Meunier, B. *Org. Biomol. Chem*. **2003**, *1*, 921.
28. Dubey, I.; Pratviel, G.; Meunier, B. *Perkin 1* **2000**, *18*, 3088.
29. Chaloin, L.; Bigey, P.; Loup, C.; Marin, M.; Galeotti, N.; Piechaczyk, M.; Heitz, F.; Meunier, B. *Bioconjugate Chem*. **2001**, *12*, 691.
30. Lapi, A.; Pratviel, G.; Meunier, B. *Metal-Based Drugs* **2001**, *8*, 47.
31. Wietzerbin, K.; Muller, J. G.; Jameton, R. A.; Pratviel, G.; Bernadou, J.; Meunier, B.; Burrows, C. J. *Inorg. Chem.* **1999**, *38*, 4123.
32. Drexler, C.; Hosseini, M. W.; Pratviel, G.; Meunier, B. *Chem. Commun.* **1998**, *13*, 1343.
33. Jakobs, A. J.; Bernadou, J. B.; Meunier, B. *J. Org. Chem.* **1997**, *62*, 3505.
34. Marguerite, P.; Meunier, B. *J. Biol. Inorg. Chem.* **1996**, *1*, 239.
35. Casas, C.; Lacey, J.; Meunier, B. *Bioconjugate Chem.* **1993**, *4*, 366.

36. Casas, C.; Bernadette, S.J.; Loup, C.; Lacey, J.; Meunier, B. *J. Org. Chem.* **1993**, *58*, 2913.

37. Maraval, A.; Franco, S.; Vialas, V.; Patviel, G.; Blasco, M. A.; Meunier, B. *Org. Biomol. Chem.* **2003**, *1*, 921.

38. Frau, S.; Bernadou, J.; Meunier, B. *Bioconjugate Chem.* **1997**, *8*, 222.

39. Silvana, F.; Jeanoseph, B.; Meunier, B.; Jean-Claude, D.; Joseph, V. *New. J. Chem.* **1995**, *19*, 873.

40. Bigey, P.; Sonnichsen, S. H.; Meunier, B.; Nielsen, P. E. *Bioconjugate Chem*. **1997**, *8*, 267.

41. Mestre, B.; Pitie, M.; Loup, C.; Claparols, C.; Pratviel, G.; Meunier, B. *Nucleic Acids Res.* **1997**, *25*, 1022.

42. Mestre, B.; Jakobs, A.; Pratviel, G.; Meunier, B. *Biochemistry* **1996**, *35*, 9140.

43. Ding, L.; Casas, C.; Etemad-Moghadam, G.; Meunier, B. *New. J. Chem*. 1990, *14*, 421.

44. Ding, L.; Etemad-Moghadam, G.; Cros, S.; Auclair, C.; Meunier, B. *J. Med. Chem.* **1991**, *34*, 900.

45. Uno, T.; Hamasaki, K.; Tanigawa, M.; Shimabayashi, S. *Inorg. Chem.* **1997**, *36*, 1676.

46. Uno, T.; Aoki, K.; Shikimi, T.; Hiranuma, Y.; Tomisugi, Y.; Ishikawa, Y. *Biochemistry* **2002,** *41*, 13059.

47. Laine, M.; Richard, F.; Tarnaud, T.; Bied-Charreton, C.; Verchere-Beaur, C. *J. Biol. Inorg. Chem.* **2004**, *9*, 550.

48. Salmon. L.; Bied-Charetton.C.; Verechere-Beaur. C.; Gaudemer. A. *Tetrahedron Lett*. **1990**, *31*, 519.

49. Tjahjono, D. H.; Mima, S.; Akutsu, T.; Yoshioka, N.; Inoue, H. *J Inorg. Chem.* **2001**, *85*, 219.

50. Wall, R. K.; Shelton, A. H.; Bonaccorsi, L. C.; Bejune, S. A.; Dube, D.; McMillin, D. R. *J. Am. Chem. Soc.* **2001**, *123*, 11480.
51. Bejune, S. A.; Shelton, A. H.; McMillin, D. R. *Inorg. Chem*. **2003**, *42*, 8465.
52. Bejune, S. A.; McMillin, D. R. *Chem. Commun.* **2004**, 1320.
53. McMillin, D. R.; Shelton, A. H.; Bejune, S. A.; Fanwick. E. P.; Wall. R. K. *Coord. Chem. Rev*. **2005**, *xx*, xxxx.
54. Pasternack, R.F.; Franscesconi, L. Raff, D.; Spiro. E. *Inorg. Chem.* **1973**, *12*, 2606.
55. Fuhrhop, J.-H.; Smith, K. M.; In *Porphyrins and Metalloporphyrins*; Smith, K. M., Ed.; Elsevier: Amsterdam, **1975**; p. 769.
56. Fuhrhop, J.-H.; Smith, K. M.; In *Porphyrins and Metalloporphyrins*; Smith, K. M., Ed.; Elsevier: Amsterdam, **1975**; p. 179.
57. Sirish, M.; Maiya, B. G. *J. Porphyrins Phthalocyanines* **1998**, *2*, 1.
58. Subramanian, J. In *Porphryins and Metalloporphyrins*; Smith, K. M., Ed.; Elsevier: Amsterdam, **1975**; p. 555.
59. Assour, J. M. *J. Chem. Phys.* **1965**, *43*, 2477.
60. Kadish, K. M.; Maiya, B. G.; Araullo-McAdams, A. *J. Phys. Chem.* **1994**, 427.
61. Mojzes, P.; Kruglik, S. G.; Baumruk, V.; Turpin, P-Y. *J. Phys. Chem. B* **2003**, *107*, 7532.
62. Kruglik, S. G.; Mojzes, P.; Mizutani, Y.; Kitagawa, T.; Turpin, P.-Y. *J. Phys. Chem. B* **2001**, *105*, 5018.
63. Kruglik, S. G.; Galievsky, V. A.; Chirvony, V. S.; Apanasevich, P. A.; Ermolenkov, V. V.; Orlovich, V. A.; Chinsky, L.; Turpin, P.-Y. *J. Phys. Chem.* **1995**, *99*, 5732.

64. Galievsky, V. A.; Chirvony, V. S.; Kruglik, S. G.; Ermolenkov, V. V.; Orlovich, V. A.; Otto, C.; Mojzes, P.; Turpin, P.-Y. *J. Phys. Chem.* **1996**, *100*, 12649.

65. Hudson, B. P.; Sou, J.; Berger, D. J.; McMillin, D. R. *J. Am. Chem. Soc.* **1992**, *114*, 8997.

66. Harriman, A. Davila, J. *Tetrahedron* **1989**, *45*, 4737.

67. Kalyanasundaram, K. *Inorg. Chem***. 1984**, *23*, 2453.

68. Sari, M. A.; Battioni, J. P.; Dupre, D.; Mansuy, D.; Lepecq. J. B. *Biochemistry* **1990**, *29*, 4205.

69. Kelly, J. M.; Murphy, M. J. *Nucleic Acids Res*. **1985**, *13*, 167.

70. Pasternack, R. F. *Chirality* **2003**, *15*, 329.

71. Catherine, V.-B.; Martine, P.-F.; Eric, T.; Gilles, A.-H.; Nathalie, B.; Alain, G. *Tetrahedron* **1996**, *52*, 13589.

72. Marzilli, L. G.; Petho, G.; Lin, M.; Kim, M. S.; Dixon, D. W. *J. Am. Chem. Soc*. **1992**, *114*, 7575.

73. Nancy, E. M.; Petho, G.; Dixon, D. W.; Marzilli, L. G. *Inorg. Chem*. **1995**, *34*, 3677.

74. Nancy, E. M.; Petho, G.; Dixon, D. W.; Kim, M. S.; Marzilli. L. G. *Inorg. Chem.* **1994**, *33*, 4676.

75. Petho, G. Nancy, B. E.; Kim, M. S.; Lin, M.; Dixon, D. W.; Marzilli, L. G. *Chem. Commun.* **1993**, 1547.

76. Schnier, H.-J.; Wang, M. *J. Org. Chem*. **1994**, *59*, 7473.

77. Fiel, R. J.; Beerman, T. A.; Mark, E. S.; Gupta, N. D. *Biochem. Biophys. Res. Commun.* **1982**, *107*, 1067.

78. Praseuth, D.; Gaudemer, A; Verlhac, J-B.; Kraljic, I.; Sissoeff, I.; Guille, E. *Photochem. Photobiol.* **1986**, *44*, 717.

CHAPTER 5

Binding studies of nucleobase appended tri-cationic porphyrins and metalloporphyrin with DNA hairpins

5.1 Introduction

The interaction of cationic porphyrins with synthetic and natural DNA has been widely studied using UV-visible absorption spectroscopy and circular dichroism (CD),[1-14] fluorescence,[15] Raman,[16] NMR,[16,17] ESR,[18] viscometry,[19,20] footprinting,[21,22] kinetic methods[23] and X-ray crystallography.[24] The external binding of porphyrin with DNA exhibits only a modest effect on $\pi-\pi^*$ absorption in the Soret region: a small bathochromic shift of $\Delta\ddot{e}$ 8 nm on the absorption maximum and weak hypochromism (H 10%) is most often observed. External binding also induces a CD signal with a positive amplitude.[1,25] The intercalative binding of porphyrin allows more intimate contact with the π system of the DNA, which results in larger spectroscopic perturbations. The Soret band not only shows a larger bathochromic shift ($\Delta\ddot{e}$ 15 nm), but stronger hypochromism (H 35%) as well. Intercalative binding also results in induced CD signal with negative amplitude.[1,25] The versatile binding nature of these porphyrins with DNA has been used to bring other moieties in the proximity of DNA. Recently, a variety of moieties have been connected to porphyrins to increase the binding affinity, to regulate the sequence specificity or to include chemical functionalities for inducing specific reactions.[26-40]

McMillin and co-workers have shown that DNA hairpins or stem-loop structures provide useful comparisons to other DNAs. Hairpin loop favors the formation of a double-stranded stem even for stems as short as six base pairs and it also paves way for varying the sequence. Base-replacement studies are also

straightforward and permit hypothesis testing.[41,42] Even though the effect on the sequence can be easily analyzed by using short length oligonucleotides for binding, the equilibrium concentration of single-stranded forms would be relatively high and they also bind the porphyrin.[43] Binding in the loop region is a potential complication. However it is comparatively rigid[44] and base-replacement studies are consistent with the assumption that cationic porphyrins bind almost exclusively in the stem region.[45] Working with large excess of the competing hairpins avoid complications associated with cooperative binding effects. The molecular dynamics calculations by Ford *et al*., indicated that contact in the major groove involving thymine methyl groups and pyridinium groups of 5,10,15,20-tetra (*N*-methylpyridinium-4-yl) porphyrin **(H_2T4)** could inhibit full intercalation of the porphyrin into a 5′TpA3′ step.[46] But it has been proved by uridine-for-thymine base replacement in the DNA hairpins that the steric bulk of the thymine methyl group does not prevent **H_2T4** from intercalating in A=T rich regions of DNA.[43] The mode of binding known as hemiintercalation, which has been observed in the solid[24] is unlikely to occur in solution at least in sequences rich in GC base pairs since the hemiintercalation would require base extrusion.[42,45,47]

Here, in this chapter, we analyse the interactions of nucleobase appended tri-cationic porphyrins (**AT4**, **TT4**, **GT4** and **CT4**) and copper(II) complex of adenine appended tri-cationic porphyrin (**CuAT4**) (Fig. 5.1) with hairpin substrates (Fig. 5.2) on the basis of changes in the Soret band and induced circular dichroism.

5.2 Experimental details

Tosylate salt of **H_2T4** was obtained commercially and used as such. Copper(II) complex of **H_2T4** (iodide salt)) (**CuT4**) was prepared by a modified reported procedure.[48] The porphyrins used in this study were synthesized as

described in chapter 3, section 3.2 and chapter 4, section 4.2.

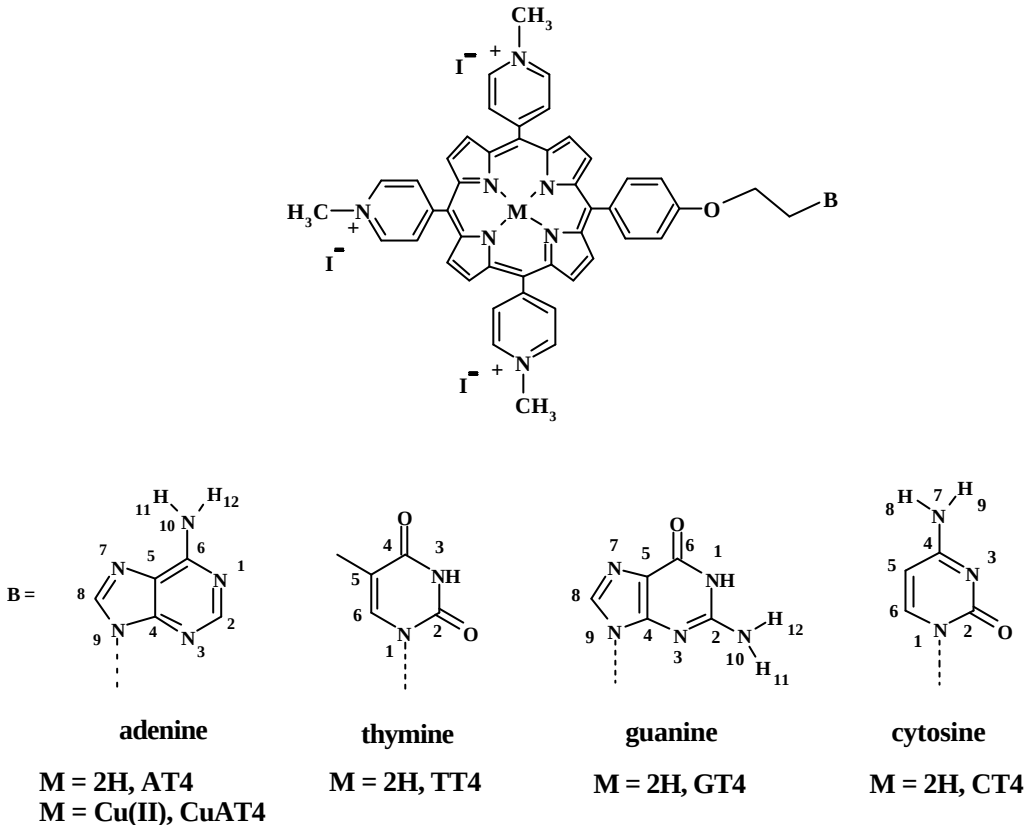

Fig. 5.1 Structures of nucleobase-appended tri-cationic porphyrins investigated in the present study.

5.3 Results and discussion

The nucleobase appended tri-cationic porphyrins and the copper(II) complex of adenine appended porphyrin (Fig. 5.1) are utilized for the studies with DNA hairpins. The interactions of porphyrins and metalloporphyrin with the DNA hairpins have been investigated and the results obtained are compared with their corresponding reference compounds. The DNA hairpins have been selected

such that the porphyrin and DNA interaction studies cover the following aspects: (a) effect on DNA hairpins rich in AT base pairs, (b) effect on DNA hairpins rich in CG base pairs and c) effect on increase in the stem length and change in the loop sequence.

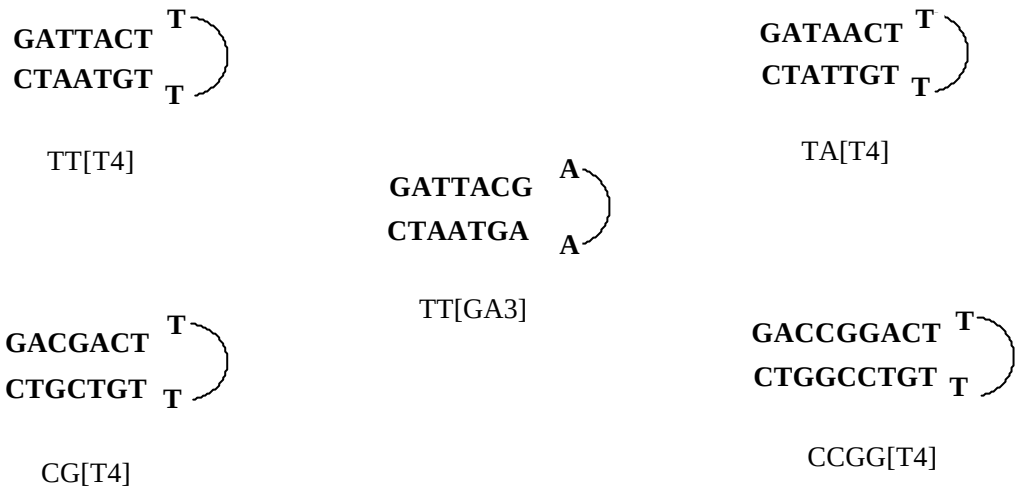

Fig. 5.2 Structures of DNA hairpins employed in this study

5.3.1 Spectral studies on the interactions of nucleobase appended tri-cationic porphyrins with DNA hairpins

Table 5.1 summarizes the spectral data obtained for the adducts of nucleobase appended tri-cationic porphyrins with TT[T4], TA[T4], CG[T4], CCGG[T4] and TT[GA3] hairpins. UV-visible titrations were performed for the **H_2T4** and nucleobase porphyrins at various r_0 values ($0.25 \leq r_0 \leq 15$). Similar to **H_2T4**, comparison of the absorption spectra of nucleobase appended tri-cationic porphyrin adduct with DNA hairpins at $r_0 \sim 5$ and $r_0 \sim 10$ (r_0 = [hairpin DNA]/[porphyrin]) reveal that adduct formation is complete at $r_0 \sim 5$ itself.[41] Spectral titrations also showed that formation of one-to-one adduct of nucleobase porphyrins with the DNA hairpin oligonucleotide was complete at $r_0 \sim 5$.[41]

Absence of an isosbestic point in almost all the systems may be due to two or more modes of binding.[39]

5.3.1.1 With TT[T4] and TA[T4] hairpins

Fig. 5.3, Fig. 5.4, Fig. 5.5 and Fig. 5.6 show the UV-visible spectra recorded with various DNA hairpins for **AT4**, **TT4**, **GT4** and **TT4**, respectively at $r_0 \sim 5$. With AT rich DNA hairpins (TT[T4] and TA[T4]) nucleobase appended porphyrins as well as **H_2T4** show 8-11 nm bathochromic shift in the Soret band. Analogous to **H_2T4**, only porphyrin in **GT4** shows hypochromism with the AT rich DNA hairpins (TT[T4] and TA[T4]). By contrast, all the other nucleobase appended porphyrins (**AT4**, **TT4** and **CT4**) show hyperchromism with the AT rich DNA hairpins. The amount of hypochromism observed for **GT4** with TT[T4] and TA[T4] DNA hairpins are 9% and 7% and with **H_2T4** the hypochromism produced are 13% and 4%, respectively.

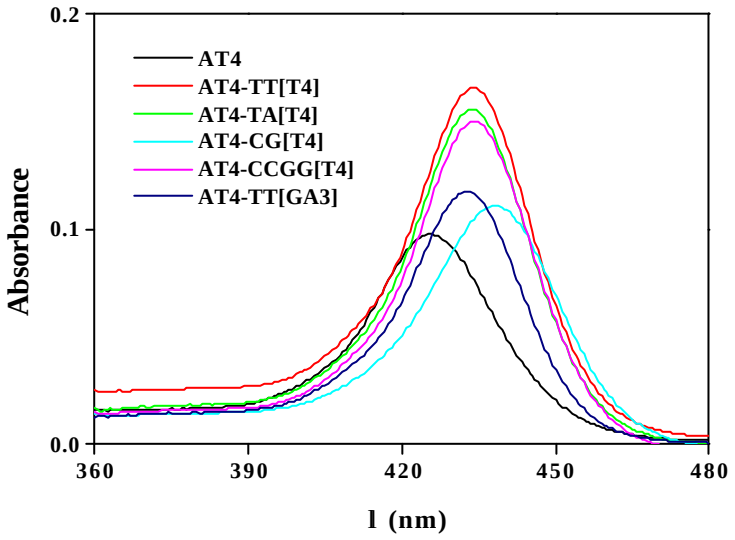

Fig. 5.3 UV-visible spectra of **AT4** recorded with various DNA hairpins in pH 6.8 phosphate buffer, μ = 0.1 M at $r_0 \sim 5$.

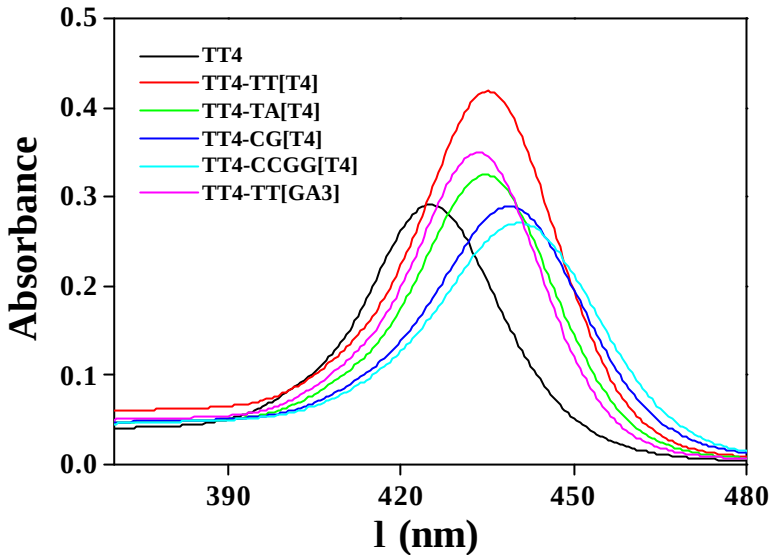

Fig. 5.4 UV-visible spectra of **TT4** recorded with various DNA hairpins in pH 6.8 phosphate buffer, μ = 0.1 M at r_0 ~ 5.

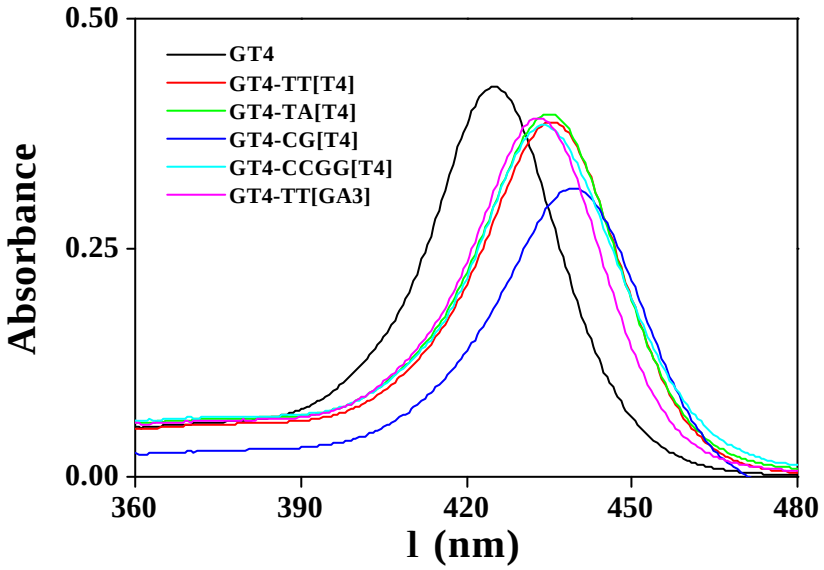

Fig. 5.5 UV-visible spectra of **GT4** recorded with various DNA hairpins in pH 6.8 phosphate buffer, μ = 0.1 M at r_0 ~ 5.

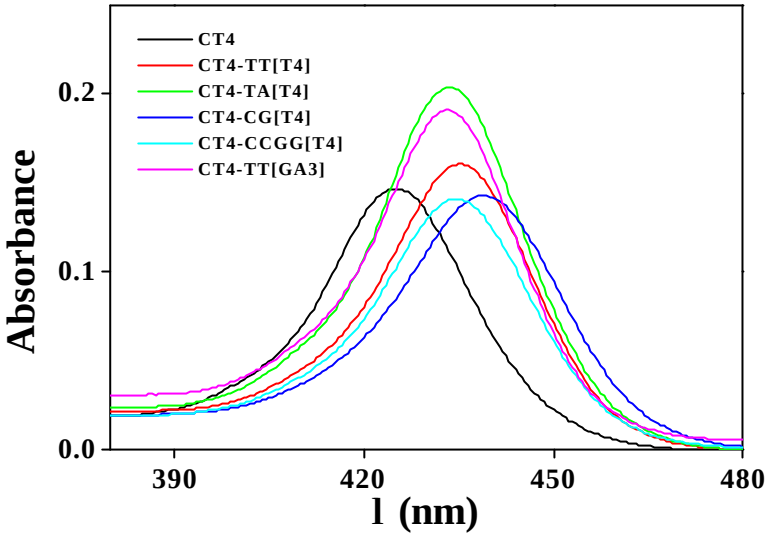

Fig. 5.6 UV-visible spectra of **CT4** recorded with various DNA hairpins in pH 6.8 phosphate buffer, μ = 0.1 M at r_0 ~ 5.

Table 5.1 Spectral data for porphyrin (nucleobase appended tri-cationic porphyrin and **H_2T4**) adducts with DNA hairpins in pH 6.8, phosphate buffer μ = 0.1 M.[a]

Compd	DNA	Soret band		CD	
		Dl, nm [b]	%H [c]	l_{max}, nm	De, M^{-1} cm^{-1}
H_2T4	TT[T4]	8	13	425	39
	TA[T4]	8	4	425	48
	CG[T4]	18	39	439	-19
	CCGG[T4]	10	24	445	-11
	TT[GA3]	7	3	426	24
AT4	TT[T4]	9	-70	427	10
	TA[T4]	9	-60	427	10
	CG[T4]	13	-13	440	-4
	CCGG[T4]	9	-54	438	-3
	TT[GA3]	8	-20	426	6

.....continued

……**Table 5.1**

TT4	TT[T4]	10	-44	425	10
	TA[T4]	10	-11	432	9
	CG[T4]	14	1	439	-7
	CCGG[T4]	16	7	437	-8
	TT[GA3]	9	-20	429	10
GT4	TT[T4]	11	9	429	19
	TA[T4]	10	7	426	22
	CG[T4]	15	26	441	-10
	CCGG[T4]	9	10	447	-16
	TT[GA3]	8	8	430	19
CT4	TT[T4]	11	-9	429	16
	TA[T4]	10	-39	426	12
	CG[T4]	14	3	441	-4
	CCGG[T4]	9	4	437	-3
	TT[GA3]	9	-30	430	8

[a] Measured at $r_0 \sim 5$.

Nucleic acids have no absorption bands in the visible region. However, the porphyrin exhibits a strong Soret band. Porphyrin does not display circular dichroism in the absence of DNA due to its achirality, whereas spectra are induced in the Soret region when they are bound to natural or artificial DNA. The induced CD spectra for **H_2T4** and the nucleobase linked porphyrins were recorded in the presence of various DNA hairpins at $r_0 \sim 5$.

Fig. 5.7, Fig. 5.8, Fig. 5.9, Fig. 5.10 and 5.11 depict the CD spectra recorded for various combinations of nucleobase appended porphyrins and **H_2T4** with TT[T4], TA[T4], CG[T4], CCGG[T4] and TT[GA3] DNA hairpins, respectively. CD spectra of the nucleobase appended porphyrins show only positive bands at 425-432 nm with AT rich DNA hairpins similar to **H_2T4** but with lesser intensity (Fig. 5.7 and Fig. 5.8; Table 5.1). These results suggest that

the nucleobase appended tri-cationic porphyrins bind only through external binding with AT rich hairpins in a manner similar to **H_2T4** but with a lesser extent.[41,49] The intensity of the positive induced CD signals are in the range $\Delta\varepsilon$ = 8-22 $M^{-1}cm^{-1}$. The lesser external binding nature of these porphyrins may be due to the presence of only three positive charges that results in decrease in the affinity.[40] Porphyrin in **GT4** shows slightly more external binding than the porphyrins connected to **AT4**, **TT4** and **CT4**. The more acidic protons to exhibit keto-enol tautomerism, extended conjugation and ability to form more number of hydrogen bonds of the bound form of guanine in **GT4** may drive the porphyrin moiety to the proximity of DNA and account for strong external interaction than the porphyrins connected to other nucleobases (**AT4**, **TT4** and **CT4**).

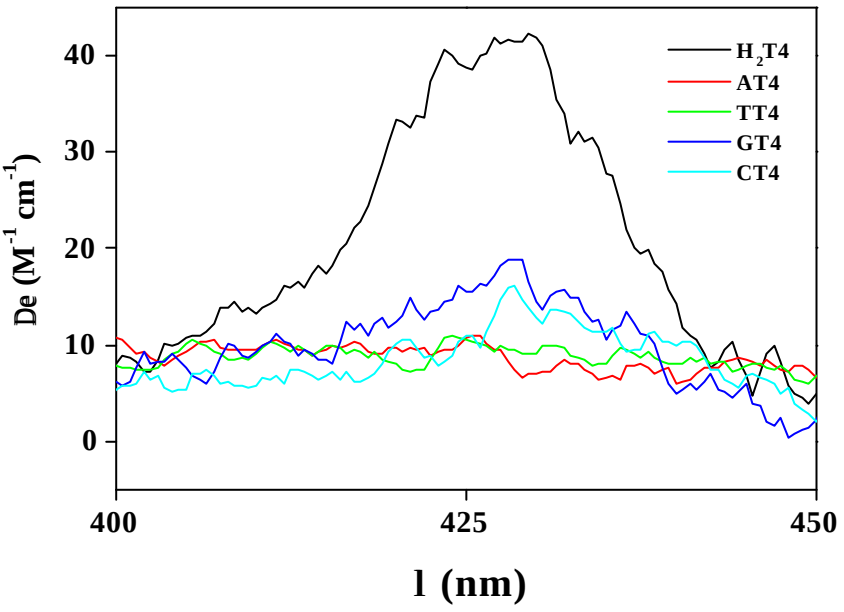

Fig. 5.7 CD spectra of TT[T4] with various nucleobase appended tri-cationic porphyrins and **H_2T4** recorded in pH 6.8 phosphate buffer, μ = 0.1 M at r_0 ~ 5.

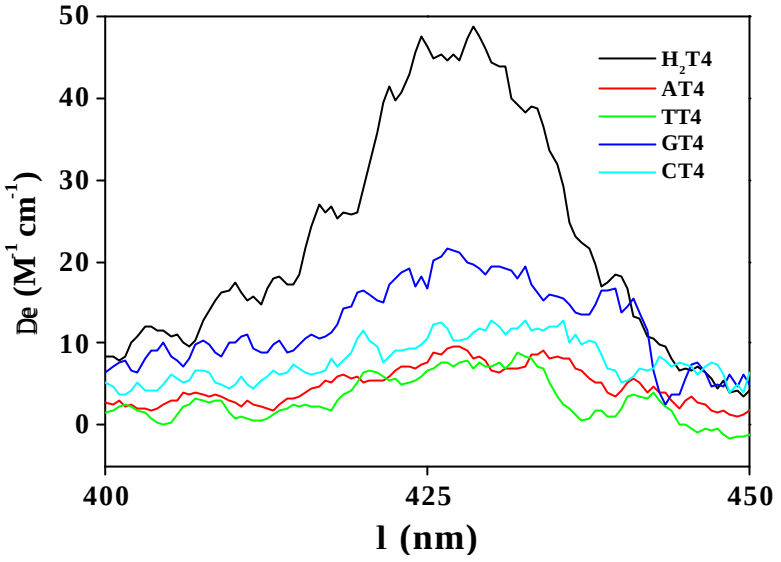

Fig. 5.8 CD spectra of TA[T4] with various nucleobase appended tri-cationic porphyrins and **H_2T4** recorded in pH 6.8 phosphate buffer, μ = 0.1 M at r_0 ~ 5.

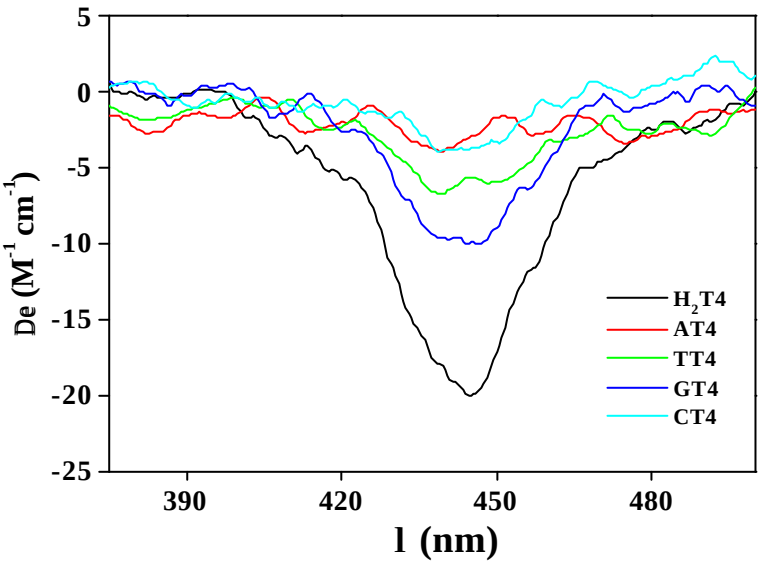

Fig. 5.9 CD spectra of CG[T4] with various nucleobase appended tri-cationic porphyrins and **H_2T4** recorded in pH 6.8 phosphate buffer, μ = 0.1 M at r_0 ~ 5.

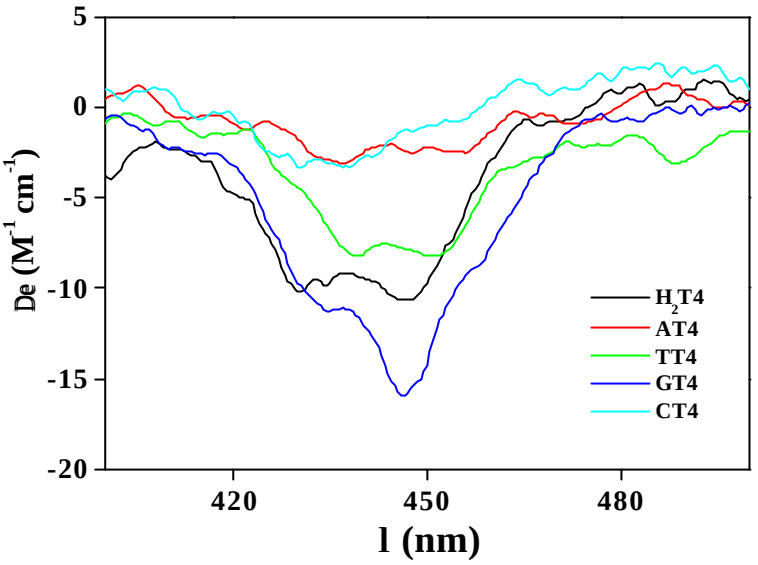

Fig. 5.10 CD spectra of CCGG[T4] with various nucleobase appended tri-cationic porphyrins and **H_2T4** recorded in pH 6.8 phosphate buffer, μ = 0.1 M at r_0 ~ 5.

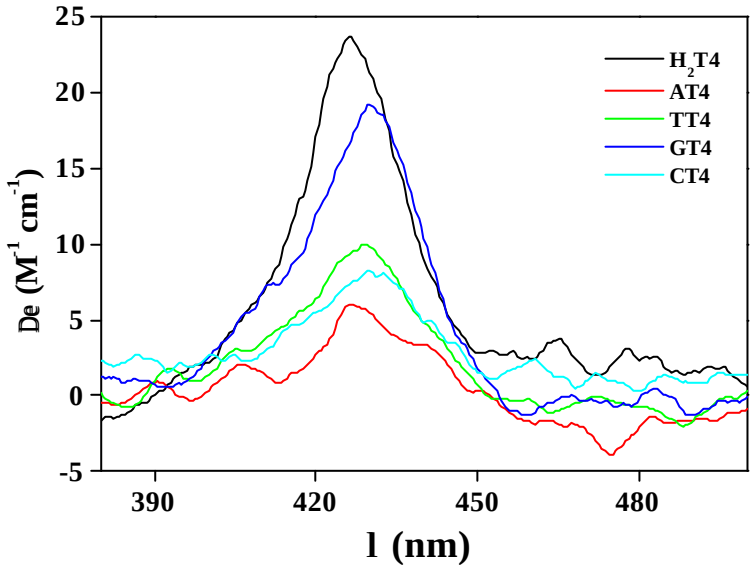

Fig. 5.11 CD spectra of TT[GA3] with various nucleobase appended tri-cationic porphyrins and **H_2T4** recorded in pH 6.8 phosphate buffer, μ = 0.1 M at r_0 ~ 5.

5.3.1.2 With CG[T4] hairpin

Similar to **H_2T4**, the nucleobase appended porphyrins show binding mode different from that of the binding with AT rich DNAs. All these porphyrins show a bathochromic shift of 13-15 nm in the Soret region whereas **H_2T4** shows 18 nm shift. The nucleobase-appended porphyrins **TT4** and **CT4** show lesser hypochromicity (1% and 3%, respectively) whereas **AT4** shows hyperchromicity (-13%) with CG[T4] hairpin substrate. Only the guanine-connected porphyrin (**GT4**) exhibits hypochromicity (26%) similar to **H_2T4** (39%). The higher bathochromicity and more hypochromism are indicative of strong coupling between the π system of porphyrin chromophore with the nucleobase of the DNA during intercalation.[50]

The CD data obtained for CG[T4] porphyrin also supports the UV-visible results (Fig. 5.9 and Table 5.1). Only negative CD signal has been observed for nucleobase porphyrins and **H_2T4** with CG[T4] hairpin but the peak intensities of nucleobase porphyrins are less than that of the **H_2T4**. Among the nucleobase porphyrins, porphyrin in **GT4** and **TT4** shows stronger intercalation than other nucleobase porphyrins. The intercalating tendency of the nucleobase appended porphyrins and standard decreases in the order **H_2T4** > **GT4** > **TT4** > **CT4** ~ **AT4** with CG[T4] DNA. Decrease in the affinity with only three positive charges may be reason for the decrease in the intercalating efficiency of these porphyrins when compared to **H_2T4**.[40]

5.3.1.3 With CCGG[T4] hairpin

The hairpin containing 20-mer CCGG[T4] is related to CG[T4] except that the stem contains two more C≡G base pair on either side of the 5′-CpG-3′ step. The bound form of **TT4** porphyrin shows 16 nm bathochromic shift whereas the other porphyrins (**AT4**, **GT4** and **CT4**) show only 9 nm shift similar to the

standard **H_2T4** porphyrin. Hyperchromism was observed with **AT4** porphyrin whereas other porphyrins show 4-10% hypochromism; among them, **GT4** porphyrin exhibits maximum hypochromism. All the nucleobase porphyrins and **H_2T4** show negative CD signal, while the porphyrin in **AT4**, **TT4** or **CT4** shows a less intense peak at 437 nm, the one in **GT4** shows a more intense peak than **H_2T4** at 447 nm. All these results reveal that porphyrin in **GT4** intercalates strongly into the long stem CCGG[T4] hairpin DNA than the other nucleobase appended porphyrins and the **H_2T4** porphyrin. Thus with CCGG[T4] the intercalating efficiency of the nucleobase appended porphyrins and reference decreases in the order **GT4** > **H_2T4** > **TT4** > **CT4** ~ **AT4**.

5.1.3.4 Comparison of CG[T4] and CCGG[T4] adducts

Mcmillin coworkers have extensively studied the interactions of **H_2T4** and **CuT4** porphyrins with various DNA hairpins.[41,42,45,47] The results reveal that the DNA containing at least 50% G≡C base pairs supports intercalative binding simply because a robust hydrogen bonding framework stabilizes the intercalated adduct and inhibits distortions that favor external binding. In accordance with these results, the interactions of nucleobase porphyrins with CG rich DNA hairpins (CG[T4] and CCGG[T4]) also exhibit absorption spectral changes and negative CD signal due to intercalative binding.

The Soret absorption band and the CD signal obtained for the adducts of **H_2T4** and nucleobase appended tri-cationic porphyrins (**AT4**, **TT4**, **GT4** and **CT4**) with CG[T4] DNA hairpin are broader than those of the adducts formed with AT rich DNA hairpins. This bandwidth could be explained on the basis that both the 5′-CpG-3′ and 5′-GpC-3′ steps support intercalation and that the two signals are different enough to broaden the envelope.[50] The negative CD signals obtained for **H_2T4**, **GT4** and **TT4** with CCGG[T4] appear bisignate compared to

that of the adducts with CG[T4]; thus can be attributed to two different binding modes.[52] The additional C≡G base pair may also support intercalation and both the intercalations (5′-CpG-3′ and 5′-GpC-3′) were strong enough to appear as bisignate signs. Among the nucleobase appended porphyins, the intercalating efficiency follows the order **GT4** > **TT4** > **CT4** ~ **AT4** with both the CG rich DNA hairpins, CG[T4] and CCGG[T4]. A similar argument as that of the intercalation of nucleobase appended porphyrins with CTDNA holds good here also. The acidity of the NH sites in nucleobase follows the order: guanine (N10H11 and N1H) > thymine (N3H) > cytosine (N7H8) > adenine (N10H11). The acidic protons present in the N1 and N3 of guanine and thymine, respectively favour keto-enol tautomerism in these nucleobases.[53] The extended conjugation and the more number of hydrogen bonding (three hydrogen bonds) capability of bound guanine drives the porphyrin connected in **GT4** to intercalate more than the porphyrin in **TT4**, in which thymine moiety can form only two hydrogen bonds and less conjugation with only six membered ring.

Comparison of the porphyrin adducts of **H_2T4** and **GT4** with CG[T4] and CCGG[T4] DNA substrates show difference in their interactions. The CD signal obtained for **GT4** and CCGG[T4] adduct is more intense than that of the **H_2T4** and CCGG[T4] adduct. In contrast, the signal intensity of **GT4** with CG[T4] is less intense compared to the intensity of **H_2T4** and CG[T4]. This difference in the intensity reveals that the porphyrin in **GT4** intercalates readily into CCGG[T4] compared to CG[T4] hairpin DNA whereas the **H_2T4** porphyrin intercalation is stronger with CG[T4] than CCGG[T4]. The other nucleobase porphyrins (**AT4**, **TT4** and **CT4**) intercalate with almost similar efficiency with CG[T4] and CCGG[T4] DNA. Co-operative interactions occur when intercalation of one porphyrin affects the binding and the spectral properties of a second porphyrin molecule usually bound nearby.[50] As discussed earlier for the interactions of

nucleobase porphyrins with AT rich DNA, the significance of the guanine moiety bound to DNA may facilitate the interaction of porphyrin moiety by bringing it into the proximity of the DNA, which in turn enhances co-operative binding of porphyin moieties. Since the overall co-operative effect also depends on the strength of the hydrogen bond of DNA hairpin, the one with high hydrogen bonding ability (CCGG[T4]) results in enhanced intercalation. Porphyrin in **AT4**, **TT4** and **CT4** shows less intercalating efficiency than **H_2T4** due to the less number of positive charges and decrease in the contribution of bound nucleobase moiety for stabilization of the intercalation of porphyrin moiety.

5.3.1.5 With TT[GA3] hairpin

The UV-visible spectra recorded for the nucleobase appended porphyrins with TT[GA3] at r_0 ~ 5 show 7-9 nm shift in the Soret region which is similar to **H_2T4**. Porphyrin in **GT4** and **H_2T4** shows hypochromism whereas hyperchromism was observed for the adducts with other nucleobase porphyrins (**AT4**, **TT4** and **CT4**). Positive CD signals were observed due to external binding of all the nucleobase porphyrins but with a lesser affinity than **H_2T4** due to the presence of only three positive charges. The CD signals fall in the range 426-430 nm. **GT4** exhibits an intense CD signal compared to **AT4**, **CT4** and **TT4** due to its stronger external binding due to the contribution of bound guanine moiety for the stabilization of porphyrin and DNA hairpin adduct. With TT[GA3], the external binding efficiency of the nucleobase appended porphyrins and standard decrease in the order **H_2T4** > **GT4** > **TT4** > **CT4** ~ **AT4**.

5.3.1.6 Comparison of TT[T4] and TT[GA3] adducts

The hydrogen bonding is inherently weaker within a 5′-T4-3′ loop as compared to a 5′-GA3-3′ loop.[54,55] The intensity of the positive CD signal

observed for the binding of **H_2T4**, porphyrin in **AT4** and **CT4** with TT[T4] hairpin is high compared to that with the TT[GA3] adducts. Intercalation is effective in the relatively rigid polymer whereas external binding becomes a higher affinity process with the more flexible polymer. [7,12,59] Due to inherently weaker hydrogen bonding in the 5′-T4-3′ loop, melting of TT[T4] hairpin may be easier and may end up with high external binding affinity.[50] By contrast, porphyrin in **GT4** and **TT4** shows similar external binding to both the hairpins TT[T4] and TT[GA3]. This may be due to the binding of guanine and thymine moieties which are strong enough to bring about structural reorganization (partial melting) of B-form DNA and promote stronger binding of the porphyrin moiety with TT[GA3] hairpin.

5.3.2 Spectral studies on the interactions of copper(II) complex of adenine appended tri-cationic porphyrin with DNA hairpins

Table 5.2 summarises the spectral data obtained for the DNA hairpin adducts of **CuAT4** and **CuT4**. UV-visible titrations have been performed with various r_0 values ($0.25 \leq r_0 \leq 15$) in a manner similar to that for nucleobase appended porphyrins. Pronounced spectral changes occurred with the addition of hairpin DNA solution into **CuAT4**, which is similar to that with **CuT4**.[42,45,47] Analogous to the absorption changes of **H_2T4** and nucleobase appended tri-cationic porphyrins, comparison of the adduct formation of **CuAT4** and **CuT4** with DNA hairpins at $r_0 \sim 5$ and $r_0 \sim 10$ reveals that adduct formation is complete at $r_0 \sim 5$ itself. Spectral titrations also confirmed that formation of the one-to-one adduct of copper complex with the DNA hairpin oligonucleotide was complete at $r_0 \sim 5$.[45] Absence of an isosbestic point in the absorption titration may be due to two or more modes of binding.[39]

The UV-visible titrations performed using AT rich DNA hairpins reveal

that upon uptake, the Soret band undergoes a small bathochromic shift and decreases in intensity. The Soret band grows smoothly as the concentration of DNA increases and exhibits hyperchromism in the presence of an excess of TT[T4] or TA[T4] hairpin substrates (Table 5.2). The bathochromic shift observed on the Soret band of **CuAT4** and **CuT4** with AT rich haipins are comparable (~4 nm) whereas the amount of hyperchromism exerted is more for porphyrin in **CuAT4** than **CuT4**. In contrast to the above, with CG rich DNA (CG[T4]) the spectral data reveal that at least two different types of adduct form depending on the amount of hairpin in solution. Thus, the absorbance goes through a minimum and then approaches a limiting value as the r_0 value increases. At the same time, the bathochromic shift of the Soret band evolves in a more monotonic fashion. Qualitatively, with CCGG[T4] hairpin also the same trend is observed. Similar bathochromic shift (~10 nm) was observed for the porphyrin in **CuAT4** and **CuT4** with CG[T4] and CCGG[T4] hairpins. The hypochromism observed for **CuAT4** and **CuT4** with CG[T4] and CCGG[T4] fall in the range 20-26%. Hairpin with long stem shows slightly higher hypochromism most likely due to increase in the number of hydrogen bonds. Between the copper complexes, **CuAT4** shows slightly less hypochromism. Interactions of both the copper complexes with TT[GA3] however, results in hyperchromism.

Fig. 5.12 illustrates the CD spectra recorded for CuAT4 with various DNA hairpins. Metalloporphyrins are achiral but induced CD signal is observed when bound to DNA. In these copper metallated complexes the high symmetry of the metalloporphyrin moiety plays a major role in its interactions with DNA. The interactions of the Cu(II) metal center with the bases of the nucleic acids via its vacant axial sites also facilitate the adduct formation. The wavelength maximum and the amplitude of the CD peaks show good agreement with the results obtained from UV-visible experiments. The addition of AT rich hairpins (TT[T4] and

TA[T4]) induces positive signal with the **CuAT4** porphyrin which is similar to that with CuT4 but with higher intensity. This shows its greater external binding ability. High symmetry of the copper(II) metallated porphyrin restricts the ease of orientation of the metalloporphyrin moiety for partial melting of the DNA and leads to less external binding than H_2T4. The binding of the adenine moiety promotes the interaction of copper(II) metalated porphyrin chromophore with DNA by distorting its B-form, which results in relatively strong external binding of porphyrin in CuAT4.

Table 5.2 Spectral data for metalloporphyrin (**CuAT4** and **CuT4**) adducts with DNA hairpins in pH 6.8, phosphate buffer μ = 0.1 M.[a]

Compd.	DNA	Soret band		CD	
		D l , nm	**%H**	**l_{max}, nm**	**De , M^{-1} cm^{-1}**
CuT4	TT[T4]	4	-24	419	14
	TA[T4]	4	-18	423	13
	CG[T4]	10	25	434	-21
	CCGG[T4]	10	27	433	-23
	TT[GA3]	3	-18	417	9
CuAT4	TT[T4]	5	-49	424	24
	TA[T4]	5	-48	427	24
	CG[T4]	10	20	437	-17
	CCGG[T4]	9	22	442	-19
	TT[GA3]	8	-22	426	33

[a] Measured at $r_0 \sim 5$.

In parallel with the absorbance spectra, interaction with the CG rich hairpins give rise to a negative peak in the Soret region due to the binding of porphyrin in the intercalation mode. Both the copper complexes show slightly highly intense signal with CCGG[T4] than with CG[T4] due to the strong hydrogen bonding of the former resulting in a more rigid nature. Comparison of

the negative CD signal obtained for the adducts of porphyrin in CuAT4 with that of CuT4 porphyrin shows that the former is slightly less efficient for intercalation. The slightly lesser intercalating capacity of CuAT4 may be explained by less number of positive charges. A positive peak has been observed as a result of interaction with TT[GA3] for both these porphyrins in agreement with the external binding. Weaker hydrogen bonding in the 5′-T4-3′ loop may facilitate external binding of CuT4 porphyrin in TT[T4] than TT[GA3] whereas the case is reverse with porphyrin in CuAT4. The strong hydrogen bonding in the loop of TT[GA3] DNA may be overwhelmed by CuAT4 since both the adenine moiety and Cu(II) metallated porphyrin core can participate in the distortion of the DNA.

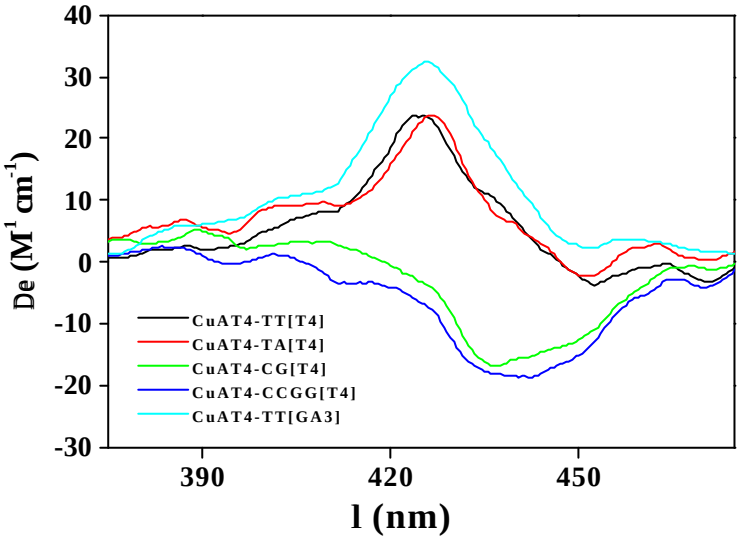

Fig. 5.12 CD spectra of **CuAT4** with various DNA hairpins recorded in pH 6.8 phosphate buffer, μ = 0.1 M at $r_0 \sim 5$.

5.4 Energy Analysis

McMillin and coworkers have successfully discussed the energy analysis involved in the interaction of porphyrins and DNA hairpins.[50,51] Parallel to their

discussions, the energy analysis of the interactions of nucleobase porphyrins with DNA hairpins can be explained as discussed below. Intercalation is a natural mechanism of DNA-binding, a simple unwinding motion normally creates the pocket needed.[56,57] In contrast, creation of an optimal external binding site for large, highly charged ligands such as tri or tetra cationic porphyrins would involve significant melting of the DNA structure.[12] The energetics of adduct formation must include endoergic as well as exoergic factors. Destabilizing factors of DNA-porphyrin adduct may include requirements for structural reorganization of the host or the guest as well as any steric strain generated by adduct formation.

In the present context, the residual steric effect is the net repulsion energy that accrues in the final, fully reorganized adduct due to unfavorable interactions between host and guest atoms. The counterbalancing forces that drive adduct formation include coulombic interactions between peripheral charges on the porphyrin and phosphate groups on the DNA backbone,[57] hydrophobic effects, van der Waals interactions[58] and any charge-transfer stabilization associated with interactions between the π systems of the ligand and the host.[41] To summarize the arguments, it is convenient to use eqn 5.1

$$\Delta G = \Delta G_R + \Delta G_B \qquad (5.1),$$

where ΔG represents the interaction energy between the porphyrin and DNA, ΔG_R denotes the free energy needed to reorganize the DNA as well as the ligand and ΔG_B is the free energy asssociated with the binding of the preorganized components.[41] Note that ΔG_B includes all terms that drive the binding as well as the steric strain. In Figure 5.13, the P + DNA state represents the unbound porphyrin and DNA. The ΔG_R^e term represents the free energy needed to prepare

DNA and the porphyrin for external binding and ΔG_B^e is the energy released upon formation of the externally bound adduct P^e/DNA^e. Likewise, the ΔG_R^i term represents the free energy needed to reorganize DNA and the porphyrin for intercalative binding and ΔG_B^i is the energy released on formation of the intercalated adduct P^i/DNA^i.

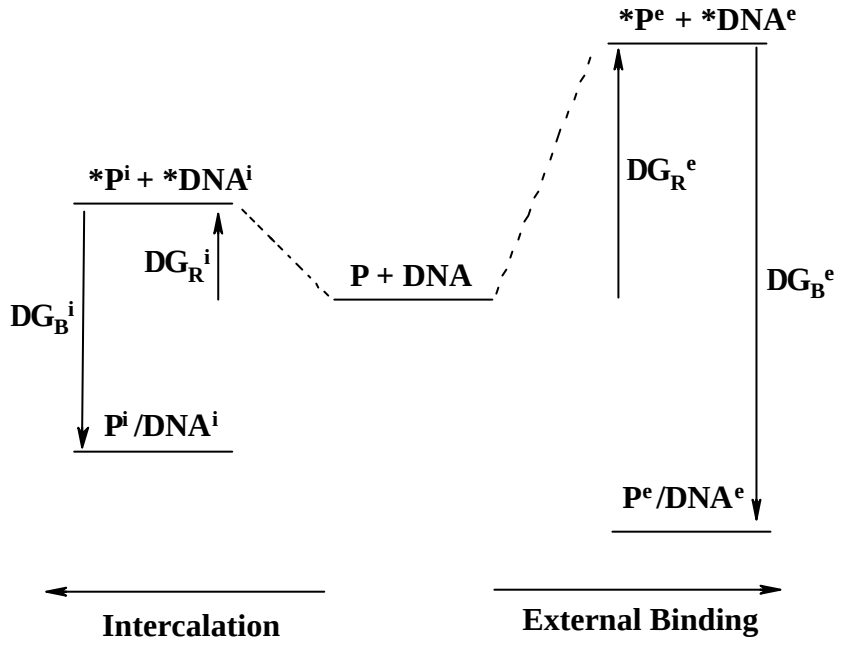

Fig. 5.13 Qualitative energy diagram for competitive binding of porphyrin moiety (tri or tetra cationic) to AT rich DNA hairpins. ΔG_R^e (ΔG_R^i) is the reorganization energy for external (intercalative) binding and ΔG_B^e (ΔG_B^i) is the energy released upon external (intercalative) binding of preorganized species. The P + DNA state corresponds to the free components and asterisk signifies reorganized for binding.

5.4.1 With AT rich porphyrins

Figure 5.13 provides a qualitative rationale for the fact that porphyrin moiety binds externally to AT rich DNA hairpins. The ease of melting of AT rich

DNA hairpins permits formation of a very favorable external binding pocket that results in a highly exoergic ΔG_B^e. While the ΔG_R term is smaller for intercalation. Strain reduces the free energy available for release during the ΔG_B^i step. The mix of factors therefore favors external binding. Comparison of the interaction of porphyrin in nucleobase appended porphyrins with that of the **H_2T4** porphyrin shows lesser amount of external binding due to the decrease in the number of positive charges (lesser Coulombic interaction) results in lesser exoergic ΔG_B^e. Porphyrin in **GT4** exhibits a slightly higher external binding efficiency. This may be due to the ease of reorganization of the porphyrin moiety directed by strong binding of guanine (depends on its more acidic protons, number of hydrogen bonding ability and extended conjugation) results in decrease in the ΔG_R^e term. Similarly decrease in ΔG_R^e term accounts for more external binding of **CuAT4** than **CuT4**.

5.4.2 With CG-rich porphyrins

Robust hydrogen bonding in DNA sequences rich in G≡C base pairs disfavors effective external binding because the ΔG_R^e term is prohibitively endoergic.[42] As a consequence, the bulky porphyrin ligand binds by intercalation despite steric strain in the minor groove that reduces the exoergonic character of the ΔG_B^i step. The loss of affinity (due to the presence of only three positive charges) results in less ΔG_B^i accounts for the less intercalating efficiency of nucleobase porphyrins than **H_2T4**. Only the interaction of porphyrin in **GT4** with CCGG[T4] hairpin exhibit higher intercalating ability than **H_2T4** due to lesser ΔG_R^i and more exoergic ΔG_B^i due to increase in co-operativite interactions. The same argument explains slightly lesser intercalating capacity of **CuAT4** when compared to **CuT4**.

5.5 Summary

Interactions of four nucleobase (A, T, G and C) appended tri-cationic porphyrins and copper(II) complex of adenine appended tri-cationic metalloporphyrin with DNA hairpins (TT[T4], TA[T4], CG[T4], CCGG[T4] and TT[GA3]) have been investigated and the results obtained were compared with their corresponding reference compounds. External binding has been observed with DNA hairpins those are rich in AT sequences whereas intercalation has been observed with CG rich DNA. Magnitude of the binding of porphyrin moiety (external or intercalative) differs among these nucleobase porphyrins and depends on the nature of the nucleobase present in it. Interestingly with the long stem DNA, CCGG[T4], porphyrin in **GT4** shows more intercalation than **H_2T4** whereas the situation was quite opposite with CG[T4] DNA. Change in the loop sequence of the DNA also affects binding. Similar to **CuT4**, **CuAT4** exhibits external binding and intercalation with AT rich and GC rich DNAs, respectively. Finally a stepwise energy analysis has been provided to illustrate the competing effects that influence the binding.

5.6 References

1. Pasternack, R. F.; Gibbs, E. J.; Villafranca, J. J. *Biochemistry* **1983**, *22*, 2406.
2. Mukundan, N. E.; Petho, G.; Dixon, D. W.; Marzilli, L. G. *Inorg. Chem.* **1995**, *34*, 3677.
3. Pasternack, R. F. *Chirality* **2003**, *15*, 329.
4. Lipscomb, L. A.; Zhou, F. X.; Presnell, S. R.; Woo, R. J.; Peek, M. E.; Plaskon, R. R.; Williams, L. D. *Biochemistry* **1996**, *35*, 2818.
5. Pasternack, R.F.; Gibbs, E.J. *Met. Ions Biol. Syst.* **1996**, *33*, 367.
6. McMillin, D. R.; McNett, K. M. *Chem. Rev.* **1998**, *98*, 1201.

7. Marzilli, L. G. *New J. Chem.* **1990**, *14*, 409.
8. Bennett, M.; Krah, A.; Wien, F.; Garman, E.; Mckenna, R.; Sanderson, M.; Niedle, S. *Proc. Natl. Acad. Sci. U.S.A.* **2000**, *97*, 9476.
9. Barnes, N. R.; Schreiner, A. F.; Finnegan, M. G.; Johnson, M. K.; *Biospectroscopy* **1998**, *4*, 341.
10. Chirvony, V. S. *J. Porphyrins and Phthalocyanines* **2003**, *7*, 766.
11. Strickland, J. A.; Banville, D. L.; Wilson, W. D.; Marzilli, L. G. *Inorg. Chem.* **1987**, *26*, 3398.
12. Gibbs, E. J.; Maurer, M. C.; Zhang, J. H.; Reiff, W. M.; Hill, D. T.; Malcika-Blaszkiewicz, M.; McKinnie, R. E.; Liu, H. Q.; Pasternack, R. F. *J. Inorg. Biochem.* **1988**, *32*, 39.
13. Hudson, B. P.; Sou, J.; Berger, D. J.; McMillin. D. R. *J. Am. Chem. Soc.* **1992**, *114*, 8997.
14. Kruk, N. N.; Shishporenok, S. I.; Korotky, A. A.; Galievsky, V. A.; Chirnovy, V. S.; Turpin, P. Y. *J. Photochem. Photobiol. B.* **1998**, *45*, 67.
15. Sari, M. A.; Battioni, J. P.; Dupre, D.; Mansuy, D.; LePecq, J. B. *Biochemistry* **1990**, *29*, 4205.
16. Butje, K.; Schneider, J. H.; Kim, J. P.; Wang, Y.; Ikuta, S.; Nakamoto, K.; *J. Inorg. Biochem.* **1989**, *37*, 119.
17. Strickland, J. A.; Marzilli, L. G.; Wilson, W. D.; Zon, G. *Inorg. Chem.* **1989**, *28*, 4191.
18. Dougherty, G.; Pasternack, R. F. *Biophys. Chem.* **1992**, *44*, 11.
19. Banville, D. L.; Marzilli, L. G.; Strickland, J. A.; Wilson, W. D.; *Biopolymers* **1986**, *25*, 1837.
20. Gray, T. A.; Yue, K. T.; Marzilli, L. G. *J. Inorg. Biochem.* **1991**, *41*, 205.
21. Ward, B.; Skorobogaty, A.; Dabrowiak, J.C. *Biochemistry* **1986**, *25*, 7827.

22. Ford, K.; Fox, K R.; Neidle, S.; Waring, M. J. *Nucl. Acids Res*. **1987**, *15* 2221.
23. Pasternack, R. F.; Gibbs, E. J.; Vilafranca, J. J. *Biochemistry* **1983**, *22*, 5409.
24. Kim, J.-O.; Lee, Y.-A.; Jin, B.; Park, T.; Song, R, Kim, S. K. *Biophys. Chem*. **2004**, *111*, 63.
25. Casas, C.; Lacey, J.; Meunier, B. *Bioconjugate Chem.* **1993**, *4*, 366.
26. Frau, S.; Bernadou, J.; Meunier, B. *Bioconjugate Chem.* **1997**, *8*, 222.
27. Silvana, F.; Jeanoseph, B.; Meunier, B.; Jean-Claude, D.; Joseph, V. *New. J. Chem.* **1995**, *19*, 873.
28. Bigey, P.; Sonnichsen, S. H.; Meunier, B.; Nielsen, P. E. *Bioconjugate Chem*. **1997**, *8*, 267.
29. Mestre, B.; Pitie, M.; Loup, C.; Claparols, C.; Pratviel, G.; Meunier, B. *Nucleic Acids Res.* **1997**, *25*, 1022.
30. Mestre, B.; Jakobs, A.; Pratviel, G.; Meunier, B. *Biochemistry* **1996**, *35*, 9140.
31. Li, H.; Fedorova, O. S.; Trumble, W. R.; Fletcher, T. R.; Czuchajowski, L.; *Bioconjugate Chem.* **1997**, *8*, 49.
32. Mohammadi, S.; Perree-Fauvet, M.; Gresh, N.; Hillairet, K.; Taillandier, E.; *Biochemistry* **1998,** *37*, 6165.
33. Steenkeste, K.; Enescu, M.; Tfibel, F.; Perree-Fauvet, M.; Fontaine-Aupart, M.-P.; *J. Phys. Chem. B* **2004**, *108*, 12215.
34. Perree-Fauvet, M.; Gresh, N. *Tetrahedron Lett*. **1995**, *36*, 4227.
35. Li, H.; Fedorova, O. S.; Grachev, A. N.; Trumble, W. R.; Bohach, G. A.; Czuchajowski, L. *Biochim. Biophys. Acta* **1997**, *1354*, 252.
36. Li, H.; Czuchajowski, L.; Trumble, W. R. *J. Heterocyclic Chem.* **1997**, *34*, 999.

37. Song, R.; Kim, Y.-S.; Lee, C. O.; Soo. Y. S.; *Tetrahedron Lett*. **2003**, *44*, 1537.

38. Ding, L.; Etemad-Moghadam, G.; Cros, S.; Auclair, C.; Meunier, B. *J. Med. Chem*. **1991**, *34*, 900.

39. Laine, M.; Richard, F.; Tarnaud, T.; Bied-Charreton, C.; Verchere-Beaur, C. *J. Biol. Inorg. Chem.*, **2004**, *9*, 550.

40. Catherine, V.-B.; Martine, P.-F.; Eric, T.; Gilles, A.-H.; Nathalie, B.; Alain, G. *Tetrahedron* **1996**, *52*, 13589.

41. Keith, E. T.; McMillin. D. R. *J. Phys. Chem. B* **2001,** *105*, 12628.

42. Tears, D. K. C.; McMillin, D. R. *Chem. Commun*. **1998**, 2517.

43. Blom, N.; Odo, J.; Nakamoto, K.; Strommen, D. P. *J. Phys. Chem*. **1986**, *90*, 2847.

44. VanDongen, M. J. P.; Mooren, M. M. W.; Willems, E. F. A.; van der Marel, G. A.; van Boom, J. H.; Wijmenga, S. S.; Hilbers, C. W. *Nucl. Acids Res*. **1997**, *25*, 1537.

45. Lugo-Ponce, P.; McMillin, D. R. *Coord. Chem. Rev*. **2000**, *208*, 169.

46. Ford, K.; Fox, K. R.; Neidle, S.; Waring, M. J. *Nucleic Acids Res.* **1987**, *15*, 2221.

47. Eggleston, M. K.; Crites, D. K.; McMillin. D. R. *J. Phys. Chem. A* **1998,** *102*, 5506.

48. Pasternack, R.F.; Franscesconi, L. Raff, D.; Spiro. E. *Inorg. Chem*. **1973**, *12*, 2606.

49. Wall, R. K.; Shelton, A. H.; Bonaccorsi, L. C.; Bejune, S. A.; Dube, D.; McMillin, D. R. *J. Am. Chem. Soc*. **2001**, *123*, 11480.

50. McMillin, D. R.; Shelton, A. H.; Stephanie A. Bejune, S. A.; Fanwick, P. E.; Wall. R. K. *Coord. Chem. Rev*. **2005**, xxx, xxxx.

51. Bejune, S. A. Shelton. A. H. McMillin, D. R. *Inorg. Chem*. **2003**, *42*, 8465.

52. Kuroda. R.; Tanaka. H. *J. Chem. Soc., Chem. Commun*. **1994**, 1575.

53. Baker. E. S.; Gidden. J.; Ferzoco. A.; Bowers. M. T. *Phys. Chem. Chem. Phys*. **2004**, *6*, 2786.

54. Bejune. S. A.; McMillin. D. R. *Chem. Commun.* **2004**,1320.

55. Nakano, M.; Moody, E. M.; Liang J.; Bevilacqua, P. C. *Biochemistry* **2002**, *41*, 14281.

56. Calladine, C. R.; Drew, H. R. *Understanding DNA*; Academic: New York, 1997.

57. Sari, M. A.; Battioni, J. P.; Mansuy, D.; Lepecq, J. B. *Biochem. Biophys. Res. Commun.* **1986**, *141*, 643.

58. Ren, J. S.; Jenkins, T. C.; Chaires, J. B. *Biochemistry* **2000**, *39*, 8439.

CHAPTER 6

Bis(aryloxo) derivatives of azo-benzene bridged tin(IV) porphyrins: Synthesis, spectroscopy and photochemistry

6.1 Introduction

In this chapter we have used 'axial-bonding' strategy to construct tin(IV) porphyrin based donor-acceptor systems. These compounds are synthesized from diporphyrinic system where azobenzene moiety is directly connected to the tin(IV) porphyrin chromophore. Here we describe the synthesis, characterization and photochemistry of these derivatives and their monomeric compounds. Unfortunately we could not observe '*cis-trans*' isomerism, which causes photoswitching function in many of the porphyrin–azobenzene conjugates reported so far.[1-9]

Tin(IV) porphyrin complexes and related macrocyclic systems have several biomedical applications. The major use has been for photodynamic therapy against cancer and non-cancerous proliferative skin conditions.[10-15] Non-cytotoxic antiproliferative action has been applied to the problem of restenosis following angioplasty.[16] A particularly useful property of tin(IV) complexes of natural porphyrins and their allies is their inhibition of heme oxygenase, making them candidates for the treatment of hyperbilirubinemia.[17,18] In addition, they offer protection against acute oxidative injury.[19] Tin(IV) porphyrins have also been included, with other metalloporphyrins, in the studies of antiviral action, particularly for preventing HIV infection.[20,21] Tin(IV) porphyrins have been studied extensively for electrochemical and fluorescence sensors for various substrates[22,23] and as catalysts for photooxidation/photoreduction reactions of water as well as a variety of organic reactants.[24-26] More recent applications of

tin(IV) macrocycles built on the porphyrin framework are concerned with their ability to act as NMR shift reagents and key components in functional supramolecular assemblies.[27-33]

All the above applications of these macrocyclic systems largely rely on their favorable chemical and spectroscopic properties.[34-40] Thus, interest in the chemistry of tin(IV) porphyrin has originated from the realization that their attractive redox and photochemical properties can be harnessed for performing potentially useful functions. Results of our efforts in this direction are discussed in this chapter which reports the synthesis, characterization and photochemical properties of 'axial-bonding' type two monomeric (**M3PY** and **M4PY**) and two dimeric (**A3PY** and **A4PY**) triads based on the tin(IV) porphyrin, Schemes 6.1 - 6.3. Finally, ground state and excited state properties of **A3PY** and **A4PY** are compared with their monomeric triads, **M3PY** and **M4PY**.

6.2 Experimental details

5,10,15,20-tetraphenylporphyrin (**H_2TPP**) and 5,10,15,20-tetraphenyl porphyrinatozinc(II) **(ZnTPP)**, reference compounds employed during this investigation were synthesized by reported procedures.[41,42]

6.2.1 Synthesis of 5,10,15,20-tetra(4-methylphenyl)porphyrin [H_2L^1][43]

Freshly distilled pyrrole (5.6 mL, 80 mmol) and reagent grade p-toluladehyde (9.6 mL, 80 mmol) were added to 200 mL of refluxing propanoic acid. The mixture was refluxed for 45 min., left overnight at 10°C and filtered. The black-violet residue was washed several times with hot water, followed by methanol and purified by chromatography on basic alumina column. Elution with chloroform gave 5,10,15,20-tetra(4-methylphenyl)porphyrin (**H_2L^1**). Yield = 2.7 g (20%).

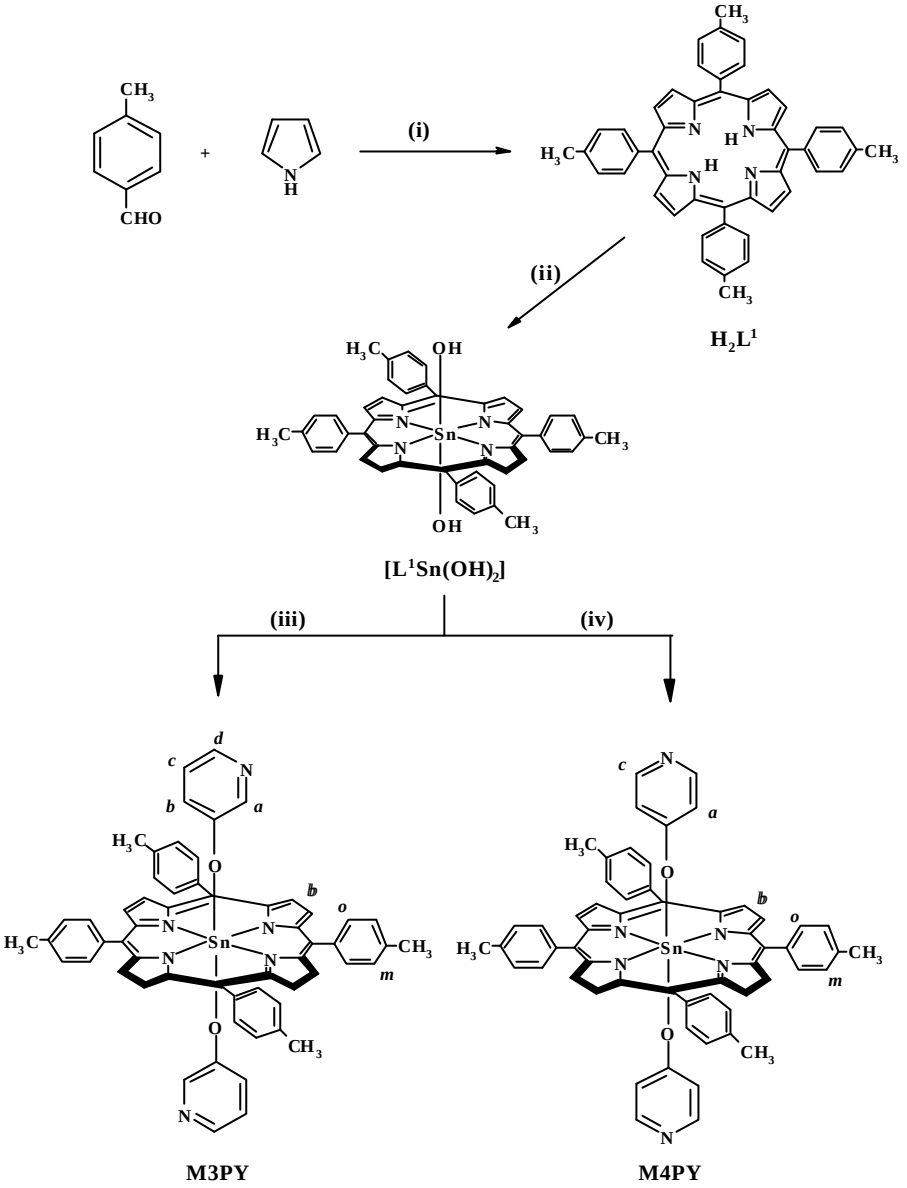

Reaction conditions: (i) propanoic acid, reflux, 45 min. (ii) $SnCl_2$, pyridine, reflux, 3 h, aq. NH_3 (iii) 3-hydroxypyridine, benzene, reflux, 4 h (iv) 4-hydroxypyridine, benzene, reflux, 4 h.

Scheme 6.1 Synthesis of **M3PY**, **M4PY** and their reference compound **$[L^1Sn(OH)_2]$.**

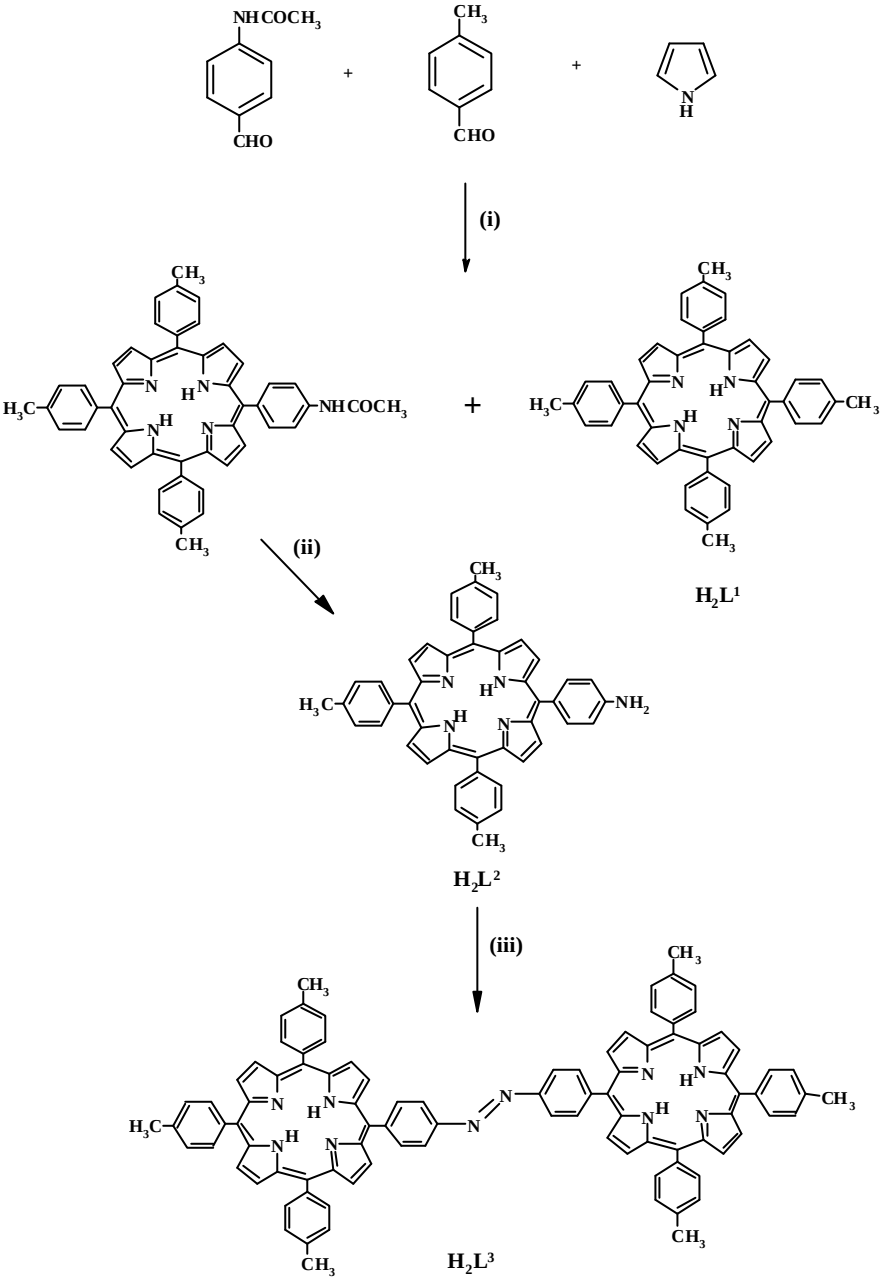

Reaction conditions: (i) propanoic acid, reflux, 1 h (ii) 20% HCl, reflux, 5 h (iii) MnO_2, $CHCl_3$, reflux, 7 h.

Scheme 6.2 Synthesis of azobenzene bridged porphyrin dimer, **[H_2L^3]**.

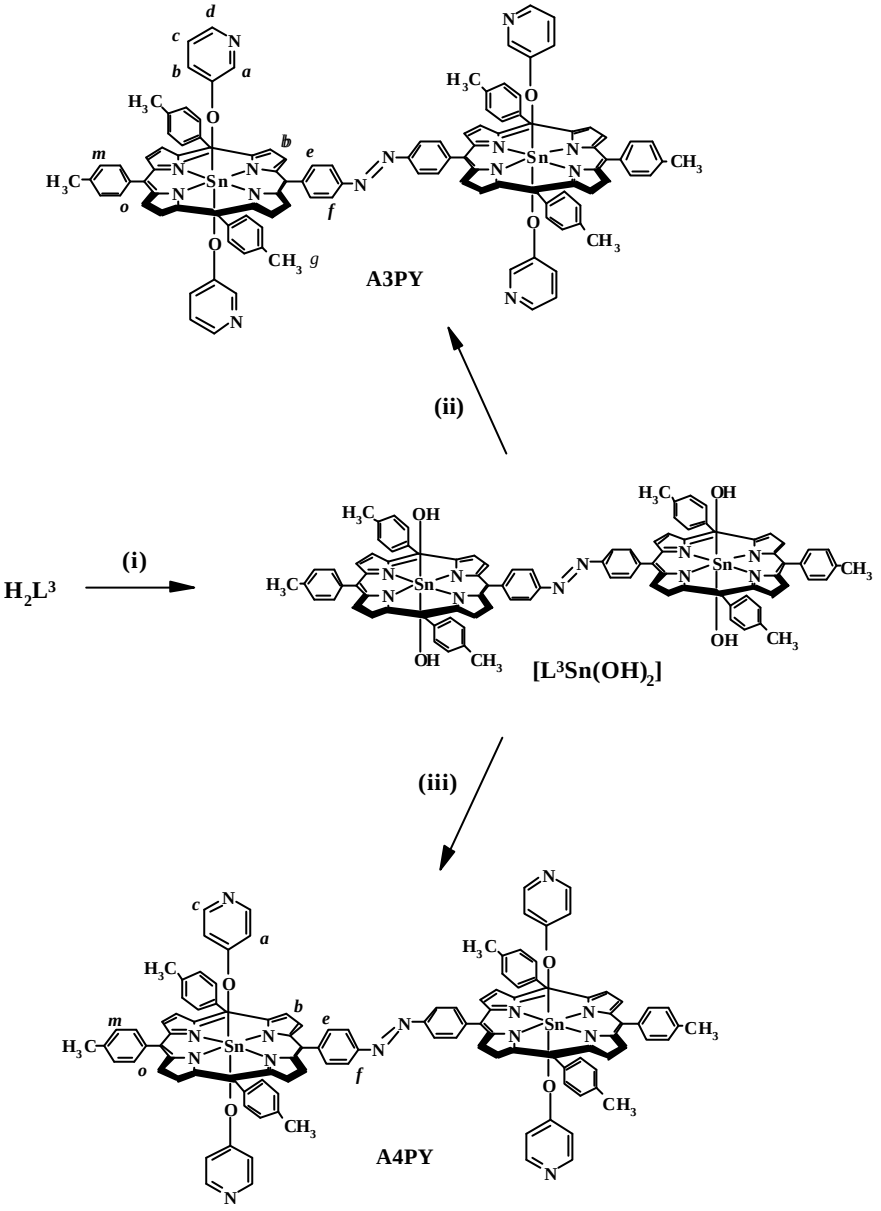

Reaction conditions: (i) $SnCl_2$, pyridine, reflux, 5 h, aq. NH_3 (ii) 3-hydroxypyridine, benzene, reflux, 5 h (iii) 4-hydroxypyridine, benzene, reflux, 5h.

Scheme 6.3 Synthesis of **A3PY**, **A4PY** and their reference compound, **$[L^3Sn(OH)_2]$**.

6.2.2 Synthesis of meso-5-(4-aminophenyl)-10,15,20-tri(4-methylphenyl) porphyrin [H_2L^2][1]

Pyrrole (5.37 g, 80 mmol) was slowly added to a refluxing solution of 4-methylbenzaldehyde (7.21 g, 60 mmol) and 4-acetamidobenzaldehyde (3.23 g, 20 mmol) in 1.5 L propanoic acid. After complete addition of pyrrole, the reaction mixture was refluxed for 1 h, cooled and left for 12 h at room temperature. The propanoic acid was removed by distillation, and the residue was dried at 100 °C in vacuum and chromatographed on a silica gel column with CH_2C1_2 as eluent. The first fraction collected was 5,10,15,20-tetra(4-methylphenyl)porphyrin. After isolation of first fraction, 5% ethyl acetate was added to the eluent. The second fraction collected was compound 5-(4-acetamidophenyl)-10,15,20-tri(4-methylphenyl) porphyrin. Yield = 0.37 g (17%).

A suspension of 5-(4-acetamidophenyl)-10,15,20-tri(4-methylphenyl) porphyrin (0.28 g 0.39 mmol) in 20% HCl was refluxed for 5 h. The solution was cooled and neutralized carefully by adding 10% KOH solution. The neutralized solution was extracted several times with CH_2Cl_2. The combined organic layers were dried (Na_2SO_4), the solvent was evaporated and the residue chromatographed on a silica gel column using CH_2C1_2 as eluent. Yield = 0.31 g (90%).

6.2.3 Synthesis of 4,4¢-bis[5-(10,15,20-tri(4-methylphenyl))porphyrinyl] azobenzene [H_2L^3][1]

Freshly prepared MnO_2 (2.0 g, 23 mmol) was added to a solution of 0.1 g (0.149 mmol) $\mathbf{H_2L^2}$ in 25 mL $CHCl_3$. The reaction mixture was refluxed for 7h. The reaction mixture was filtered, and the residue washed several times with $CHCl_3$ (100 mL). The solution was dried over $MgSO_4$ and the solvent evaporated.

The remaining solid was chromatographed on a silica gel column with $CHCl_3$ as eluent. Yield = 0.06 g (60%). MALDI MS: $[M]^+$ = 1340.

6.2.4 Synthesis of 5,10,15,20-tetra(4-methylphenyl)porphyrinatodihydroxide-tin(IV) $[L^1Sn(OH)_2]$[44,45]

A sample of $\mathbf{H_2L^1}$ (2.0 g, 3.0 mmol) and $SnCl_2$ (2.0 g, 8.0 mmol) were taken up in 40 mL of pyridine. The reaction mixture was refluxed for 2 h. To this, 5 mL of aq. ammonia was added and the resulting mixture was stirred for 1 h at 50°C. The solvent was evaporated to dryness under reduced pressure. The residue was dissolved in ca. 50 mL of $CHCl_3$ and was washed repeatedly with water. The $CHCl_3$ solution was dried over anhydrous Na_2SO_4, after which it was evaporated to ca. 5 mL. This solution was applied on to a neutral alumina column. The desired product was eluted using $CHCl_3$-CH_3OH (97:3, v/v). Solvents were evaporated and the product was precipitated from CH_2Cl_2-hexane. Yield = 2.4 g (90%).

6.2.5 Synthesis of 4¢-bis[5-(10,15,20-tri(4-methylphenyl))porphyrinato-dihydroxidetin(IV)]azobenzene $[L^3Sn(OH)_2]$

A mixture of $\mathbf{H_2L^3}$ (0.5 g, 0.37 mmol) and $SnCl_2$ (0.56 g, 2.98 mmol) were dissolved in 60 mL of pyridine. The resulting mixture was refluxed for 5 h, after which pyridine was removed under reduced pressure the crude product was dissolved in $CHCl_3$ and washed several times with water. The organic layer was dried by passing through anhydrous Na_2SO_4 and chromatographed over basic alumina. Elution with $CHCl_3$:CH3OH (98:2 V/V) gave the $\mathbf{[L^3SnCl_2]}$. Yield: 0.61 g (95%). To the $CHCl_3$ solution of $\mathbf{[L^3SnCl_2]}$, 10% aqueous NaOH was added and the reaction mixture was stirred at room temperature for 2 h. The organic layer was separated and dried to get violet solid of $\mathbf{[L^3Sn(OH)_2]}$ which was

recrystallized from CH_2Cl_2-hexane. Yield: 0.54 g (92%). MALDI MS: $[M]^+$ = 1642, $[M\text{-}OH]^+$ = 1625, $[M\text{-}2OH]^+$ = 1608.

6.2.6 Synthesis of $L^1Sn(3\text{-pyridoxy})_2$ [M3PY]

A solution containing **$[L^1Sn(OH)_2]$** (0.1 g, 0.12 mmol) and 3-hydroxypyridine (3-PY**,** 0.11 g, 1.2 mmol) in 30 mL of dry benzene was refluxed under the nitrogen atmosphere for 3 h. After cooling to room temperature, the excess 3-PY was removed by filtration through sintered crucible. The solvent was removed under reduced pressure and the crude solid was dissolved in minimum amount of CH_2Cl_2. This solution was precipitated by addition of CH_3CN and heated to 80 °C for 1 h. It was then filtered in hot condition to remove traces of 3-PY. This process was repeated several times to get 3-PY free compound. Finally it was precipitated from $CHCl_3$-hexane to give the desired product. Yield = 0.14 g (80%). FAB-MS: $[M+H]^+$ = 976, $[M\text{-}C_5H_4NO]^+$ = 882, $[M\text{-}2(C_5H_4NO)]^+$ = 788.

6.2.7 Synthesis of $L^1Sn(4\text{-pyridoxy})_2$ [M4PY]

This compound was prepared, starting with **$[L^1Sn(OH)_2]$** (0.1 g, 0.12 mmol) and 4-hydroxypyridine (4-PY**,** 0.11 g, 1.2 mmol), in a manner analogous to that described above for **M3PY**. Yield: 0.11 g (90 %). LCMS: $[M]^+$ = 975, $[M\text{-}C_5H_4NO]^+$ = 881, $[M\text{-}2(C_5H_4NO)]^+$ = 788.

6.2.8 Synthesis of $L^3Sn(4\text{-pyridoxy})_2$ [A3PY]

This compound was prepared, starting with **$[L^3Sn(OH)_2]$** (0.1 g, 0.061 mmol) and 3-PY (0.12 g, 1.22 mmol), in a manner analogous to that described above for **M3PY**. Yield: 0.09 g (80%). FAB-MS: $[M\text{-}(C_5H_4NO)]^+$ = 1854, $[M\text{-}3(C_5H_4NO), H]^+$ = 1665, $[M\text{-}4(C_5H_4NO)]^+$ = $[C_{94}H_{65}N_{10}Sn_2]^+$ = 1571,

$[C_{47}H_{33}N_5Sn]^+$ = 785, $[C_{47}H_{33}N_4Sn]^+$ = 771. (A few low intensity peaks around 1918 and 1969 were also observed).

6.2.9 Synthesis of $L^3Sn(4\text{-pyridoxy})_2$ [A4PY]

This compound was prepared, starting with **$[L^1Sn(OH)_2]$** (0.1 g, 0.061 mmol) and 4-PY (0.12 g, 1.2 mmol), in a manner analogous to that described above for **A3PY**. Yield: 0.1 g (85%). LCMS: $[M-(C_5H_4NO)-H]^+$ = 1853.

6.3 Results and discussion

The well-known oxophilicity of tin(IV) porphyrin have been exploited to synthesize functionally-active, 'axial-bonding' type monomers and dimers of tin(IV) porphyrin-$(pyridoxo)_2$ triads. Details of spectroscopic, electrochemical and fluorescence properties of these new compounds are described below.

6.3.1 Design and Synthesis

The synthetic routes leading to synthesis of new compounds are shown in Schemes 6.1 - 6.3. Reaction of excess of 3- or 4-hydroxypyridine with tin(IV) porphyrins in refluxing benzene offered desired compounds. Relying largely on the oxophilicity of the tin(IV) ion, synthesis of all new compounds has been accomplished here, in good-to-moderate yields, following a step-wise protocol that we had adopted earlier for the synthesis P(V), Sn(IV) and Al(III) porphyrin triads.[8,9,38-40,46,47] Pure compounds were obtained by simple precipitation methods in suitable spectroscopic grade solvents.

6.3.2 Ground state properties

Mass (FAB or MALDI or LCMS) spectra of reference compounds **H_2L^3** and **$[L^3Sn(OH)_2]$** show the expected molecular ion peak and peaks due to

fragments upon removal of the axial hydroxy group/s in **$L^3Sn(OH)_2$**. These data are summarized in experimental section. Newly synthesized dimeric triads, **A3PY** and **A4PY** did not show the expected molecular ion peak whereas **M3PY** and **M4PY** monomeric triads show an intense molecular ion peak. In all these compounds peaks are obtained due to fragments upon removal of the axial pyridoxy (**-O-PY**) subunit/s.

The ^{1}H NMR spectrum of each newly synthesized porphyrin during this study was analyzed on the basis of resonance position, integrated intensity data and ^{1}H-^{1}H coupling patterns observed in the 2D (^{1}H-^{1}H COSY) spectra. Schemes 6.1 and 6.3 illustrate the various types of protons present in the investigated compounds.

The ^{1}H NMR spectral data of the triads along with those of the individual compounds are summarized in Table 6.1 and the spectra of **A3PY** and **A4PY** are shown in Fig. 6.1. Each compound showed features typical of a diamagnetic porphyrin and, moreover, it was possible to distinguish between the resonances due to protons present on the porphyrin ring and those on the axial ligands, as was the case with the tin(IV) porphyrins reported earlier.[38-40,47] From Table 6.1, it is clear that the resonance positions of the protons (type *b*, *o*, *m*, *e* and *f*) on the basal Sn(IV) porphyrin components of **M3PY**, **M4PY**, **A3PY** and **A4PY** are more or less similar to those of their precursor compounds, **[$L^1Sn(OH)_2$]** or **[$L^3Sn(OH)_2$]**. Resonance due to the *b*-pyrrole protons appears in the region 9.16 - 9.26 ppm as singlet with two minor peaks or multiplet. These minor peaks are due to the ^{117,119}Sn-H coupling and the coupling constants span a range of 12-15 Hz consistent with the earlier reported aryloxo derivatives analogous.[48,49] Resonance due to protons (type *o* and *m*) on the meso-tolyl rings of these triads are not much influenced by type of the axial ligand and appear as a pair of sharp doublets/multiplets. The azobenzene bridging protons (type *e* and *f*) appear as a

pair of doublets in **A3PY** and **A4PY**. The singlet observed between 2.74 to 2.78 ppm for all triads is due to the methyl protons of tolyl groups.

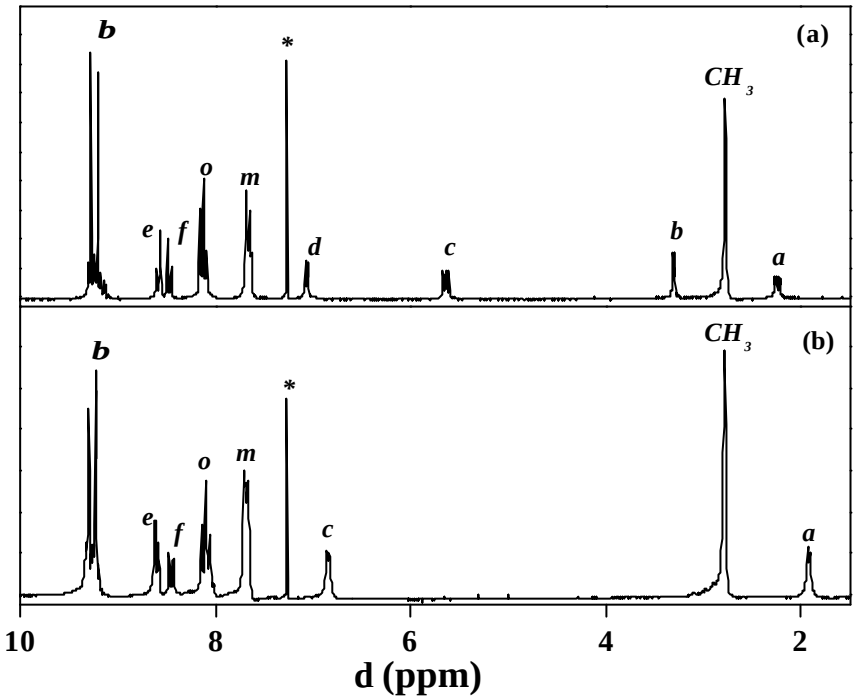

Fig. 6.1 ^{1}H NMR spectra of (a) **A3PY** and (b) **A4PY** in $CDCl_3$, TMS (200 MHz, 300K, * peak is due to solvent).

On the other hand, the resonance positions and also the splitting patterns of the protons on their axial pyridoxy are quite different from those of 3- or 4-hydroxypyridine as a result of the ring current effect exerted by the basal Sn(IV) porphyrin.[50,51] As such, the ortho, meta and para (with respect to the axial 'oxo' group) protons of the bound porphyrin-aryloxo ligand in **A3PY** are shielded and resonate at 2.17 (m, 2H, type *a*), 3.25 (d, 2H, type *b*), 5.57 (m, 2H, type *c*) and 7.00 (d, 2H, type *d*) ppm, respectively (identified by ^{1}H-^{1}H COSY experiment). Analysis of the ^{1}H NMR spectrum of **A3PY** proved to be inconclusive with

respect to assigning the axial ligand proton resonances and hence a ^{1}H-^{1}H COSY spectrum was run for this triad.

Table 6.1 ^{1}H NMR data (for proton assignments see Schemes 6.1 and 6.3) [a]

Compound	d ppm [J, Hz] {Dd}	
	Porphyrin ***(b-pyrrole, H_e, H_f, H_o, H_m, -CH_3)***	**Aryloxo** ***(H_d, H_c, H_b, H_a)***
3-PY	-	8.28 (d, 1H) [2.0], 8.09 (dd, 1H) [2.0, 2.0], 7.30 (m, 2H)
4-PY	-	7.61 (d, 2H), 6.47 (d, 2H)
H_2L^3	8.90 (m, 16H), 8.45 (s, 8H), 8.10 (m, 12H), 7.52 (m, 12H), 2.70 (s, 18H), -2.81 (s, 4H)	
[$L^1Sn(OH)_2$]	9.15 (m, 8H), 8.22 (d, 8H) [7.8], 7.63 (d, 8H) [7.8], 2.74 (s, 12H)	-
[$L^3Sn(OH)_2$]	9.21 (m, 16H), 8.61 (m, 8H), 8.26 (m, 12H), 7.67 (m, 12H), 2.77 (s, 18H)	-
M3PY	9.16 (m, 8H), 8.09 (d, 8H) [7.8], 7.63 (d, 8H) [7.8], 2.74 (s, 12H)	7.00 (d, 2H) [2.8] {1.28}, 5.57 (m, 2H) {2.52}, 3.25 (d, 2H) [2.8] {4.05}, 2.17 (m, 2H) {5.13}
M4PY	9.17 (m, 8H), 8.06 (d, 8H) [7.8], 7.64 (d, 8H) [7.8], 2.75 (s, 12H)	6.78 (d, 4H) [5.8] {0.83}, 1.85 (d, 4H) [5.6] {4.62}
A3PY	9.24 (m, 16H), 8.58 (d, 4H) [8.8], 8.47 (d, 4H) [8.8], 8.12 (m, 12H), 7.67 (m, 12H), 2.78 (s, 18H)	7.06 (d, 4H) [5.8] {1.22}, 5.63 (m, 4H) {2.46}, 3.29 (d, 4H) [3.0] {4.01}, 2.23 (dd, 4H), [3.0, 6.8] {5.07}
A4PY	9.26 (m, 16H), 8.60 (d, 4H) [5.8], 8.45 (d, 4H) [8.6], 8.10 (m, 12H), 7.69 (m, 12H), 2.78 (s, 18H)	6.84 (d, 8H) [4.8] {0.77}, 1.92 (d, 8H) [6.0] {4.55}

[a] Spectra were run in $CDCl_3$, TMS. Error limits: δ, ± 0.01 ppm, J: ± 1 Hz.

The representative ^{1}H-^{1}H COSY spectrum of **A3PY** is displayed in Fig. 6.2. The $\Delta\delta$ (i.e. δ(3-PY) - δ(**A3PY**)) values for protons type *a*, *b*, *c* and *d* of 5.07, 4.01, 2.46 and 1.22 ppm are a function of their separation distance from the

porphyrin ring (see Table 6.1) as expected. There is an obvious absence of protons of type *b* in **A4PY** due to its architectural symmetry; a symmetric resonance pattern is observed for protons *a* and *c*. The corresponding resonances for **A4PY** are seen to be similarly shifted upfield (compared to the corresponding protons on 4-PY) and resonate at 1.92 (d, 2H, type *a*) and 6.84 (d, 2H, type *c*) ppm with the $\Delta\delta$ values (i.e. δ(4-PY) - δ(**A4PY**)) of 4.55 and 0.77 ppm, respectively. Similar results were obtained for monomeric triads **M3PY** and **M4PY**, except the absence of azobenzene bridging peaks.

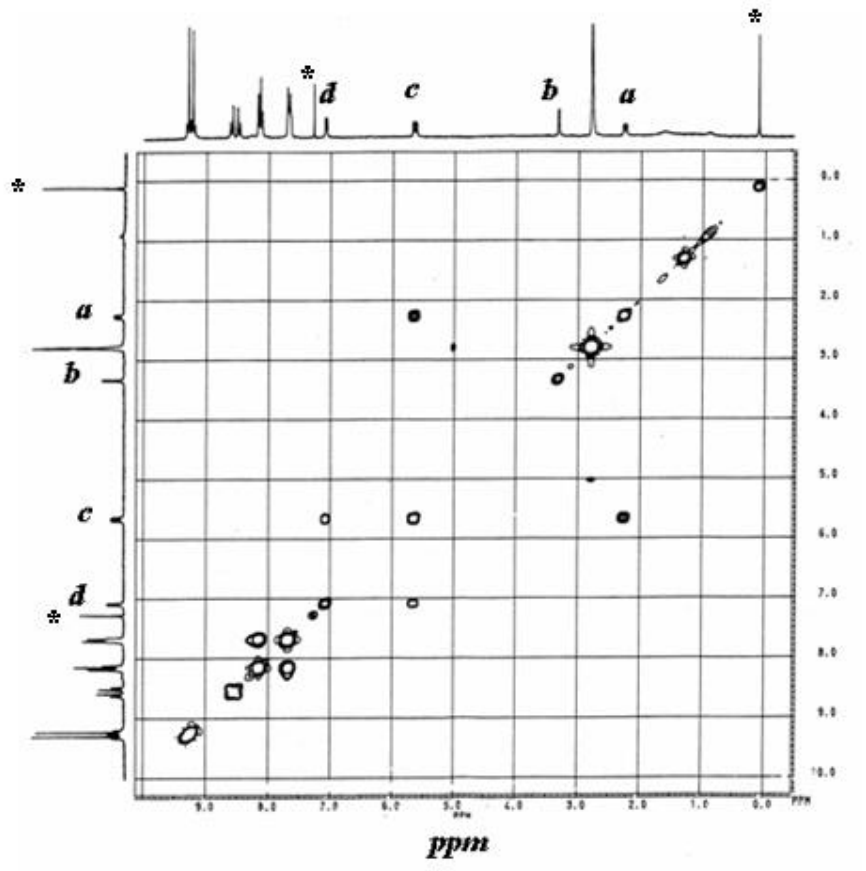

Fig. 6.2 ^{1}H-^{1}H COSY NMR of **A3PY** in $CDCl_3$, TMS (200 MHz, 300K, * peak is due to solvent).

The wavelengths of maximum absorbance (λ_{max}) and molar extinction coefficient (ε) of the newly synthesized triads and those of their constituent individual components obtained from the UV-visible studies are summarized in Table 6.2. Fig. 6.3 illustrates the absorption spectra of **A3PY** and **A4PY**. Comparison of spectra and the data given in Table 6.2 suggests that the axially connected pyridine subunit in these compounds predominantly absorbs between 230-350 nm, a region in which porphyrin part of each molecule shows its so-called N and L bands. Bands at 286 nm and 317 nm for **A3PY** corresponds to the absorbance (π-π* transition) of the pyridine moiety and N, L bands of tin(IV) porphyrin, respectively. Similarly band at 317 nm for **A4PY** is due to absorbance of both pyridine moiety and N, L bands of tin(IV) porphyrin. Beside porphyrin absorption bands, **A3PY** and **A4PY** show relatively weak and broadened bands of *trans*-azobenzene moiety between 305 and 320 nm.[1] Although from the spectroscopic data it is not clear whether the *cis*- or *trans*-isomer or a mixture of the isomers of the diporphyrins is formed, we think that the *trans*-isomer is formed in the synthesis due to thermodynamic reasons. On the other hand, porphyrin parts of these compounds show two less intense Q-bands and one intense Soret band (B-band) in the wavelength region (400-700 nm) where the pyridine moiety does not absorb.

The newly synthesized porphyrins show interesting absorption properties. Fig. 6.4 shows the overlay of Soret band in dichloromethane for all newly investigated compounds in this study. The Soret band of **[L^3Sn(OH)$_2$]** is broadened when compared with monomeric compound, **[L^1Sn(OH)$_2$]** indicating a ground state interaction of the azobenzene and porphyrin chromophore.[1] The same trend was observed for **M3PY** and **M4PY** when compared with **A3PY** and **A4PY** triads, respectively. Dilute solutions containing 1:2 molar equivalents of **[L^1Sn(OH)$_2$]** or **[L^3Sn(OH)$_2$]** and 3- or 4-hydroxypyridine generate UV-visible

spectra that are close to the spectra of triads, **M3PY**, **M4PY**, **A3PY** and **A4PY**. The absorption maxima (λ_{max}) and molar extinction coefficient (ε) values of the Soret and Q-bands in these triads were not shifted from those of respective bands in reference compounds. Finally, it was observed that the λ_{max} and spectral shapes of the bands of these newly synthesized compounds are more or less similar to individual components, implying that the π-electronic systems are not significantly perturbed.

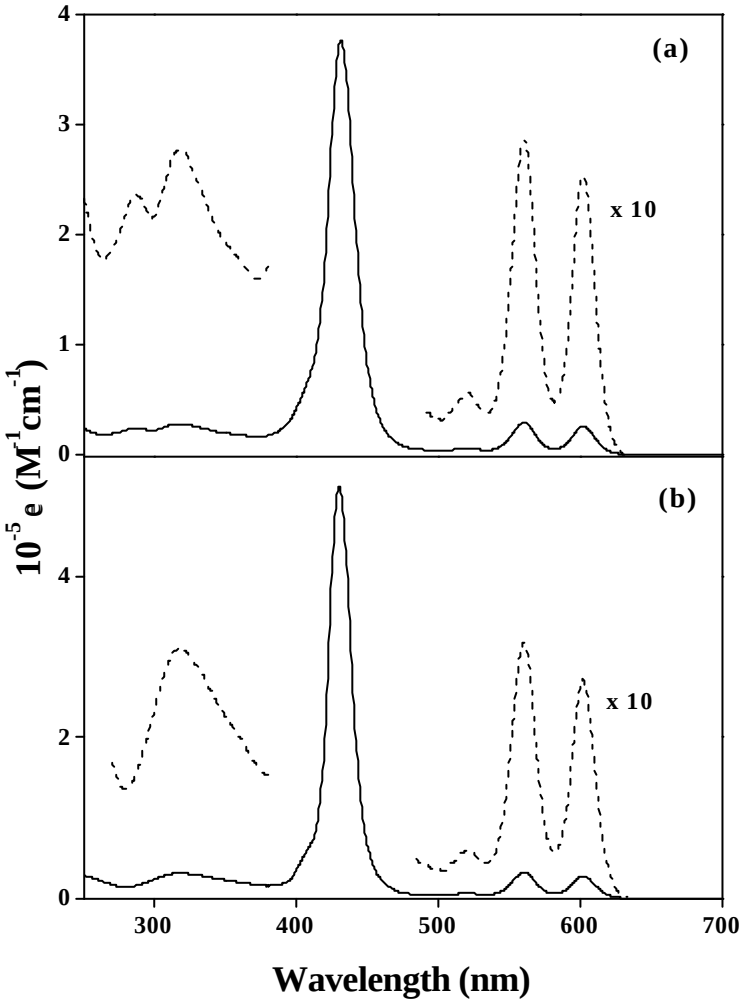

Fig. 6.3 UV-visible spectra of (a) **A3PY** and (b) **A4PY** in dichloromethane.

Table 6.2 UV-visible data of all investigated compounds [a]

Compound	l_{max}, nm (log e)		
	Soret band	Q-bands	Azo- & Aryl group
3-PY	-	-	275 (3.59)
4-PY	-	-	260 (4.13)
H_2L^1	419 (5.73)	648 (3.84), 592 (3.81), 552 (4.10), 516 (4.33)	-
***H_2L^3**	422 (5.74)	649 (3.99), 592 (4.02), 557 (4.36), 519 (4.52)	305 (4.47)
[$L^1Sn(OH)_2$]	428 (5.76)	604 (4.32), 563 (4.36), 524 (3.72)	-
[$L^3Sn(OH)_2$]	430 (5.76)	606 (4.53), 564 (4.54), 524 (3.89)	320 (4.58)
M3PY	429 (5.53)	601 (4.28), 560 (4.37), 521 (3.64)	289 (4.32)
M4PY	428 (5.44)	600 (4.28), 559 (4.36), 521 (3.63)	314 (4.31)
A3PY	432 (5.58)	603 (4.56), 561 (4.61), 521 (3.93)	317 (4.61), 286 (4.54)
A4PY	430 (5.71)	602 (4.58), 561 (4.64), 521 (3.96)	317 (4.65)

[a] Spectra were recorded in CH_2Cl_2. Error limits: λ_{max}, ± 1 nm, log ε, ± 10%, * recorded in $CHCl_3$.

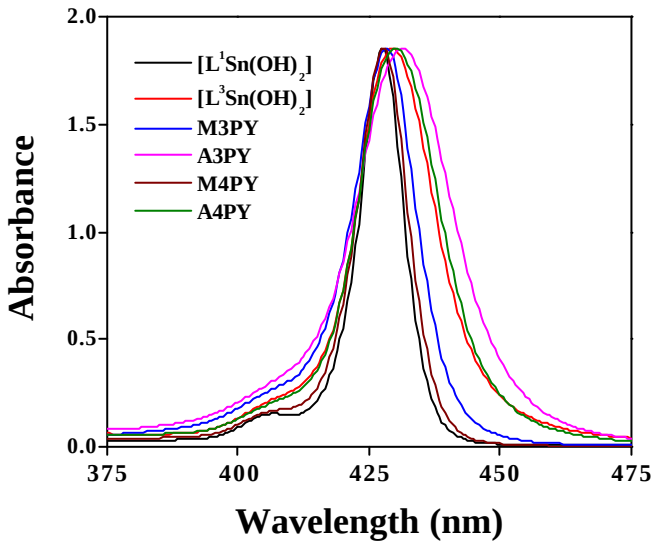

Fig. 6.4 Soret band of all newly investigated compounds in CH_2Cl_2; all bands are normalized to equi absorbance.

Table 6.3 summarizes the redox potential data (CH_2Cl_2, 0.1 M TBAP) of newly synthesized triads along with the reference compounds investigated in this study. Fig. 6.5 illustrates the cyclic and differential pulse voltammograms of **M3PY**, **M4PY** and reference compound **[L[1]Sn(OH)$_2$]**. As seen in Fig. 6.5, each triad undergoes two stepwise reduction reactions. Wave-analysis (from cyclic voltammetry) suggested that both these electrode processes are reversible (i_{pc}/i_{pa} = 0.9 - 1.0) and diffusion controlled ($i_{pc}/\nu^{1/2}$ = constant in the scan rate (ν) range 50 - 500 mV s^{-1}) one-electron transfer (ΔE_P = 60 - 70 mV; ΔE_P = 65 ± 3 mV for Fc^+/Fc couple) reactions.[52] Based on the redox potential data reported earlier for 'axial-bonding' type tin(IV) porphyrins,[38-40] and also on the basis of the diagnostic criteria developed by Fuhrhop, Kadish and Davis for porphyrin ring reduction[53] ($\Delta E_{1/2}$ i.e. the difference in potential between the first one-electron and second one-electron addition = 0.42 ± 0.05 V**;** see Table 5.2 where $\Delta E_{1/2}$ = 0.42 - 0.48 V), the first two reduction waves observed for the D-A conjugates investigated here can be assigned to successive, one-electron additions to the porphyrin ring. Reduction peak due to the pyridine subunits was not observed for these compounds within the solvent window.

Scanning the potential in the positive range (0-1.8 V) for solutions containing the investigated (**M3PY**, **M4PY**, **A3PY** and **A4PY**) triads gave ill-defined voltammograms with a large background current. However, pyridine (3-**PY**/4-**PY**) employed here for synthesis of the aryloxo tin(IV) porphyrins could be irreversibly oxidized in dichloromethane: 0.1 M TBAP. Analysis of the data given in Table 6.3 reveals that the electrochemical redox potentials of the **M3PY**, **M4PY**, **A3PY** and **A4PY** are in the same range as those of the corresponding reference compound **[L[1]Sn(OH)$_2$]/ [L[3]Sn(OH)$_2$]**. Overall, the spectroscopic and electrochemical features described above suggest that electronic communication

between the porphyrin and pyridoxo subunits is quite negligible in these new D-A systems.

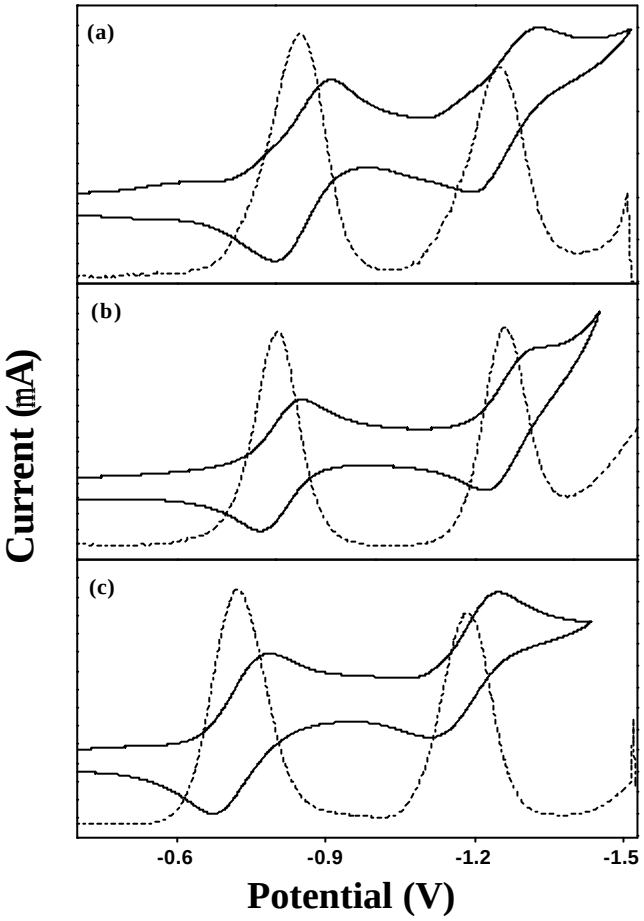

Fig. 6.5 Cyclic (——) and differential pulse (……..) voltammograms of (a) **[L^1Sn(OH)$_2$]** (b) **M3PY** and (c) **M4PY** in CH_2Cl_2, 0.1 M TBAP (scan rate = 100 mVs^{-1}, modulation amplitude = 10 mV).

6.3.3 Excited state properties

The UV-visible spectral data of **M3PY, M4PY, A3PY** and **A4PY** indicate that it is possible to address photochemistry of the porphyrin subunit in these bichromophoric systems. Steady state fluorescence spectra of these D-A systems

Table 6.3 Redox potential data in CH_2Cl_2, 0.1M TBAP [a]

Compound	Potential (V, vs SCE)	
	Oxidation (V)	**Reduction (V)**
3-PY	1.04	-
4-PY	1.54	-
$[L^1Sn(OH)_2]$	1.57	-0.85, -1.25
$[L^3Sn(OH)_2]$	1.56	-0.80, -1.24
M3PY	1.64	-0.80, -1.26
M4PY	1.55	-0.72, -1.18
A3PY	1.68	-0.75, -1.25
A4PY	1.54	-0.68, -1.14

[a] Error limits: $E_{1/2}$, ± 0.03 V

have been measured in different solvents (toluene, dichloromethane, acetonitrile, N,N-dimethylformaide) by exciting the solutions at 600 nm (exclusively porphyrin absorption). The wavelengths of emission maxima ($ë_{em}$) and the quantum yield (ϕ) data are summarized in Table 6.4. The resulting spectra are compared with those of the corresponding individual components constituting them, i.e. **$[L^1Sn(OH)_2]$** or **$[L^3Sn(OH)_2]$**. In Fig. 6.6, the steady state fluorescence spectra of these compounds measured in dichloromethane are compared with spectra of the corresponding individual components. Upon excitation at 600 nm, porphyrin component of each compound showed fluorescence spectrum that is typical of a hexa-coordinated tin(IV) porphyrin.[33-36,41-43] Spectral shapes and wavelengths of emission maxima (λ_{em}) of **M3PY** or **M4PY** and **A3PY** or **A4PY**

are similar to the spectra of **[L^1Sn(OH)$_2$]** and **[L^3Sn(OH)$_2$],** respectively. From an overlay of the absorption and fluorescence spectra of these D-A systems, the 0-0 spectroscopic transition energies ($E_{0\text{-}0}$) of the tin(IV) porphyrin (2.04 ± 0.04 eV) moieties have been estimated and found to be close to those of the corresponding unlinked chromophores. The quenching efficiency values (Q) have been calculated with eqn. 6.1 in different solvents using the quantum yield data, and are summarized in Table 6.4.

$$Q = (\phi_{ref} - \phi_{triad}) / \phi_{ref} \qquad (6.1)$$

Here, ϕ_{triad} and ϕ_{ref} refers to the quantum yields of given triad and the appropriate reference compound, respectively.

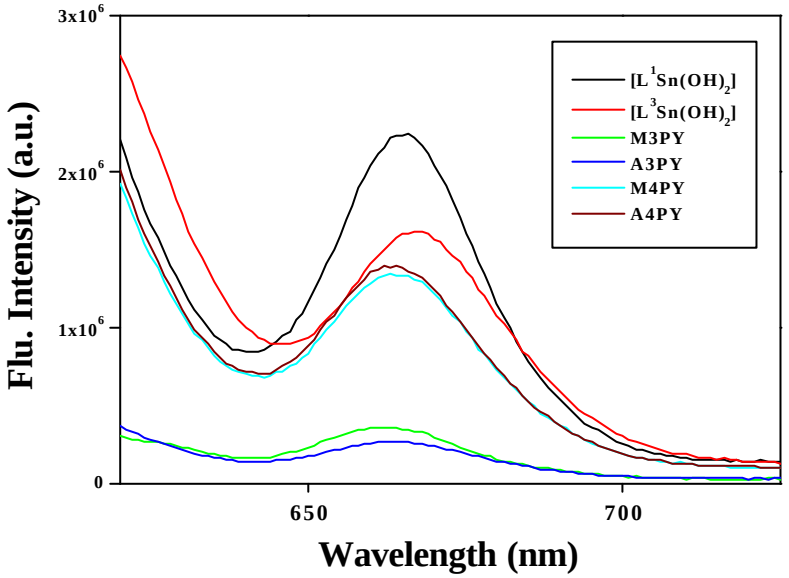

Fig. 6.6 Fluorescence spectra of newly investigated triads in CH_2Cl_2, λ_{exc} = 600 nm., OD = ~0.2.

Table 6.4 Fluorescence spectroscopic data of triads and their monomeric analogues (λ_{ex} = **600 nm**) [a]

Compounds	λ_{em} (f, %Q)			
	Toluene	**DCM**	**Acetonitrile**	**DMF**
$L^1Sn(OH)_2$	665 (0.020)	666 (0.048)	664 (0.040)	667 (0.055)
$L^3Sn(OH)_2$	667 (0.013, 35)	668 (0.041, 15)	664 (0.030, 25)	671 (0.033, 40)
M3PY	662 (0.0058, 71)	661 (0.0084, 82)	659 (0.0044, 89)	662 (0.0047, 91)
M4PY	663 (0.031, 0)	665 (0.034, 29)	664 (0.026, 35)	664 (0.035, 36)
A3PY	666 (0.0051, 61)	663 (0.007, 83)	661 (0.0038, 87)	663 (0.0042, 87)
A4PY	663 (0.034, 0)	664 (0.033, 20)	662 (0.024, 20)	664 (0.034, 30)

[a] Error limits: λ, ± 1 nm; ϕ, ± 10%

A variety of excited state processes including EET, enhanced internal conversion and intersystem crossing, ion-association, PET etc. can be thought to be operative in the quenching of fluorescence observed in these D-A systems. Obviously, it is not going to be easy to estimate the contribution from each of these excited state processes. However, an intramolecular EET from the singlet tin(IV) porphyrin to the pyridoxo ligand is less likely to occur because singlet states of the axial pyridine ligands employed here (E_S > 3.0 V)[47] lie higher than singlet state of the basal porphyrin chromophore (E_S ~ 2.04 V). Therefore, the contribution of this process to the overall decrease in the ϕ values is considered to be minimal for these complexes. Similarly, the observed general dependence of the ϕ values on the solvent polarity indicates that it is difficult to rationalize these trends solely on the basis of differences in the rates of internal conversion and

intersystem crossing reactions of the aryloxo porphyrins among themselves and also in relation to the dihydroxy analogue. As far as the PET-based mechanism is concerned, two types of reactions can be envisaged for these complexes (equations 6.2 and 6.3).

$$Sn^* - OPY \quad Sn(IV)^+ - OPY^- \tag{6.2}$$

$$Sn^* - OPY \quad Sn(IV)^- - OPY^+ \tag{6.3}$$

where Sn* - OPY represents the singlet state of porphyrin and $Sn^+ - OPY^-$ and $Sn^- - OPY^+$ represent the charge separated species. The free energy changes (ΔG_{PET}) required for the PET reaction between two chromophores are calculated by the simplified Rehm-Weller method,[57] eqn. 6.4.

$$\Delta G_{PET} = E_{CT} - E_{0\text{-}0} \tag{6.4}$$

Here E_{CT} refers to energy of the charge transfer state ($E[Sn^+\text{-}OPY^-] = E_{1/2}{}^{OX}(Sn) - E_{1/2}{}^{RED}(OPY)$ or $E[Sn^-\text{-}OPY^+] = E_{1/2}{}^{OX}(OPY) - E_{1/2}{}^{RED}(Sn)$) and $E_{0\text{-}0}$ is energy of the singlet state of the tin(IV) porphyrin. In these calculations, reduction potential of pyridoxo subunit is assumed to be cathodic to -1.40 V, respectively (solvent limit in our experimental conditions). The positive ΔG_{PET} (1.00, 0.91, 1.04 eV and 0.90 eV for **M3PY**, **M4PY**, **A3PY** and **A4PY**, respectively) values for processes 6.2 suggest that, electron transfer from the singlet porphyrin to the axially bound pyridoxo subunit is thermodynamically unfavorable processes in all investigated triads. On the other hand, process represented by eqn. 6.3 is thermodynamically favorable process and the extent of exoergicity (i.e. -0.20, 0.22, -0.25 and 0.18 eV for **M3PY**, **M4PY**, **A3PY** and **A4PY**, respectively) suggests that this process

(electron transfer from the pyridoxo subunit to the porphyrin moiety) can, in principle, occur in these new D-A systems. The observed general decrease of the ϕ values (or the increase in the %Q values, see Table 6.4) with increasing polarity of the solvent is consistent with the participation of a charge transfer state in the excited state deactivation of the tin(IV) porphyrin.[58] For processes 6.3, due to positive ΔG_{PET} value for **M4PY** and **A4PY** triads, explain low quenching values compared with **M3PY** and **A3PY** triads.

Based on the above observations that relaxation of the singlet state to the thermodynamically accessible charge transfer state (Sn^{-} - OPY^{+}) is responsible for the observed fluorescence quenching of the porphyrin chromophore in all triads. Despite the above analysis of the fluorescence data of triads based on the PET mechanism, we note that it is not generally correct to consider exclusively an electron transfer mechanism relying only on the thermodynamic criteria and solvent dependence of the ϕ values. It is reasonable to expect that contribution from the PET based mechanism is high these triads having axial ligand; this analysis is quite consistent with that made earlier for the analogous series of phosphorus(V) porphyrins,[46,47,59] the Sn(IV) porphyrin based arrays and other donor-acceptor compounds.[38,39,54,55]

6.4 Summary

In summary, a series of bis(aryloxo) tin(IV) porphyrins have been synthesized and fully characterized by mass, UV-visible and ^{1}H NMR methods. The spectral data reveal that the two trans axial ligands are symmetrically disposed with respect to the basal porphyrin and that there exists no ð–ð interaction between the porphyrin and pyridoxo ligands in **M3PY, M4PY, A3PY** and **A4PY** triads. A photoinduced electron transfer from the axial pyridoxo ligands to the singlet tin(IV) macrocycle has been suggested to occur in these

systems by the combined application of redox and emission data. Although, we could not effect *cis-trans* isomerism of **A3PY** and **A4PY** triads under our experimental conditions, further investigations (perhaps under laser induced conditions) may provide fruitful results.

6.5 References

1. Hombrecher, H. K., Ludtke, K. *Tetrahedron*, **1993**, *49*, 9489.
2. Otsuki, J.; Harada, K.; Araki, K. *Chem. Lett*. **1999**, 269.
3. Tsuchiya, S. *J. Am. Chem. Soc*. **1999**, *121*, 48.
4. Hunter, C. A.; Sarson, L. D. *Tetrahedron Lett*. **1996**, *37*, 699.
5. Autret, M. ; le Plouzennec, M. ; Moinet, C. ; Simmonneaux, G. *J. Chem. Soc., Chem. Commun*. **1994**, 1169.
6. Hombrecher, H. K.; Ludtke, K.; Koll, D. *J. Prakt. Chem*. **1996**, *338*, 257.
7. Neumann, K. H.; Vogtle, F. *J. Chem. Soc., Chem. Commun*. **1988**, 520.
8. Reddy, D. R.; Maiya, B. G. *Chem. Commun*. **2001**, 117.
9. Reddy, D. R.; Maiya, B. G. *J. Phys. Chem. A* **2003**, *107*, 6326.
10. Dierickx, C. C. *Compr. Ser. Photosci*. **2001**, *2*, 271.
11. Pogue, B. W.; Ortel, B.; Chen, N.; Redmond, R. W.; Hasan, T. *Cancer Res*. **2001**, *61*, 717.
12. Renno, R. Z.; Miller, J. W. *Adv. Drug Deliv. Rev*. **2001**, *52*, 63.
13. Kaplan, M. J.; Somers, R. G.; Greenberg, R. H.; Ackler, J. *J. Surg. Oncol*. **1998**, *76*, 121.
14. Kessel, D.; Morgan, A.; Garbo, G. M. *Photochem. Photobiol*. **1991**, *54***,** 193.
15. Embleton, M. L.; Nair, S. P.; Cookson, B. D.; Wilson, M. *J. Antimicrob. Chemother*. **2002**, *50*, 857.
16. Coates Jr. W. D.; Currie, J. W.; Mejias, Y.; Narciso, H. L.; Faxon, D. P. *Biochem. Cell Biol*. **1996**, *74*, 325.

17. Philippova, T. O.; Galkin, B. N.; Golovenko, N. Y.; Zhilina, Z. I.; Vodzinskii, S. V. *J. Porphyrins Phthalocyanines* **2000**, *4*, 243.
18. Drummond, G. S.; Smith, T. J.; Kappas, A. *Pharmacology* **1996**, *52*, 178.
19. Dwyer, B. E.; Lu, S.-Y.; Laitinen, J. T.; Nishimura, R. N. *J. Neurochem.* **1998**, *71*, 2497.
20. Compans, R. W.; Marzilli, L. G.; Sears, A. E.; Dixon, D. W. *International Patent WO 0,* **2003**, *357*, 176.
21. Neurath, A. R.; Jiang, S.; Debnath, A. K. *International Patent WO 9,* **1995**, *517*, 893.
22. Chaniotakas, N. A.; Park, S. B.; Meyerhoff, M. E. *Anal. Chem*. **1989**, *61*, 566.
23. Grigg, R.; Norbert, W. D. J. A. *Chem. Commun*. **1992**, 1298.
24. Szulbinski, W.; Strojek, J. W. *Inorg. Chim. Acta*. **1986**, *118***,** 91.
25. Harel, Y.; Manassen, J. *J. Am. Chem. Soc*. **1977**, *99***,** 5817.
26. Whitten, D. G.; You, J. C.; Carroll, F. A. *J. Am. Chem. Soc*. **1971**, *93*, 2291.
27. Tong, Y.; Hamilton, D. G.; Meillon, J.-C.; Sanders, J. K. M. *Org. Lett*. **1999**, *1*, 1343.
28. Hawley, J. C.; Bampos, N.; Abraham, R. J.; Sanders, J. K. M. *Chem. Commun*. **1998**, 661.
29. Kim, H.-J.; Bampos, N.; Sanders, J. K. M. *J. Am. Chem. Soc*. **1999**, *121*, 8120.
30. Redman, J. E.; Feeder, N.; Teat, S. J.; Sanders, J. K. M. *Inorg. Chem*. **2001**, *40*, 2486.
31. Webb, S. J.; Sanders, J. K. M. *Inorg. Chem*. **2000**, *39*, 5920.
32. Fallon, G. D.; Langford, S. J.; Lee, M. A.-P.; Lygris, E. *Inorg. Chem. Commun*. **2002**, *5*, 715.

33. Crossley, M. J.; Thordarson, P.; Wu, R. A.-S. *J. Chem. Soc., Perkin Trans. 1* **2001**, 2294.
34. Arnold, D. P.; Blok, J. *Coord. Chem. Rev*. **2004**, *248*, 299.
35. Hawley, J. C.; Bampos, N.; Sanders, J. K. M. *Chem. Eur. J*. **2003**, *9*, 5211.
36. Fallon, G. D.; Lee, M. A.-P.; Langford, S. J.; Nichols, P. *J. Org. Lett*. **2002**, *4*, 1895.
37. Smith, G.; Arnold, D. P.; Kennard, C. H. L.; Mak, T. C. W. *Polyhedron* **1991**, *10*, 509.
38. Reddy, D. R.; Maiya, B. G. *J. Porphyrins Phthalocyanines* **2002**, *6*, 3.
39. Giribabu, L.; Kumar, A. A.; Neeraja, V.; Maiya, B. G. *Angew. Chem., Int. Ed*. **2001,** *40*, 3621.
40. Kumar, A. A.; Giribabu, L.; Reddy, D. R.; Maiya, B. G. *Inorg. Chem*. **2001**, *40*, 6757.
41. Fuhrhop, J.-H.; Smith, K. M.; In *Porphyrins and Metalloporphyrins*; Smith, K. M., Ed.; Elsevier: Amsterdam, **1975**; p. 769.
42. Fuhrhop, J.-H.; Smith, K. M. in *Porphyrins and Metalloporphyrins*; Smith, K. M., Ed.; Elsevier: Amsterdam, **1975**; p. 179.
43. Alder, A. D.; Longo, F. R.; Finarelli, J. D.; Goldmacher, J.; Assour, J.; Korsakoff, L. *J. Org. Chem.* **1962**, *32*, 476.
44. Kadish, K. M.; Xu, Q. Y. Y.; Maiya, B. G.; Barbe, J.-M.; Guilard, R. *J. Chem. Soc., Dalton Trans*. **1989**, 1531.
45. Corwin, A. H.; Collins III, O. D. *J. Org. Chem*. **1962**, *27*, 3060.
46. Prashanth, P.K.; Maiya, B. G. *New J. Chem.* **2003**, *27*, 619.
47. Rao, T. A.; Maiya, B. G. *Inorg. Chem.* **1996**, *35*, 4829.
48. Arnold, D. P. *Polyhedron* **1986**, *5*, 1957.
49. Arnold, D. P.; Bartley, J. P. *Inorg. Chem.* **1994**, *33*, 1486.

50. Abraham, R. J.; Bedford, G. R.; McNeillie, D.; Wright, B. *Org. Magn. Reson*. **1980**, *14*, 418.
51. Fallon, G.D.; Langford, S.J.; Lee, M.A.-P.; Lygris, E. *Inorg. Chem. Commun.*, **2002**, *5*, 715.
52. Nicholson, R. S.; Shain, I. *Anal. Chem*. **1964**, *36*, 706.
53. Fuhrhop, J. H.; Kadish, K. M.; Davis, D. G. *J. Am. Chem. Soc*. **1973**, *95*, 5140.
54. Giribabu, L.; Rao, T. A.; Maiya, B. G. *Inorg. Chem.* **1999,** *38*, 4971.
55. Maiya, B. G.; Bampos, N.; Kumar, A. A.; Feeder, N.; Sanders, J. K. M. *New J. Chem.* **2001**, *25*, 797.
56. Sayer, P.; Gouterman, M.; Connell, C. R. *Acc. Chem. Res.* **1982,** *15*, 73.
57. Rehm, D.; Weller, A. *Isr. J. Chem*. **1970**, *8*, 259.
58. Suppan, P. *Chimia* **1988**, *42*, 320.
59. Hirakawa, K.; Segawa, H. *J. Photochem. Photobiol. A: Chem.* **1999**, *123*, 67.

CHAPTER 7

Conclusions

Photochemically active porphyrin arrays and porphyrin-based donor-acceptor (D-A) systems are of immense utility in various research areas including biomimetic photosynthesis, molecular catalysis, molecular electronics and photodynamic therapy.[1] Water-soluble, cationic porphyrin systems are receiving attention because of their affinity for DNA and the potential they have for applications in photodynamic therapy.[2] A great variety of monomeric and oligomeric porphyrin species bearing electron donor/acceptor groups at their peripheral or axial positions also have been synthesized to investigate the photochemical activity. Literature on recently reported systems that bear relevance to the present thesis has been reviewed in chapter 1. Results obtained during the present investigation that deal with the design, synthesis, characterization of tri-cationic porphyrins and metalloporphyrins and their DNA interaction studies are reported in chapters 3, 4 and 5. The photochemical properties of D-A systems derived from 'axial' substitution of metalloid porphyrins are reported in chapter 6.

7.1 Interactions of DNA with nucleobase appended tri-cationic porphyrins and metalloporphyrins

The rationale for the design of nucleobase appended tri-cationic porphyrins was based on the following two essential considerations:

(1) Choice of the Porphyrin: The nucleobase appended tri-cationic porphyrins are derivatives of **H_2T4**, which is able to bind strongly to GC-rich sequences by intercalation.[3] Mode of binding of cationic porphyrins is influenced by coulombic, hydrophobic and steric constraints, which can be varied by modifying the structure of the porphyrin as well as the composition of DNA. The

mode of binding (intercalation or groove binding) also depends on the [porphyrin]/[DNA] ratio. At low [porphyrin]/[DNA] ratios, the groove binding mode and intercalation have been suggested for **H_2T4** complexed with AT and GC site of DNA, respectively. As the ratio increases, the outside binding mode, represented by a bisignate excitonic circular dichroism (CD) in the Soret region, dominates for both AT-rich and GC-rich DNAs. The cationic porphyrins are endowed with strong antitumor activities, while eliciting weak toxic effects. Furthermore, cationic porphyrins and metalloporphyrins are shown to display nuclease activities. The versatile binding nature of these porphyrins with DNA can be used to bring other moieties into the proximity of DNA.

(2) Selection of nucleobase: In literature, a few reports involving porphyrin connected with nucleobase[4] or nucleoside[5,6] subunit/subunits are available. It is of interest to investigate the interactions of nucleobase with DNA, since nucleobase moieties are part of the building blocks of the DNA.

The present work has been undertaken to scrutinize the interaction of the nucleobase appended tri-cationic porphyrins with calf thymus DNA (CTDNA). Details of the design, synthesis and characterization of the nucleobase (A, T, G and C) appended tri-cationic porphyrins (**AT4**, **TT4**, **GT4** and **CT4**) are discussed in chapter 3 of this thesis. Interactions of these porphyrins with CTDNA have been investigated using UV-visible, fluorescence, circular dichroism and thermal melting experiments. Finally, a comparison is made between the results obtained for well-established **H_2T4** system with that of the nucleobase appended porphyrins. Extent of cleavage (in the presence of light) of these porphyrins with pBR 322 DNA was calculated through photocleavage experiments. The singlet oxygen mechanism, which is responsible for the cleavage of DNA, is confirmed by conducting photocleavage inhibition experiments using various inhibitors.

Interactions of the metalloporphyrins with nucleic acid duplexes are also significant since the binding mode of porphyrin to nucleic acid duplexes (i.e., intercalative or outside binding mode) can be easily tuned by varying the metal center.[3,7,8] Insertion of various metal ions in the porphyrin ring makes it suitable for specific interactions. Chapter 4 presents the details of the design, synthesis and characterization of the Cu(II) and Zn(II) complexes of adenine appended tri-cationic porphyrins (**CuAT4** and **ZnAT4**). Interactions of these metalloporphyrins with calf thymus DNA (CTDNA) have been investigated using UV-visible, fluorescence, Circular Dichroism (CD) and thermal melting experiments and the results obtained were compared with those obtained for **AT4** and Cu(II) or Zn(II) complex of **H_2T4**. Extent of cleavage in DNA (in the presence of light) of these porphyrins with pBR 322 DNA was calculated through photocleavage experiments.

Chapter 5 describes the interactions of nucleobase appended tri-cationic porphyrins (**AT4**, **TT4**, **GT4** and **CT4**) and Cu(II) complex of adenine appended porphyrin (**CuAT4**) with DNA hairpins using UV-visible and CD techniques. A stepwise energy analysis also has been provided to illustrate the competing effects that influence the binding.

7.2 Axial-bonding type porphyrin arrays and D-A systems

While majority of the reported porphyrin arrays have been obtained *via* cumbersome and often, low-yielding organic synthesis protocols which involve manipulation at either the pyrrole-β or the meso-phenyl position/s of the monomers,[9] relatively less studies have been carried out on the so-called 'axial bonding' type systems. In addition, less attention seems to have been paid towards the construction of functionally active, hybrid systems. Chapter 6 deals with the synthesis, characterization and photochemical properties of 'axial-bonding' type

two monomeric (**M3PY** and **M4PY**) and two dimeric (**A3PY** and **A4PY**) triads based on the tin(IV) porphyrin scaffolds. The ground state spectral data reveal that there exists no ð-ð interaction between the porphyrin and pyridoxo ligands. A photoinduced electron transfer from the axial pyridoxo ligands to the singlet tin(IV) macrocycle has been suggested to occur in the excited state of these systems.

7.3 Future scope of work

The present study has been helpful in formulating strategies towards the design of new types of derivatives of **H_2T4** connected with other moieties to target the DNA with different specific characteristics. It has also been valuable in probing the intricacies involved in the binding as well as cleaving with DNA in these compounds. The interactions of these porphyrins with DNA may further be analyzed using other techniques like Topoisomerisation, Resonance Raman Studies, NMR (^{1}H NMR and ^{31}P NMR), Viscosity, Flash photolysis, Stopped-flow and Temperature-jump techniques. Cationic porphyrins bind with telomeric DNA and act as inhibitors of telomerase, an enzyme that has a significant role in extending the life-time of tumor cells.[10] This provides insight in the direction of binding of these nucleobase appended porphyrins with quadruplex DNAs. The degradation of quadruplex DNA also can be assayed *in vitro* with these newly synthesized nucleobase appended porphyrins and metalloporphyrins through telomeric repeat amplification protocol (TRAP) assay experiments.

The results described in chapter 6 provide some insight into the design aspects of new, architecturally more-appealing supramolecular arrays. The well known binding of zinc(II) and ruthenium(II) metal centers of porphyrin to nitrogen can be employed to construct heterometallic porphyrin oligomers with

these tin(IV) porphyrin-(pyridoxy)$_2$ monomeric and dimeric triads through metal-ligand interactions.

7.4 References

1. Henderson, B. W.; Dougherty, T. J. *Photochem. Photobiol.* **1992**, *55*, 145.
2. Ali, H.; van Lier, J. E. *Chem. Rev.* **1999**, *99*, 2379.
3. Pasternack, R. F.; Gibbs, E. J. In *Porphyrin and metalloporphyrin interactions with nucleic acids*; Elsevier: Amsterdam, The Netherlands, **1996**, Vol. 33, p. 367.
4. Sirish, M.; Maiya, B. G. *J. Porphyrins Phthalocyanines*, **1998**, *2*, 1.
5. Goh, G. K. -M.; Czuchajowski, L. *J. Porphyrins Phthalocyanines* **1997**, *1*, 281.
6. Masiero, S.; Gottarelli, G.; Pieraccini. S. *Chem. Commun*. **2000**, 1995.
7. Lipscomb, L.A.; Zhou, F.X.; Presnell, S.R.; Woo, R.J. Peek, M.E. Plaskon, R.R.; Williams, L.D. *Biochemistry* **1996**, *35*, 2818.
8. Bennett, M.; Krah, A.; Wien, F.; Garman, E.; Mckenna, R.; Sanderson, M.; Niedle, S. *Proc. Natl. Acad. Sci. U.S.A.* **2000**, *97*, 9476.
9. Wasielewski, M. R. *Chem. Rev*. **1992**, *92*, 435.
10. Han, H.; Langley, D. R.; Rangan, A.; Hurley, L. H. *J. Am. Chem. Soc*. **2001**, *123*, 8902.

Appendix I

List of publications

1. Porphyrin-anthraquinone dyads: Synthesis, spectroscopy and photochemistry. P. Prashanth Kumar, **G. Premaladha** and Bhaskar G. Maiya, *J. Chem. Sci.* **2005**, 117, 193.
2. Axial bis(terpyridoxy)phosphorus(V) porphyrin: Modulation of PET and EET by Zn^{2+} or Cd^{2+} ions. P. Prashanth Kumar, **G. Premaladha** and Bhaskar G. Maiya, *Chem. Commun.* **2005**, 3823.
3. Nucleobase (A, T, G and C) appended tri-cationic water-soluble porphyrins: Synthesis, characterization, binding and photocleavage studies with DNA. **G. Premaladha**, P. Prashanth Kumar and Bhaskar G. Maiya (communicated *to J. Porphyrins and Phthalocyanines*).
4. Adenine appended tri-cationic water-soluble metalloporphyrins: Synthesis, characterization, binding and photocleavage studies with DNA. **G. Premaladha** and Bhaskar G. Maiya (*manuscript under preparation*).
5. Interactions of DNA hairpin substrates with nucleobase appended tri-cationic porphyrins and metalloporphyrin. **G. Premaladha** and Bhaskar G. Maiya (*manuscript under preparation*).
6. Bis(aryloxo) derivatives of azo-benzene bridged tin(IV) porphyrin dimers: Synthesis, spectroscopy and photochemistry. **G. Premaladha,** P. Prashanth Kumar and Bhaskar G. Maiya (*manuscript under preparation*).

7. Porphyrin dyads and triads with ruthenium(II) bis-terpyridine complex: Synthesis, spectroscopy and photochemistry. P. Prashanth Kumar**, G. Premaladha** and Bhaskar G. Maiya (*to be communicated)*.
8. Axial bis(terpyridoxy)tin(IV) and phosphorous(V) porphyrin triads: Characterization, crystal structure and photochemistry. P. Prashanth Kumar, **G. Premaladha** and Bhaskar G. Maiya (*to be communicated*).